Investigation of Toll-Like Receptor Tolerance in the Regulation of Inflammation

Submitted to the National University of Ireland, Cork in fulfilment of the requirements for the degree of Doctorate of Philosophy

by

Christine Elizabeth O'Carroll, BSc.

Department of Biochemistry

Alimentary Pharmabiotic Centre,

National University of Ireland, Cork

November 2013

Supervisor: Dr. Ruaidhrí J. Carmody

Table of Contents

Declaration

I hereby declare that this thesis is the result of my own work and has not been submitted in whole or in part elsewhere for any award. Any assistance and contribution by others to this work is duly acknowledged within the text.

_____

Christine Elizabeth O'Carroll, BSc

List of Publications

This work has been published in the following formats

Journal Article

C O'Carroll, G Moloney, G Hurley, S Melgar, E Brint, K Nally, RJ Nibbs, F Shanahan, RJ Carmody.

Bcl-3 deficiency protects against dextran-sodium sulphate-induced colitis in the mouse. Clinical and Experimental Immunology. 2013 Aug;173(2):332-42. doi: 10.1111/cei.12119

C O'Carroll, A Fagan, F Shanahan, RJ Carmody.

Identification of A Unique Hybrid Macrophage Polarisation State Following Recovery from LPS Tolerance

Journal of Immunology, In press

Poster Presentation

"Dr. Jekyll and Mr. Hyde: The Macrophage in Inflammation and Immunity"

C O'Carroll, A Fagan, F Shanahan, RJ Carmody.

Identification of A Novel Macrophage Polarisation State Following Recovery from LPS Tolerance

American Association of Immunology (Boston, 2012)

C O'Carroll, A Fagan, F Shanahan, RJ Carmody.

Identification of A Novel Macrophage Polarisation State Following Recovery from LPS Tolerance

Irish Society of Immunology (Galway, 2011)

C O'Carroll, A Fagan, F Shanahan, RJ Carmody.

Identification of A Novel Macrophage Polarisation State Following Recovery from LPS Tolerance

3rd UK & Ireland NF-κB workshop (Maynooth, 2011)

C O'Carroll, A Fagan, F Shanahan, RJ Carmody.

Identification of A Novel Macrophage Polarisation State Following Recovery from LPS Tolerance

Oral Presentations

Alimentary Pharmabiotic Centre Launch (Cork, 2013)

C O'Carroll, A Fagan, F Shanahan, RJ Carmody.

Identification of A unique Macrophage activation state post microbial tolerance

"Thesis in Three" Science Foundation Ireland national competition (Dublin, 2012)

Tolerance: The fine balance between good and evil

"Science for all" postgraduate student public presentation final (Cork, 2012)

Macrophage: Friend or Foe?

Alimentary Pharmabiotic Centre annual symposium (Cork, 2012)

C O'Carroll, A Fagan, F Shanahan, RJ Carmody.

Identification of A Novel Macrophage Polarisation State Following Recovery from LPS Tolerance

Other publications

C O'Carroll. Macrophage: Friend or Foe? (Issue; A closer look at Science)

Evening Echo Newspaper, Cork June 2012

Colleran A, Collins PE, O'Carroll C, Ahmed A, Mao X, McManus B, Kiely PA, Burstein E, Carmody RJ.

Deubiquitination of NF-κB by Ubiquitin-Specific Protease-7 promotes transcription. Proceedings of the National Academy of Sciences of the United States of America (PNAS) 2013 Jan 8;110(2):618-23

O'Gorman DM, O'Carroll C, Carmody RJ.

Evidence that marine-derived, multi-mineral, Aquamin inhibits the NF-κB signaling pathway *in vitro*. Phytotherepy Research. 2012 Apr;26(4):630-2

Abstract

Inflammation is a complex and highly organised immune response to microbes and tissue injury. Recognition of noxious stimuli by pathogen recognition receptor families including Toll-like receptors results in the expression of hundreds of genes that encode cytokines, chemokines, antimicrobials and regulators of inflammation. Regulation of TLR activation responses is controlled by TLR tolerance which induces a global change in the cellular transcriptional expression profile resulting in gene specific suppression and induction of transcription. In this thesis the plasticity of TLR receptor tolerance is investigated using an *in vivo*, transcriptomics and functional approach to determine the plasticity of TLR tolerance in the regulation of inflammation. Firstly, using mice deficient in the negative regulator of TLR gene transcription, Bcl-3 (Bcl-$3^{-/-}$) in a model of intestinal inflammation, we investigated the role of Bcl-3 in the regulation of intestinal inflammatory responses. Our data revealed a novel role for Bcl-3 in the regulation of epithelial cell proliferation and regeneration during intestinal inflammation. Furthermore this data revealed that increased Bcl-3 expression contributes to the development of inflammatory bowel disease (IBD).

Secondly, we demonstrate that lipopolysaccharide tolerance is transient and recovery from LPS tolerance results in polarisation of macrophages to a previously un-described hybrid state (RM). In addition, we identified that RM cells have a unique transcriptional profile with suppression and induction of genes specific to this polarisation state. Furthermore, using a functional approach to characterise the outcomes of TLR tolerance plasticity, we demonstrate that cytokine transcription is uncoupled from cytokine secretion in macrophages following recovery from LPS

tolerance. Here we demonstrate a novel mechanism of regulation of TLR tolerance through suppression of cytokine secretion in macrophages. We show that TNF-α is alternatively trafficked towards a degradative intracellular compartment. These studies demonstrate that TLR tolerance is a complex immunological response with the plasticity of this state playing an important role in the regulation of inflammation.

Acknowledgements

I would like to thank the many people who have directly and indirectly contributed to my thesis and PhD experience. I first would like to give a special thank you my supervisor Dr Ruaidhrí Carmody, for his time, dedication and endless encouragement throughout the last four years of my PhD studies. I am grateful to the Alimentary Pharmabiotic Centre and Science Foundation Ireland for providing the excellent facilities, support and funding to complete my studies.

I have been fortunate to be a member of two dynamic and vibrant research groups, which allowed me to navigate successfully through my research. To all members of the Carmody Lab and the Host Response and Inflammation Group past and present, I wish you all the very best and I value the time I have spent working with you. I would like to give a special acknowledgment to Dr Ailís Fagan for her support and training of bioinformatics and microarray data processing. Much of this work presented in this thesis could not have been completed without her help and expertise.

I would especially like to thank my collaborators, Professor Mary McCaffrey, Professor Allan Mowat and their lab members particularly Dr Conor Horgan, Sara Hanscom and Dr Calum Bain for endless supply of reagents and technical assistance during my studies. The assistance and suggestions you provided greatly enhanced the quality of each study.

To Grainne, Carola and Collette, a special thanks is owed for your technical help throughout my studies and most importantly your friendship. To my fellow

researchers and friends, whose splendid company and constant banter put a smile on my face every day both in and outside the lab.

Finally, to my family and to Alan, my number one supporters who have provided unwavering encouragement and helped me keep everything in perspective every step of the way; it is to you I dedicate this thesis.

List of Figures

List of Tables

List of Abbreviations

7-AAD	7-amino-actinomycin D
AF	alexafluor
AhR	aryl hydrocarbon receptor
AIM2	absent in melanoma 2
APC	allophallocyanin
Atg16L1	Autophagy 16-like 1
β-actin	beta-actin
Bcl-3	B cell (B-CLL) lymphoma 3
BM	bone marrow
BMDM	bone marrow derived macrophage
BSA	bovine serum albumin
CCL	C-C chemokine ligand
CCR	C-C chemokine receptor
CD	Crohn’s disease
CD	cluster of differentiation
CDH	Chronic granulomatous disease
CD40L	CD40 Ligand
cDNA	complementary DNA
CLR	C-type lectin receptor
CNS	central nervous system
COPD	chronic obstructive pulmonary disease
CXCL	C-X-C chemokine ligand
CXCR	C-X-C chemokine receptor
CYLD	cylindromatosis protein
DAI	disease activity score
DAMP	danger associated molecular pattern

DSS	dextran sodium sulphate
EDTA	ethylenediaminetetraacetic acid
EGF-TM7	epidermal growth factor seven transmembrane receptor
FACS	fluorescent activated cell sorter
FCS	foetal calf serum
FITC	fluorescein isothiocyanate
FMO	fluorescence minus one
GWAS	genome wide association studies
HSC	haematopoietic stem cell
HSP	heat shock protein
HRP	horseradish peroxidase
IBD	inflammatory bowel disease
IFN	interferon
IL	interleukin
iNOS	inducible nitric oxide synthase
i.p	intraperitoneal
IRF	interferon regulatory factor
IVCs	individually ventilated cages
KO	knockout
LBP	LPS binding protein
LPS	Lipopolysaccharide
M1	classically activated macrophage
M2	alternatively activated macrophage
mAB	monoclonal antibody
MAP	mitogen activated protein
MARCO	macrophage receptor with collagenous structure
MD2	myeloid differentiation factor 2
M-CSF	monocyte macrophage colony stimulating factor
miRNA	microRNA

mRNA	messenger RNA
MR/MRC1	mannose receptor
MSD	meso scale discovery
MFI	mean fluorescence intensity
MyD88	myeloid differentiation primary response gene
NF-κB	nuclear factor kappa b
NLR	nucleotide binding oligomerisation domain receptor
NOD2	nucleotide binding oligomerisation domain protein 2
NO	nitric oxide
OCT	optimal cutting temperature compound
PAMP	pathogen associated molecular pattern
PBS	phosphate buffered saline
Pen/Strep	penicillin/streptomycin
PE	phycoerythrin
PFA	paraformaldehyde
PGN	peptidoglycan
PRR	pathogen recognition receptor
PVDF	polyvinyl difluoride
RA	rheumatoid arthritis
RHIM	rip homotypic interaction motif
RIPA	radio-immunoprecipitation assay
RLR	RIG-I-like receptor
RM	recovered macrophage
RT	room temperature
ROS	reactive oxygen species
RT enzyme	reverse transcriptase
SARM	sterile alpha and armadillo motif containing protein
SEM	standard error of the mean
SHP2	src homology -2 domain containing protein tyrosine phosphate

SLE	systemic lupus erthymatosis
Th	T helper
TIR	Toll/interleukin-1 (IL-1) receptor domain
TLR	toll-like receptor
TNF-α	tumour necrosis factor alpha
Tregs	T regulatory cells
TREM-1	triggering receptor expressed on myeloid cells-1
UC	ulcerative colitis
qRT-PCR	quantitative real time polymerase chain reaction

1. General Introduction

1.1 Inflammation

Inflammation is a complex and tightly regulated immunological response to pathogen invasion and tissue injury largely controlled by cells of the innate and adaptive immune system. Innate immune cells such as macrophages are central mediators of inflammatory responses through recognition of microbial pathogens and host tissue injury by different pathogen recognition receptor (PRR) families [1]. Following pathogen or injury recognition, production of soluble inflammatory mediators including cytokines, chemokines, enzymes, vasoactive peptides and amines, complement components and lipid mediators orchestrates leukocyte recruitment and migration to inflammatory tissue sites. This in turn activates cytotoxic and tissue remodelling innate and adaptive immune cells which ultimately clear infection, promote tissue repair and the resolution of inflammation [2]. While a robust microbicidal inflammatory response is critical to fighting infection, prolonged responses can have devastating tissue destructive effects. Excessive or uncontrolled inflammation can result in a pleiotropic range of chronic inflammatory and autoimmune diseases in addition to cancer, heart disease and diabetes. Thus a physiological adjustment of inflammatory responses is critical to promoting tissue homeostasis and resolution of inflammation post inflammatory challenge [2, 3].

1.2 Pathogen recognition

Pathogen recognition is central to innate immunity and mediated through germ-line encoded pathogen recognition receptors found on both immune and non-immune

cells. These receptors include Toll-like receptors (TLRs), RIG-I-like receptors (RLRs), nucleotide-binding oligomerization domain (NOD-like) receptors (NLRs) and C-type lectin receptor (CLRs) families which recognise a vast repertoire of microbial pathogen associated molecular patterns (PAMPS) and tissue derived danger associated molecular patterns (DAMPS) [1, 4-6]. PRRs can be soluble or membrane bound however they are limited in number in contrast to the number of stimuli that they recognise. Soluble PRRs include pentraxins, collectins, ficolins and complement which recognise and bind to foreign molecules which are then cleared by opsonic mediated phagocytosis by host phagocytic cells [7]. Membrane bound PRRs directly bind microbes or tissue injury signals and can be found at both the cell surface and intracellular compartments. Furthermore PRRs have the ability to discriminate between different microbial species including bacteria, viruses, parasites and fungi. This further extends to discrimination between RNA and DNA viruses, gram negative and gram positive bacteria in addition to bacterial flagellin in order to mediate tailored and stimulus specific immune responses [1, 6] (Table 1.1 and Figure 1.1)

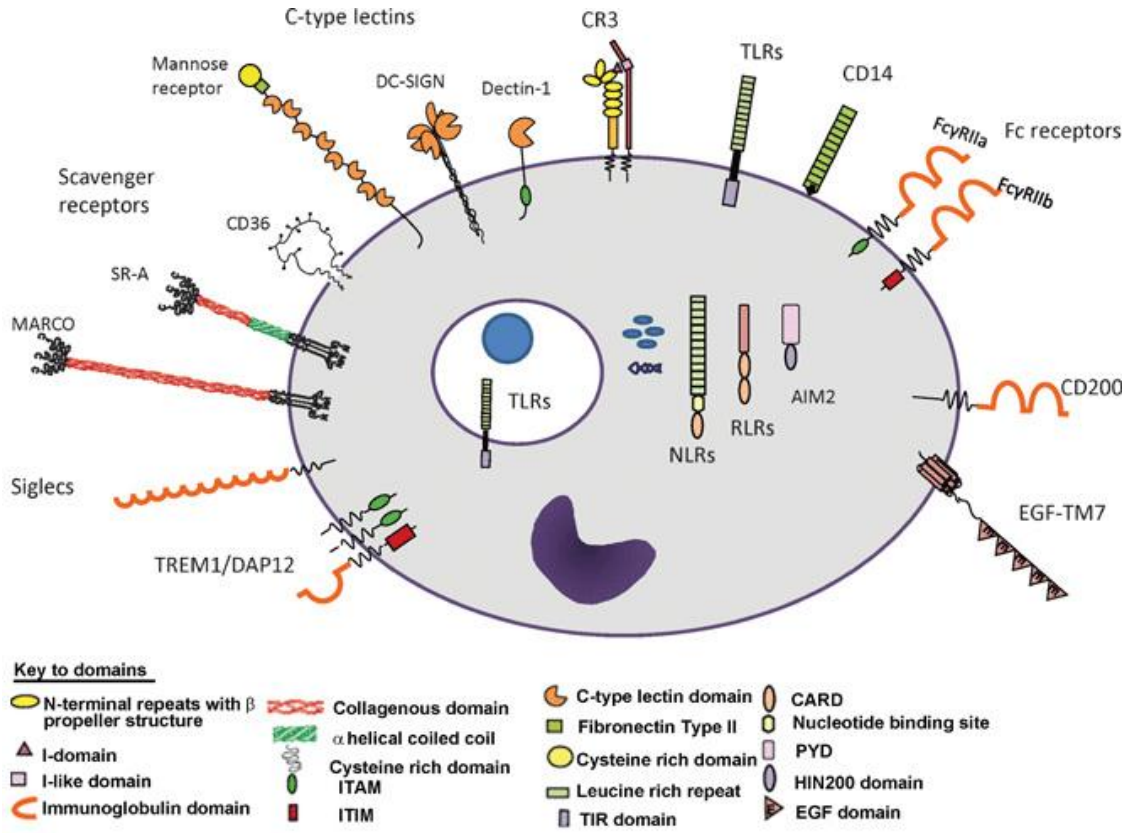

Figure 1.1: Pathogen recognition receptors

C-type lectins (DC-SIGN, Dectin-1, siglecs) and scavenger receptors (CD36, mannose receptor - MR, scavenger receptor A - SR-A, macrophage receptor with collagenous structure - MARCO) and complement receptors (CR3). TLRs, NLRs, RLRs, opsonic receptors (Fc receptors). Surface receptors; activating receptors - EGF-TM7 (epidermal growth factor seven transmembrane receptor), TREM-1 (triggering receptor expressed on myeloid cells – 1), inhibitory receptors - CD200. [8]

1.3 Toll-like receptors

Toll-like receptors (TLRs) are the most extensively studied and widely characterised family of PRRs. TLRs are evolutionary conserved type 1 transmembrane proteins homologus to the protein TOLL in Drosophila [9]. TOLL was originally found to be important for dorso-ventral polarity in drosophila embryonic development with its cytoplasmic domain later found to be important in anti-fungal responses [10]. This

cytoplasmic Toll/interleukin-1 (IL-1) receptor (TIR) domain region of TOLL shares amino acid homology with the interleukin 1 receptor (IL-1R) and is important for NF-κB activation. It was in 1997 that the mammalian homologue hTOLL (TLR4) was cloned and shown to be involved in NF-κB activation and inflammatory gene expression [11].

Discovery of the human TOLL homologue has since led to the discovery of 12 TLRs in mice and 10 in humans. Structurally, TLRs contain an ectodomain rich in leucine repeats which recognises a variety of PAMPs and DAMPS, a transmembrane domain and cytoplasmic TIR domain which mediates downstream signalling and transcriptional events. TLR1, TLR2, TLR4, TLR5 and TLR6 are embedded in the plasma membrane at the cell surface and recognise microbial components expressed on their surface. TLRs are the most extensively studied PRR in innate immunity which recognise a variety of fungal (mannan), viral (envelope proteins, RNA and DNA), bacterial (lipopolysaccharide (LPS), lipotechoic acids, peptidoglycan and DNA) and host DAMPS (heat shock proteins and fibrinogen) (Table 1.1). TLR4 primarily recognises LPS, an outer membrane cell wall component of gram negative bacteria. TLR4 also recognises mannan, heat shock proteins and fibrinogen. TLR2 is important for detection of gram positive bacteria. It recognises peptidoglycan (PGN) and lipotechoic acid, lipoarabinomannan and zymosan from mycobacterium and fungi in addition to hemagglutinin protein from measles virus. TLR2 can form heterodimers with TLR1 and TLR6 to detect microbial triacylated and diacylated lipoproteins respectively. TLR5 specifically recognises flagellin while its closely associated murine family member TLR11 recognises uropathogenic bacteria and profilin like molecules (Table 1.1) [1, 12, 13].

TLR3, TLR7, TLR8 and TLR9 specifically recognise RNA and DNA viruses; therefore these TLRs are strategically located within cytosolic compartments such as endosomes and lysosomes to detect nucleic acids from virally infected cells. TLR7 and TLR8 are closely related and recognise single stranded RNA (ssRNA) viruses such as Influenza A and HIV while TLR9 recognises unmethlyated CpG DNA motifs found in viruses and bacteria but not in mammals. TLR3 specifically recognises double stranded RNA (dsRNA) viruses and signals through a distinct signally pathway from all other TLRs to mediate robust antiviral responses (Table 1.1) [1, 12, 13].

Table 1.1: Pathogen Recognition Receptors and ligands

Source	PAMP	TLR	PRR
Bacterial	Triacyl Lipopeptides	TLR1/TLR2	
	Diacyl Lipopeptides	TLR6/TLR2	
	LPS	TLR4	
	Lipotechoic acid	TLR2	NOD1/NOD2
	Peptidoglycan	TLR2	NOD1/NOD2
	Flagellin	TLR5	
	DNA	TLR9	AIM2
	Lipoarabinomannan	TLR2	
	Porins	TLR2	
	Uropathogenic bacteria	TLR11	
Viral	dsRNA	TLR3	RIG-I, MDA5, LGP2
	ssRNA	TLR7 & TLR8	RIG-I, MDA5, LGP2
	DNA	TLR9	AIM2
	Envelope proteins	TLR4	
	Hemagglutinin	TLR2	
Fungal	Profilin like molecules	TLR11	
	Glycoinositolphospholipids	TLR4	
	Mannan	TLR2/4	
	Zymosan	TLR2/6	Dectin1
	Phospholipomannan	TLR2	
	Hemozoin	TLR9	
Host	HSP	TLR4	
	Fibrinogen	TLR4	

1.4 Lipopolysaccharide and TLR4 signalling

Lipopolysaccharide (LPS) is a complex glycolipid of gram negative bacteria and an extremely potent activator of innate immune responses towards microbial infections. TLR4 recognition of LPS requires a number of co-factors to facilitate effective recognition and activation. LPS is transported in the blood by LPS binding protein (LBP), a soluble plasma carrier protein that binds the glycosylphosphatidylinositol

linked protein, CD14. The interaction between CD14 and LBP facilitates the recognition of LPS by the TLR4 - myeloid differentiation factor 2 (MD2) complex thereby conferring TLR4 responsiveness to LPS [14-17]. *Park et al* demonstrated that successful TLR4 activation requires five of the six LPS lipid chains to bind the hydrophobic region of MD2 [18]. This intricate interaction results in stabilisation of the LPS-TLR4-MD2 complex, dimerisation and activation of the receptor complex and subsequent downstream TLR signalling [18].

1.5 MyD88 dependent pathway

TLR inducible immunological responses are tailored according to specific TLR activation signals by PAMPs or DAMPs. TLR3 TLR7, TLR8 and TLR9 recognise viral RNA and DNA and drive anti-viral immunity though induction of interferon response genes. TLR1/TLR2, TLR6/TLR2 and TLR5 mainly mount pro-inflammatory cytokine responses. All TLRs except TLR3 exclusively signal through an adaptor protein MyD88, which leads to a robust activation of pro-inflammatory cytokine production through activation of NF-κB and mitogen activated protein (MAP) kinase gene expression. In addition TLR4 is the only TLR that can utilise both MyD88 dependent and independent pathways further emphasising the robust immunological potential of TLR4 signalling responses towards infection [12, 13, 19].

Activation of all TLRs signalling events requires the recruitment of a combination of TIR domain adaptor proteins. These include MyD88, TRIF, TIRAP (MAL), TRAM and the recently identified adaptor protein SARM [20]. The activated TLR signalling complex recruits MyD88 to the plasma membrane through TIR domain interactions facilitated by the bridging adaptor molecule TIRAP. MyD88 interacts through death

domain interactions with IRAK4 leading to its activation. IRAK4 phosphorylates IRAK1 and IRAK2, both of which detach from this adaptor group and form a new complex with TRAF6, an E3 ubiquitin ligase and an E2 ubiquitin enzyme complex composed of Ubc13 and Uev1. This E2 complex is responsible for mediating K63 mediated poly-ubiquitination of TRAF6 and generation of a free unconjugated polyubiquitin chain which leads to recruitment of another complex comprising of TAK1, TAB1, TAB2 and TAB3. TAK1 is an IKK kinase and therefore phosphorylates specific serine residues on IKKβ in the IKK complex involved in NF-κB activation. Activated IKKβ phosphorylates and targets the predominant IκB protein IκBα for proteosomal degradation by triggering K48 polyubiquitination. Degradation of IκBα allows movement of the transcription factor NF-κB into the nucleus to promote the transcription of pro-inflammatory mediators. In addition, TAK1 phosphorylates MAP kinase 6 which in turn leads to activation of JNK and p38 stress response pathways and subsequent activation of the transcription factor AP1 [12, 13, 21] (Figure 1.2).

Deficiencies in these signalling adaptor molecules results in altered immunological responses and subsequently increased susceptibility to microbial infections. MyD88 and TIRAP deficient mice display reduced NF-κB inducible pro-inflammatory gene expression in response to LPS activation [22, 23]. Furthermore, MyD88 deficiency renders mice highly susceptible to the development of intestinal inflammation and colitis [24]. Similarly, IRAK4 deficiency leads to defective IL-1 and TLR signalling [25, 26]. Interestingly, deficiency in MyD88 identified a MyD88 independent pathway downstream of TLR4 which led to the induction of type 1 interferons and delayed NF-κB gene expression [27].

1.6 MyD88 independent pathway

The MyD88 independent TLR signalling pathway employs the adaptor and TIR domain protein TRIF. TRIF dependent signalling is utilised by TLR3 to activate interferon gene expression tailored specifically towards viral infection. However TRIF signalling is not exclusively employed by TLR3 as TLR4 can also signal though TRIF independently of MyD88 to mediate both pro-inflammatory and interferon responses. Activated TLR3 can directly interact with TRIF through its TIR domain, however TLR4 requires an additional bridging adaptor protein, TRAM to mediate TLR4 interactions with TRIF. TRIF interacts with TRAF3 and TRAF6 in addition to RIP1 through its RIP homotypic interaction motif (RHIM). A complex comprising of TRAF6, RIP1, pellino and TRADD is required for activation of the IKK kinase TAK1, which in turn leads to activation of the IKK complex and subsequently NF-κB and MAP kinase activation. TRIF signalling also gives rise to the induction of interferon response genes through the transcription factor IRF3. TRAF3 is responsible for activating TBK1 and IKKi which are responsible for phosphorylation of IRF3 and IRF7 and subsequent transcription of type 1 interferons [1, 12, 13, 21] (Figure 1.2). Deficiencies in TRIF signalling can lead to significant impairment in anti-viral responses through repression of IRF3 and IFNβ production [28].

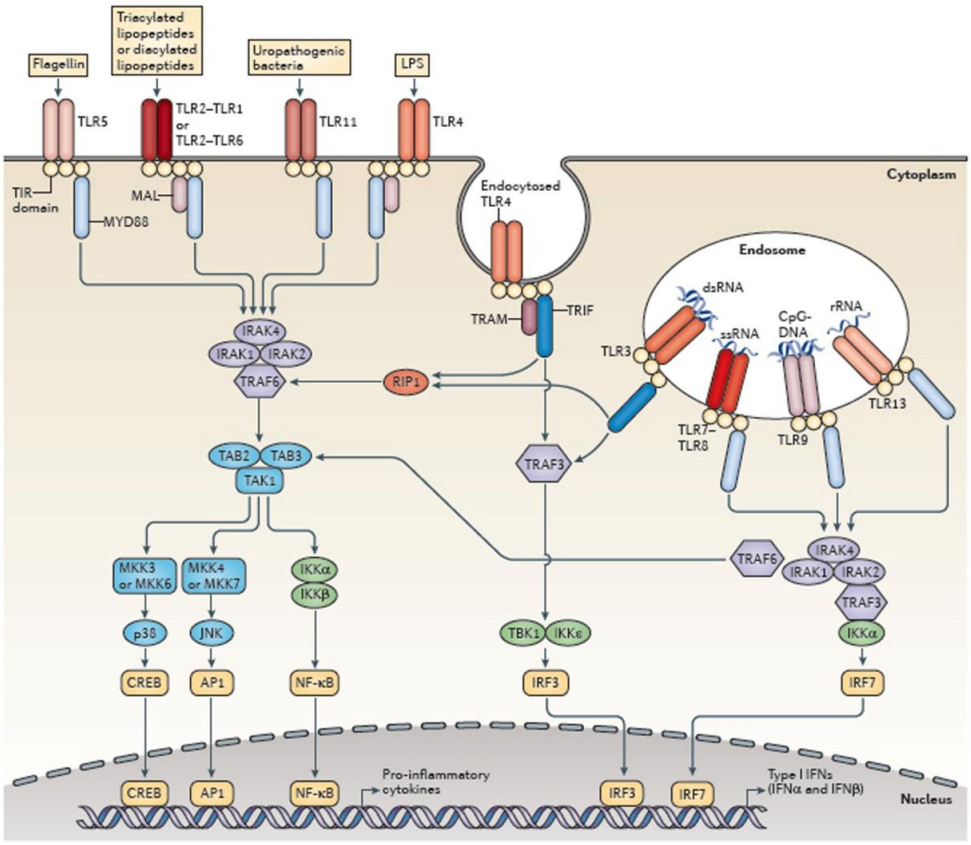

Figure 1.2: TLR signalling pathways

MyD88 dependent and MyD88 independent (TRIF) TLR signalling pathways are utilised by different TLRs. TLR4 uses both pathways to activate pro-inflammatory cytokines through NF-κB and stress response pathways (p38 and JNK). Interferon inducible genes are activated by both NF-κB and IRF3 [9].

1.7 Negative regulation of TLR induced inflammation

TLR signalling induces a rapid yet tailored and robust immune response towards a broad repertoire of stimuli. However uncontrolled and excessive TLR signalling can have devastating pathological consequences. Excessive TLR signalling and subsequent transcription of cytokines and chemokines can result in induction of unregulated cellular recruitment of innate immune cells such as neutrophils, TNF-α induced cellular apoptosis in addition to excessive production of reactive oxygen and

nitrogen species all which can result in tissue and organ damage. This necessitates the need for strict control of TLR signalling responses to maintain immune homeostasis. To limit host tissue damage, TLR inflammatory responses are controlled by a number of molecular processes that include inhibition of signal transduction and repression of gene transcription (Table 1.2 and Figure 1.3) [29-32].

1.7.1 Negative regulators of TLR signalling

Soluble decoy receptors target the early stages of TLR signalling by altering TLR activation and therefore represent one of the first lines of negative regulation of TLR signalling [31]. sTLR4 has been proposed to directly attenuate TLR activation and downstream signalling events by blocking the interaction between TLR4 and the accessory proteins MD2 and CD14 [33, 34]. In support of this, sTLR2 and sTLR4 have been shown to reduce NF-κB activation and pro-inflammatory gene expression [29]. ST2 is a type 1 transmembrane bound glycoprotein and negative regulator of both TLR4 and IL-1R1 signalling which sequesters the adaptor proteins MyD88 and TIRAP preventing their recruitment to the activated TLR complex. Moreover, ST2 deficient mice were found to be hyperresponsive towards repeated challenges with LPS and failed to develop LPS tolerance, a protective regulatory response towards repeated challenges with LPS [35, 36]. Similar to ST2, the orphan receptor SIGIRR (TIR8) has been demonstrated to prevent adaptor protein recruitment to the TLR receptor with increased MyD88 dependent NF-κB activation measured in SIGIRR deficient mice [37]. SIGIRR is a negative regulator of both TLR and IL-1R1 signalling but it is only the TIR domain of SIGIRR that has been shown to be specific for interaction with IRAK1 and TRAF6 in TLR signalling [38].

In addition to SIGIRR and ST2 there are many more negative regulators which affect adaptor protein recruitment to the TLR adaptor protein complex. IRAK-M is an inducible intracellular negative regulator of both IL-1 and TLR signalling which inhibits IRAK1 and IRAK4 dissociation from MyD88 by preventing them from forming a complex with TRAF6, required for downstream activation of TLR signalling. IRAK-M$^{-/-}$ mice and macrophages are hyperresponsive towards both TLR/IL-1 stimulation and display a defect in LPS tolerance similar to that of ST2 deficient mice [39]. Reduced IRAK-M expression in germ-free mice highlighted the importance of IRAK-M in regulation of intestinal immune responses towards the intestinal microbial community [40]. Furthermore a number of conditions including asthma and cystic fibrosis have been associated with a loss of function mutations for IRAK-M which further supports its role as an important upstream negative regulator of TLR signalling [41, 42]. In addition, the TLR and IL-1 signalling negative regulator Tollip directly interferes with IRAK1 inhibiting its phosphorylation and kinase activity [43, 44]. Similarly, MyD88s has been demonstrated to inhibit the phosphorylation of IRAK1 by IRAK4 thereby inhibiting downstream signalling and NF-κB activation [45, 46]. Sterile-alpha and armadillo-motif containing protein (SARM) represents another negative regulator of the MyD88 independent TLR pathway. SARM is a TIR domain adaptor protein which inhibits the essential adaptor protein TRIF with its mechanism unknown [20].

Table 1.2: Negative regulators of TLR signalling

Site	Negative regulator	Target
Signalling	ST2	MyD88, TIRAP
	SIGIRR	IRAK1, TRAF6
	IRAK-M	IRAK1, IRAK4 MyD88
	TOLLIP	IRAK1
	MyD88s	IRAK1/IRAK4
	sTLR2/sTLR4	TLR receptor complex
	SARM	TRIF
	A20	TRAF6
	USP4	TRAF6
	CYLD	TRAF6/TRAF7
	SHP2	TRIF/TBK1
	SOCS1	TIRAP, MAPK, p38, JNK
	PDLIM2	p65
	TRIM30α/TRIM38	TAB2/TAB3/TRAF6
	IL10, TGFβ	IRAK1, IRAK4, ↑negative regulators
	IL1RA	IL1R signalling
	TGF-β	↑ SHIP1
	PI3K	TLR9 signalling
	ATG16L	ROS, IL1 signalling
	IRF4/IRF5	MyD88
	TIPE2	Activating protein 1 (NF-Kb)
Transcription	Bcl-3	p50 homodimers
	IκBNS	NF-κB target genes
	Nurr1	p65 bound promoters
	Ahr	Pro-inflammatory gene expression
	Micro-RNAs	Repress transcription
	ATF3	chromatin

Phosphorylation and ubquitination events play an important role in shaping a tailored TLR induced response following pathogen recognition. Therefore it is not surprising that post-translational modifications play a central role in negative regulation of TLR signalling [30]. The deubiquitinating enzyme A20 is a TLR inducible negative

regulator of both MyD88 dependent and independent TLR induced responses through removal of K63 linked polyubiquitin chains on activated TRAF6 [47]. A20 also regulates TLR3 signalling by preventing IRF3 dimerisation [48] in addition to negatively regulating TNF signalling [49] and NOD2 signalling [50] through removal of K63 polyubiquitin chains on RIP proteins. Furthermore, A20 has been associated with a number of inflammatory diseases, with A20 deficiency in enterocytes and dendritic cells implicated in the development of spontaneous inflammation including colitis [51, 52]. Additionally loss of function polymorphisms are associated with rheumatoid arthritis (RA) and systemic lupus erythematosus (SLE) [53, 54].

Similarly to A20, ubiquitin specific peptidase 4 (USP4) negatively regulates TLR signalling by removing ubiquitin chains from TRAF6 and a deficiency in USP4 leads to an increase in pro-inflammatory cytokines upon LPS and IL-1 stimulation [55]. Moreover while the deubiquitinylating enzyme cylindromatosis protein (CYLD) has been identified as a negative regulator of NF-κB and the IκB protein Bcl-3, it also plays a role in negatively regulating TLR2 signalling by deubiquitinating TRAF6 and TRAF7 [56, 57]. In addition Src homology 2 domain-containing protein tyrosine phosphatase 2 (SHP2) has been shown to be a negative regulator of TRIF dependent pathways by targeting TBK1. This was supported by SHP2 knockdown studies in macrophages which resulted in increased IFN-β production [58].

Suppressor of cytokine signalling 1 (SOCS1) is an important negative regulator of TLR signalling due to its multiple targets of regulation. $SOCS1^{-/-}$ mice are hypersensitive to LPS stimulation and produce more IFN-γ than their WT counterparts [31, 32]. This has been associated with influencing susceptibility to

endotoxin shock [59, 60]. SOCS1 inhibits the JAK-STAT pathway and suppresses NF-κB activation by targeting the adaptor protein TIRAP in addition to binding to the NF-κB member p65 targeting them for ubiquitination and subsequent degradation [61]. Furthermore, SOCS1 also regulates stress response MAP kinase, JNK and p38 pathways [61]. Moreover, deficiencies in TAM (Tyro3, Axl and MER) receptors have been shown to lead to a reduction in SOCS1 expression and subsequently an increase in cytokine secretion [62]. In addition, TRIM30α was identified as an important negative regulator of TLR signalling with both *in vitro* and *in vivo* studies emphasising its importance in protection against endotoxin shock [63]. TRIM30α negatively regulates TLR signalling by targeting TAB2 and TAB3 of the TAK1-TAB2-TAB3 complex for degradation and therefore inhibiting the activation of NF-κB [63]. Furthermore the TRIM38 family member has also been shown to act as a negative regulator of TLR signalling by targeting TRAF6 for proteosomal degration following its poly-ubquitination by TRIM38 [64].

Negative regulation of TLR signalling can be brought about through the expression of soluble mediators including IL-10, TGF-β and IL-1RA. TGF-β and IL-10 are anti-inflammatory mediators of TLR signalling and deficiencies in IL-10 or TGF-β renders mice more susceptible to developing colitis [65]. IL-10 reduces pro-inflammatory gene expression resulting from degradation of IRAK1 and IRAK4 in addition to altering macrophage antigen presentation capacity [66]. Furthermore IL-10 expression leads to an increase in a number of negative regulators of TLR signalling including IL-1RA, SOCS3 and Bcl-3 in addition to increased activity of STAT3 and PI3K pathways [32, 67, 68]. TGF-β alters pro-inflammatory gene expression by altering NF-κB activation and leading to an increase of an additional negative regulator SHIP1 with $SHIP1^{-/-}$ macrophages defective in endotoxin

tolerance [69]. Moreover TGF-β has been shown to play an important role in dampening MyD88 dependent TLR signalling pathways by inducing the ubiquitination and subsequent degradation of MyD88 [70]. Furthermore, deficiency in IL-1RA rendered mice highly susceptible to endotoxin shock with altered IL-1R signalling decreasing pro-inflammatory cytokine production [71].

In addition to the expression of soluble mediators, components of other cellular signalling pathways play a role in regulating TLR responses. The induction of PI3K has been shown to play a role in negative regulation in response to TLR9 signalling [29]. A loss of Atg16L1, a component of the autophagy pathway is associated with increased risk of inflammatory bowel disease in addition to elevated production of reactive oxygen species and IL-1 signalling suggesting it plays a regulatory role in response to TLR signalling [72]. Furthermore competition between the transcription factors IRF4 and IRF5 for the adaptor protein MyD88 represents another level of complexity to negative regulation of TLR signalling with IRF4 affecting IRF5 transcription [30, 73]. In addition TIPE2 was identified as a negative regulator of TLR signalling though caspase 8 activity with TIPE2 deficiency resulting in a state of cellular hyperresponsiveness [74]. The large number of negative regulators and the extent of different modes of negative regulation demonstrate the complexity of the TLR signalling pathway and the necessity to tightly control TLR responses to generate an appropriate tailored immune response.

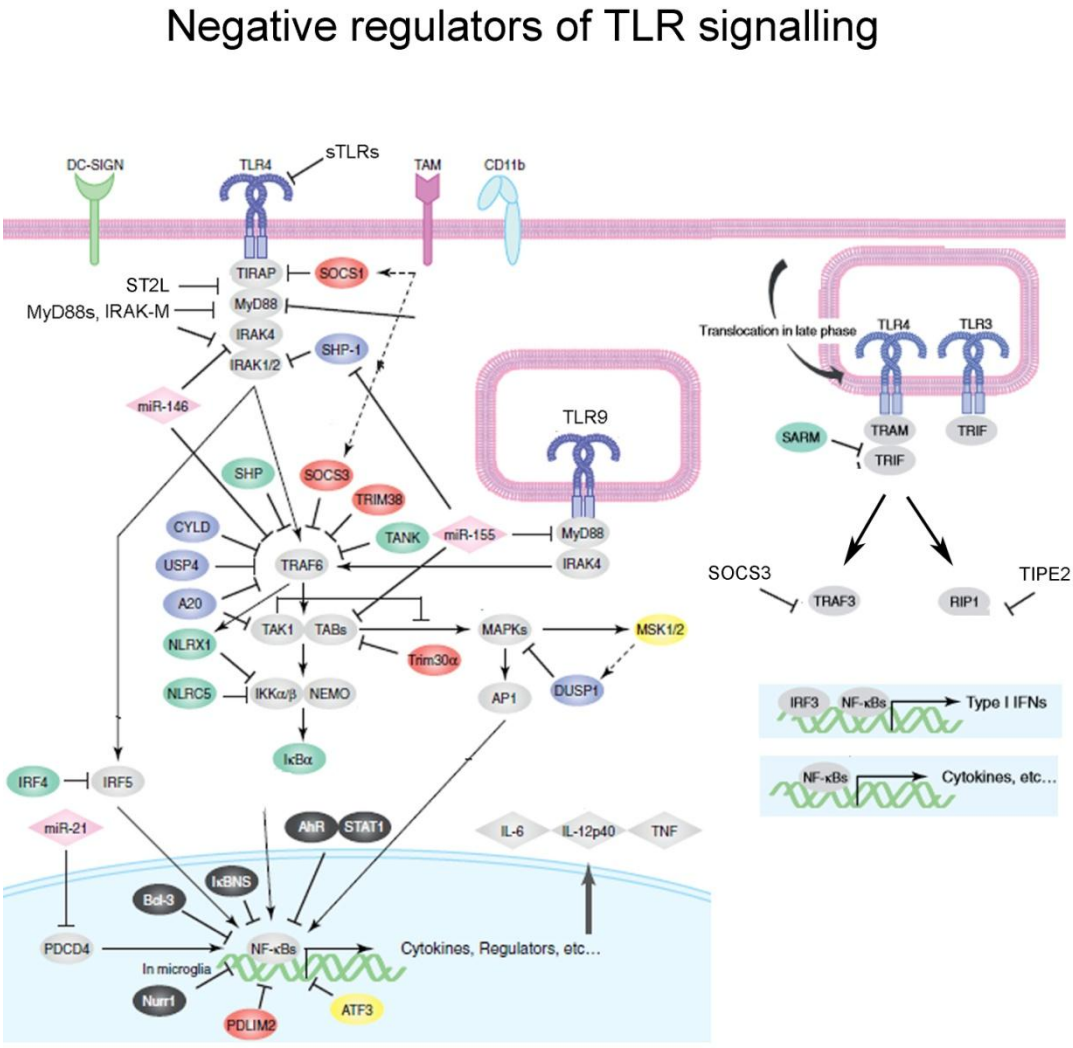

Figure 1.3: Negative regulators of TLR signalling

Negative regulators of MyD88 and TRIF dependent TLR pathways through inhibition of TLR signal transduction and TLR inducible gene transcription mechanisms. Adapted from *Kondo et al, 2011*[30]

1.7.2 Negative regulators of TLR gene transcription

Transcriptional analysis of TLR4 induced gene expression reveals a large number of LPS inducible genes which can be divided into different subgroups dependent on their function. The array of functions ranging from pro-inflammatory, anti-inflammatory, anti-microbial, tissue remodelling, wound repair and metabolic

suggests that these genes are differentially regulated dependent upon their requirements for immunological or normal physiological responses [75]. Transcriptional regulation of TLR signalling involves a number of mechanisms including the expression of negative regulators affecting transcription, in addition to gene specific regulation at individual promoters by chromatin remodelling and histone modifications [29, 30, 32, 61, 75].

1.7.2.1 Transcriptional factors

The negative regulator Nurr1 was shown to be involved in terminating NF-κB responses in microglia cells of the central nervous system (CNS) in a negative feedback system. Nurr1 was shown to be recruited to p65 on inflammatory gene promoter sites which in turn led to the recruitment of a CoREST repression complex resulting in termination of NF-κB transcriptional responses [76]. The aryl hydrocarbon receptor (AhR) transcription factor is a LPS inducible transcriptional negative regulator of TLR induced responses with AhR deficiency in mice resulting in increased susceptibility to LPS induced lethal shock. Furthermore $AhR^{-/-}$ macrophages are hyperresponsive following LPS stimulation resulting in increased production of TNF-α and IL-6 pro-inflammatory cytokines [77]. Moreover transcriptional regulation by AhR was shown to require the transcription factor STAT1, with deficiency in STAT1 and AhR leading to further increased IL-6 production. It has been demonstrated that the activity of the IL-6 promoter was affected by an inhibitory complex composed of NF-κB, STAT1 and the Ah Receptor in TLR4 stimulated macrophages resulting in decreased LPS induced IL-6 gene expression [77].

1.7.2.2 MicroRNAs

MicroRNAs (miRNA) represent another level of complexity to transcriptional regulation of TLR signalling. miRNAs are short (22nt) non-coding evolutionarily conserved molecules which regulate a number of biological processes post transcriptionally [78]. miRNAs have been shown to play a role in regulating immune responses. miR-146a, miR-155 and miR-132/-212 are induced upon TLR activation and lead to the repression of pro-inflammatory gene transcription in a negative feedback loop [78]. miR-146a inhibits IRAK1 and TRAF6 thus inhibiting NF-κB activation and pro-inflammatory gene expression. miR-146a deficiency has demonstrated NF-κB dysregulation. Mice deficient in miR-146a are hyperresponsive and polymorphisms have been identified in inflammatory conditions including rheumatoid arthritis. [30, 79].

More recently, a bioinformatics target scan approach revealed miR-132 and miR-212 (miR-132/-212) as miRNAs that target IRAK4. This revealed that miR-132/-212 was induced by peptidoglycan, Pam3CSK4 and flagellin in a cREB dependent manner where it promoted tolerance to TLR stimulation. miR-132/-212 was shown to be induced rapidly upon TLR stimulation and to target the adaptor protein kinase IRAK4 [80]. In addition, miR-21 was identified as another negative regulator of TLR4 signalling where it was shown to target the tumour suppressor PDCD4 thereby inhibiting pro-inflammatory gene expression and promoting the expression of IL-10 [81]. Furthermore miR-155 plays a dual role in the regulation of TLR immune responses. While miR-155 positively regulates TLR induced responses by repressing SHIP1 [82], it plays a crucial role in negatively regulating TLR responses by targeting TAB2, IKKι and MyD88 [83, 84].

1.7.2.3 Chromatin remodelling

Chromatin remodelling plays an essential role in regulating TLR induced gene transcription by modifying DNA containing chromatin structures making promoter regions of DNA accessible or inaccessible to the transcriptional machinery. Histone modifications are the principal epigenetic modifications associated with chromatin remodelling in response to LPS signalling. Histone proteins which package chromatin structures are subject to addition or removal of acetylation, methylation, phosphorylation and ubiquitination markers by a number of different enzymes including histone acetlytransferases, demethylases, kinases and methyltransferases. The addition or removal of histone modifications determines the accessibility of promoter regions to transcription factors and additional transcriptional machinery [85]. Regulation of TLR induced responses during LPS tolerance was recently shown be regulated by chromatin remodelling with the inhibitory histone methylation mark H3K27 observed on pro-inflammatory genes. This inhibitory histone modification prevented pro-inflammatory gene promoter accessibility to the transcriptional machinery resulting in repression of gene expression [75, 85]. ATF3 is a member of the CREB/ATF family of transcription factors with $ATF3^{-/-}$ macrophages displaying increased gene expression of IL-6 and IL-12p40 following TLR4 stimulation with LPS. ATF3 has been shown to bind to acetylation sites within chromatin structures resulting in recruitment of the histone deacetylase HDAC1. ATF3 negatively regulates gene expression by facilitating an alteration in the chromatin conformational structure resulting in an inhibition of access of activating transcription factors to gene promoter sites [86, 87].

1.7.2.4 Additional transcriptional regulators of TLR gene transcription

PDLIM2, a PDZ and LIM domain protein targets the p65 NF-κB subunit for proteosomal degradation thereby negatively regulating NF-κB activation. PDLIM2$^{-/-}$ mice displayed increased NF-κB activation and are hyperresponsive towards TLR stimulation. PDLIM2 binds to p65 in the nucleus and promotes K48-linked polyubiquitination resulting in sequestering of p65 to PML nuclear bodies followed by subsequent degradation [88]. IκBNS is a member of the IκB inhibitory proteins which negatively regulates gene expression of pro-inflammatory genes including IL-6 and IL-12p40 but not TNF-α or IRF3 target genes. IκBNS deficient mice are susceptible to endotoxin shock and intestinal inflammation with IκBNS deficient macrophages displaying increased NF-κB activation. Therefore IκBNS represents a selective transcriptional negative regulator of NF-κB target genes [89].

1.8 B cell Leukemia-3 in inflammation and immunity

B cell leukemia-3 (Bcl-3) is an atypical member of the IκB family which regulates NF-κB transcription [90]. Bcl-3 is predominantly nuclear in localisation and is not degraded upon activation of the IKK complex. Bcl-3 selectively binds the REL homology domain region of p50 and p52 homodimers through its ankyrin repeat domain thereby modulating NF-κB gene transcription. Bcl-3 was originally identified in a subset of chronic lymphocytic leukaemia (B-CLL) patients containing a recurring t(14:19) chromosomal translocation [91, 92]. As a result Bcl-3 has since been implicated in cell survival and tumorigenesis [93-96]. Increased expression of NF-κB subunits in addition to Bcl-3 was observed in breast cancer tumours and epithelial cancer cells [97, 98]. Additionally, a loss of function mutation in the CYLD gene which negatively regulates Bcl-3 expression is associated with benign

skin tumours, cylindromas [56, 99]. Bcl-3 has been shown to play an important role in cell survival. Bcl-3 deficient T cells demonstrated reduced survival while over-expression of Bcl-3 increased T cell survival [100-102]. Bcl-3 is a regulator of cyclin D1 and is important in cell cycle regulation. Over-expression of Bcl-3 has been shown to shorten the G1 phase of cell cycle in breast cancer epithelial cells which coincided with elevated cyclin D1 expression levels [96]. Bcl-3 also regulates HDM2, an inhibitor of p53 induced apoptosis by promoting its expression [103].

Bcl-3 has also been shown to play a critical role in immunological development, the negative regulation of autoreactive thymocytes and altering T cell responses [104, 105]. Bcl-3 deficient mice revealed impaired differentiation of naïve T helper cells into Th2 immune cells as a result of a lack of the transcription factor GATA3 expression and subsequent induction of IL-4 [106]. In addition, Bcl-3 deficient mice were found to display defects in lymphoid organogenesis including a defective follicular dendritic cell network, reduced germinal centre formation and secondary lymphoid organ development including reduced numbers of Peyer's patches and defective lymph node structure. [104, 107, 108]. Bcl-3 has recently been shown to play a regulatory role by limiting granulopoiesis under inflammatory conditions with Bcl-3 deficient myeloid progenitors demonstrating increased granulocyte proliferation and differentiation [109]. Furthermore, Bcl-3 deficiency in haematopoietic cells led to increased susceptibility of mice to develop diabetes. In this study Bcl-3 was shown to play a regulatory role in autoimmune diabetes by limiting pro-inflammatory cytokine and chemokine gene expression [110].

Bcl-3 is an important negative regulator of TLR and NF-κB induced responses. Bcl-3 is essential for induction of TLR tolerance and Bcl-$3^{-/-}$ mice and macrophages are

hyperresponsive to TLR stimulation and are defective in LPS tolerance. Furthermore Bcl-3 deficiency revealed increased susceptibility of mice to endotoxin shock resulting from uncontrolled pro-inflammatory gene expression at the transcriptional level. Bcl-3 negatively regulates NF-κB gene expression by stabilising inhibitory p50 homodimers at κB promoter sites of pro-inflammatory genes by inhibiting p50 ubiquitination and subsequent proteasomal degradation. This in turn prevents activating NF-κB heterodimers (p65/p50) from occupying NF-κB gene promoter sites and promoting transcription [111]. Additionally Bcl-3 deficiency in mice led to increased susceptibility to microbial infections with *Klebsiella pneumoniae, Streptococcus pneumoniae* and *Listeria monocytogenes* [68, 108, 111, 112]. Thus, Bcl-3 plays an important role in inflammation, immunological development and cell cycle however it is critical in negatively regulating TLR signalling and TLR induced gene expression.

1.9 LPS Tolerance – historical and physiological perspective

Paul Beeson first identified the novel phenomenon of LPS tolerance as a physiological adaptation following inflammatory challenge in the 1940's. Beeson demonstrated that rabbits displayed a reduction in fever following repeated challenges with typhoid vaccine and induced a state of tolerance towards repeated exposure [113]. This was one of the first pieces of evidence that the inflammatory response adapts to limit the deleterious consequences of excessive inflammation. This was later repeated with endotoxin (LPS) which demonstrated similar suppressed responses to the typhoid vaccine findings. Beeson defined this physiological immune adaption as endotoxin tolerance. He postulated that the cells of the reticuloendothelial system were involved in promoting tolerance towards

endotoxin with this state later demonstrated to be transferrable from one animal to another [114-116]. In support of this pioneering work, patients recovering from polynephritis, malaria, typhoid and paratyphoid fever displayed reduced fever responses when challenged with endotoxin [117]. Furthermore reports suggested this protective phenomenon was used in fever therapies over 100 years ago to treat neurological related illnesses such as depression [118].

Following Beesons pioneering work, Freudenberg and Galanos demonstrated that a pre-stimulation with LPS protected mice against lethal doses of LPS even when LPS responsiveness was increased upon galactosamine treatment [119]. Importantly, they elegantly demonstrated that monocytes and macrophages were responsible for mediating tolerance towards LPS [119]. This work indicated that innate immunity played a pivotal role in regulating inflammation by inducing a state of unresponsiveness or tolerance towards repeated exposure to inflammatory signals such as LPS. However, the molecular events leading to this essential protective phenomenon remained to be elucidated at this time with the lack of identification of a recognition receptor playing a central role. This work did however pave the way for extensive research into pathogen recognition by the immune system first postulated by Charles Janeway [4]. Following the discovery of PRRs, genetic studies identified TLR4 as the LPS receptor [120]. This data was supported by the findings of the spontaneous mutation in the LPS^{D} gene which encodes for TLR4, in the C3H/HeJ mouse colony which rendered them insensitive to LPS [120]. In addition TLR4 deficient mice were found to be unresponsive to LPS thus confirming TLR4 as the LPS receptor [19].

1.10 LPS Tolerance – transcriptional regulation

Since the discovery of TLRs, extensive study of the intricate regulation of TLR signalling pathways has led to significant developments in elucidating the molecular mechanisms involved regulating TLR signalling in addition to induction of LPS tolerance. LPS tolerance is defined as a state of altered responsiveness in cells such as macrophages as a result of a global change in the cellular transcriptional profile from that of a pro-inflammatory to anti-inflammatory resolving state. Prior to transcriptomics analysis of LPS tolerance, TLR4 signalling studies revealed LPS tolerance as a state of hyporesponsiveness or refractoriness towards repeated challenges with LPS. It was proposed that induction of this state of reduced responsiveness resulted in suppression of TLR signalling and NF-κB inducible expression of pro-inflammatory cytokines including TNF-α. These studies defined LPS tolerance as an essential suppressed inflammatory state resulting from inhibition of adaptor protein recruitment and TLR receptor desensitisation mediated through induction of multiple negative regulators (Table 1.2) [121-125].

Recently, a transcriptomics profiling study identified two classes of LPS responsive genes; those that are suppressed during LPS tolerance, so-called tolerisable (Class T) genes and those whose expression is maintained or even increased during LPS tolerance, so called non-tolerisable genes (class NT). Pro-inflammatory genes including TNF-α and IL-6 were found to be rapidly tolerised upon prolonged LPS exposure while anti-microbial peptides, tissue remodelling factors, mediators of phagocytic activity and genes promoting the resolution of inflammation were induced during this state. Upon further examination it was found that chromatin modification plays a central role in regulation of LPS tolerance gene expression.

Selective histone deacetylation and chromatin remodelling of tolerisable genes reduced promoter access and Pol II recruitment preventing gene transcription. In contrast acetylation of histones and Pol II recruitment remained intact on NT gene promoters [75].

This pivotal finding revealed that TLR induced gene transcription is required to suppress transcription of tolerisable genes in addition to promoting expression of NT genes. Furthermore, this data confirmed that LPS tolerance is a gene specific regulatory mechanism which results in altered gene expression of different functional groups rather than global suppression of TLR induced gene expression, LPS signalling and receptor desensitisation. In support of this study, it was later confirmed that NF-κB specific motifs within promoters of genes specified TLR induced gene repression. Furthermore the interaction between the NF-κB motifs and the NcoR repressosome was found to be essential in the induction of TLR tolerance [126]. This study showed that NF-κB sites were significantly enriched within promoter regions of TLR4 induced tolerisable genes. However these sites were not enriched in non-tolerisable gene promoters. Interestingly mutations in these NF-κB motifs resulted in an inability of tolerisable genes to be suppressed during LPS tolerance. Mutation in NF-κB motifs converted LPS tolerisable genes into non-tolerisable genes. In addition, inserting NF-κB motifs into promoter sites on non-tolerisable genes converted them into tolerisable genes. Both these studies provide molecular insight into the physiological adaption of the inflammatory response towards TLR challenge with LPS tolerance inducing a global shift in the transcriptional profile of macrophages from a pro-inflammatory to anti-inflammatory pro-resolution state [75].

1.11 Macrophage activation response upon microbial challenge

Macrophages are key components of the innate immune system and are central mediators of inflammation and disease. Macrophages also play important physiological roles involving tissue repair and remodelling, phagocytosis of cellular debris and apoptotic cells in addition to having essential metabolic functions [127]. Macrophages can be divided into two populations; inflammatory and tissue resident macrophages both of which are members of the mononuclear phagocyte system (MPS) [128]. The MPS was originally described by Van Furth and colleagues in the early 1970's where they described the MPS as comprising of different cell types (monocytes, macrophages and dendritic cells) which are all derived from a common bone marrow progenitor cell [129]. Macrophages can be further divided into two subgroups based on whether they are tissue resident or recruited to different anatomical sites under inflammatory cues. Macrophages can be found at a variety of anatomical tissue sites including the lungs, spleen, intestines and the CNS with each site determining specific macrophage environmental characteristics and biological functions [130-132] (Figure 1.4). Recently, significant insight has been provided into macrophage origins independent of the haematopoietic stem cell (HSC). The resident macrophage population of the CNS, microglia cells, have recently been shown by fate mapping studies to originate from the yolk sac [132]. Furthermore a number of additional resident macrophage populations including pleural macrophages, Langerhans cells and Kupffer cells have been shown to proliferate independently of the bone marrow through the primitive yolk sac macrophage lineage [133].

Tissue resident macrophages are one of the first activators of inflammation at sites of infection as they detect pathogens through their pathogen recognition receptors. This

initiates a local inflammatory response characterised by production of cytokines and chemokines which instigate leukocyte recruitment and migration to the site of infection. Inflammatory macrophages are not terminally differentiated but are recruited from the $GR1^{+}$ $CX3CR1^{Low}$ pool of circulating monocytes in the blood. Upon recruitment and migration of monocytes to sites of infection, they differentiate into inflammatory macrophages where they perform pro-inflammatory and cytotoxic activities to fight and clear infection. In addition these cells have pro-resolution properties and function to restore tissue homeostasis. Thus macrophages play a dual role in fighting infection and restoring tissue homeostasis post infection [127, 134].

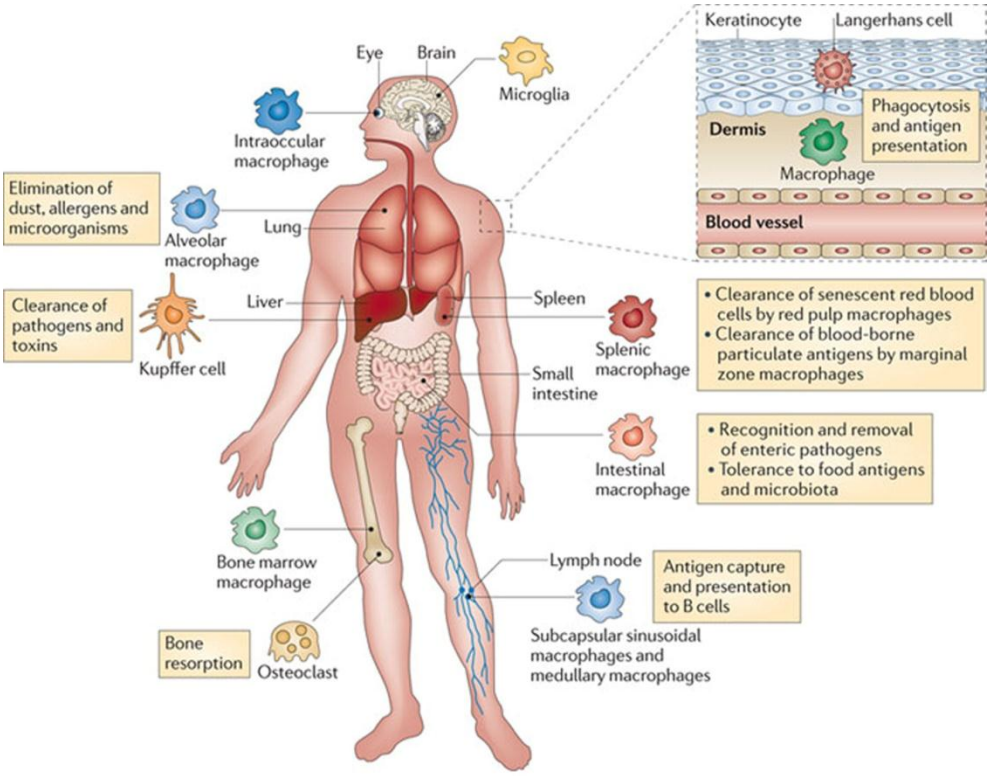

Figure 1.4: Macrophage origins and tissue resident macrophage populations

Differentiation of the haematopoietic stem cell (HSC) in response to monocytes/macrophage colony stimulating factor leads to commitment to the monocyte lineage. Monocytic cells exit the bone marrow and enter circulation giving rise to two populations, resident monocytes (GR1 negative, CX3CR1 high) and inflammatory monocytes (GR1 positive, CX3CR1 low) which migrate into tissue to become resident and inflammatory macrophage populations. Recent evidence suggests that microglia cells originate from the yolk sac rather from the haematopoietic lineage described above [130, 132]. Adapted from *Murray and Wynn, 2011 [130]*.

1.12 Macrophage activation and plasticity

Macrophages are highly plastic and adaptable professional phagocytes which play important roles in a wide range of biological activities. This is reflected in the emerging spectrum of macrophage activation states based around the M1 pro-inflammatory and M2 anti-inflammatory classification system.

1.12.1 Classical macrophage activation (M1)

Classical activation of macrophages results primarily in a pro-inflammatory microbicidal state. Macrophages are polarised into classically activated M1 phagocytes following stimulation with TNF-α or a TLR ligand such as LPS in addition to a second signal, interferon-gamma (IFN-γ), produced by natural killer (NK) cells and Th1 cells in response to infection. Upon activation M1 macrophages produce type 1 interferons including IFN-β which can signal in an autocrine manner and replace the short lived cellular immune source (NK cell and Th1 cells) of IFN-γ in addition to further enhancing M1 polarisation. Classical macrophage activation results in production of pro-inflammatory cytokines such as TNF-α, IL-6, IL-1, IL-12, and IL-23 leading to recruitment of both innate and adaptive immune cells including the expansion of Th17 helper cells. This results in a robust inflammatory response towards pathogenic infection and tissue injury. In addition to production of pro-inflammatory mediators of inflammation, M1 macrophages play an important role in antigen presentation and activation of Th1 immune responses against infection. Furthermore, these cells are critical for destruction and elimination of intracellular and phagocytosed pathogens through production of reactive oxygen and nitrogen species [127, 130, 135-138].

Defects in nitric oxide (NO) production can lead to the inability of macrophages to effectively kill and clear intracellular pathogens such as *Mycobacterium tuberculosis* [127]. Furthermore a defect in the membrane bound enzyme complex NADPH oxidase involved in superoxide production has been found in chronic granulomatous disease (CDH) patients rendering them susceptible to infections [139]. In addition, combined stimulation of macrophages with IFN-γ and a TLR ligand is essential to lead to full activation and effective clearance of intracellular bacteria. A single signal can render macrophages less efficient at clearing infection. *Leishmania* species and *Mycobacterium tuberculosis* are two intracellular pathogens that can interfere with IFN-γ signalling, effectively dampening the immune response and enhancing their survival. Thus a combination of M1 polarisation stimuli is required for effective killing and clearance of intracellular pathogens [127].

Recently, transcriptional profiling has been used to define macrophage polarisation in combination with surface markers [140]. Classically activated M1 macrophages have a unique transcription factor signature. Macrophages deficient in the transcription factor IRF5 displayed impaired pro-inflammatory (M1) cytokine expression suggesting IRF5 is an essential M1 polarisation factor [141]. In addition, classically activated macrophage markers including IL-12, inducible nitric oxide synthase (iNOS) activity and antigen presentation are all regulated by JAK-STAT signalling with STAT1 playing an important role [142, 143]. While classically activated M1 macrophages are essential in fighting and clearing bacterial infections, they have strong potential to inflict host tissue and organ damage. Thus strict regulation of M1 responses through induction of negative regulatory pathways and TLR tolerance is important.

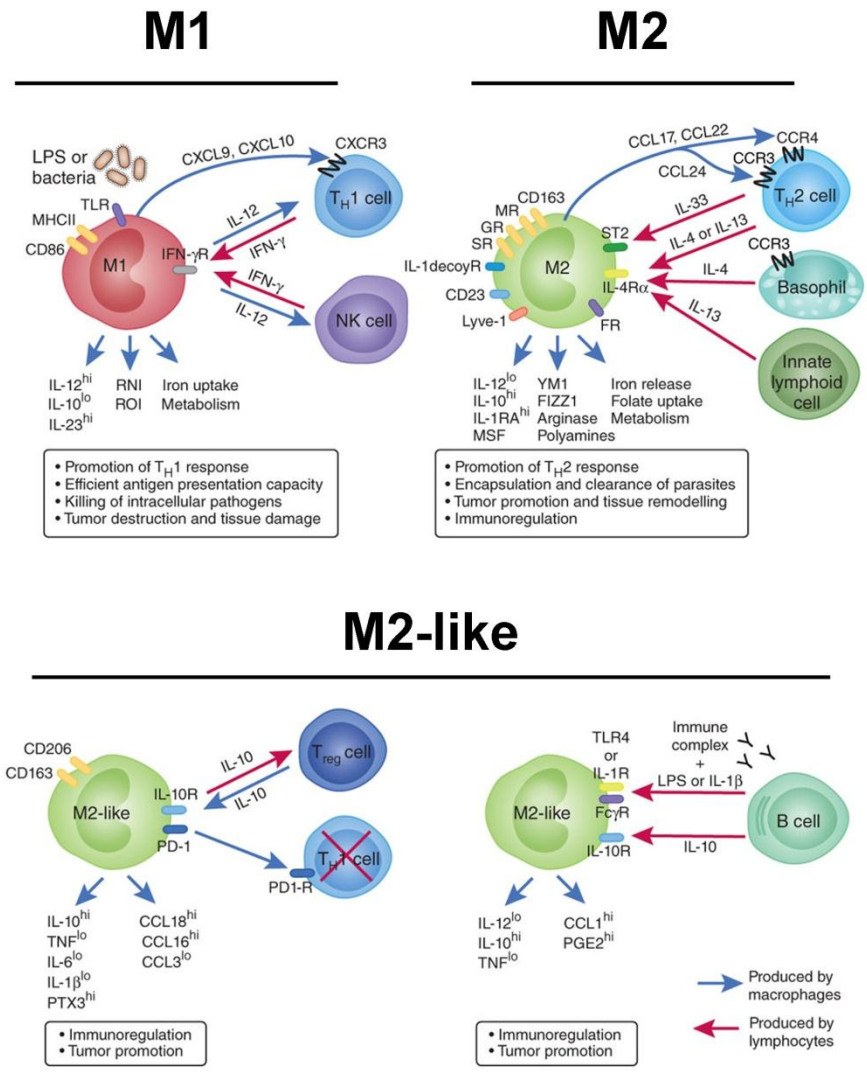

Figure 1.5: Macrophage activation states

Macrophages can be polarised into a spectrum of activation states with the main polarisation states illustrated. M1 macrophages are primarily pro-inflammatory and activated by bacterial infections. M2 macrophages are anti-inflammatory cells strictly polarised by IL-4, IL-13 and parasitic infection. Many hybrid macrophage populations exist in the emerging spectrum of macrophage polarisation which encompasses multiple anti-inflammatory M2-like states. These include, tumour associated macrophages, regulatory macrophages, endotoxin tolerant macrophages. Illustration adapted from *Biswas and Mantovani, 2010* [135].

1.12.2 Alternative macrophage activation (M2)

Alternatively activated macrophages (M2) have a unique transcriptional and biological signature initiated by IL-4 and IL-13 which are produced by immune cells of the Th2 adaptive immune response including basophils, eosinophils and mast cells. Furthermore, parasitic infections are powerful drivers of M2 polarisation and Th2 immunity. Two additional cytokines, IL-21 and IL-33 have also been implicated in M2 macrophage polarisation. IL-21 drives increased expression of the IL-4 receptor (IL-4R) promoting M2 macrophage polarisation [127, 144, 145]. Wound healing and tissue remodelling are key biological functions of M2 macrophages which are reflected in increased arginase activity. IL-4 drives a shift from iNOS enzyme activity to that of increased expression of arginase 1 activity in M2 cells. Arginase 1 facilitates wound healing responses by converting L-arginine to L-ornithine, a polyamine and proline (collagen) precursor, which is required for generation of the extracellular matrix in tissue remodelling, repair and parasite capture [127, 138]. M2 macrophages are highly phagocytic and uniquely express the mannose receptor MRC1 (CD206) [144]. In addition to reduced reactive oxygen species mediated microbicidal activities, M2 cells have reduced ability to kill intracellular pathogens such as mycobacteria [146].

In contrast to the pro-inflammatory profile of M1 macrophages, gene expression of TNF-α, IL-6 and IL-12 is greatly suppressed in M2 cells. However M2 macrophage activation induces the expression of anti-inflammatory mediators IL-10, TGF-β and VEGF in addition to a number of unique markers YM1 (CHI3L3), FIZZ1 (RELM-α), CCL17, CCL22 and CCL24 which are potent inducers of Th2 responses [127]. IRF4, STAT6 and PPARγ transcription factors play a central role in M2 macrophage

polarisation [140]. IL-4 stimulation of macrophages from a myeloid specific knockout of the IL-4 receptor (IL-4RA) fail to polarise towards the M2 alternative state emphasising the importance of IL-4 signalling in M2 macrophage polarisation [147, 148]. While STAT1 plays an important role in M1 pro-inflammatory gene expression STAT6 regulates the transcription of M2 specific genes including Arg1, MRC1, FIZZ1 and YM1. In addition, PPAR-γ is involved in M2 polarisation and uses STAT6 as a co-factor. IL-4 induction via STAT6 in addition to PI3K and IRF4 has been shown to be an important pathway involved in M2 polarisation [140]. Recently IRF4 and the histone demethylase JMJD3 have been shown to be involved in polarisation of M2 macrophages in response to chitin, a component found in the cell walls of fungi and parasites [149]. Additionally mice which lack CREB promoter binding sites in C/EBPβ displayed specific suppression in M2 associated genes in addition to defects in wound healing following muscle injury suggesting that the transcription factors CREB and CEBPβ are essential for M2 polarisation and gene expression [150].

One of the hallmarks of bacterial infections is the recruitment and migration of inflammatory M1 macrophages to sites of infections. In contrast to this, recent evidence has suggested that M2 macrophages are not recruited from the circulation Rather resident macrophages proliferate locally and polarise towards an M2 alternatively activated state upon parasitic infection [151]. In summary, M2 macrophages are anti-inflammatory macrophages specifically activated by IL-4/IL-13 cytokines in addition to parasitic infections. These cells have unique biological functions including tissue remodelling and mounting Th2 immune responses as a result of a unique transcriptional profile distinct from that of pro-inflammatory M1 macrophages.

1.12.3 Regulatory Macrophages and Hybrid activation states

Due to the highly plastic and adaptable nature of macrophages it is difficult to designate all macrophage polarisation states to the M1 and M2 classification system. Rather M1 and M2 represent two contrasting states in the emerging spectrum of macrophage activation. Furthermore this classification fails to account for the many hybrid macrophage populations which display overlapping and unique activation properties largely influenced by the variety of environmental specific stimuli they encounter *in vivo* [127, 135] (Figure 1.5).

Regulatory macrophages are immune regulatory cells that display both anti-inflammatory and pro-inflammatory features through suppression of some pro-inflammatory genes including TNF-α, IL-6 and IL-12 and increased production of IL-10 and TGF-β. In addition, these cells are highly phagocytic, antigen presenting macrophages however unlike M2 macrophages, these cells do not perform wound healing or tissue remodelling functions. Immune complexes in conjunction with TLR activation polarise macrophages into a regulatory state. In addition, other stimuli including glucocorticoids, prostaglandins and apoptotic cells have been implicated in regulatory macrophage polarisation. While regulatory macrophages are distinct from both M1 and M2 macrophages, these cells share some overlapping anti-inflammatory properties with M2 cells [127]. These three macrophage populations represent the main groups in the emerging spectrum of macrophage polarisation however many hybrid macrophage activation states exist owing to the large number of activation stimuli that macrophages encounter *in vivo*. Tumour associated macrophages, intestinal macrophages, placental macrophages, Kupffer cells and LPS tolerised macrophages are described as representing hybrid macrophage

populations which share overlapping M1/M2 and regulatory properties while expressing distinct features unique to their polarisation state and microenvironment. [135, 152-156].

Intestinal macrophages represent a unique macrophage population that does not belong to either the M1 or M2 groups. Intestinal macrophages display some feature of M2 activation including increased phagocytic capacity and reduced pro-inflammatory responses. Importantly, while intestinal macrophages display M2-like characteristics they are not M2 cells as the M2 polarising cytokines IL-4, IL-13 and IL-33 are in low abundance in the intestine [157]. Rather the intestinal microenvironment, composed of a variety of antigens and the microbial community, influences the polarisation of intestinal macrophages towards a hybrid M2-like immune regulatory state [131, 157]. LPS tolerant macrophages have been shown to display anti-inflammatory [158] properties including reduced bactericidal activity and increased phagocytic capacity. Furthermore pro-inflammatory responses are suppressed while anti-microbial peptides and pro-resolution factors are induced during this state [36, 153, 154]. Importantly, LPS tolerant macrophages are not M2 cells. M2 polarisation is mediated by IL-4 and the IL-13 pathway and is therefore distinct from LPS tolerance and TLR4 signalling [144, 152]. LPS tolerant macrophages display a hybrid regulatory phenotype which shares some features of M2 polarisation similar to that of intestinal macrophages. These different populations possess unique biological functions dependent on their specific environment; however they share many anti-inflammatory M2-like features.

1.13 Macrophage TLR tolerance

TLR tolerance is an essential immune homeostatic response in macrophages. As previously mentioned, LPS tolerance induces a global change in the gene expression profile of macrophages with suppression of pro-inflammatory genes including IL-6 and TNF-α, and up-regulation of anti-microbial peptides, anti-inflammatory cytokines and chemokines in addition to pro-resolution factors. Thus LPS tolerance induces a switch in macrophage polarisation from that of a M1 pro-inflammatory state to that of an anti-inflammatory activation state. LPS tolerant macrophages share some M2 properties including reduced cytotoxic and antigen presenting capacity but maintain increased phagocytic activity [36, 42, 135, 152-154] (Figure 1.6).

The plasticity of macrophages can have different outcomes depending on the local environmental requirements and activation stimuli that macrophages encounter. While an LPS tolerant state may limit excessive inflammation, maintenance of this state can have devastating consequences in cases of septic shock, cystic fibrosis and cardiovascular complications. Monocytes isolated from patients of these groups displayed reduced responsiveness towards *ex vivo* challenges with LPS as determined by pro-inflammatory cytokine production [159]. These cells remained locked in an LPS tolerant state and contributed to patient mortality due to the inability to respond to secondary infection. Interestingly patients who recovered from sepsis displayed responsiveness towards LPS upon LPS challenge *ex vivo* [159, 160]. Furthermore, monocytes isolated from cystic fibrosis patients also displayed a tolerant-like state with patient mortality linked to secondary infections [42]. In addition monocytes isolated from patients with acute coronary syndrome displayed an LPS tolerant phenotype [161]. This suggests that prolonged TLR tolerance is a

pathophysiological immunosuppressive state rather than a protective physiological immune response.

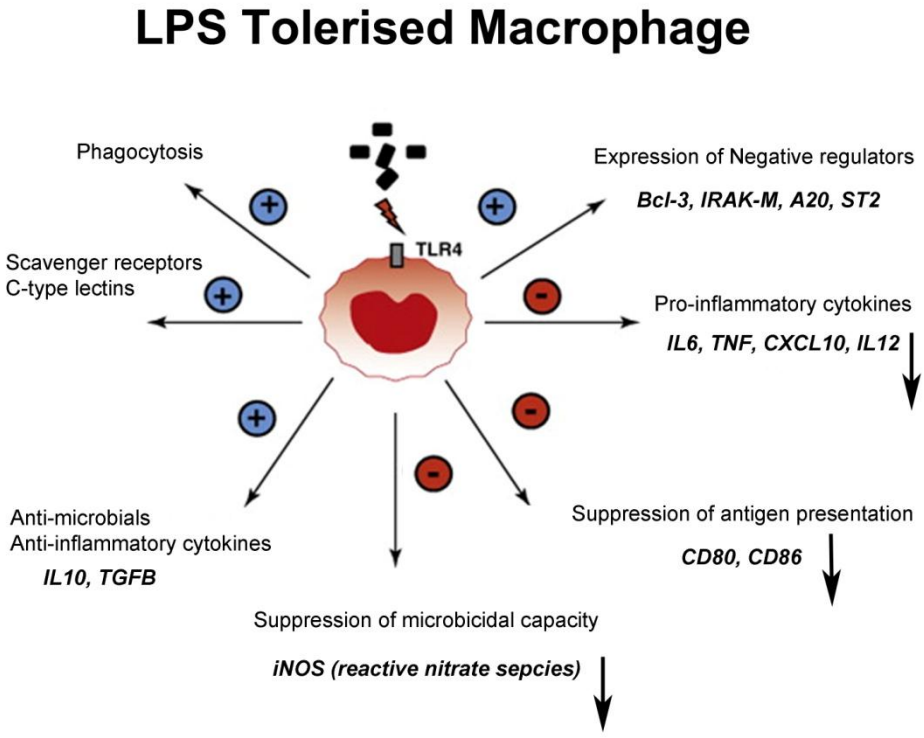

Figure 1.6 LPS tolerised macrophage

LPS tolerant macrophages are anti-inflammatory cells. Pro-inflammatory cytokines, antigen presenting markers and iNOS activity all illustrated in red are classical M1 features which are suppressed (-) in LPS tolerant macrophages. Increased expression of negative regulators of TLR signalling, anti-microbial peptides, anti-inflammatory cytokines and enhanced mediators of phagocytosis illustrated in blue are all inducible (+) properties of LPS tolerant macrophages . Adapted from *Biswas SK, 2009* [36]

TLR and microbial tolerance is also central to maintaining environment specific homeostasis. The gastrointestinal tract is home to the largest microbial community in humans, which does not lead to robust activation of the immune system. While multiple factors are involved in the regulation of the complex interplay between the host immune response and the intestinal microbial community, macrophages significantly contribute to this by adopting an anti-inflammatory tolerant state towards the local environmental stimuli which include the intestinal microbiota. This environment is enriched in the M2-like polarising cytokines IL-10 and TGF-β which contribute to generating an anti-inflammatory tolerant environment in the gut [131]. Furthermore these cells produce reduced amounts of pro-inflammatory cytokines upon TLR challenge [162]. In addition, the resident liver macrophage population, Kupffer cells adopt a unique tolerant-like phenotype specific to the liver microenvironment where they are exposed to numerous gut derived and environmental toxins under the normal physiologic conditions. Upon LPS challenge, induction of both pro-inflammatory and immunmodulatory responses control inflammation in this environment including increased arginase activity which inhibits TNF-α expression by Kupffer cells [163-165]. These two macrophage populations reside in environments where maintenance of tolerance is a physiological protection mechanism. Alcoholic liver disease, viral infections and inflammatory bowel disease (IBD) are all associated with a loss in the normal environmental tolerogenic state [158, 165-169]. Thus macrophage plasticity is central to their physiological and immunological functions. While maintenance of the resident macrophage population in anti-inflammatory tolerant states may be essential to certain environments, prolonged or inappropriate tolerance could have devastating consequences to the host post infection clearance.

1.14 Aims of thesis

Since the discovery of TLRs, extensive research has lead to the characterisation of the acute response to TLR activation. Furthermore, the necessity for strict control of these responses is evident by the numerous mechanisms of negative regulation of TLR signalling and TLR induced gene expression including TLR tolerance. The first aim of this study was to investigate the role of Bcl-3 in inflammation in the gut, an environment colonised by a large microbial community. Recently, a single nucleotide polymorphism (SNP) associated with reduced Bcl-3 gene expression has been identified as a potential risk factor for Crohn's disease [170]. Bcl-3 is an important anti-inflammatory factor and therefore we postulated that Bcl-3 may play a protective role in the gut to prevent intestinal inflammation. To test this theory, an *in vivo* approach was utilised to model intestinal inflammation using mice deficient in Bcl-3 [108] as illustrated in Chapter 3. An acute model of inflammation using the dextran sodium sulphate model of murine colitis was used in these studies as it has been shown to be highly reproducible, of short duration, technically straightforward and mimics aspects of human IBD [65, 171-174].

The second aim of this thesis was to investigate the transcriptional plasticity of TLR tolerance. Chapter 4 sets out to use a transcriptomics approach to investigate the plasticity of LPS tolerance in macrophages. The aim of this chapter was to first design a model of recovery from LPS tolerance in macrophages. Once the model was established microarray profiling and subsequent downstream bioinformatics analysis generated a gene expression profile of macrophages that recovered from LPS tolerance.

The final aim of this thesis was to characterise the functional outcomes of TLR tolerance plasticity. Chapter 5 represents a continuation of the previous chapter which provided transcriptional analysis of TLR tolerance and is based on an observed uncoupling of cytokine transcription and secretion in macrophages following TLR tolerance Here, cytokine secretion is examined in recovered macrophages by flow cytometry, cytokine intracellular trafficking by immunofluorescence, inhibitor studies and cytokine secretion by ELISA. In summary, this thesis utilised both *in vivo* and molecular approaches to provide in-depth analysis and characterisation of TLR tolerance plasticity.

2. Materials and Methods

2.1 Materials

All reagents were stored and prepared according to the manufacturer's guidelines.

2.1.1 Reagents

- Bovine serum albumin (BSA) (Sigma Aldrich Ltd. Dublin, Ireland)
- Bafilomycin A (Sigma)
- BD GolgiPlug (BD Biosciences, NJ, USA)
- Ca074me (Calbiochem/Merck KGaA, Darmstadt, Germany)
- Dextran Sodium Sulfate (DSS) 45 kDa (TdB Consultancy, Uppsala, Sweden)
- Dulbecco's modified eagles medium (DMEM) (Sigma Aldrich)
- DPX mounting medium (Sigma Aldrich)
- Ethylenediaminetetraacetic acid (EDTA) (Sigma Aldrich)
- Eosin (Sigma Aldrich)
- Goat serum (Dako Diagnostics, Dublin, Ireland)
- Harris haemotoxylin (Sigma Aldrich)
- Heat-inactivated foetal calf serum (FCS) (Gibco, Life Technologies, NY, USA)
- Histochoice clearing agent (Sigma Aldrich)
- Hoechst (Invitrogen, Life Technologies, USA)
- Human Tissue Array (Crohn's/Colitis) (Origene, Rockville, MD, USA)
- IL-1β (Peprotech, London, UK)
- L-Glutamine (Sigma Aldrich)

- Lipopolysaccharide K12 Ultrapure (LPS) (Invivogen, Toulouse, France)
- MDL28170 (Sigma)
- Monensin (Biolegend, San Diego, CA, USA)
- Non essential amino acids (Sigma)
- OCT compound (Tissue-Tek, Sakura, Finetek, USA)
- Pam3CSK4 (Invivogen)
- Paraformaldehyde (Sigma Aldrich)
- PBS (Sigma Aldrich)
- Penicillin/Streptomycin (Sigma)
- Pepstatin A (Sigma)
- Prolong gold antifade reagent (Molecular probes/ Invitrogen)
- Rat serum (Sigma Aldrich)
- SYBR safe DNA gel stain (Invitrogen)
- Trypan blue (Sigma Aldrich)
- Tween (Sigma Aldrich)
- Lightcycler 480 Probes Master mix (Roche Applied Sciences, West Sussex, UK)
- 5X Transcriptor Buffer (Roche)
- Deoxyribonucleotide triphosphate - dNTPs (Roche)
- Nuclease free water (Sigma)
- RNAse inhibitor (Roche)
- Random primers (Roche)
- Rneasy mini RNA isolation kit (Qiagen, Manchester, UK)
- Taqman gene expression assays (Life technologies, USA)
- Transcriptor reverse transcriptase enzyme (Roche)

2.1.2 Mice

Bcl-3$^{-/-}$C57BL/6 (B6) mice were generated as described previously [108, 111]. Bcl-3$^{-/-}$C57BL/6 (B6) male mice were generously provided for establishment of homozygous breeding by Professor Y. Chen (University of Pennsylvania, Philadelphia, Pennsylvania, USA). Wild-type (WT) C57BL/6 mice were purchased from Harlan laboratories, UK at 6 - 8 weeks of age. Atg16L1$^{-/-}$ female mice [175] (6 – 8 weeks) were provided by Dr Silvia Melgar for generation of bone marrow derived macrophage experiments. Bcl-3$^{-/-}$ and WT littermate controls were group housed in individually ventilated cages (IVC's), (OptiMice, Animal Care Systems, UK) with WT C57BL/6 mice housed in conventional mouse housing units under specific pathogen free (SPF) conditions. Standard housing and environmental conditions were maintained (temperature 21°C, 12 hours light and 12 hours darkness with 50% humidity). Animals were fed sterile standard pellet diet and water *ad libitum*. Animal husbandry and experimental procedures were approved by the University College Cork Animal Experimentation Ethics Committee (AEEC).

Table 2.1: Antibody Table

Target	Species	Clone	Host	Conjugate	Source
CD80	Mouse	B7-1	Hamster	FITC	eBiosciences
CD86	Mouse	GL1	Rat	APC	BD Biosciences
F4/80	Mouse	BM8	Rat	APC	eBiosciences
F4/80	Mouse	BM8	Rat	PE	eBiosciences
CD11b	Mouse	M1/70	Rat	PE	BD Biosciences
TNF	Mouse	MP6-XT22	Rat	PEcy7	BD Biosciences
CCR3	Mouse	83103	Rat	AF647	BD Biosciences
CD16/CD32	Mouse	2.4G2	Rat	N/A	BD Biosciences
TNF	Mouse	Polyclonal	Rabbit	N/A	Abcam
GM130	Mouse	35	Mouse	N/A	BD Biosciences
LAMP1	Mouse	1D4B	Rat	N/A	Santa Cruz
p65	Mouse	Polyclonal C20	Rabbit	N/A	Santa Cruz
p105/p50	Mouse	Polyclonal C19	Goat	N/A	Santa Cruz
RELB	Mouse	Polyclonal C19	Rabbit	N/A	Santa Cruz
cREL	Mouse	Polyclonal	Rabbit	N/A	Santa Cruz
ERK 1/2	Mouse	p44/p42	Rabbit	N/A	Cell signalling
Phospho ERK 1/2	Mouse	Thr202/Tyr204	Rabbit	N/A	Cell signalling
p38	Mouse	Polyclonal	Rabbit	N/A	Cell signalling
Phospho p38	Mouse	Thr180/Tyr182	Rabbit	N/A	Cell signalling
IRF5	Mouse	10T1	Mouse	N/A	Abcam
IRF4	Mouse	H140	Rabbit	N/A	Santa Cruz
HDAC	Mouse	H-51	Rabbit	N/A	Santa Cruz
B-actin	Mouse	AC-74	Mouse	N/A	Sigma
Bcl-3	Mouse + (H)	C14	Rabbit	N/A	Santa Cruz
Secondary	Rat	Whole Ab	Goat	Alexa 594	Molecular Probes
Secondary	Rabbit	Whole Ab	Gorat	Alexa 594	Molecular Probes
Secondary	Mouse	Whole Ab	Goat	Alexa 488	Molecular Probes
Secondary	Rat	Polyclonal	Goat	HRP	Dako Diagnostics
Secondary	Rabbit	Polyclonal	Rabbit	HRP	Dako Diagnostics
Secondary	Mouse	Polyclonal	Rabbit	HRP	Dako Diagnostics

Table 2.2: Oligonucleotide Primers and Universal probe Library probes

Gene Name	NCBI reference	Forward (5'-3')	Reverse (5'-3')	UPL probe
18s	NR_003278.3	aaatcagttatggttcctttggtc	gctctagaattaccacagttatccaa	**55**
IL6	NM_031168.1	tctaattcatatcttcaaccaagagg	tggtccttagccactccttc	**78**
TNF-α	NM_001278601.1	tcttctcattcctgcttgtgg	ggtctgggccatagaactga	**49**
IL1β	NM_008361.3	tgtaatgaaagacggcacacc	tcttctttgggtattgcttgg	**78**
CXCL10	NM_021274.2	gctgccgtcattttctgc	tctcactggcccgtcatc	**3**
CXCL1	NM_008176.3	agactccagccacactccaa	tgacagcgcagctcattg	**83**
NFIL3	NM_017373.3	gttacagccgccctttcttt	gagcctttcatgggttatcg	**32**
IL10	NM_010548.2	cagagccacatgctcctaga	gtccagctggtcctttgttt	**41**
IFNA5	NM_010505.2	gccttaaccctcctggtaaaa	tcctgtgggaatccaaagtc	**51**
BCL3	NM_033601.3	gaacaacagcctgaacatgg	tctgaccgttcacgttgg	**18**
IL17A	NM_010552.3	cagggagagcttcatctgtgt	gctgagctttgagggatgat	**28**
IL22	NM_016971.2	tttcctgaccaaactcagca	ctggatgttctggtcgtcac	**49**
CCL5	NM_013653.3	tgcagaggactctgagacagc	gagtggtgtccgagccata	**110**
IL33	NM_001164724.1	cacattgagcatccaaggaa	aacagattggtcattgtatgtactcag	**51**
BCL3	N/A	cggaagtgcttgacattgg	gtattgaccgattccttgcg	**N/A**
IL2	N/A	catacagaaggcgttcattg	tacctgtgtggcagaaagc	**N/A**

2.2 Methods

2.2.1 Genotyping

Bcl-3$^{-/-}$ and WT littermate control mice were ear clipped and genotyped upon weaning to confirm their genetic status. DNA was extracted by incubating the ear clip sample in a solution containing 0.2mM EDTA and 25mM NAOH for 45 minutes at 99ºC. The reaction was neutralised by addition of an equal volume of 40mM Tris-CL (pH 5). Bcl-3 deficiency was confirmed by measuring expression of the Bcl-3 targeting cassette construct which results in Bcl-3 becoming functionally inactive [108]. Homozygous Bcl-3$^{-/-}$ mice contain two copies of the Bcl-3 construct in comparison to the one copy for heterozygotes. WT mice contain no copy of the Bcl-3 cassette. Primers were designed to measure expression of the Bcl-3 construct compared with the IL-2 promoter control (Table 2.2). The genetic status of each mouse was determined by measuring the ratio of the Bcl-3 targeting construct to the IL-2 promoter followed by visualisation of amplified DNA on a 2% agarose gel containing SYBR safe DNA gel stain (Invitrogen). WT mice contain only the IL-2 promoter with heterozygotes containing both the Bcl-3 construct and the IL-2 promoter in a 1:1 ratio. All Bcl-3 deficient homozygous mice have a 2:1 Bcl-3 construct: IL-2 promoter ratio. All Bcl-3$^{-/-}$ and WT littermate controls were genotyped prior to breeding and experimental usage.

2.2.2 DSS induced colitis – an acute model of colonic inflammation

Mice were administered dextran sodium sulphate (DSS) (45 kDa) *ad libitum* in their drinking water to induce colitis as previously described [176]. 1%, 2% and 2.5% DSS solutions were prepared freshly and administered on a daily basis for six days

followed by administration of water only from day six to eight to induce acute disease. Body weight, stool consistency and posture/fur texture were recorded daily to determine the daily disease activity index (DAI). DAI scoring was assessed blinded with a maximum score of 10 as previously described [176, 177]. DAI scoring combined scoring from weight loss (% change) 0 – 4, stool consistency 0 – 4 and posture/fur texture 0 – 2 (Table 2.3). Mice were sacrificed at day 8 with colons removed from anus to caecum and washed in PBS. Colons were measured, cut longitudinally and divided into the distal and proximal colon segments. Both proximal and distal colons were weighed and processed for histology, protein and gene expression analysis according to sample requirements. Distal colon samples were further divided into three segments with one snap frozen in liquid nitrogen for protein analysis. For histological analysis a segment of distal colon was rolled in a "swiss roll", embedded in optimal cutting temperature (OCT) compound (Tissue-tek) and snap frozen with liquid nitrogen. The final distal colon segment was transferred in to 1ml of RNA later (Sigma) and snap frozen with liquid nitrogen. All samples were stored at -80ºC until required for analysis

Table 2.3: Daily disease activity Index scoring system (DAI)

Score	Weight loss	Stool consistency	Fur/posture
0	No change	No change	No change
1	1-3% weight loss	Minor change	Mildly hunched
2	3-6% weight loss	Loose stool	Hunched & reduced movement
3	6-9% weight loss	Loose stool & rectal bleeding	-
4	>9% weight loss	Diarrhoea & rectal bleeding	-

2.2.3 Colon histology

2.2.3.1 Tissue Sectioning

Distal colons (3cm) were cut longitudinally into three sections with one rolled in a "swiss roll" for histological analysis as described in section 2.2.2. Frozen sections were cut using a Leica CM1900 cryostat (Leica Microsystems, Ireland) and allowed to air dry prior to staining. Alternatively, frozen sections were stored at -80ºC until required for tissue staining.

2.2.3.2 Haematoxylin and Eosin tissue staining

Frozen distal colonic sections (6μm) were fixed in an ice cold acetone/ethanol 3:1 solution and stained with haematoxylin and eosin according to standard histological staining procedures. Briefly, distal colon sections were stained with Harris haematoxylin for 10 minutes, washed in running tap water for 5 minutes and differentiated in 1% acid alcohol for 30 seconds. Sections were then stained with eosin for 30 seconds prior to dehydration steps through increasing ethanol concentrations. Sections were then incubated with histochoice clearing reagent (Sigma), allowed to air dry followed by mounting with DPX mounting media (Sigma). Stained sections were allowed to dry overnight prior to histological analysis. Stained sections were analysed using an Olympus BX51 camera and Cell F software (Olympus, Germany). Images captured are representative of greater than seven fields of view at 20X magnification per mouse. Histological scoring was performed in a blinded fashion. Scoring of tissue damage was quantified as previously described with a maximum combined score of 12 [177, 178] as follows: 0 – no infiltration, no injury, no crypt damage; 1 - minor infiltration, mucosal injury, damage at crypt base; 2 – moderate infiltration (foci formation), mucosal and sub

mucosal injury, damage at crypt base and centre; 3 – severe infiltration, transmural injury, only epithelium intact; 4 – loss of whole crypt and epithelium (Table 2.4).

Table 2.4: Colon histological scoring (H&E)

Injury	Cell infiltration	Extent of Injury	Crypt Damage
0	No change	No change	No Change
1	Minor	Mucosal	Base
2	Moderate (Foci formation)	Mucosal & Submucosal	Base and centre
3	Severe (loss of architecture)	Transmural	Only epithelium intact
4	-	-	Crypt and epithelium loss

2.2.4 Cell culture

2.2.4.1 L929 cell culture

The L929 fibroblast cell line NCTC clone 929 [L cell, L-929, derivative of Strain L] (ATCC® CCL-1™) was cultured to provide a source of the growth factor M-CSF used for the differentiation of macrophages from bone marrow. Murine L929 fibroblasts were seeded in tissue culture flasks with Dulbecco's Modified Eagles Medium (DMEM), 10% foetal bovine serum (FBS), 1% penicillin/streptomycin and 1% L-glutamine (Sigma) and grown to confluency in a T175 tissue culture flask. Cells were maintained at 37ºC in a humidified environment with 5% CO_2. Confluent L929 fibroblasts were incubated with 50ml of L929 culture media for a further 7 days to allow for production and secretion of M-CSF by the cells. After 7 days the supernatants were removed and filter sterilised, aliquoted and stored at -80°C until required. L929 fibroblasts were passaged by mechanical disruption using a cell scraper and re-seeded in a T175 tissue culture flask. Every 7 days after the cells reached confluency supernatants were removed and stored as described. L929 fibroblast cell line stocks were cryopreserved in FCS supplemented with 10% DMSO at a cell density of 2 x 10^6/ml.

2.2.4.2 Murine bone marrow isolation

Bone marrow was isolated from female C57BL/6 and Atg16L1$^{-/-}$ mice at 6 - 8 weeks old for generation of primary bone marrow derived macrophages (BMDM) *in vitro*. Mice were sacrificed by cervical dislocation with both hind legs removed at the hip joint. Excess tissue was removed from the femur and tibia bones and then cleaned in 1X sterile PBS and 70% ethanol. Using a 21 gauge needle and syringe bone marrow was isolated by flushing ice cold sterile PBS through the femur and tibia bones and

collected in a 50 ml falcon tube. Isolated bone marrow was re-suspended to generate a single cell suspension and passed through a 70μM cell strainer to remove any debris. The bone marrow suspension was washed twice in BMDM culture media (DMEM, 10% FBS, 1% penicillin/streptomycin, 1% L-glutamine, 1% non-essential amino acids), and centrifuged at 4°C at 300 x g for 5 minutes. Bone marrow was cryopreserved in foetal calf serum (FCS) supplemented with 10% DMSO until required for use.

2.2.4.3 Bone Marrow derived Macrophage (BMDM) differentiation

Bone marrow was cultured following isolation or from cryopreserved stocks in BMDM culture media supplemented with 30% L929 conditioned media for seven days. The cells were cultured on sterile non tissue culture treated petri dishes. On day 3 BMDM differentiation media was removed and replaced with fresh differentiating BMDM culturing media with any non-adherent cells removed at this stage. Adherent monocytes/macrophage progenitors differentiated into BMDMs by day 7. Differentiated BMDMs were removed from the petri dishes by incubating the cells with 5mM EDTA in sterile PBS at 37°C for 5 minutes. Cells were collected and washed twice in BMDM culture media at 4°C for 5 minutes at 300 x g, re-suspended in BMDM culture media and transferred to tissue culture treated dishes for downstream experimental use. The purity of BMDMs was assessed by flow cytometry and was typically greater than 95% F4/80 positive.

2.2.4.4 Peritoneal Macrophage isolation

Peritoneal macrophages were isolated from C57BL/6 female mice (6 – 8 weeks). Macrophages were recruited to the peritoneal cavity by administration of 1ml of sterile 4% thioglycollate to mice via intraperitoneal injection. Three days post i.p

injection recruited macrophages were isolated by peritoneal lavage. Mice were euthanized using CO_2 to ensure the peritoneal cavity remained intact. Briefly, 10ml of ice cold sterile PBS was injected into the peritoneal cavity. The peritoneal cavity was gently massaged to allow cells to be collected and withdrawn from the cavity. Collected cells from three mice were pooled, passed through a 70μM cell strainer (BD Biosciences) and centrifuged at 4°C for 5 minutes at 300 x g. Isolated peritoneal cells were plated in tissue culture dishes overnight to allow for adherence of macrophages. Non-adherent cells were removed prior to experimental use. The purity of the population was measured by flow cytometry using CD11b and F4/80 double positive staining.

2.2.5 LPS Tolerance Recovery Model

BMDM were differentiated for 7 days in BMDM differentiating media, removed from petri dishes and washed in BMDM culture media as described in section 2.2.4.3. Cells were quantified using trypan blue exclusion dye and a Neubauer haemocytometer counting chamber. Roughly 2 x 10^8 BMDMs were derived from the femurs and tibias of three C57BL/6 mice at 6 - 8 weeks of age. BMDMs were seeded at various densities in tissue culture dishes for experimental treatment.

LPS tolerance was induced in BMDMs by stimulating cells for 8 hours with 100ng/ml ultrapure LPS-EK (K12) (Invivogen). After 8 hours the media was removed and the cells were washed twice with sterile PBS. The cells were allowed to rest and recover in fresh BMDM culture media for a further 16 hours before a second stimulation with LPS was given. These cells were described as being LPS tolerised macrophages (T). Recovery from LPS tolerance (R – recovered macrophage) was achieved by inducing LPS tolerance in BMDMs as described, however the period of

rest and recovery with the fresh culture media extended beyond 16 hours to that of 64 to 136 hours (2 to 4 days) before they received a second challenge with LPS. All data including transcriptional profiling experiments were performed on macrophages rested for three days prior to re-stimulation (Recovery – R) as determined by recovery time optimisation experiments. Additional analysis of recovery from LPS tolerance on day 2 and day 4 is specified within the text where appropriate. The acute LPS response group (A) received a single LPS stimulation for 1, 4, 8 or 24 hours depending on protein or gene expression analysis requirements. Macrophages that received no stimulation with LPS were described as Naïve macrophages (N). LPS tolerant and recovered macrophages received a second challenge of LPS for 1, 4, 8 or 24 hours depending on protein or gene expression analysis requirements.

2.2.6 Gene expression analysis

2.2.6.1 RNA isolation

BMDMs were washed twice in cold 1X PBS and removed from tissue culture dishes by mechanical disruption using a cell scraper. The cell suspension was centrifuged at 4°C for 5 minutes at 300 x g with RNA isolated using the RNeasy mini RNA isolation kit (Qiagen) according to the manufacturer's guidelines. Briefly, supernatants were discarded and the cell pellet was lysed in RLT lysis buffer containing 10% β-mercaptoethanol (Sigma). The lysates were homogenised using Qiashredders (Qiagen) and total RNA was extracted using the RNeasy mini kit with an optional DNase step included using the RNase free DNase kit (Qiagen).

Distal colon tissue samples were stored at -80ºC in RNA-later to preserve RNA integrity. Samples were thawed on ice, removed from RNA-later and transferred to magNALyser green bead tubes (Roche) and homogenised using the magNALyser

homogeniser three times for 15 seconds at 6500 x g (Roche). Colonic tissue was homogenised in RLT lysis buffer (Qiagen) with homogenised samples centrifuged for 5 minutes at 4°C at 200 x g. RNA was isolated using the RNeasy mini kit according to the manufacturer's guidelines. RNA purity and quantification was measured using a nanodrop ND1000 spectrophotometer (Thermo Scientific) and stored at -80°C until required. All work was performed under nuclease free conditions.

2.2.6.2 Complementary DNA (cDNA) Synthesis: RT-PCR

1µg total RNA was used to synthesise complementary DNA (cDNA) with random hexamer primers using Transcriptor Reverse Transcriptase (Roche). Briefly, the reverse transcription reaction mix was incubated for 10 minutes at 25°C to allow efficient annealing of random primers. This was followed by incubating the reaction at 55°C for 30 minutes. The reaction mix was finally incubated at 85°C for a final 5 minutes to inactivate the enzyme (Table 2.5). Synthesised cDNA was diluted with nuclease free water in a 1:5 dilution. Two negative controls were included in each RT-PCR reaction. A no RT control (reverse transcriptase enzyme) was included which contained RNA and all the reaction mix except the enzyme. A second negative control contained the reverse transcriptase enzyme however RNA was not included to determine non specific DNA amplification. cDNA was stored at -20°C until required for experimental use.

2.2.6.3 Quantitative/ Real Time PCR (qRT-PCR)

Gene expression was measured by quantitative real time PCR (qRT-PCR) using the LightCycler 480® (Roche) in combination with the Universal Probe Library system (Roche) (Table 2.6). Primers sequences and corresponding probes can be found in

Table 2.2. Gene expression was measured from triplicate wells with mRNA levels made relative to the housekeeper gene 18s ribosomal RNA (rRNA). Human tissue arrays (Crohn's/Colitis cDNA Array, Origene) were used to measure Bcl-3 expression. Gene expression was measured using the LightCycler 480 system in combination with Taqman gene expression assay for Bcl-3 (Applied Biosystems). Gene expression changes were calculated using the $2^{-\Delta\Delta CT}$ method [179] and represented as relative mRNA.

Table 2.5: cDNA synthesis – Reaction master mix

cDNA Master Mix	Volume (1 reaction)
5X Transcriptor Buffer	5µl
RT enzyme (500 Units)	0.5µl
RNase Inhibitor (2000 Units)	0.5µl
Random primers (200ng/µl)	3µl
dNTP mix (10mM each)	1µl
Nuclease free water	Max 10µl – sample dependent
1µg Total RNA	Volume – sample dependent
Total Volume	**20µl**

Table 2.6: qRT-PCR reaction master mix

qRT-PCR Master Mix	Volume (1 reaction)
Lightcycler® 480 Enzyme mix	5µl
Forward primer (10mM)	0.5µl
Reverse primer (10mM)	0.5µl
Probe (UPL) (10mM)	0.1µl
Nuclease free water	1.9µl
cDNA (1:5 dilution)	2µl
Total volume	**10µl**

2.2.7 Microarray profiling

Total RNA was isolated using the RNeasy mini kit (Qiagen) with all samples DNase treated as described in section 2.2.6.1. RNA quantification and purity were measured using the Nanodrop ND1000 spectrophotometer (Thermo Scientific). Triplicate biological replicate samples submitted for microarray profiling met all sample submission criteria (Beckman Coulter Genomics, NC, USA). Briefly, 200ng of total RNA was fluorescently labelled with Cy3 nucleotides. Labelled RNA (cRNA) was hybridised to Agilent mouse 8 x 60K microarrays (Agilent-028005). Hybridised arrays were washed and scanned and data extrapolated for downstream bioinformatics analysis. Each experiment is representative of BMDM derived from bone marrow pooled from three mice.

2.2.8 Bioinformatics

All data processing was carried out using Bioconductor packages [180] in the R software environment with the data background corrected using Limma package [181]. The data was then corrected for batch effects using the ComBat script [182]. The corrected data was then normalised between arrays using quantile normalisation [181]. Differentially expressed genes were found using the Limma package [181]. These genes were then corrected for multiple testing using the Benjamini-Hochberg method. Data was corrected with an adjusted p-value cut off of $p<0.05$ and a 1.5 fold change. Further bioinformatics analysis was performed using DAVID [183] to perform gene ontology and pathway analysis. Gene expression changes and gene expression trends were visualised by hierarchical and *K* means clustering using Genesis software [184]. Gene expression profiling was independently validated by real time quantitative PCR (qRT-PCR). Gene expression profiling data (GSE47783)

has been deposited in the National Center for Biotechnology Information Gene Expression Omnibus database (http://www.ncbi.nlm.nih.gov/geo/query/acc.cgi?token=bxoxxisyouyoulw&acc=GSE47783). Transcriptional profiling of Crohn's disease and Ulcerative Colitis tissue was performed using a dataset of sigmoid biopsy patient samples published by *Costello et al*. (GEO dataset ID GDS1330) [185] (Crohn's disease n = 10, Ulcerative Colitis n = 10, normal controls n = 11).

2.2.9 Western blotting

Cells were initially washed in ice cold PBS to remove any remaining stimuli followed by removal of cells from tissue culture treated dishes using a cell scraper. Cells were transferred into ice cold PBS and washed twice by centrifugation at 300 x g for 5 minutes at 4°C. Total protein was isolated from both BMDMs and distal colonic tissue samples by lysing the cell pellet or tissue sample in radio-immunoprecipitation assay (RIPA) buffer (150 mM NaCl, 50 mM Tris-Cl, pH 7.4, 1% NP-40, 0.25% sodium deoxycholate, 1mM Na_3VO_4, 1mM EDTA) supplemented with a protease and phosphatase inhibitor cocktail (Sigma). Cells were lysed for 30 minutes on ice followed by centrifugation at 14000 x g for 10 minutes to remove cellular debris. Supernatants were removed and stored at -20ºC until required.

Cytoplasmic and nuclear proteins were isolated from cells using the nuclear extract kit (Active Motif, Carlsbad, CA, USA). Briefly, cells were washed with 5ml of an ice-cold PBS/Phosphatase inhibitor solution and removed from the dishes by mechanical disruption using a cell scraper. Cytoplasmic protein was isolated by re-suspending the cell pellet in a 1X hypotonic solution for 15 minutes on ice followed

by addition of detergent. The cell suspension was centrifuged at 4°C for 30 seconds at 14000 x g. Supernatants containing cytoplasmic proteins were removed and stored at -80°C. The pellet was re-suspended in a nuclear lysis solution for 30 minutes shaking gently followed by centrifugation of the nuclear lysates at 4°C for 10 minutes at 14000 x g. Supernatants containing nuclear protein were removed and stored at -80°C.

Distal colon tissue samples were washed in PBS and snap frozen with liquid nitrogen. Tissue samples were thawed and transferred to magNA Lyser green bead tubes (Roche) and homogenised using the Magna lyser instrument three times for 15 seconds at 6500 x g (Roche) in RIPA lysis buffer supplemented with a protease and phosphatase inhibitor cocktail (Sigma). Homogenised tissue lysates were centrifuged at 14000 x g for 10 minutes to remove cellular debris. Distal colon lysates were stored at -20ºC until required for use.

Protein concentration quantification was measured for all protein samples using the Bio-Rad protein assay solution (Bio Rad, Hertfordshire, UK) with absorbance measured at 595nm using an absorbance plate reader. 30µg of protein from each sample was resolved by SDS-polyacrylamide gel electrophoresis (SDS-PAGE), transferred to methanol activated polyvinyl difluoride (PVDF) membrane (Millipore Billerica, MA, USA) and incubated for antibodies of interest according to manufacturer's guidelines (Table 2.1). Membranes were incubated with horseradish-peroxidise (HRP) labelled secondary antibodies (1:1000) for 1 hour at room temperature. Membranes were analysed by electrochemiluminescence detection using Super Signal® West Dura Extended Duration kit (Thermo Scientific, USA).

2.2.10 Electrophoretic mobility shift assay (EMSA)

Nuclear protein was isolated as described above using the nuclear extract kit (Active Motif). NF-κB consensus double stranded oligonucleotides (5'AGTTGAGGGGACTTTCCCAGG-3') were purchased from Santa Cruz Biotechnology (Santa Cruz, CA). 10μg of nuclear protein was incubated with the NF-κB consensus probe for 15 minutes at room temperature in a 25μl binding reaction containing 1μg/μl Poly dI:dC (Roche), Ficoll (Sigma), DTT, orange G and 10X EMSA buffer (10mM HEPESKOH (pH7.9), 50mM KCL, 2.5mM MgCl2, 1mM DTT, 40μg/ml BSA). The reaction was resolved in the dark on a 5% non-denaturing polyacrylamide gel running at 300 Volts for 3 hours at 4°C in 0.5X TBE buffer. The gel was visualised using the Odyssey Infrared Imager system and Odyssey software (Li-Cor Biosciences, USA).

2.2.11 Cytokine and Chemokine secretion

2.2.11.1 ELISA/MSD

BMDM were plated in 96 well flat bottom tissue culture plates at a cell density of 0.6 x 10^5 / well. Each time point was performed in triplicate with supernatants removed at specific time points for cytokine and chemokine measurement; TNF-α (8 hours), IL-6, IL-12p70, CXCL1, RANTES and IL-10 (24 hours). For secretion experiments, BMDMs were re-stimulated with LPS for 8 or 24 hours in the presence or absence of additional inflammatory ligands including IL-1β (10ng/ml), Pam3CSK4 (100ng/ml), CpG (1μM), IFN-γ (50ng/ml) and CD40L (10μg/ml). BMDMs were also re-stimulated in the presence or absence of Bafilomycin A (1μM) in addition to intracellular enzymatic inhibitors including pepstatin A (10μM), ca074me (10μM) and MDL28170 (10μM) for 8 hours during LPS re-stimulation for

inhibitor experiments. Secretion was measured using murine Meso Scale Discovery (MSD) tissue culture single spot plates in conjunction with the electrochemiluminescence system Sector 2400 imager from Meso Scale Discovery (Gaithersburg, MD). Cytokine and chemokine secretion was measured in pg/ml.

2.2.11.2 Cytokine antibody array

BMDM were seeded in 6 well plates at 2 x 10^6/ well. Supernatants after 24 hours LPS re-stimulation were removed following experimental treatment (24 hours) and stored at -80ºC until required. Supernatants were incubated on mouse cytokine arrays for 32 cytokines (Ray Biotech, Inc, USA) according to manufacturer's guidelines Cytokine arrays were visualised and captured using electrochemiluminescence HRP detection (Appendix 2).

2.2.12 Flow cytometry

2.2.12.1 Surface staining

Macrophages were surface stained with a panel of antibodies (Table 2.1) with expression measured using the C6 Accuri Flow cytometer (BD Bioscience). Macrophages were removed from tissue culture dishes following experimental conditions and washed three times in ice cold staining buffer composed of 1X PBS, 0.5% BSA, 1% FBS and 0.1% sodium azide (Sigma). Cells were incubated with CD16/CD32 (Fc Block - 1μg/10^6 cells) antibody for 15 minute to block non-specific binding of antibodies to the Fc receptors on macrophages. Cells were surface stained in the dark on ice for 30 minutes, washed in staining buffer three times and re-suspended in running buffer (1X PBS, 1mM EDTA, 0.5% BSA) prior to analysis on the flow cytometer. Data was controlled for using isotype and by fluorescence minus

one (FMO) controls. Data was analysed using FCS express flow cytometry software (De Novo Software, Los Angeles, CA).

2.2.12.2 Intracellular staining

To stain for intracellular cytokines, macrophages were initially stimulated in combination with Golgi plug (Brefeldin A) at 1μg/10^6 cells (BD Bioscience). To stain for TNF-α intracellularly, cells were stimulated for 8 hours with LPS and Brefeldin A. Cells were removed from tissue culture treated dishes and washed in staining buffer as described above. Cells were also incubated with Fc block to block non-specific binding to the Fc receptors. Following surface staining (if applicable), cells were fixed and permeablised using the Cytofix/Cytoperm^{TM} kit (BD Biosciences) according to the manufacturer's guidelines. Briefly cells were fixed and permeabilsed for 20 minutes in the dark on ice with FIX/Perm buffer, washed twice in 1X FIX/Perm wash buffer and incubated with the intracellular cytokine antibody for 30 minutes on ice in the dark. After intracellular staining, the cells were washed three times in 1X FIX/Perm wash buffer and re-suspended in flow cytometry running buffer prior to analysis. Data was controlled for using isotype and by fluorescence minus one (FMO) controls. Mean fluorescence intensities were calculated from three independent experiments. Data was analysed using FCS express flow cytometry software (De Novo Software).

2.2.13.3 Assessment of phagocytosis

BMDM were seeded at 5x10^5 per well in a 24 well plate with cells treated according to experimental requirements. The phagocytic capacity of cells was measured using pHrodo *E.coli* bioparticles (molecular probes). Briefly, pHrodo *E.coli* bioparticles were incubated with each macrophage group for 3 hours in the dark at 37°C

according to the manufacturer's protocol. After incubation, the bioparticles were removed and the cells were vigorously washed in ice cold PBS three times. Phagocytosis was measured by flow cytometry using the FL2/PE channel of the Accuri C6 flow cytometer (BD Biosciences).

2.2.14 Immunofluorescence staining

2.2.14.1 Distal Colon tissue Immunofluorescence staining

Frozen colonic sections (6μm) were fixed in an ice cold acetone/ethanol 3:1 solution and incubated with blocking buffer (10% rat/mouse/goat serum, 5% fish gelatine, 0.05% Tween-20, 1% BSA, 0.1% sodium azide) for 45 minutes at room temperature. Distal colon sections were incubated with directly conjugated anti mouse antibodies specific to the protein of interest (Table 2.1) and counterstained with Hoechst 1μg/ml (Molecular Probes). Stained tissue sections were mounted with Prolong Gold antifade mounting medium (Molecular probes) and visualised using a fluorescence microscope (Olympus BX51, Olympus, Germany). Fluorescence images were captured using Cell F software (Olympus). Images captured are representative of greater than seven fields and 10 fields of view at 20X and 40X magnification respectively per mouse. Quantification was performed on greater than 10 fields of view per tissue section at 100X magnification. Quantification was performed on all mice per group.

2.2.14.2 TUNEL

The extent of apoptosis in distal colonic tissue was measured by terminal deoxynucleotidyl transferase-mediated deoxyuridine triphosphate nick end labelling (TUNEL). Frozen distal colon sections (6μm) were thawed at room temperature and

initially incubated with 3% hydrogen peroxide (Sigma) and a 4% DEPC (Sigma) solution to eliminate background fluorescence from both peroxidase and endonuclease enzyme activity in the tissue. The colon sections were incubated for one hour in a reaction using Terminal Deoxynucleotidyl Transferase (Promega) and Fluorescein 12 - dUTP (Roche) at 37ºC. Nuclei were counterstained with Hoechst 1μg/ml (Molecular Probes). Stained distal colon sections were imaged and analysed using a fluorescence microscope (Olympus BX51, Olympus, Germany) and Cell F software (Olympus). Images captured are representative of greater than seven fields of view at 20X magnification per mouse. Quantification of TUNEL positive cells was performed in a blinded manner on greater than 10 fields of view per tissue section at 100X magnification. Quantification was performed on all mice per group.

2.2.14.2 BMDM Immunofluorescence staining

BMDM were seeded in 12 well tissue culture dishes with inserted sterile glass coverslips at a density of 0.8 x 10^6 per well. BMDM were allowed to adhere overnight prior to experimental treatment. For immunofluorescence inhibitor experiments, BMDMs were re-stimulated with LPS for 1.5 hours in the presence or absence of intracellular enzymatic inhibitors including pepstatin A (1μM), ca074me (10μM) and MDL28170 (10μM). BMDMs were also re-stimulated with Bafilomycin A (1μM) and monensin (2μg/10^6 cells) for 1.5 hours during LPS re-stimulation for immunofluorescence analysis. At the experimental endpoint, cells were fixed in 3% paraformaldehyde for 15 minutes followed by quenching of free aldehyde groups using 50mM ammonium chloride (NH_4Cl) for an additional 15 minutes. BMDMs were permeabilsed in permeabilisation buffer (PBS, 2% BSA, 0.05% saponin. Primary antibody and secondary antibody (Table 2.1) incubation steps were carried

out in a humidified chamber in the dark at room temperature. Cells were incubated with anti-TNF-α (1:200) and anti-GM130 (1:4000) for 1 hour and washed twice in permeabilisation buffer. Coverslips were then incubated with anti rabbit and anti mouse secondary antibodies (1:400) in addition to the DAPI nuclear stain for an additional hour at room temperature. All antibodies were diluted in 5% FBS/PBS. Coverslips were mounted onto glass slides with mowiol and dried over night prior to imaging. Fluorescence images were captured using a Nikon Digital Sight DS Fi1C camera (Nikon) and NIS element software (Nikon). Images captured are representative of greater than 10 fields of view / sample at 100x magnification. Quantification was performed in a blinded manner on greater than 10 fields of view per sample at 100X magnification. Quantification of GM130 and TNF-α co-localisation is represented as percentage co-localisation per field of view at 100X magnification. Quantification was performed on triplicate experiments.

2.2.15 Statistical analysis

Statistical analysis was determined using one-way ANOVA/ two-way ANOVA with post hoc analysis (Tukey's post hoc test and Bonferroni post hoc test). qRT-PCR expression data was calculated using the $2^{-\Delta\Delta CT}$ [179] followed by unpaired and Mann Whitney U Test or one–way ANOVA with Tukey's post hoc test to compare differences between groups. Statistical analysis was performed using GraphPad software, (San Diego, CA, USA). Data is represented by mean ± SEM with $p<0.05$ considered statistically significant.

3. Bcl-3 deficiency protects against DSS-induced colitis in the mouse

3.1 Abstract

Bcl-3 is a member of the IκB family of proteins and is an essential negative regulator of Toll-like receptor induced responses. Recently, a single nucleotide polymorphism associated with reduced Bcl-3 gene expression has been identified as a potential risk factor for Crohn's disease. Here we report that in contrast to the predictions of SNP analysis, patients with Crohn's disease (CD) and Ulcerative Colitis (UC) demonstrate elevated Bcl-3 mRNA expression relative to healthy individuals. To further explore the potential role of Bcl-3 in inflammatory bowel disease (IBD) we used the dextran-sodium sulphate (DSS) induced model of colitis in Bcl-$3^{-/-}$ mice. We found that Bcl-$3^{-/-}$ mice were less sensitive to DSS-induced colitis compared to wild type controls and demonstrated no significant weight loss following treatment. Histological analysis revealed similar levels of oedema and leukocyte infiltration between DSS treated wild type and Bcl-$3^{-/-}$ mice but showed that Bcl-$3^{-/-}$ mice retained colonic tissue architecture which was absent in wild type mice following DSS treatment. Analysis of the expression of the pro-inflammatory cytokines IL-1β, TNF-α and IL-6 revealed no significant differences between DSS-treated Bcl-$3^{-/-}$ and wild type mice. Analysis of intestinal epithelial cell proliferation revealed enhanced proliferation in Bcl-$3^{-/-}$ mice which correlated with preserved tissue architecture. Our results reveal that Bcl-3 has an important role in regulating intestinal epithelial cell proliferation and sensitivity to DSS induced colitis which is distinct from its role as a negative regulator of inflammation.

3.2 Introduction

The nuclear factor (NF)-κB transcription factor family controls the inducible expression of more than 500 genes, including cytokines, chemokines and regulators of cell survival and proliferation [186, 187]. The dual role of NF-κB as a key regulator of inflammation and cell survival makes it a critical factor in the pathogenesis of chronic diseases such as inflammatory bowel disease (IBD). Increased NF-κB activation is observed in the mucosa of IBD patients and the requirement for NF-κB for the expression of pro-inflammatory cytokines supports a contributory role for NF-κB in IBD [188, 189]. Indeed, in the IL-$10^{-/-}$ mouse model of colitis, increased activation of NF-κB in myeloid cells is critical for the development of disease, while mice lacking CYLD or A20, two important negative regulators of NF-κB, show increased sensitivity to dextran-sodium sulphate (DSS)-induced colitis [51, 189-191]. Moreover, the pharmacological inhibition of NF-κB by anti-sense oligonucleotides or inhibitory peptides can prevent DSS-induced colitis in mice [192].

Genetic studies have identified an equally important role for NF-κB in maintaining the homeostasis of the intestinal epithelium. Mice lacking NF-κB essential modulator (NEMO) in intestinal epithelial cells ($NEMO^{\Delta IEC}$) develop spontaneous and severe colitis resulting from elevated intestinal epithelial cell apoptosis [189, 193]. A similar phenotype is observed in mice lacking both the IKKα and IKKβ subunits in intestinal epithelial cells ($IKK\alpha\backslash\beta^{\Delta IEC}$) and mice lacking the NF-κB subunit RelA in intestinal epithelial cells are hypersensitive to DSS-induced colitis [189, 194]. Toll-like receptors (TLRs) are the key sensors of microbial products in innate immunity and are critical in initiating NF-κB activation in intestinal epithelial

cells. Thus, mice lacking MyD88, a key component downstream of a number of TLRs, are also hyper-responsive to DSS-induced colitis [24, 195]. Together these studies indicate that while NF-κB activity is critical for inflammation in IBD, NF-κB activity in the epithelium is critical for tissue homeostasis and its inhibition can have severe consequences including the development of IBD. Thus a further understanding of the regulation of NF-κB during inflammation in the intestine and the contribution of components of the NF-κB pathway to inflammation and epithelial proliferation in the mucosa, are critical for the development of effective therapies for IBD.

Bcl-3 is a member of the IκB family of proteins as determined by sequence homology and the presence of ankyrin repeat domains which mediate interaction with NF-κB dimers [108, 196, 197]. Bcl-3 is largely a nuclear protein and only binds homodimers of the p50 or p52 NF-κB subunits [197]. Interestingly, these two subunits lack a transactivation domain and thus have generally been regarded as repressors of NF-κB transcription when present in the homodimeric form. Bcl-3 is an essential negative regulator of TLR induced responses. Bcl-$3^{-/-}$ macrophages and mice are hyper-responsive to TLR stimulation and are defective in lipopolysaccharide tolerance [111]. Recently, a single nucleotide polymorphism (SNP) associated with reduced Bcl-3 gene expression has been identified as a potential risk factor for Crohn's disease [170]. However, the role of Bcl-3 in IBD has not been investigated to date.

In this chapter the regulation of gut homeostasis by Bcl-3 is analysed using a murine acute model of intestinal inflammation. Measurements of Bcl-3 mRNA in patient groups with Crohn's disease (CD), Ulcerative Colitis (UC) and healthy control

individuals reveal elevated Bcl-3 expression associated with IBD, in contrast to the predictions of the SNP analysis [170]. To further explore the potential role of Bcl-3 in IBD we used the DSS-induced model of colitis in Bcl-$3^{-/-}$ mice. Considering the previously described anti-inflammatory role of Bcl-3 as a negative regulator of cytokine expression and an inducer of TLR tolerance [111], we were surprised to find that Bcl-$3^{-/-}$ mice were less sensitive to DSS-induced colitis. Measurement of the inflammatory response in the colon by analysis of the expression levels of pro-inflammatory cytokines and the recruitment of T-cells, neutrophils, macrophage and dendritic cells, revealed no significant differences between DSS-treated Bcl-$3^{-/-}$ and wild type mice. Analysis of intestinal epithelial cell death and proliferation revealed increased proliferation and regeneration of the epithelium in Bcl-$3^{-/-}$ mice identifying Bcl-3 as an important factor in regulating epithelial cell turnover and sensitivity to colitis. Our study suggests that Bcl-3 may be an effective target for promoting regeneration of the epithelium in the colon.

3.3 Results

3.3.1 Elevated Bcl-3 mRNA is found in the colon of IBD patients

To assess the role of Bcl-3 in IBD the Bcl-3 mRNA expression levels were initially analysed from a previously published study which identified a large number of genes associated with inflammatory bowel diseases [185]. In that study, transcriptional profiles were generated from biopsies taken from the sigmoid colon of patients with Crohn's disease (CD) (n = 10) and ulcerative colitis (UC) (n = 10) and those of normal controls (n = 11). Bioinformatics analysis of this dataset revealed that Bcl-3 mRNA expression levels were significantly increased in both CD ($p<0.01$) and UC ($p<0.05$) (Figure 3.1A). The elevated Bcl-3 mRNA levels in CD and UC were unexpected considering a SNP in the *BCL3* locus predicted reduced expression of Bcl-3 mRNA was associated with in CD [170].

To confirm this analysis Bcl-3 mRNA expression was measured by real time quantitative PCR (qRT-PCR) in an additional, independent patient cohort of 21 CD, 21 UC and 6 normal control colon tissue samples. Importantly, this independent analysis of Bcl-3 mRNA expression also revealed a statistically significant increase in Bcl-3 gene expression in Crohn's disease tissue samples relative to normal healthy controls ($p<0.05$) (Figure 3.1B). Moreover, the magnitude of increase of Bcl-3 mRNA levels in CD and UC relative to normal controls was similar in these tissue samples and in those contained in the previous microarray analysis. However, although an increase in Bcl-3 mRNA expression was observed in UC tissue samples, this did not meet statistical significance. To gain an insight into the association of elevated Bcl-3 mRNA with sites of inflammation in CD, Bcl-3 mRNA expression levels were further investigated in tissue samples of the ileum and colon from CD

patients and from normal patient control samples. Real time PCR (qRT-PCR) analysis of Bcl-3 mRNA in CD ileum and colon tissue revealed increased Bcl-3 mRNA expression in colon tissue samples of Crohn's disease relative to normal controls (Figure 3.1C). Increased Bcl-3 mRNA expression was not observed in ileum tissue of CD tissue samples suggesting that elevated Bcl-3 mRNA levels may be associated with specific anatomical regions of the intestine (Figure 3.1C). No difference was seen in Bcl-3 expression levels between rectal and colon UC tissue (Figure 3.1D). Taken together, these data demonstrate a strong correlation between increased Bcl-3 mRNA expression and colitis in human IBD.

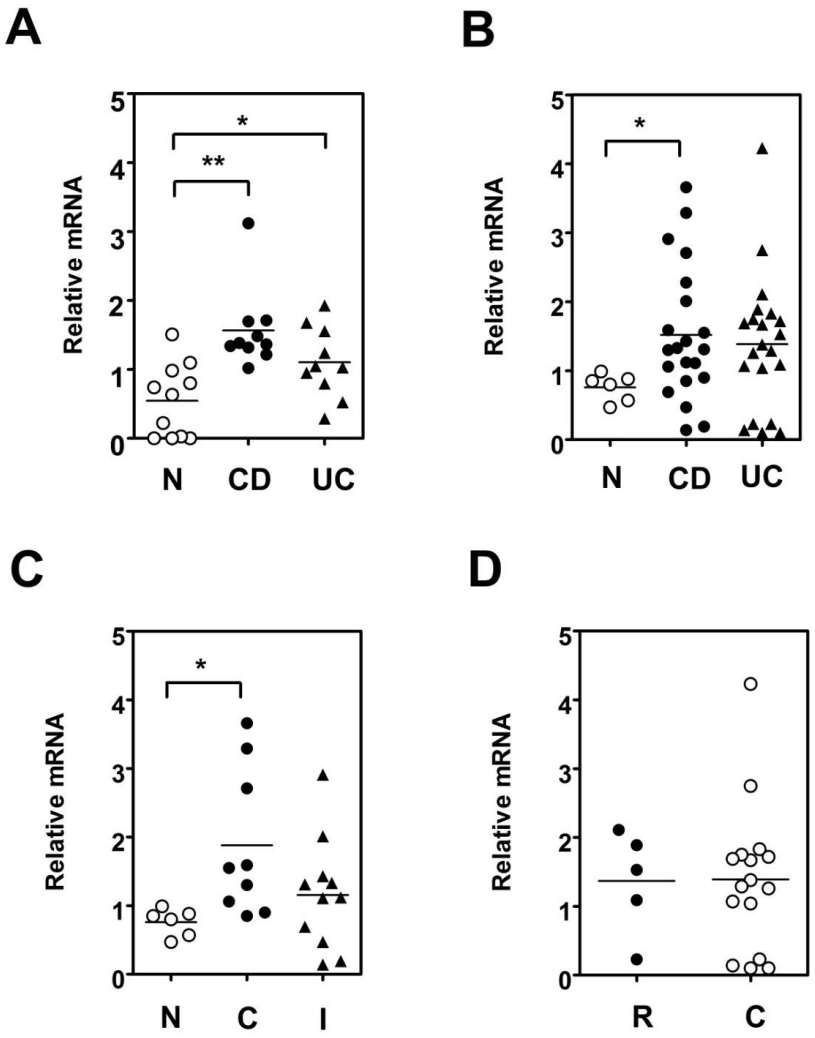

Figure 3.1: Bcl-3 expression in inflammatory bowel disease.

(**A**) Bcl-3 mRNA levels in normal (N, n = 11), Crohn's disease (CD, n = 10) and ulcerative colitis (UC, n = 10) colon tissue. Data extracted from the NCBI GEO dataset GDS1330. (**B**-**D**) Real time PCR (qRT-PCR) analysis of Bcl-3 gene expression relative to normal controls (Human inflammatory bowel disease (IBD) tissue array library) (**B**) Bcl-3 mRNA levels in Crohn's disease (CD, n = 21) and ulcerative colitis (UC, n = 21) tissue samples relative to normal (N, n = 6) controls ($p<0.05$ *). (**C**) Increased Bcl-3 expression in Crohn's disease colon (C) tissue relative to normal control tissue (N). (**D**) Differences in Bcl-3 gene expression between colon (C) and rectal (R) UC tissue samples were found to be not statistically significant. Data is expressed as means ± standard error of the mean (SEM). Statistical significance was determined using Mann Whitney U Tests. N = Normal, C = Colon, I = Ileum, R = Rectal, CD = Crohn's Disease, UC = ulcerative colitis.

3.3.2 DSS colitis experimental design

In order to investigate further the potential role of Bcl-3 in IBD, the murine model of dextran-sodium sulphate (DSS) induced colitis was performed using male Bcl-$3^{-/-}$ and wild-type littermate controls as described in chapter 2. Briefly, Bcl-$3^{-/-}$ and wild-type (WT) litter mate controls were group housed with administration of DSS in their drinking water. Three concentrations of DSS (1%, 2% and 2.5%) were tested to determine the optimal DSS concentration to induce disease. Fresh DSS solutions were administered daily to the mice for six days (D0 – D6) followed by removal of DSS and replacement with water only for a further two days. Disease scoring was performed daily on each group with weight loss, stool consistency and fur/posture individually measured to calculate the daily disease activity index (DAI). On day 8, mice were sacrificed for further downstream tissue analysis. Colons were weighed, measured and divided into different sections for tissue processing. Tissue samples were further processed according to sample requirements (Figure 3.2).

3.3.3 Bcl-$3^{-/-}$ and WT litter mate controls - genotype confirmation

Bcl-$3^{-/-}$ and WT littermates were genotyped to confirm their genetic status prior to experimental use. Bcl-$3^{-/-}$ expression was analysed by measuring expression of the Bcl-3 targeting neocassette construct which results in Bcl-3 becoming functionally inactive [108]. Homozygous Bcl-$3^{-/-}$ mice contain two copies of the Bcl-3 construct in comparison to the one copy for heterozygotes. WT animals contain no copy of the Bcl-3 neocassette as determined by analysing the PCR amplified DNA by agarose gel electrophoresis. Expression of the Bcl-3 construct was compared with the IL-2 promoter with the genetic status of each mouse determined by measuring the ratio of the Bcl-3 construct to the IL-2 promoter. WT mice contain only the IL-2 promoter

with heterozygotes containing both the Bcl-3 construct and the IL-2 promoter in a 1:1 ratio. All Bcl-3 deficient homozygous mice were found have a 2:1 ratio, when comparing the Bcl-3 construct with the IL-2 promoter. Following confirmation of the genetic status, validated WT and Bcl-3 deficient mice were used in the DSS colitis experiment (Figure 3.3).

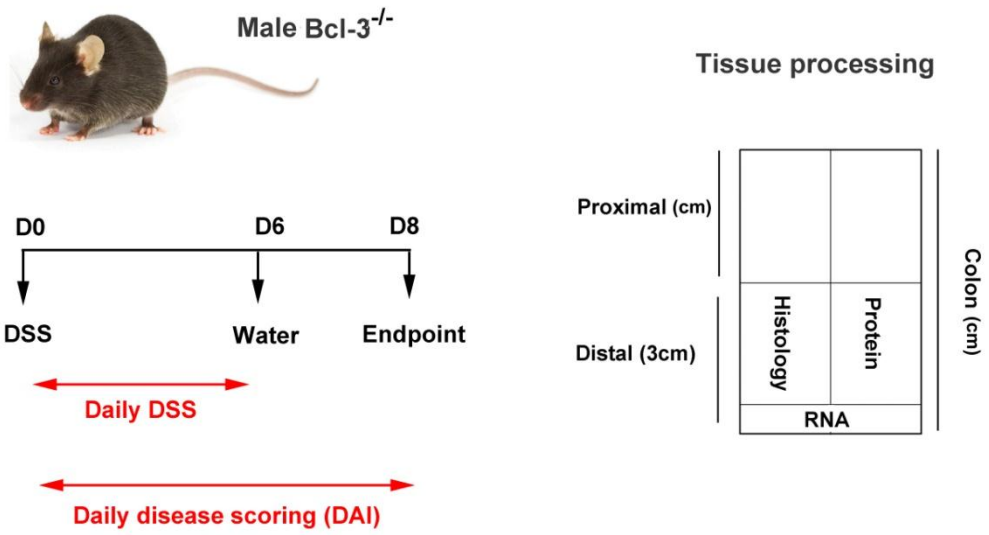

Figure 3.2: DSS colitis experimental design

Bcl-3$^{-/-}$ and WT litter mate control male mice (10 -12 weeks) were fed a daily solution of DSS (1%, 2% and 2.5%) in their drinking water for 6 days. DSS was removed and replaced with water only for two days prior to experimental endpoint. Daily disease scoring was measured by the daily disease activity index scoring system (DAI). Colons were removed at experimental endpoint, opened longitudinally and divided into different sections for tissue processing. Colon weight and length were influenced by experimental treatment (untreated, DSS treated). The distal colon was determined using a 3cm cut off from the base of the colon. Samples were processed according to specific sample requirements.

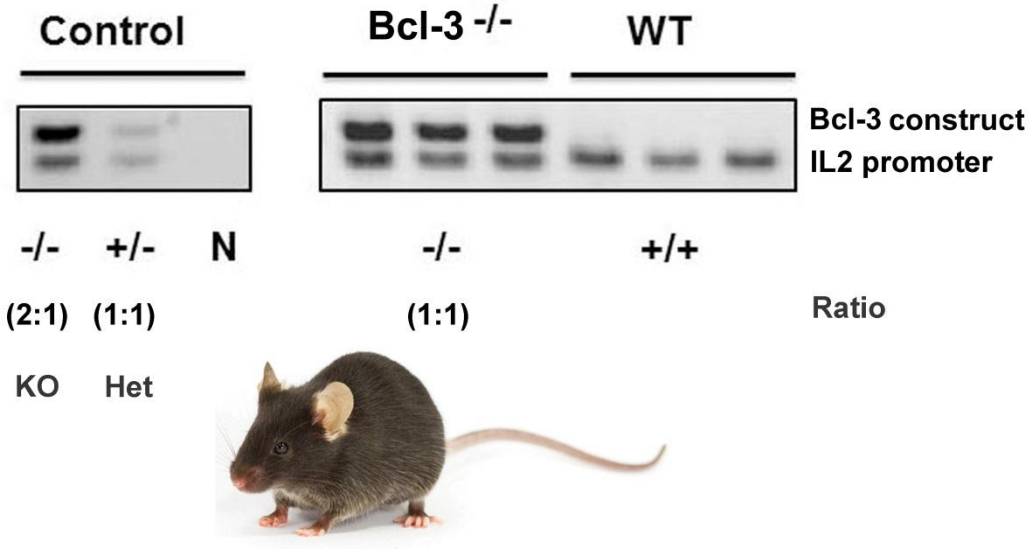

Figure 3.3: Genotype confirmation of Bcl-3$^{-/-}$ and WT litter mate control mice

Bcl-3$^{-/-}$ and WT litter mate controls were all genotyped prior to DSS experimental trial. Data is representative of total mice used for DSS trial. N = negative control (no template control), +/+ = Wild type control (WT), -/- = Bcl-3$^{-/-}$ (KO – knockout) and +/- = Heterozygous (Het). Amplified PCR products for the Bcl-3 construct (209 base pairs) and IL-2 promoter control (170 base pairs) were ran on a 2% agarose gel containing SYBR safe DNA gel stain.

3.3.4 Bcl-3$^{-/-}$ mice are protected against DSS-induced colitis

To assess the optimal concentration of DSS required to induce colitis in Bcl-3 deficient mice, we administered three doses of DSS for six days followed by replacement of DSS with water until day eight. Administration of a 1% DSS solution did not have a significant effect on either WT or Bcl-3$^{-/-}$ DSS groups when compared with healthy untreated groups as determined by DAI score. In contrast a 2.5% DSS dose induced a significant change in DAI score for both WT and Bcl-3$^{-/-}$ DSS groups when compared to untreated healthy control mice (Day 4; $p<0.05$, Day 5 – Day 8; $p<0.001$). Interestingly no difference in DAI score was observed between WT and Bcl-3$^{-/-}$ 2.5% DSS groups suggesting that both Bcl-3$^{-/-}$ and WT mice develop a similar colitis phenotype based on DAI scoring analysis (Figure 3.4).

Within four days of beginning 2% DSS administration both Bcl-3$^{-/-}$ and WT mice developed characteristic symptoms associated with DSS-induced colitis. This data suggests that the 2% dose of DSS was sufficient to induce colitis in WT and Bcl-3$^{-/-}$ mice (Day 5 – 8; $p<0.001$). However when rectal bleeding, diarrhoea, hunched posture, and weight loss of 2% DSS treated and untreated mice were analysed, the DAI score revealed that Bcl-3$^{-/-}$ mice developed a significantly less severe form of DSS-induced colitis when compared with WT DSS treated mice (Day 7; $p<0.01$, Day 8; $p<0.001$) (Figure 3.4). Importantly, the reduced disease observed in the Bcl-3$^{-/-}$ mice (2% DSS group) was not a consequence of reduced DSS intake, since water consumption was equivalent between groups during the experiment (Figure 3.5).

Furthermore breakdown analysis of the DAI scoring revealed a large difference in weight loss between the WT and Bcl-3$^{-/-}$ 2% DSS group. By day eight following DSS treatment WT mice had lost greater than 12% of their body weight (Day 6;

$p<0.01$, Day 7; $p<0.001$, Day 8; $p<0.001$) (Figure 3.6A). In contrast, DSS treated Bcl-$3^{-/-}$ mice did not demonstrate any significant loss of body mass when compared to untreated Bcl-$3^{-/-}$ mice up to 8 days following the initial DSS treatment. Differences between the WT and Bcl-$3^{-/-}$ 2% DSS groups were found to be statistically significant at day 7 ($p<0.05$) and day 8 ($p<0.001$) (Figure 3.6A). WT and Bcl-$3^{-/-}$ mice treated with 2% DSS demonstrated rectal bleeding and alterations in stool consistency between day 5 to day 8 relative to their respective healthy untreated groups ($p<0.001$) (Figure 3.6B). However, stool consistency in the 2% DSS treated Bcl-$3^{-/-}$ group began to resolve between day 6 and day 8 when compared with the WT 2% DSS group (Day 8; $p<0.001$). This difference in stool consistency correlated with the difference in weight loss between the 2% DSS groups with WT mice severely losing weight between day 6 to day 8 in comparison to Bcl-$3^{-/-}$ mice. In addition treatment with 2% DSS lead to an alteration in fur and posture of both WT and Bcl-$3^{-/-}$ 2% DSS treated mice when compared with healthy untreated controls (Day 4 – 8; $p<0.001$) however no significant difference was observed between these DSS groups (Figure 3.6C).

The 1% DSS dose did not lead to any weight loss or difference in stool consistency when compared with healthy untreated mice (Figure 3.7A-B). A minor change in fur and posture score was observed in the 1% DSS groups relative to healthy untreated controls however this was not found to be statistically significant (Figure 3.7C). This was consistent with the low DAI score for the 1% DSS group (Figure 3.4). The 2.5% dose of DSS led to the development of colitis in both WT and Bcl-$3^{-/-}$ mice. Despite a robust induction of inflammation as determined by DAI score, the 2.5% DSS dose resulted in no difference in weight loss, stool consistency and fur/posture between WT and Bcl-$3^{-/-}$ groups. This indicated that this dose exceeded the minimal DSS dose

required to induce colitis in these mice (Figure 3.8). Taken together, individual scoring analysis of weight loss, stool consistency and fur/posture score revealed that the 2% DSS dose was the optimal concentration of DSS to induce colitis in both WT and Bcl-3$^{-/-}$ mice. Importantly, this also resulted in a differential response between WT and Bcl-3 deficient mice towards DSS. Therefore the 2% DSS concentration was used for all subsequent analyses of the role of Bcl-3 in acute colitis unless otherwise stated. This data demonstrates clearly that Bcl-3 contributes to colitis with WT mice developing a more severe disease in comparison to Bcl-3$^{-/-}$ mice when administered 2% DSS.

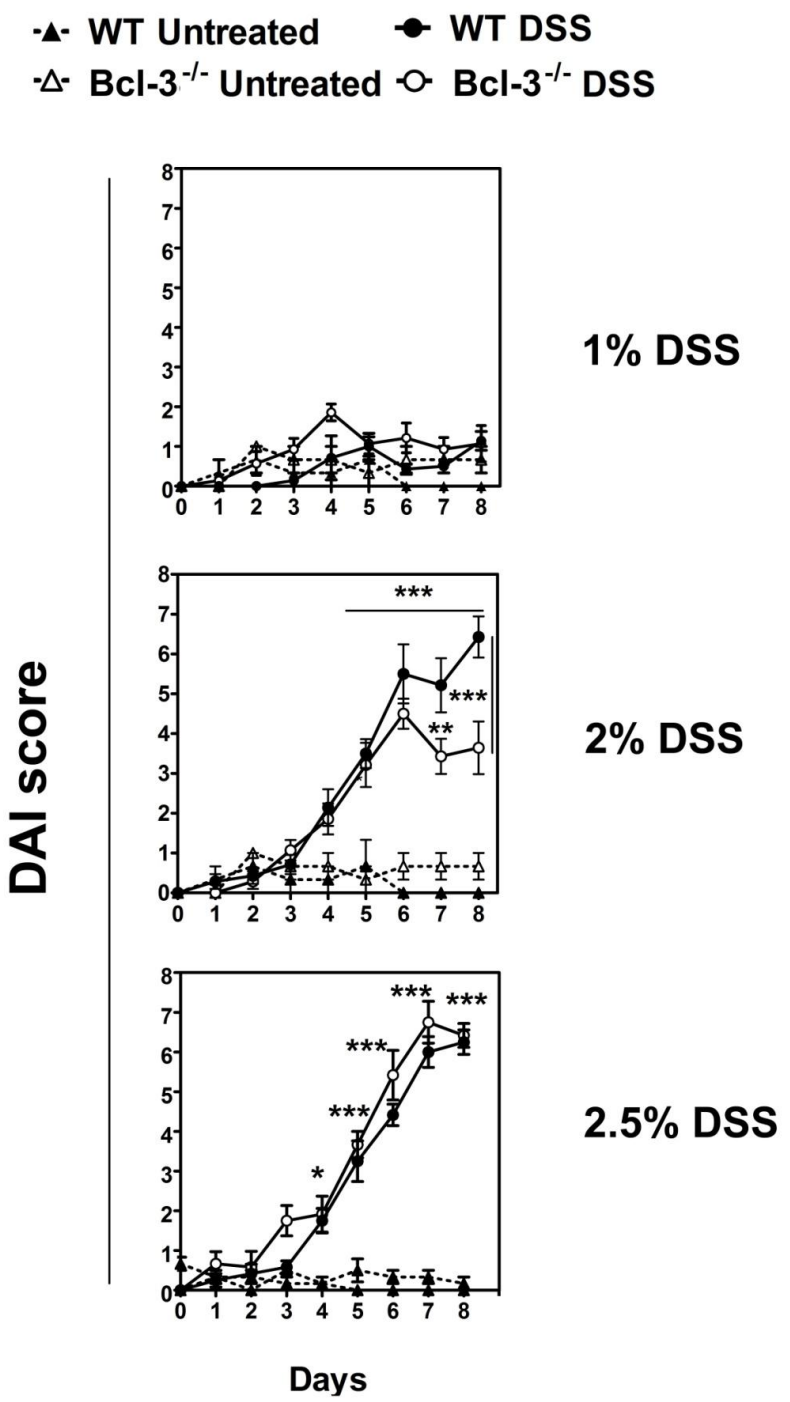

Figure 3.4: Bcl-3$^{-/-}$ mice develop a milder colitis phenotype when administered a 2% DSS dose

WT and Bcl-3$^{-/-}$ mice were administered DSS for 6 days followed by water for an additional 2 days. Weight loss (A), stool consistency (B) and fur/posture (C) were measured each day to determine the DAI score for each DSS dose group. Statistical significance in DAI scores were calculated over time by Two-way ANOVA with Bonferroni post hoc test with $p<0.001$ (***), $p<0.01$ (**) and $p<0.05$ (*) (n = 7/group).

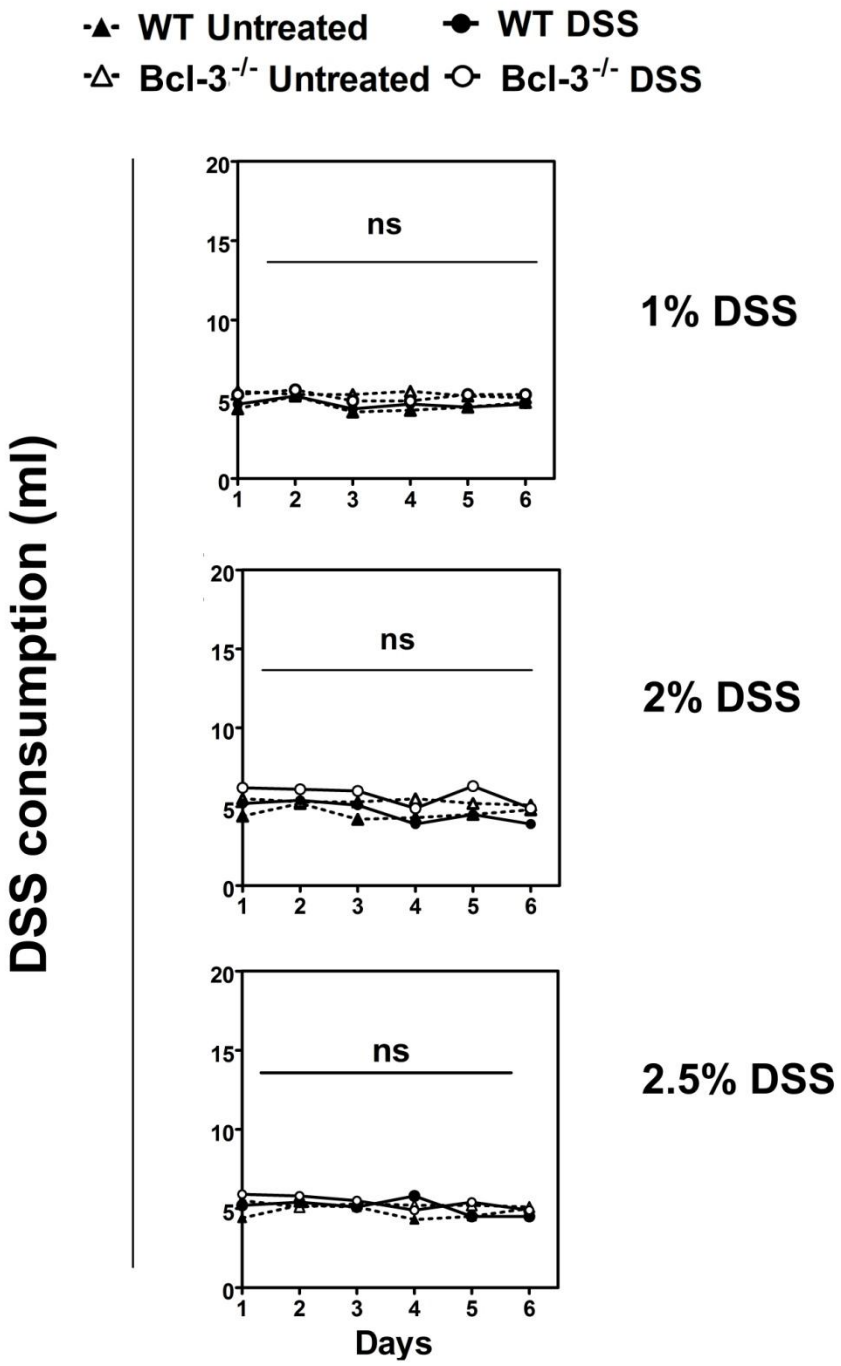

Figure 3.5: WT and Bcl-3$^{-/-}$ mice – Daily DSS consumption

WT and Bcl-3$^{-/-}$ mice were administered DSS for 6 days followed by water for an additional 2 days. Average daily DSS consumption was measured in each group every day during DSS consumption. Statistical significance in DSS consumption was calculated over time by Two-way ANOVA with Bonferroni post hoc test (ns – not statistically significant). (n = 7/group).

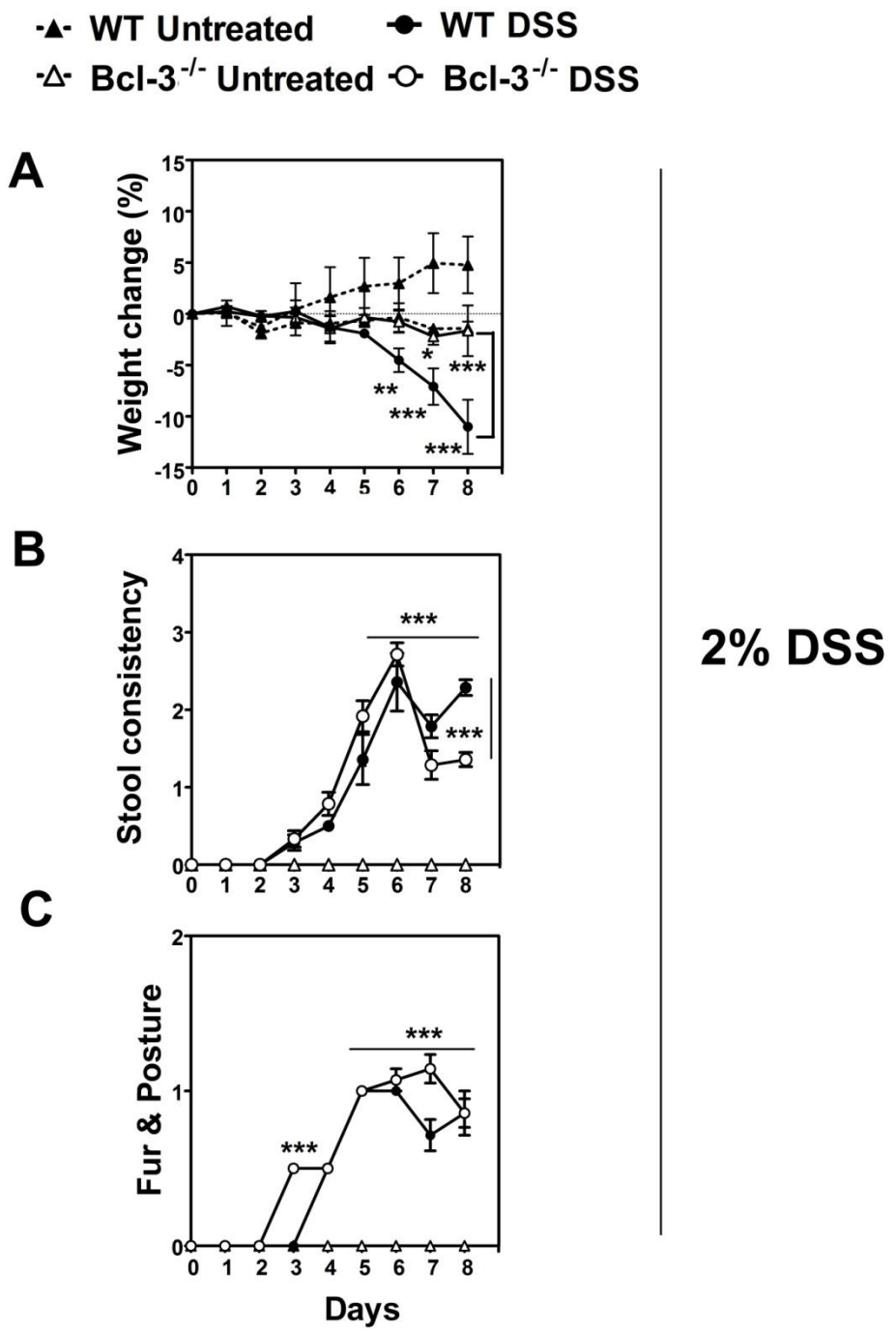

Figure 3.6: DSS administration (2%) induces a milder colitis phenotype in Bcl-3$^{-/-}$ mice

WT and Bcl-3$^{-/-}$ mice were administered 2% DSS for 6 days followed by water for an additional 2 days. Weight loss (A), stool consistency (B) and fur/posture (C) were measured each day to determine the DAI score. Statistical significance in weight loss (% change), stool consistency and fur/posture scores were calculated over time by Two-way ANOVA with Bonferroni post hoc test with $p<0.001$ (***), $p<0.01$ (**) and $p<0.05$ (*) (n = 7/group).

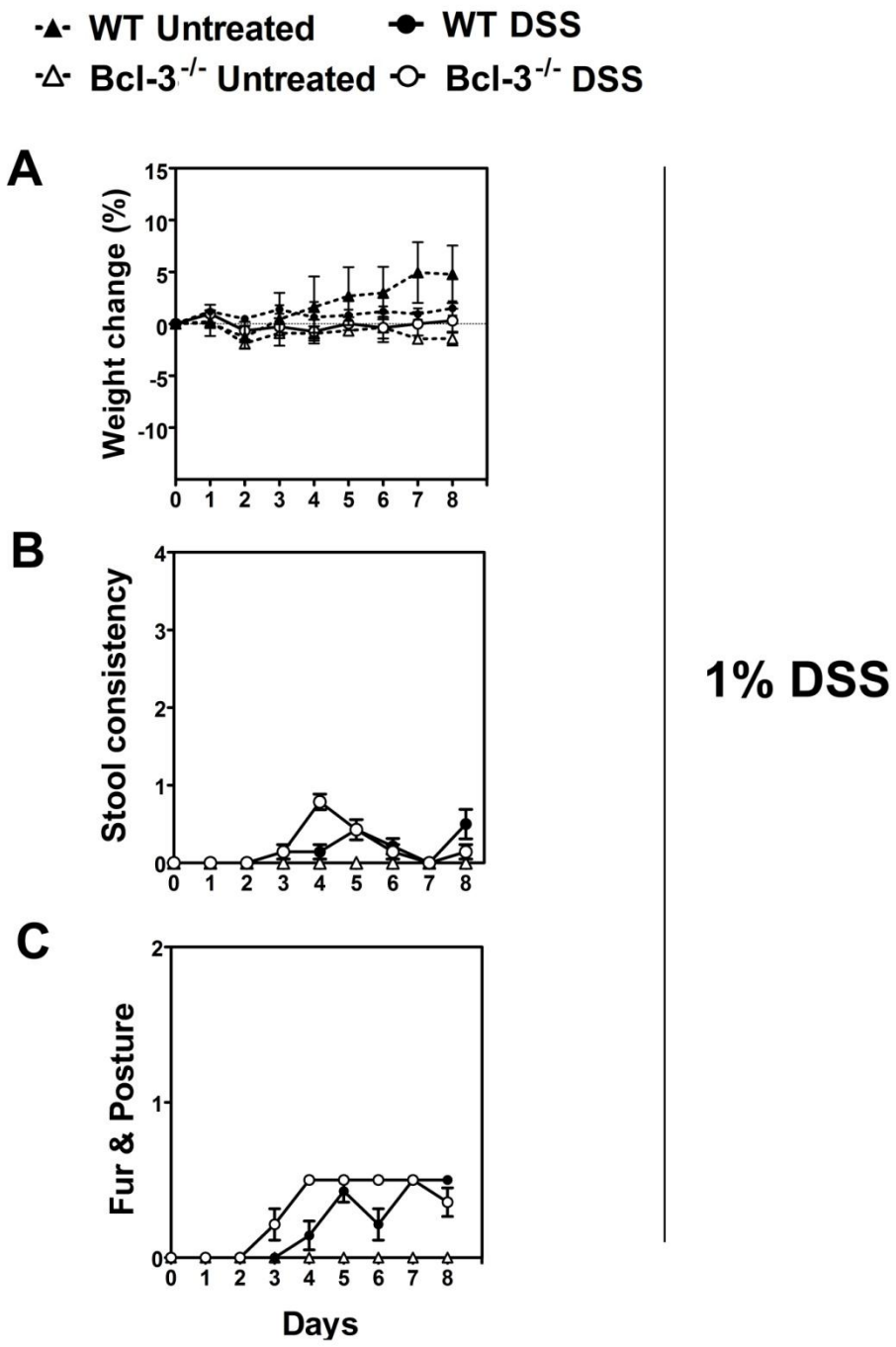

Figure 3.7: 1% DSS administration is not sufficient to induce the colitis phenotype in Bcl-3$^{-/-}$ and WT mice

WT and Bcl-3$^{-/-}$ mice were administered 1% DSS for 6 days followed by water for an additional 2 days. Weight loss (A), stool consistency (B) and fur/posture (C) were measured each day to determine the DAI score. Statistical significance in weight loss (% change), stool consistency and fur/posture scores were calculated over time by Two-way ANOVA with Bonferroni post hoc test with $p<0.001$ (***), $p<0.01$ (**) and $p<0.05$ (*) (n = 7/group).

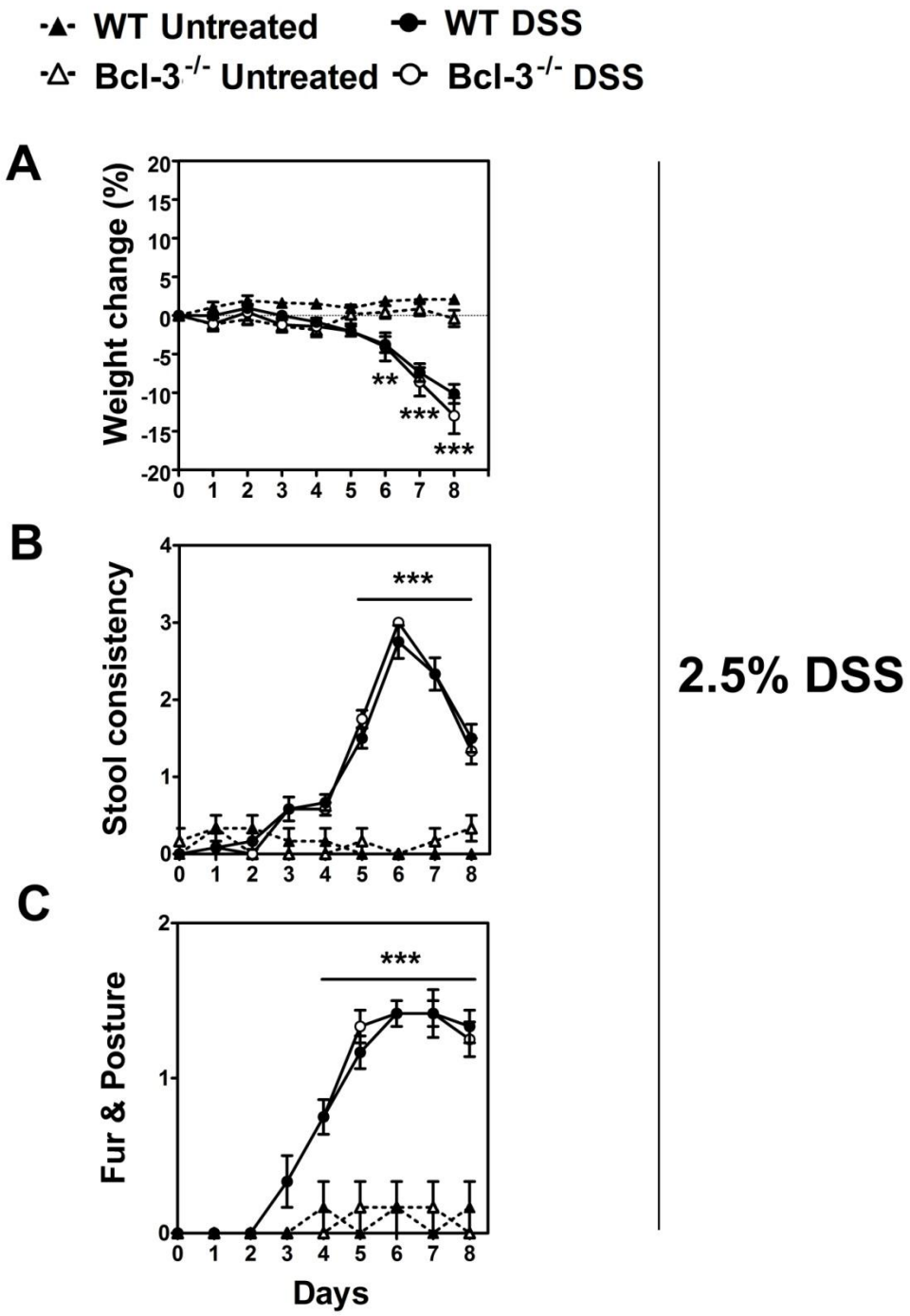

Figure 3.8: 2.5% DSS administration leads to an equivalent colitis phenotype in both WT and Bcl-3$^{-/-}$ mice

WT and Bcl-3$^{-/-}$ mice were administered 2.5% DSS for 6 days followed by water for an additional 2 days. Weight loss (A), stool consistency (B) and fur/posture (C) were measured each day to determine the DAI score. Statistical significance in weight loss (% change), stool consistency and fur/posture scores were calculated over time by Two-way ANOVA with Bonferroni post hoc test with $p<0.001$ (***), $p<0.01$ (**) and $p<0.05$ (*) (n = 7/group).

3.3.5 Macroscopic analysis of colon tissue in DSS treated WT and Bcl-3$^{-/-}$ mice

Macroscopic analysis of colon tissue was performed on day eight following termination of the experiment. WT 2% DSS-treated mice demonstrated significant shortening of the colon when compared to untreated healthy controls ($p<0.05$; Figure 3.9A). Surprisingly, a similar degree of colon shortening was observed in 2% DSS treated Bcl-3$^{-/-}$ mice when compared to untreated healthy Bcl-3$^{-/-}$ controls (Figure 3.9A). Moreover, the significantly increased colonic weight of 2% DSS treated WT mice relative to untreated controls was also observed in 2% DSS treated Bcl-3$^{-/-}$ mice ($p<0.05$; Figure 3.9B). Thus, although the macroscopic inflammation of colonic tissue was similar in both 2% DSS treated WT and Bcl-3$^{-/-}$ mice, the clinical indices of the DSS-induced colitis, in particular weight loss, were significantly reduced in Bcl-3$^{-/-}$ mice.

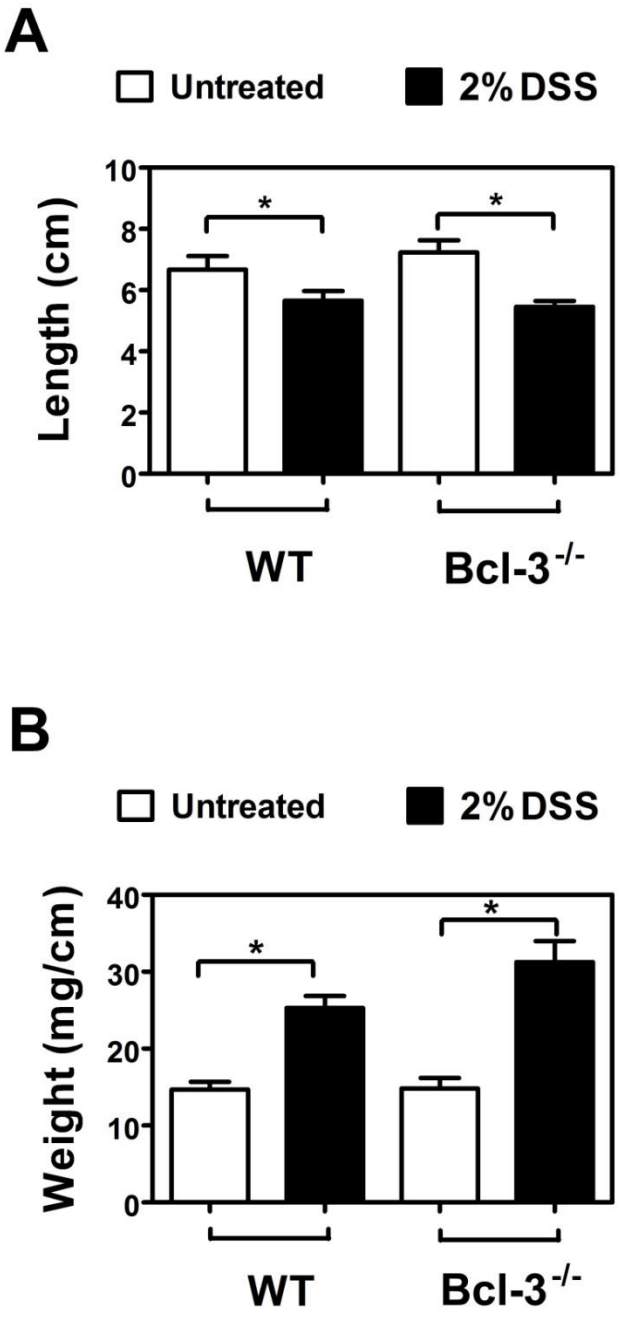

Figure 3.9: Macroscopic analysis of colon tissue in DSS treated WT and Bcl-3$^{-/-}$ mice

Differences in (A) colon length and (B) distal colon weight between in both WT and Bcl-3$^{-/-}$ mice was relative to healthy untreated controls and found to be statistically significant ($p<0.05$). Data is expressed as mean ± SEM. Statistical significance was determined using Mann Whitney U Tests with $p<0.05$ (*) (n = 7/group).

3.3.6 Bcl-3$^{-/-}$ mice show reduced tissue pathology following DSS treatment

To further investigate the differences in DSS-induced colitis (2% DSS) between WT and Bcl-3$^{-/-}$ mice histological examination of distal colon tissue sections from untreated and DSS treated WT and Bcl-3$^{-/-}$ mice was performed (Figure 3.10A). No differences were observed between untreated WT and untreated Bcl-3$^{-/-}$ distal colonic tissue samples by haematoxylin and eosin (H&E) staining. Both WT and Bcl-3$^{-/-}$ mice displayed normal epithelial architecture with intact goblet cells and crypts with no discernible inflammatory influx. DSS treatment of WT mice induced a dramatic alteration in the colonic mucosal tissue with extensive oedema, large cellular infiltrates and a severe loss of tissue organisation with destruction of crypts and loss of goblet cells. Although histological analysis revealed similar levels of oedema and cellular infiltrates in Bcl-3$^{-/-}$ mice there was significantly less destruction of the tissue architecture following DSS treatment (Figure 3.10A). Quantitative histopathology analysis of the distal colon tissue from DSS treated Bcl-3$^{-/-}$ mice revealed significantly reduced epithelium damage and loss of tissue architecture compared to WT mice (Figure 3.10B). However, there were no significant differences in the extent of inflammation, the degree of cellular infiltration and oedema between DSS-treated WT and Bcl-3$^{-/-}$ mice. This histological analysis provides insight into the reduced weight loss and overall clinical disease score observed in DSS-treated Bcl-3$^{-/-}$ mice relative to WT mice, which would appear to result from an intact or regenerated epithelium rather than reduced leukocyte infiltration in Bcl-3$^{-/-}$ mice.

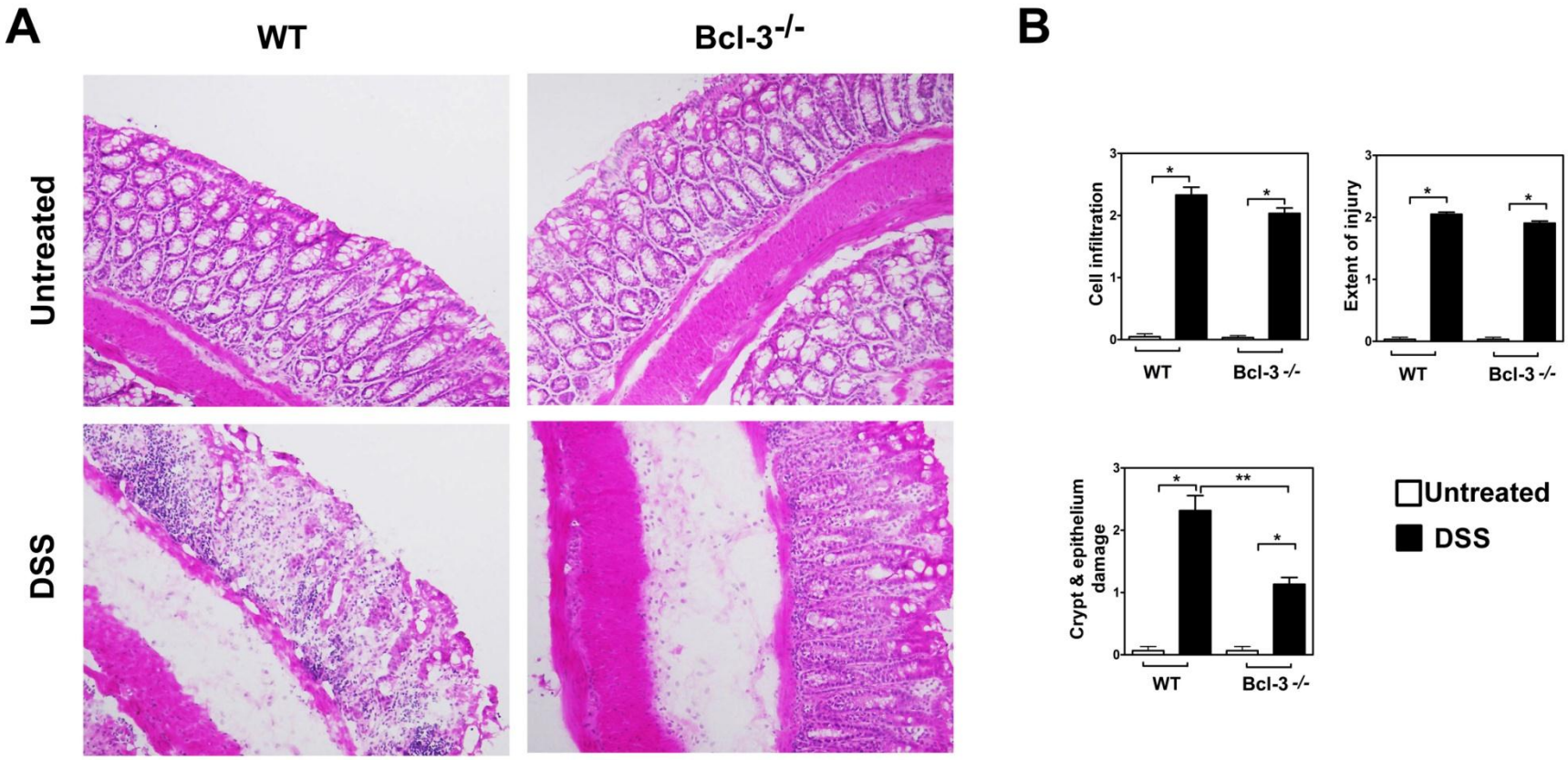

Figure 3.10: Reduced histological damage in Bcl-3$^{-/-}$ mice following DSS induced colitis (Figure legend – Next page)

Figure 3.10: Reduced histological damage in Bcl-3$^{-/-}$ mice following DSS induced colitis

(**A**) Representative H&E of untreated (control) and DSS treated wild type (WT) and Bcl-3$^{-/-}$ mice. **(B)** Histological sections were scored for cellular infiltration, extent of injury and epithelium/crypt damage. DSS induced cellular infiltration, extent of injury, and epithelium and crypt damage scores were increased in WT and Bcl-3$^{-/-}$ mice relative to untreated controls. Statistical significance was determined using the Mann Whitney U test with $p<0.05$ (*), $p<0.01$ (**) and $p<0.001$ (***). DSS treated WT mice showed greater crypt and epithelium damage relative to DSS treated Bcl-3$^{-/-}$ mice ($p<0.01$). Data is representative of greater than 7 fields of view per tissue section at 20X magnification (n = 7 per group).

3.3.7 DSS induces similar levels of cytokines in the colon of Bcl-3$^{-/-}$ and WT mice

Although histological analysis showed similar levels of oedema and leukocyte infiltration in DSS treated WT and Bcl-3$^{-/-}$ mice, it is possible that the inflammation may be qualitatively different between these groups. In order to characterise the inflammation associated with DSS-induced colitis in Bcl-3$^{-/-}$ mice we next measured inflammatory gene expression in distal colon tissue from untreated and DSS treated WT and Bcl-3$^{-/-}$ mice by qRT-PCR. Surprisingly, although Bcl-3 has previously been described as a negative regulator of Toll-like receptor induced pro-inflammatory gene expression, we found no significant difference in the expression of TNF-α, IL-6, CXCL1 and IL-1β between DSS-treated WT and Bcl-3$^{-/-}$ mice (Figure 3.11A). Measurement of distal colon Bcl-3 protein expression by immunofluorescence was unsuccessful using commercially available antibodies (Figure 3.12A) however previous studies have demonstrated Bcl-3 mRNA expression in intestinal epithelial cells [198, 199]. In support of this we measured increased Bcl-3 mRNA in DSS treated WT mice when compared to untreated controls (Figure 3.12B). This suggests that although Bcl-3 is inducible upon DSS challenge, its loss does not appear to lead to a hyperresponsive immune response.

Recent studies have identified a protective role for the cytokines IL-17A and IL-22 [200-202] in DSS colitis by inducing anti-bacterial peptide expression and epithelial cell regeneration in the colon. To assess any role for these cytokines in the observed resistance of Bcl-3$^{-/-}$ mice to DSS induced colitis and maintenance of intestinal epithelium we next measured their expression in the colon of WT and Bcl-3$^{-/-}$ mice. In line with previous reports, the expression of both IL-17A and IL-22 is robustly induced by DSS treatment in WT mice, however no significant differences in the

expression of these cytokines was found between DSS treated WT and Bcl-3$^{-/-}$ mice Figure 3.11B).

We next analysed the cellular composition of the leukocyte infiltrates in DSS-treated WT and Bcl-3$^{-/-}$ mice using immunofluorescence microscopy and antibodies against the cell surface markers F4/80 (macrophage), CD3 (T cell), Ly6G (neutrophil) and CD11c (dendritic cells) (Figure 3.13A). Quantitative analysis of tissue sections demonstrated recruitment of macrophages, neutrophils and to a lesser degree T cells and dendritic cells to the distal colon of DSS treated mice. No significant differences in the recruitment of these cell types were found between WT and Bcl-3$^{-/-}$ mice (Figure 3.13B). These data demonstrate that the inflammatory component of DSS-induced colitis is similar between WT and Bcl-3$^{-/-}$ mice and suggest that the reduced susceptibility of Bcl-3$^{-/-}$ mice to DSS induced colitis may result from altered epithelial responses to treatment.

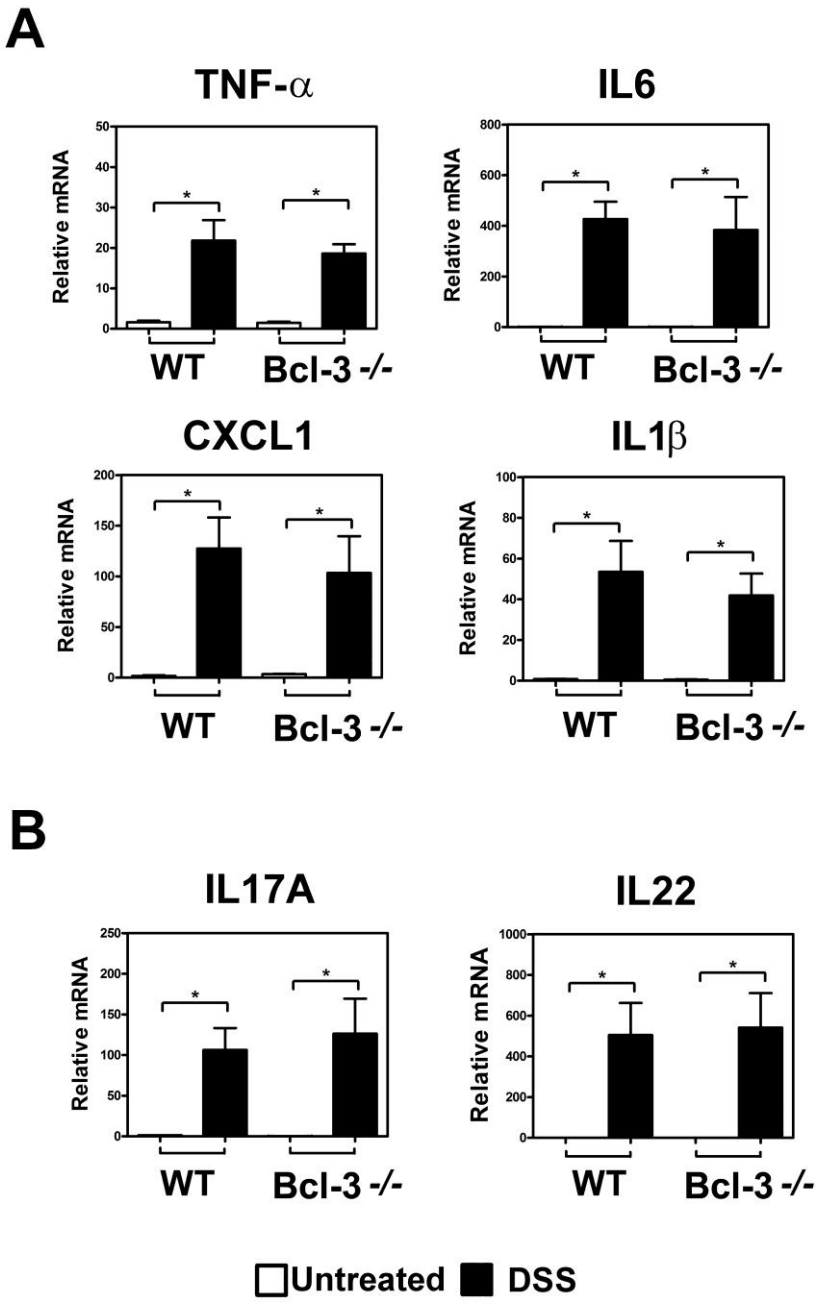

Figure 3.11: Inflammatory cytokine expression in mucosal tissue of DSS-treated Bcl-3$^{-/-}$ mice

Distal colon tissues were analysed for changes in immune gene expression relative to the housekeeping gene 18s rRNA. (A) Increased pro-inflammatory gene expression was found in the DSS group of WT and Bcl-3$^{-/-}$ mice relative to untreated control groups ($p<0.05$). (B) Increased IL-17A and IL-22 gene expression in DSS treated WT and Bcl-3$^{-/-}$ mice relative to untreated controls. Data is represented as relative mRNA expression as determined by the $2^{-\Delta\Delta CT}$ method. Statistical significance was calculated using Mann Whitney U Tests ($p<0.05$ *). Data expressed as mean ± SEM (n = 7).

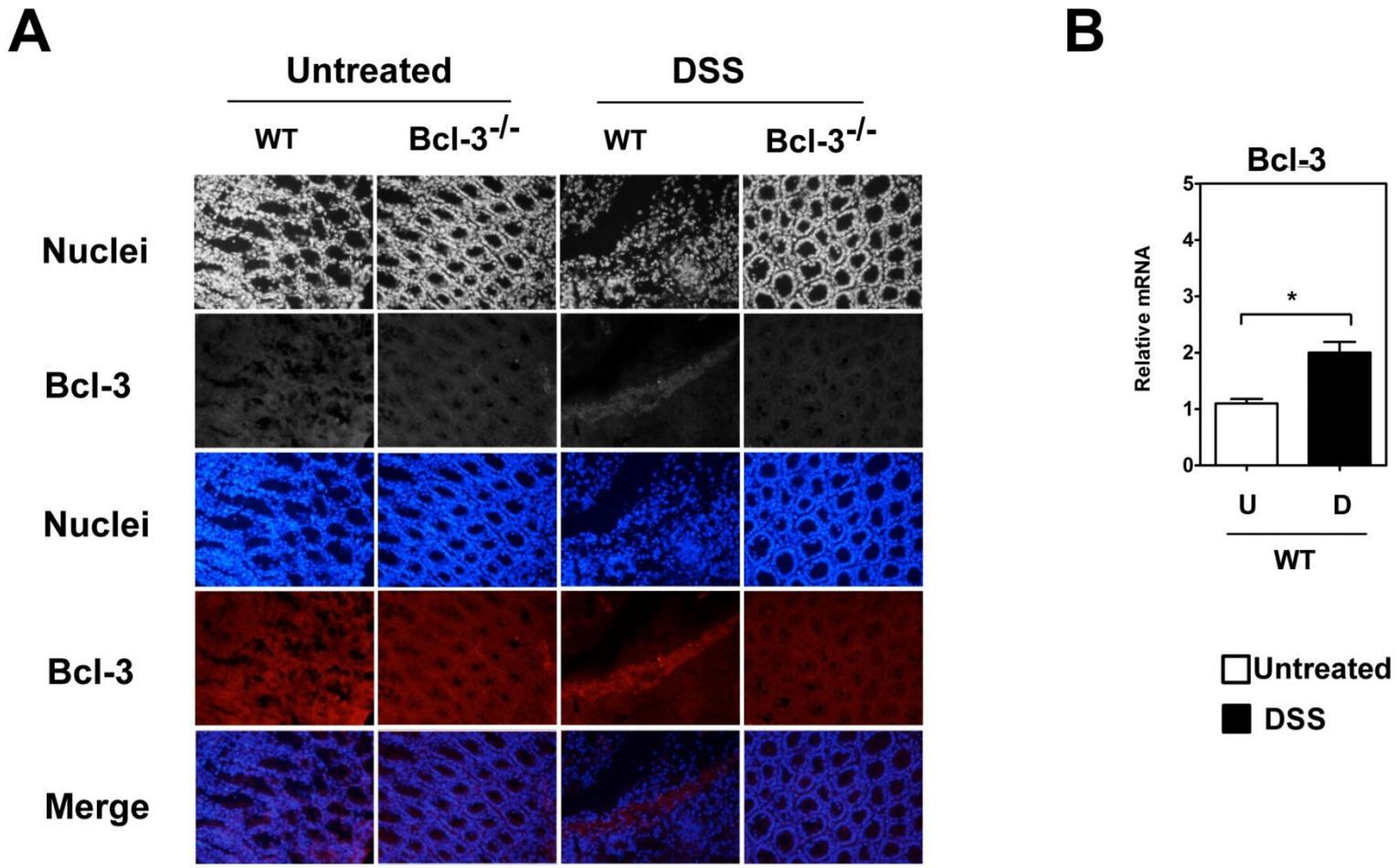

Figure 3.12: Inducible gene expression in DSS induced colitis (Figure Legend – next page)

Figure 3.12: Inducible gene expression in DSS induced colitis

(A) Immunofluorescent staining for Bcl-3 protein expression in distal colon frozen sections (6μm) at 40X magnification. **(B)** Inducible Bcl-3 gene expression in WT DSS treated mice measured by qRT-PCR. Data is represented as relative mRNA expression as determined by the $2^{-\Delta\Delta CT}$ method. Statistical significance was calculated using Mann Whitney U Tests ($p<0.05$ *). Data expressed as mean ± SEM (n = 7) U = untreated, D = DSS.

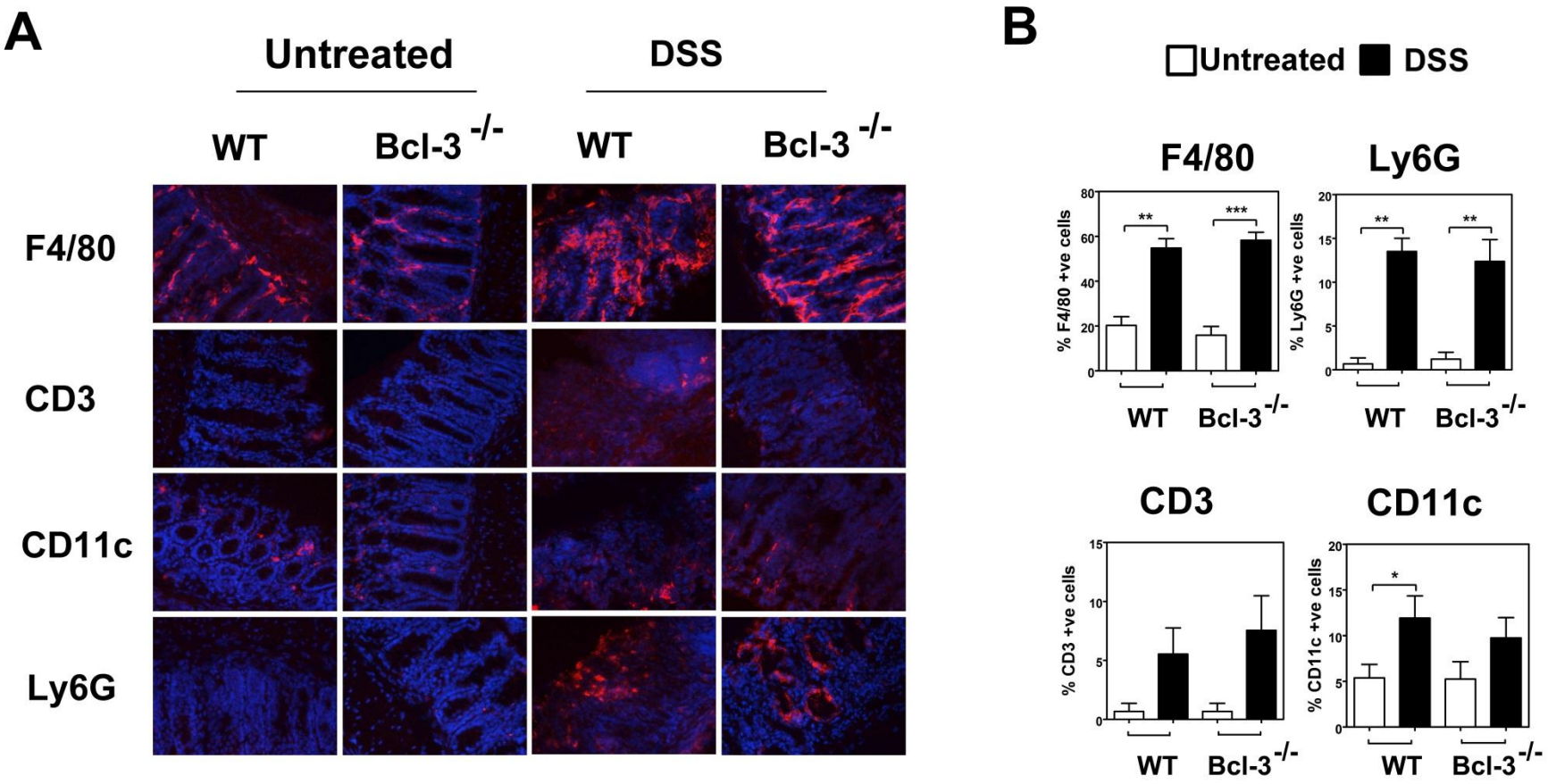

Figure 3.13: Analysis of inflammatory cell infiltration during colitis in Bcl-3$^{-/-}$ mice (Figure Legend – next page)

Figure 3.13: Analysis of inflammatory cell infiltration during colitis in Bcl-3$^{-/-}$ mice

(**A**) Immunofluorescent staining of 6μm distal colon section at 40X magnification for macrophages (F/480), dendritic cells (CD11c), T cells (CD3) and neutrophils (Ly6G). (**B**) Quantification of F4/80, CD3, Ly6G and CD11c positive cellular populations was performed on seven fields of view per section. Data is representative of scoring of all sections per treatment group (n =7). Statistical significance was determined using Mann Whitney U Tests with $p<0.05$ (*), $p<0.01$ (**) and $p<0.001$ (***).

3.3.8: Increased epithelial cell proliferation in DSS treated Bcl-3$^{-/-}$ mice

Since DSS induces epithelial cell damage to initiate colonic inflammation and colitis we next measured cell death in the colon of WT and Bcl-3$^{-/-}$ mice using terminal dUTP nick end labelling (TUNEL) of tissue sections followed by fluorescence microscopy analysis. In both untreated WT and untreated Bcl-3$^{-/-}$ mice we observed a small number of TUNEL positive nuclei in the top of the crypts representing the normal turnover of epithelial cells in this tissue (Figure 3.14A). However, following DSS treatment we observed a dramatic increase in TUNEL positive cells in both WT and Bcl-3$^{-/-}$ mice. Quantitative analysis of TUNEL staining demonstrated no significant differences in the number of cells undergoing apoptosis in both groups (Figure 3.14B). Immunoblot analysis of caspase-3 cleavage in colonic tissues also demonstrated a significant increase in apoptosis in WT and Bcl-3$^{-/-}$ mice following DSS treatment (Figure 3.14C). Densitometric analysis of cleaved caspase-3 levels normalised to β-actin level revealed no significant difference between WT and Bcl-3$^{-/-}$ mice (Figure 3.14D). Analysis of the mRNA levels of the apoptotic regulators PUMA, Bcl-XL, cIAP1/2 and NOXA by qRT-PCR also revealed no significant differences in gene expression between WT and Bcl-3$^{-/-}$ mice (Figure 3.14E).

Next the extent of epithelial cell proliferation was assessed in tissue sections using the cell proliferation marker Ki67. Immunofluorescence microscopy analysis of untreated WT and Bcl-3$^{-/-}$ mucosal colonic tissue revealed equivalent numbers of Ki67 positive cells at the base of the crypts (Figure 3.15: A and Figure 3.15: B). Ki67 staining was largely absent in WT mucosal tissue following DSS treatment and coincided with the extensive destruction and loss of tissue architecture (Figure 3.10). In contrast, widespread and strong Ki67 staining was found throughout the crypts of

colonic tissue taken from DSS-treated Bcl-3$^{-/-}$ mice, indicating significantly enhanced proliferation of Bcl-3$^{-/-}$ epithelial cells following treatment (Figure 3.15: A and Figure 3.15: B). Taken together these data suggest that Bcl-3$^{-/-}$ mice develop less severe clinical and histopathological colitis due to an increase in epithelial proliferation, which leads to regeneration of the damaged epithelium. Our data also demonstrate that this regeneration occurs despite the presence of on-going inflammation in the colonic mucosa.

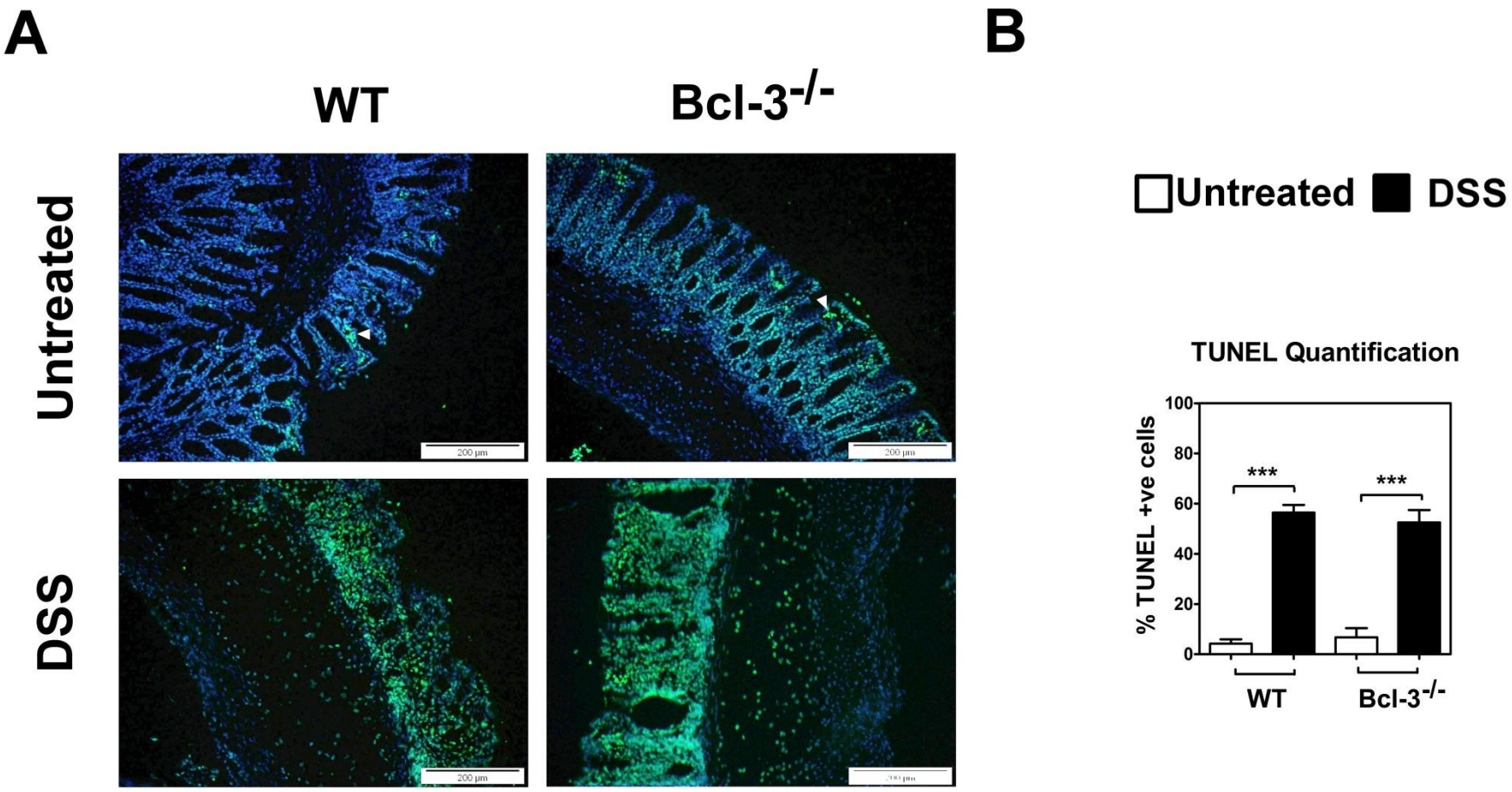

Figure 3.14: Analysis of cell death during colitis in Bcl-3$^{-/-}$ mice (Figure Legend – next page)

Figure 3.14: Analysis of cell death during colitis in Bcl-3$^{-/-}$ mice

(A) TUNEL stained distal colon 6μm sections. Arrows indicate TUNEL positive cells. Quantification of TUNEL positive cells was performed on seven fields of view per tissue section at 20X magnification (n = 7 per group). Statistical significance was calculated using Mann Whitney U Tests with $p<0.05$ (*), $p<0.01$ (**) and $p<0.001$ (***).White bars represent 200μM scale bar.

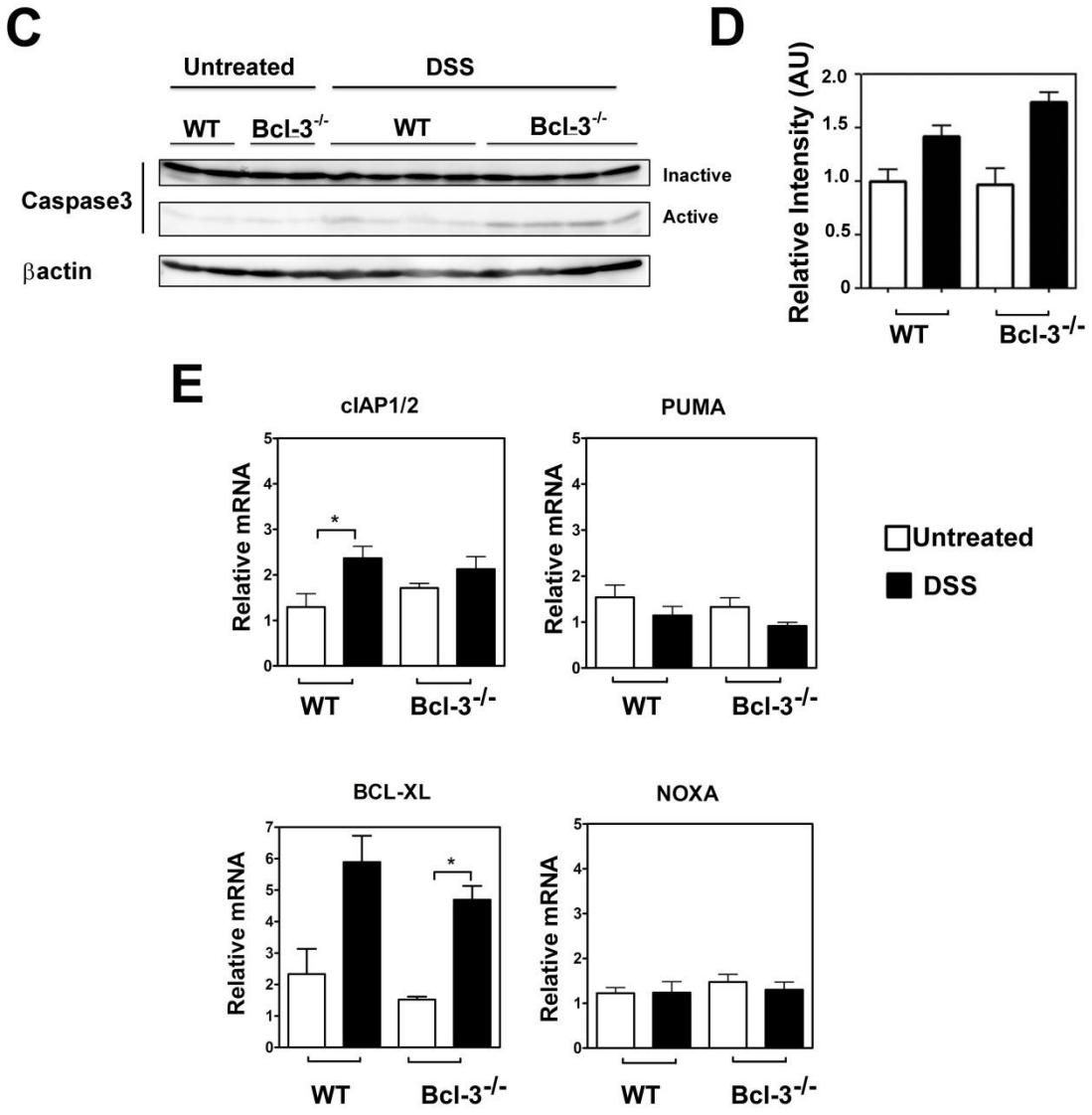

Figure 3.14: Analysis of cell death during colitis in Bcl-3$^{-/-}$ mice

(C) Western blotting for inactive (32kDa) and active (17kDa) caspase-3 in distal colon tissue of control and DSS treated WT and Bcl-3$^{-/-}$ mice. (C) qRT-PCR analysis of PUMA, Bcl-XL, cIAP1/2 and NOXA mRNA in distal colon tissue of control and DSS treated WT and Bcl-3$^{-/-}$ mice. Data is represented as relative mRNA expression as determined by the $2^{-\Delta\Delta CT}$ method. Statistical significance was calculated using Mann Whitney U Tests with $p<0.05$ (*), $p<0.01$ (**) and $p<0.001$ (***). Data expressed as mean ± SEM (n = 7). White bars represent 200μM scale bar.

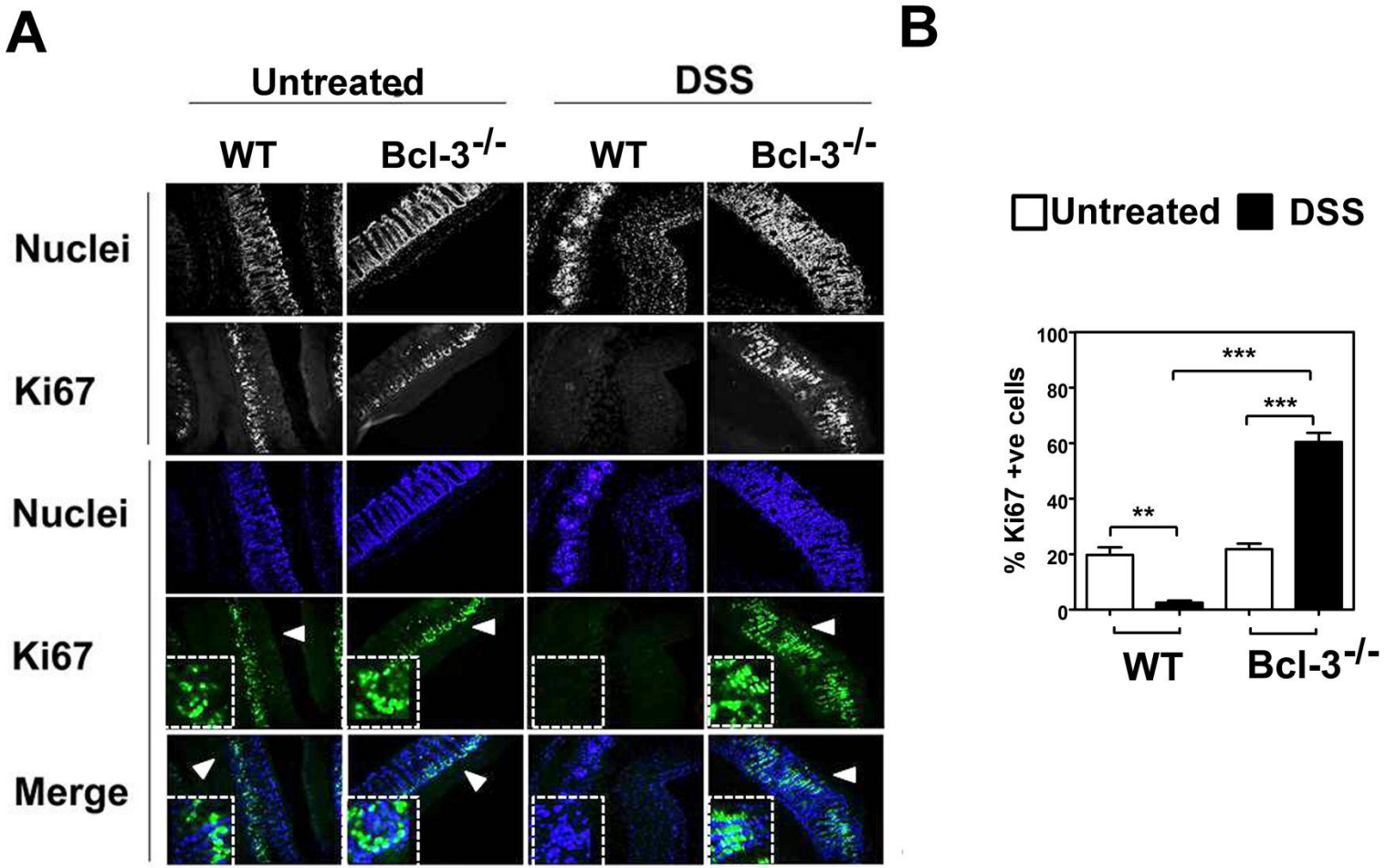

Figure 3.15: Elevated epithelial cell proliferation in DSS treated Bcl-3$^{-/-}$ mice (Figure Legend – next page)

Figure 3.15: Elevated epithelial cell proliferation in DSS treated Bcl-3$^{-/-}$ mice

(**A**) Ki67 immunofluorescence staining of 6μm distal colon sections. Data is representative of greater than seven fields of view per tissue section at 20X (n = 7 per group). (**B**) Quantification of Ki67 positive cells was performed on seven fields of view per tissue section at 20X (n = 7 per group). Statistical significance was determined using Mann Whitney U Tests with $p< 0.001$ (***), $p<0.01$ (*) and $p<0.05$ (*).

3.4 Discussion

This study investigated the expression of Bcl-3 in human IBD and also the role of Bcl-3 in DSS-induced colitis in the mouse. We found that Bcl-$3^{-/-}$ mice develop less severe colitis compared to litter mate control wild type mice. These findings were unexpected given the previously described role of Bcl-3 as a negative regulator of inflammatory gene expression [111] and the recent identification of reduced Bcl-3 expression as a potential risk factor for Crohn's disease [170]. However, the resistance of Bcl-$3^{-/-}$ mice to experimentally induced colitis correlates with our analysis of Bcl-3 expression in the colon of IBD patients which was significantly increased when compared to healthy individuals. It is possible that the identified SNPs [170] may lead to increased Bcl-3 expression rather than decreased expression as predicted. Thus, our findings suggest that increased expression of Bcl-3 rather than reduced expression may be a potential risk factor for IBD. This study also identifies a novel role for Bcl-3 in regulating intestinal epithelial cell proliferation during DSS-induced colitis.

DSS has shown differential sensitivity in different murine strains [203, 204]. Therefore we tested 1%, 2% and 2.5% DSS doses to determine the minimal dose of DSS required to induce colitis in Bcl-$3^{-/-}$ and WT litter mate control mice. Analysis of DAI scoring revealed that the 2% dose was the minimal dose required to induce colitis in the WT littermate controls. Furthermore, this dose identified Bcl-$3^{-/-}$ mice as less sensitive to DSS than their WT counterparts. This difference was not evident in the 2.5% DSS dose with both WT and Bcl-$3^{-/-}$ mice demonstrating equivalent sensitivity towards DSS. In addition, the 1% DSS dose was not sufficient to induce intestinal inflammation in both groups. This data suggested that the higher dose of

DSS induced a powerful inflammatory response in both groups masking the role of Bcl-3 in regulating intestinal inflammation in this model. Thus, the 2% DSS dose was chosen for all downstream experiments.

Analysis of cytokine expression during DSS-induced colitis in Bcl-3$^{-/-}$ mice revealed a robust inflammatory response following DSS treatment characterised by significantly elevated levels of pro-inflammatory cytokines TNF-α, IL-6 and IL-1β. The levels of these cytokines in Bcl-3$^{-/-}$ mice were similar to WT mice indicating that Bcl-3 does not act as a negative regulator of TNF-α, IL-6 and IL-1β expression in the context of DSS-induced colonic inflammation. Histological analysis further supported this observation as significant oedema and leukocyte infiltration were present in Bcl-3$^{-/-}$ colonic tissue sections and to a similar degree as that seen in WT mice. Furthermore, equivalent composition of cellular infiltrates was observed between WT and Bcl-3$^{-/-}$ mice which demonstrated that the inflammation was qualitatively, as well as quantitatively, similar to WT mice. This data suggests that Bcl-3 may not play a significant role in the regulation of inflammation in the colon. Of note, gene expression analysis and histological analysis was performed at the experimental endpoint therefore there may have been increased inflammation after DSS treatment. Thus analysis of gene expression and cellular infiltration at an earlier time point during DSS treatment may give additional information of the role of Bcl-3 in the induction of intestinal inflammation.

Despite a robust inflammatory response following DSS treatment, the colonic tissue architecture in Bcl-3$^{-/-}$ mice, in particular the epithelial features remain intact. Following DSS treatment intestinal epithelial cell proliferation in Bcl-3$^{-/-}$ mice was significantly enhanced whereas in WT mice it was absent. The increased proliferation in Bcl-3$^{-/-}$ mice correlates with the maintenance of tissue architecture

and structure and suggests that the resistance to DSS-induced colitis of Bcl-3$^{-/-}$ mice results from increased regeneration of the epithelium. It is also noteworthy that Bcl-3 acts a negative regulator of myeloid progenitor proliferation and differentiation, and is essential for limiting granulopoiesis under inflammatory conditions [109]. This study identifies a novel role for Bcl-3 in regulating intestinal epithelial cell proliferation under inflammatory but not homeostatic conditions. Our identification of Bcl-3 as a negative regulator of intestinal epithelial cell proliferation during colitis suggests additional physiological functions for Bcl-3 beyond its role as a negative regulator of pro-inflammatory gene expression.

The dual role of NF-κB as a key mediator of inflammation and a critical driver of epithelial cell survival and proliferation has rendered it a complex and difficult therapeutic target in IBD. Transgenic mice in which NF-κB activity has been selectively inhibited in the intestinal epithelium develop spontaneous colitis due to failure of the epithelial barrier function while an increase in intestinal NF-κB activity also leads to severe inflammation [189]. The data obtained in this study however suggests that certain regulatory components of the NF-κB pathway such as Bcl-3 may play a more important role in the epithelium rather than the immune system in the colon. We have previously demonstrated that Bcl-3 expression is induced by inflammation [111]. Given that the proliferation of intestinal epithelial cells is normal in Bcl-3$^{-/-}$ mice it is likely that inflammation induced expression of Bcl-3 in the epithelium during colitis contributes to the development of disease. Thus, by targeting Bcl-3 it may be possible to enhance epithelial cell proliferation and regeneration without exacerbating inflammation in the intestine. The potential therapeutic benefits to IBD are highlighted by the reduced clinical score and lack of weight loss in DSS-treated Bcl-3$^{-/-}$ mice.

In summary, we describe a novel function for Bcl-3 in regulating epithelial cell proliferation during DSS-induced colitis. The increased epithelial cell proliferation and regeneration in Bcl-3$^{-/-}$ mice further supports a role for NF-κB in maintaining the integrity of the intestinal epithelium. This report suggests that targeting Bcl-3 in colitis may be therapeutically beneficial in IBD through increasing tissue regeneration and repair in the colon without exacerbating the inflammatory response.

4. Identification of a novel hybrid macrophage polarisation state following recovery from LPS tolerance

4.1 Abstract

Lipopolysaccharide (LPS) tolerance is an essential immune-homeostatic response towards repeated exposure to LPS which prevents excessive inflammatory responses. LPS tolerance induces a state of altered responsiveness in macrophages resulting in repression of pro-inflammatory gene expression and increased expression of factors which mediate the resolution of inflammation. In this study the transcriptional plasticity of macrophages was analysed following LPS tolerance using genome-wide transcriptional profiling. We demonstrate that LPS tolerance is a transient state and that the expression of pro-inflammatory genes is restored to levels comparable to the acute response to LPS. However, following recovery from LPS tolerance a number of genes remained locked in a tolerisable state including IL-33, CD86, IL-10 and NFIL3. Furthermore, we identify of a number of genes uniquely induced following recovery from LPS tolerance. Thus, macrophages adopt a unique transcriptional profile following recovery from LPS tolerance and have a distinct expression pattern of regulators of antigen presentation, antiviral responses and transcription factors. Our data suggests that recovery from LPS tolerance leads to a novel hybrid macrophage activation state which is pro-inflammatory and microbicidal in nature but which possesses a regulatory anti-inflammatory profile distinct from that of LPS tolerant and LPS activated (M1) macrophages.

4.2 Introduction

Inflammation is a powerful, organised and complex immunological response towards infection and tissue damage. Toll-like receptors (TLR) are central to innate inflammatory responses and are key sensors of microbial presence and host damage [5]. Toll-like receptor 4 (TLR4) is the most extensively studied TLR which recognises lipopolysaccharide (LPS), an outer membrane cell wall component of gram negative bacteria. Ligation of TLR4 triggers intracellular signalling pathways culminating in the production of pro-inflammatory cytokines, chemokines and type 1 interferons to effectively clear infection [5, 12, 13]. Chronic or repeated exposure of macrophages to LPS leads to a phenomenon termed LPS tolerance which represents a state of altered responsiveness towards additional LPS challenge. The most notable feature of LPS tolerance is the sharp reduction in pro-inflammatory cytokine expression in response to LPS stimulation, including TNF-α and IL-6. LPS tolerance is critical in limiting the innate response to infection in order to reduce host damage and promote the resolution of inflammation [36, 125, 205]. Failure to enforce LPS tolerance may have profound consequences including death due to excessive and uncontrolled cytokine production [36, 206].

Recent transcriptional profiling of macrophages identified two classes of LPS induced genes; those that are suppressed during LPS tolerance, so-called *tolerisable* (class T) genes which include TNF-α and IL-6, and those genes whose expression is maintained or even increased during LPS tolerance, so called *non-tolerisable* genes (class NT) which include anti-microbial and anti-inflammatory genes. This study identified inducible chromatin modifications associated with LPS tolerance which promoted a global transcriptional switch in macrophage gene expression. This

unique transcriptional signature drives a phenotypic switch in macrophage polarisation from a pro-inflammatory to an anti-inflammatory pro-resolution state [75]. A number of negative regulators of TLR-induced responses have been identified which are critical in promoting LPS tolerance. These include regulators of TLR4 induced signal transduction such as IRAK-M, TOLLIP, SHIP, A20 and transcriptional regulators such as Bcl-3 [39, 43, 47, 49, 69, 111, 207, 208].

Macrophages display a spectrum of activation states which are broadly described as classical (M1), alternative (M2) and regulatory (M2-like/M2b) [127, 140]. M1 macrophages are pro-inflammatory cytotoxic phagocytes and promote Th1 adaptive immune responses following TLR and IFN-γ challenge [127, 140]. In contrast, IL-4 and IL-13 specifically polarise macrophages to an alternatively activated M2 state. These cells are anti-inflammatory, promote tissue remodelling and are important in mediating Th2 immunity towards fungal and parasitic infections in addition to mounting allergic responses [127, 144, 145]. Regulatory macrophages are immune regulatory cells that display both anti-inflammatory and pro-inflammatory features through suppression of some pro-inflammatory genes and increased production of IL-10, while maintaining antigen presenting capacity. Immune complexes in conjunction with TLR activation polarise macrophages into a regulatory state. In addition, other stimuli including glucocorticoids, prostaglandins and apoptotic cells have been implicated in regulatory macrophage polarisation. While regulatory macrophages are distinct from both M1 and M2 macrophages, these cells share some overlapping anti-inflammatory properties with M2 cells [127]. These three macrophage populations represent the main groups in the emerging spectrum of macrophage polarisation however many hybrid macrophage activation states exist owing to the large number of activation stimuli that macrophages encounter *in vivo*.

Tumour associated macrophages, intestinal macrophages and LPS tolerised macrophages are described as representing hybrid macrophage populations which share overlapping M1/M2 and regulatory properties while expressing distinct features unique to their polarisation state and the microenvironment they reside. [152-154].

LPS tolerance polarises macrophages into an anti-inflammatory macrophage activation state [152-154]. Although transcriptomics analysis has been performed on LPS tolerance [42, 75, 153], the plasticity of this state has not been explored using the same approach. In this chapter the persistence of LPS tolerance was analysed using transcriptional profiling and bioinformatics analysis. We utilised a model of LPS activation of murine macrophages which generated naïve (N), LPS activated/ acute response to LPS (A = M1) and LPS tolerised (T) polarisation states. Our data demonstrates that LPS tolerance is a transient state in macrophages and that following LPS tolerance macrophages adopt a previously unreported hybrid activation state, which we here term recovered macrophage (RM) to reflect the recovery from LPS tolerance. Using transcriptional analysis we demonstrate that recovery from LPS tolerance, as defined by cytokine expression, is associated with a global change in the transcriptional profile of macrophages. Thus RM cells display increased expression of tolerisable genes such as TNF-α and IL-6 following LPS stimulation, equivalent to that of an LPS activated M1 polarised cell. However, a number of genes, including IL-33 remained locked in an LPS tolerisable state and do not recover from LPS tolerance a feature not typical of M1 cells. Furthermore, recovered macrophages express a subset of inducible genes not observed in M1 or the LPS tolerised states. In addition, RM cells display a distinct pattern of expression of regulators of antigen presenting and anti-viral responses. Our data suggests that

recovery from LPS tolerance leads to a novel hybrid macrophage activation state which is pro-inflammatory and cytotoxic in nature but which possesses a regulatory anti-inflammatory profile distinct from that of LPS tolerant and LPS activated (M1) macrophages.

4.3 Results

4.3.1 LPS Tolerance Recovery Model

A model of LPS tolerance was designed using murine bone marrow derived macrophages (BMDMs) based on previous studies of TLR tolerance in human monocytes and murine BMDMs [42, 75]. In addition to naïve (N), acute response to LPS – M1-like (A) and LPS tolerant (T) macrophages, we also analysed macrophages for up to four days following the induction of LPS tolerance (R). Briefly, LPS tolerance (T) was induced by stimulation with LPS (100ng/ml) for 8 hours followed by washout of LPS with fresh culture medium. Cells were then rested for an additional 16 hours prior to re-stimulation with LPS (100ng/ml) for 4 hours. Recovery from LPS tolerance (R) was analysed following an additional resting period of three days prior to re-stimulation with LPS (100ng/ml) for 4 hours. Additional resting days (D2, D4) are specified within the text where appropriate. The acute response to LPS was measured in cells which received no pre-stimulation with LPS prior to stimulation with 100ng/ml LPS for 4 hours (A). Naïve macrophages (N) remained untreated (Figure 4.1).

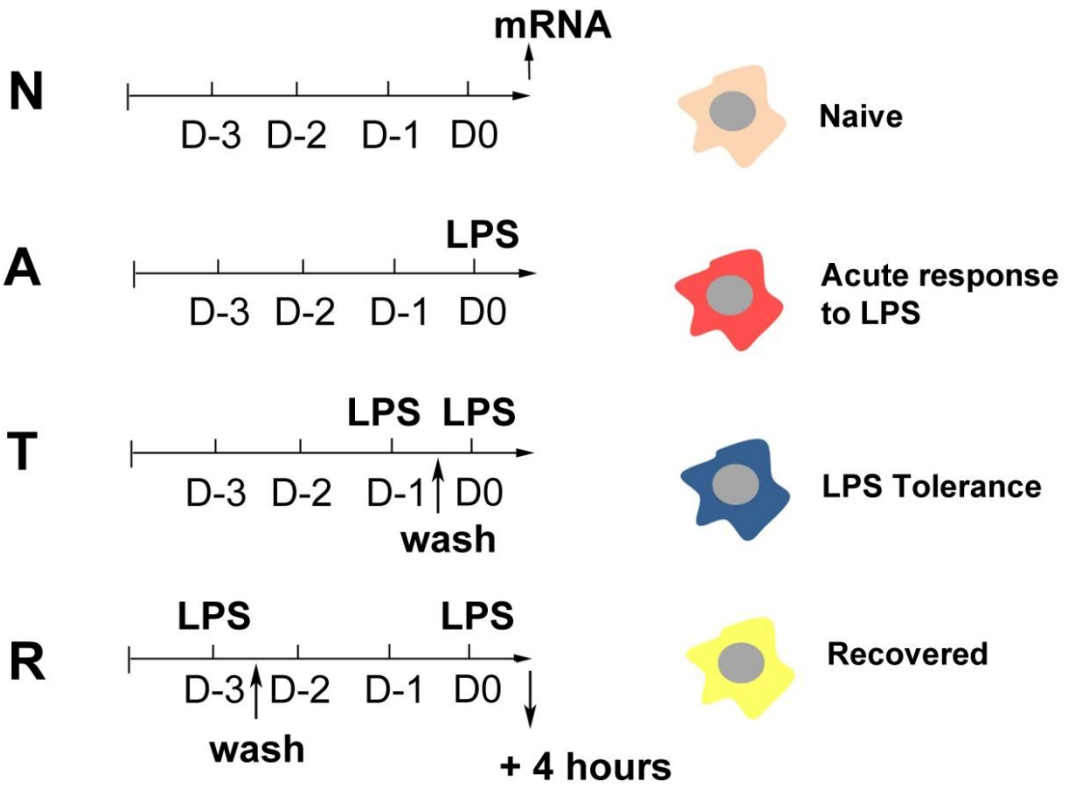

Figure 4.1: LPS Tolerance Recovery model

Four individual macrophage activation states were induced in the LPS tolerance recovery model; Naïve macrophage (N), Acute response to LPS/ M1 (A), LPS tolerant (T) and Recovered macrophage (R).

4.3.2 Confirmation of LPS tolerance induction

To confirm suppression of pro-inflammatory gene expression and successful induction of an LPS tolerant state in macrophages, gene expression for a validated LPS tolerisable pro-inflammatory cytokine, IL-6 [75] was measured by qRT-PCR (Figure 4.2). LPS inducible IL-6 mRNA levels were suppressed in the tolerant group (T) when compared to the cells of the acute response to LPS ($p<0.001$) (A). In contrast, cells stimulated with LPS two to four days (D2 – D4) prior to re-stimulation (recovery) demonstrated inducible gene expression at all stages of recovery from LPS tolerance (D2, D3 and D4) when compared to the LPS tolerant group ($p<0.001$ D2 and D3, $p<0.05$ D4). No difference in IL-6 gene expression was found between the day 2 and day 3 recovered groups and the acute response group (A) (Figure 4.2). Day 3 was found to represent the optimal time point of recovery from LPS tolerance with IL-6 gene expression returning to comparable expression levels as the acute response group (A). All subsequent experiments performed used day 3 (D3) as the time point of recovery from LPS tolerance.

To investigate if recovery from LPS tolerance was specific to IL-6, gene expression of two additional LPS inducible tolerisable genes (T genes) [75, 111] was measured by qRT-PCR. The pro-inflammatory genes CXCL10 and TNF-α were induced in the recovered group (R) to comparable levels as the LPS activated group (A) (Figure 4.3). In addition, gene expression for CXCL10 and TNF-α was measured in an independent macrophage population to determine if interferon priming of BMDM resulting from CSF-1 dependent induction of type 1 interferons was responsible for the responses we observed in each macrophage group (N, A, T and R) [209]. Thioglycollate elicited macrophages were treated as per the tolerance recovery

model and no difference in gene expression patterns for CXCL10 and TNF-α was found in these cells when compared with BMDMs (Figure 4.3). This data indicates that LPS tolerance is a transient macrophage activation state with recovery of pro-inflammatory gene expression from LPS tolerance optimally achieved three days post LPS tolerance induction.

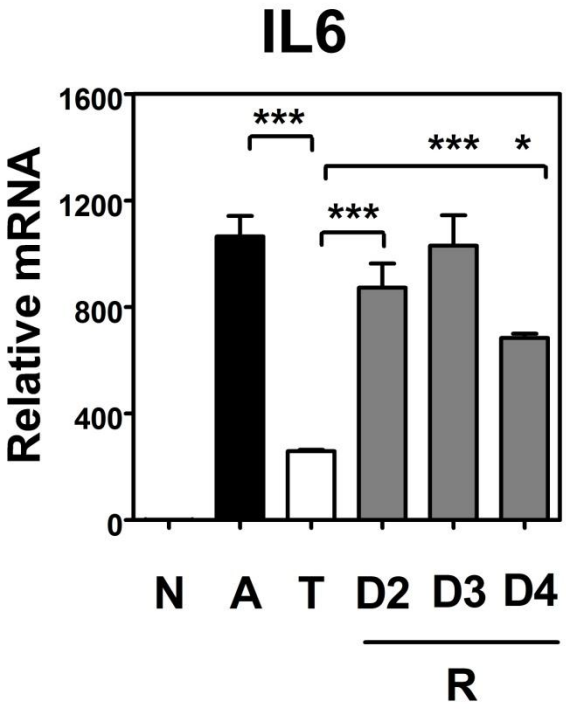

Figure 4.2: Confirmation of LPS tolerance induction

IL-6 gene expression was measured for each macrophage activation state in the LPS tolerance recovery model following 4 hours of re-stimulation by qRT-PCR. Differences between groups were measured by one-way ANOVA with Tukey's post hoc test with $p<0.05$ (*), $p<0.01$ (**) and $p<0.001$ (***). N = Naïve, A = acute response to LPS, T = LPS Tolerance and R = Recovery (D2 = 2 days rest, D3 = 3 days rest and D4 = 4 days rest). Data is representative of greater than four independent experiments and measured as relative mRNA as determined by the $2^{-\Delta\Delta CT}$ method.

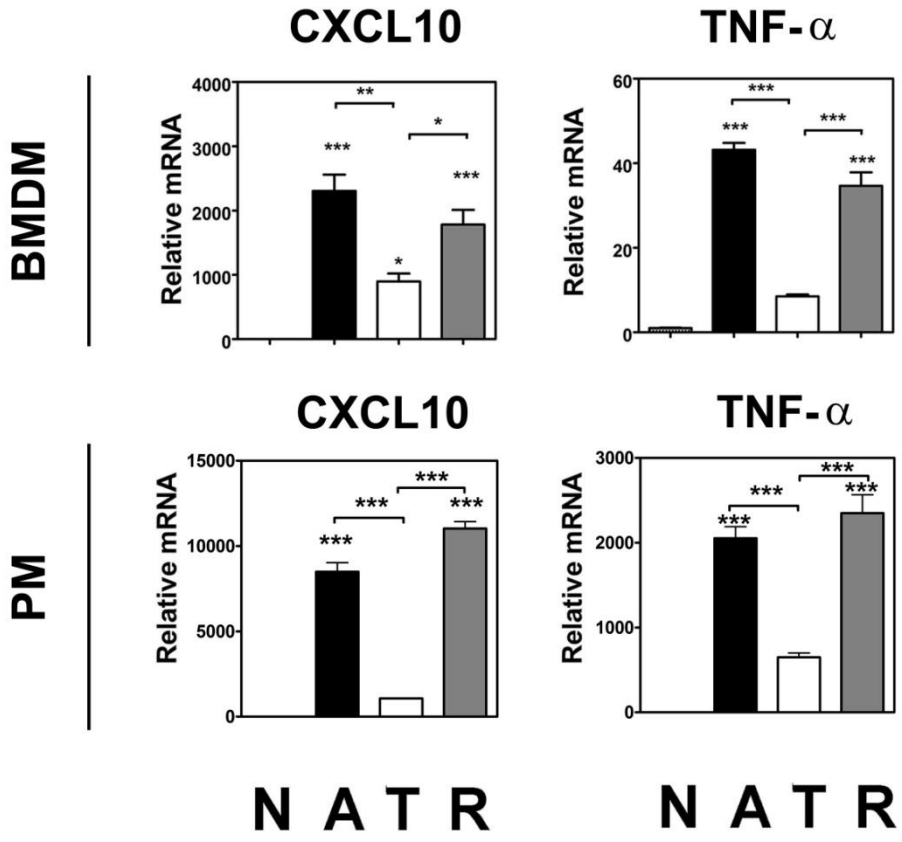

Figure 4.3: Pro-inflammatory gene induction following recovery from LPS Tolerance

Gene expression of CXCL10 and TNF-α was measured for each macrophage activation state in the LPS tolerance recovery model following 4 hours of re-stimulation by qRT-PCR. Differences between groups were measured by one-way ANOVA with Tukey's post hoc test with $p<0.05$ (*), $p<0.01$ (**) and $p<0.001$ (***). N = Naïve, A = activated, T = LPS Tolerance and R = Recovery. Data is representative of greater than four independent experiments and measured as relative mRNA as determined by the $2^{-\Delta\Delta CT}$ method. BMDM (bone marrow derived macrophage), PM (thioglycollate elicited peritoneal macrophage).

4.3.3 Recovery from LPS Tolerance results in a global shift in the gene expression profile of macrophages

To investigate the global gene expression profile of macrophages that recovered from LPS tolerance, microarray analysis was performed on all four macrophage groups (N, A, T and R). Initial *K*-means clustering analysis revealed a unique transcriptional signature for each macrophage treatment group with 10 unique gene clusters (Figure 4.4A-B). Cluster 1 contains genes that are specifically induced by LPS in the tolerant group (T) but not the acute response (A) or recovered groups (R). Interestingly, while a reduction in expression of these genes was measured in the recovered group compared to the LPS tolerant group (T), gene expression levels were increased when compared with the acute response group (A). In contrast, clusters 3 and 5 contain genes that were suppressed in the LPS tolerant group (T) but were inducible again following recovery from LPS tolerance. This data supports our initial pro-inflammatory inducible gene expression findings following recovery from LPS tolerance (Figure 4.2). Interestingly, cluster 5 genes were induced to a greater level in the recovered group relative to the acute response group (A) while cluster 3 genes were induced to a lesser degree. Of note, cluster 6 contains genes that are highly induced following recovery from LPS tolerance when compared to all other groups, thus identifying a unique transcriptional signature for this group (Figure 4.4A and B).

Correspondence analysis (COA) identified a 30% (PC1) measure of variance between the different macrophage groups (Figure 4.5). This suggests that each macrophage group in our model represents a distinct macrophage state. The acute response (A) and recovered (R) macrophage populations clustered closely together

indicating overlapping transcriptional profiles between these groups. However, upon closer examination PC4 (8% variance between groups) measured differences between the acute response (A) and the recovered group (R) further supporting a unique gene expression profile in RM cells. This finding indicates a high degree of macrophage plasticity following the induction of LPS tolerance. Taken together, these initial bioinformatics findings confirm that LPS tolerance is a transient transcriptional macrophage state and that recovery from LPS tolerance involves a global change in the macrophage gene expression profile. This gene expression profile of macrophages following recovery from tolerance shares similarity to the profile of the acute response group (A) suggesting that recovery from tolerance polarises macrophages towards a pro-inflammatory classically activated like (M1-like) state.

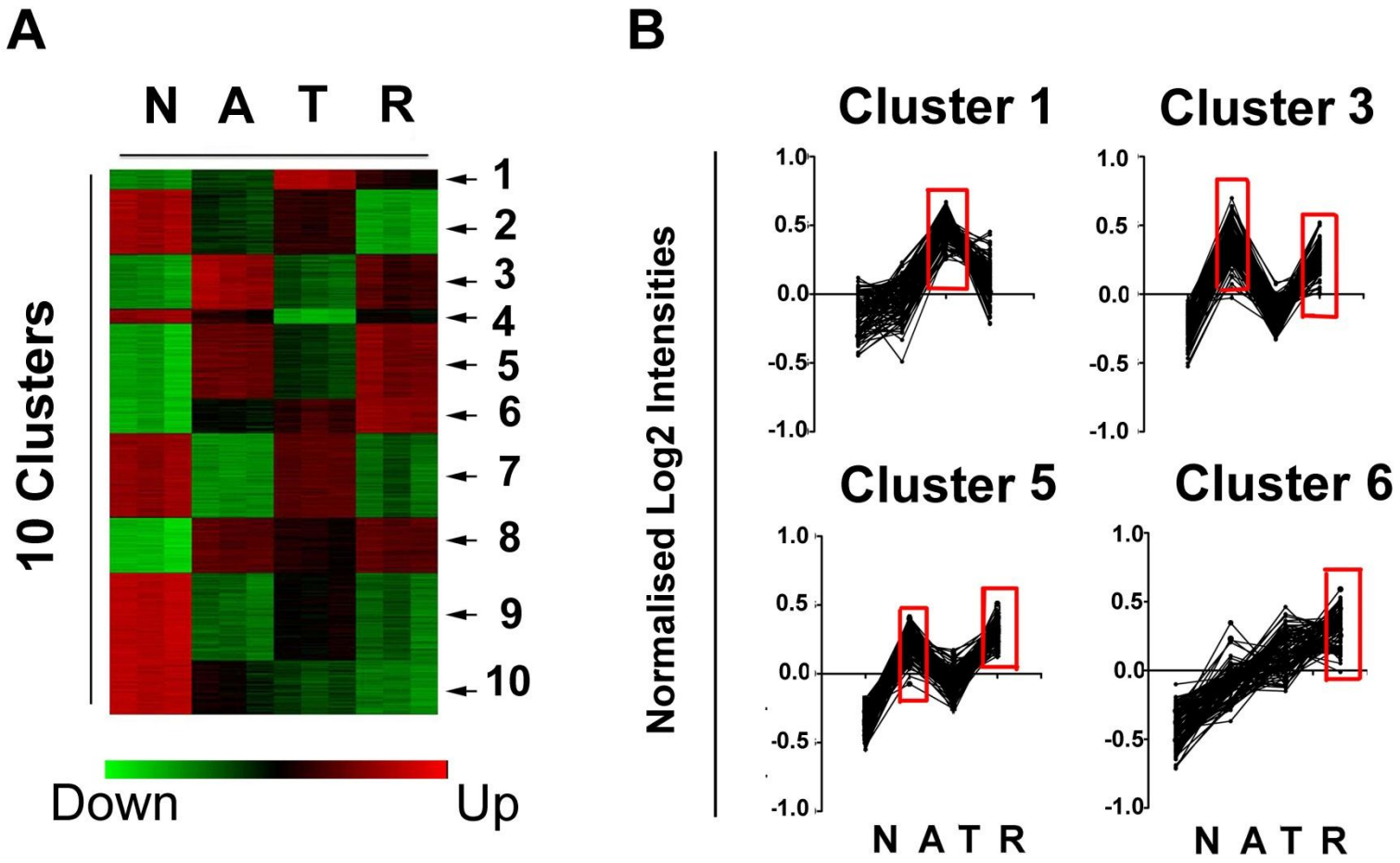

Figure 4.4: Recovery from LPS Tolerance results in a global shift in the transcriptional profile of macrophages (Figure legend –Next page)

Figure 4.4: Recovery from LPS Tolerance results in a global shift in the transcriptional profile of macrophages

(A) Microarray gene expression profiling was performed on Naive, Activated, Tolerant and Recovered macrophages (N, A, T and R). Transcriptional profiling was analysed using *K*-means clustering and identified 10 unique gene profile clusters. (B) Extrapolated individual gene clusters representing unique gene expression trends. Normalised expression values are represented in Log2. Statistical significance was determined using Benjamini Hochberg multiple correction testing. Data is represented as log2 fold change of ± 0.585 (1.5 fold) and $p<0.05$. N = Naïve, A = acute response to LPS, T = LPS Tolerance and R = Recovery.

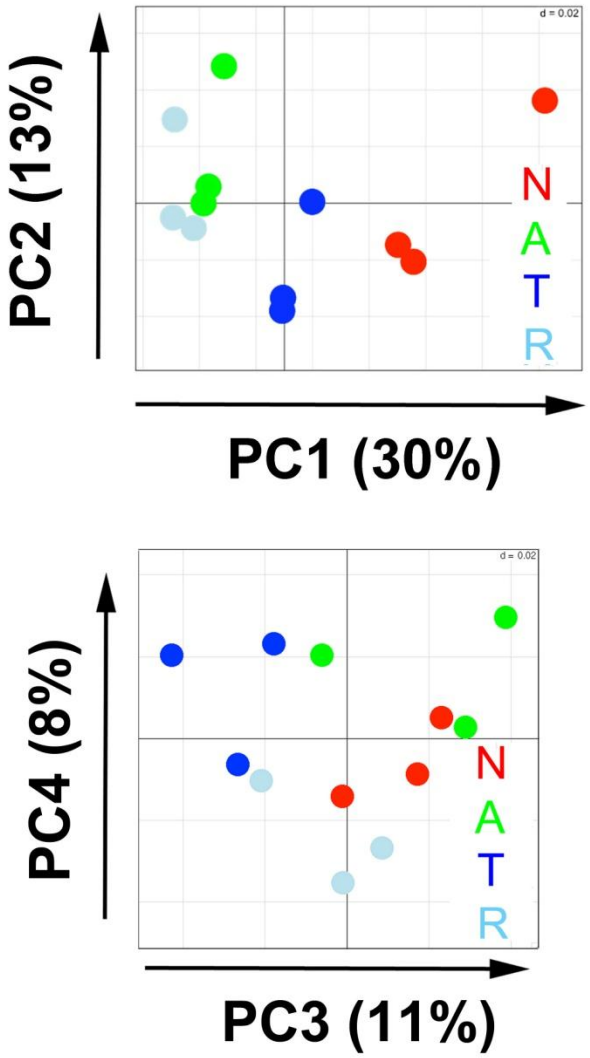

Figure 4.5: Correspondence analysis (COA): Recovery from LPS Tolerance involves a global shift in the transcriptional profile of macrophages

Correspondence analysis (COA) was performed on the LPS tolerance recovery microarray experiments. PC1 identified 30% variance between individual groups (N, A, T and R). PC2 revealed 13% variance between individual microarray replicate experiments. PC3 (11%) identified differences between the naïve (N) and tolerant (T) group with PC4 (8%) revealing differences between the acute response (A) and recovered (R) groups. N = Naïve, A = acute response to LPS, T = LPS Tolerance and R = Recovery. Statistical significance was determined using Benjamini Hochberg multiple correction testing (log2 fold change of ± 0.585 (1.5 fold) and $p<0.05$).

4.3.4 Differentially expressed genes and gene ontology enrichment

To further characterise the gene expression signature of recovered macrophages (R), we identified differentially expressed genes in the recovered group relative to naïve (N), acute response (A) and tolerant (T) groups (± 1.5 fold change, $p<0.05$). Recovery from LPS tolerance resulted in induced expression of 3,536 genes with 4,813 suppressed when compared with the naïve group. This gene list was visualised by hierarchical clustering analysis which revealed that a large proportion of LPS tolerisable genes (T genes) were re-induced following recovery from LPS tolerance to levels comparable with the LPS activated group (Figure 4.6A and B). Upon further examination the top 30 up-regulated and down regulated genes identified in the recovered group relative to the naïve group, revealed striking similarities with cells of the acute response group (Figure 4.6A and B, Table 4.1, Table 4.2). The pro-inflammatory genes CXCL10, TNF-α, IL-27, CD40, CD69, SOCS3 and MX2 were all found to be within the top 30 inducible genes in the recovered group based on fold change relative to the naïve group (Figure 4.6B and Table 4.1). When expression levels of these seven pro-inflammatory genes were compared with the levels induced in LPS activated cells relative to naïve cells, no difference in gene induction was found (Table 4.3).

Gene ontology analysis using the online bioinformatics tool DAVID [183] was then used to determine the biological significance of differentially expressed genes. Unsurprisingly, *immune response*, *TLR signalling*, *antigen presentation*, *cytokine regulation*, and *defence response* were found to be the most significantly enriched gene ontology terms from the genes up-regulated in the recovered group relative to the naïve group (Table 4.4 – Table 4.5). This data correlates with differentially

expressed genes and biological processes associated with macrophages of the acute response compared with untreated controls from this study (Figure 4.7, Table 4.6 and Table 4.7) Furthermore the gene ontology terms *cell cycle*, *cell division* and *mitosis* were the most significantly enriched biological processes found from the analysis of genes up-regulated in the recovered group (R) relative to the tolerant group (T) (Figure 4.8, Table 4.8 – Table 4.11). This data suggests that following recovery from LPS tolerance macrophages are pro-inflammatory cells with increased cellular proliferative capacity compared to anti-inflammatory tolerised cells.

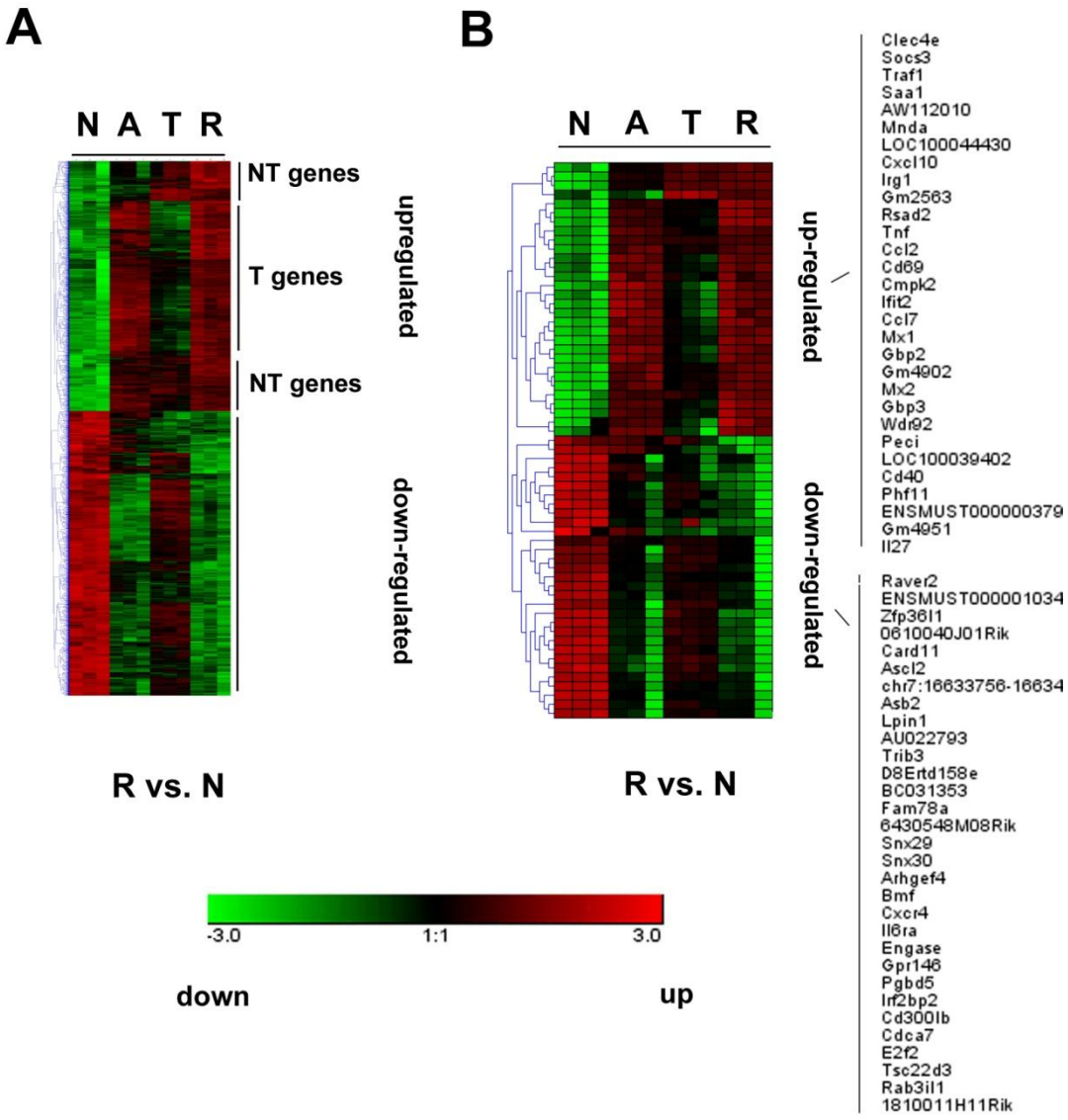

Figure 4.6: Differentially expressed genes: Recovery (R) vs. Naïve (N)

(A) Hierarchical clustering heatmap illustrating up-regulated (red) and down regulated (green) genes identified by pairwise comparisons between the recovered group (R) relative to the Naïve group (N). (B) Hierarchical clustering heatmap representing the top 30 (largest to smallest fold change) differentially expressed up-regulated and down-regulated genes in the recovered group (R) relative to the naïve group (N) (data extrapolated from total differential expressed genes - Figure 4.6A). Differentially expressed genes were identified using fold change ± 1.5 fold (0.585 Log2) and a *P* value of less than 0.05 ($p<0.05$). N = Naïve, A = Activated, T = LPS Tolerance and R = Recovery. T gene = toleriable gene, NT gene = non-tolerisable gene.

Table 4.1: Top 30 up-regulated genes – Recovery (R) vs. Naïve (N)

Differentially expressed genes were identified using a 1.5 fold change and a *P* value of less than 0.05 ($p<0.05$). Genes are ranked by largest to smallest fold change.

Rank	Gene Name	Fold change	*P* value
1	**Cxcl10**	202.95	1.49E-02
2	**Irg1**	162.80	1.76E-02
3	**Rsad2**	155.63	2.21E-02
4	**Cmpk2**	128.80	1.64E-02
5	**Cd40**	125.45	2.56E-03
6	**TNF**	108.53	2.92E-02
7	**Mnda**	108.46	1.24E-02
8	**Mx1**	103.18	1.07E-02
9	**Gbp2**	101.76	1.27E-02
10	**AW112010**	98.70	2.13E-02
11	**Clec4e**	97.34	2.41E-02
12	**Ifit2**	96.47	1.41E-02
13	**Socs3**	96.40	6.12E-03
14	**Traf1**	94.75	6.09E-03
15	**Cd69**	93.38	8.39E-03
16	**LOC100044430**	85.51	1.83E-02
17	**Wdr92**	81.80	1.62E-02
18	**Mx2**	81.01	1.01E-02
19	**Gm4902**	79.62	1.16E-02
20	**Gbp3**	79.18	9.70E-03
21	**Peci**	78.74	1.34E-02
22	**Gm2563**	76.48	2.90E-02
23	**Ccl2**	76.37	3.51E-02
24	**Phf11**	72.71	8.63E-03
25	**Ccl7**	71.95	2.14E-02
26	**Saa1**	69.60	4.67E-02
27	**Gm4951**	68.45	3.55E-03
28	**LOC100039402**	64.31	1.76E-02
29	**ENSMUST00000037976**	63.78	9.80E-03
30	**Il27**	60.46	8.89E-03

Table 4.2: Top 30 down-regulated genes – Recovery (R) vs. Naïve (N)

Differentially expressed genes were identified using a 1.5 fold change and a *P* value of less than 0.05 ($p<0.05$). Genes are ranked by largest to smallest fold change.

Rank	Gene Name	Fold change	*P* value
1	**Fam78a**	-31.41	4.67E-02
2	**BC031353**	-28.09	2.50E-02
3	**6430548M08Rik**	-24.74	3.27E-02
4	**D8Ertd158e**	-22.90	2.34E-02
5	**Rab3il1**	-21.10	6.12E-03
6	**Bmf**	-17.08	1.89E-02
7	**Snx30**	-16.47	3.40E-03
8	**Il6ra**	-14.93	1.84E-04
9	**Asb2**	-14.67	1.09E-04
10	**0610040J01Rik**	-14.66	1.73E-04
11	**Irf2bp2**	-14.61	1.91E-04
12	**Cdca7**	-13.73	3.57E-03
13	**Tsc22d3**	-13.29	1.74E-02
14	**E2f2**	-13.13	6.11E-03
15	**Ascl2**	-12.28	1.40E-05
16	**Snx29**	-12.25	1.13E-02
17	**Card11**	-11.76	7.00E-06
18	**chr7:16633756-16634410_F**	-11.67	1.50E-05
19	**Arhgef4**	-11.20	1.06E-03
20	**Zfp36l1**	-11.17	1.41E-03
21	**Gpr146**	-11.08	9.60E-05
22	**Raver2**	-11.04	4.20E-05
23	**Engase**	-10.67	1.14E-04
24	**Cxcr4**	-9.95	2.60E-05
25	**Lpin1**	-9.84	1.22E-04
26	**ENSMUST00000103426**	-9.58	1.90E-05
27	**AU022793**	-9.55	1.02E-04
28	**Pgbd5**	-9.49	1.82E-04
29	**Trib3**	-9.34	3.21E-03
30	**Cd300lb**	-9.20	1.27E-03

Table 4.3: Inflammatory expression differences; Recovery (R) and acute response (A)

Differentially expressed genes selected from the top 30 inducible gene lists (Table 4.1 and Table 4.6). Genes were identified using a 1.5 fold change and a *P* value of less than 0.05 ($p<0.05$) of either group relative to the naïve group (R vs. N, A vs. N). Genes are ranked by largest to smallest fold change.

	Acute response (A)		Recovered (R)	
Gene Name	**Fold change**	***P* value**	**Fold change**	***P* value**
CXCL10	209.82	5.48E-02	202.95	4.68E-02
TNF	104.91	1.02E-02	108.53	2.93E-02
IL27	56.65	4.07E-02	60.46	3.19E-02
SOCS3	58.12	5.12E-02	96.40	2.48E-02
CD69	129.61	2.65E-02	93.38	3.02E-02
MX2	92.35	3.13E-02	81.01	3.55E-02
CD40	88.59	2.35E-02	125.45	1.30E-02

Table 4.4: Gene Ontology – Recovery (R) vs. Naïve (N)

Gene ontology terms were identified using DAVID based on differentially expressed inducible genes identified using a 1.5 fold change and a *P* value of less than 0.05 ($p<0.05$).

Recovery vs. Naïve: Gene list up-regulated	
Term	***P*-value**
immune response	2.30E-32
phosphoprotein	5.10E-20
Toll-like receptor signaling pathway	1.00E-13
inflammatory response	2.00E-12
antigen processing and presentation	2.70E-12
regulation of cytokine production	4.50E-12
Cytokine-cytokine receptor interaction	1.80E-11
response to wounding	4.70E-11
inflammatory response	5.10E-11
defense response	2.00E-10
positive regulation of cytokine production	2.60E-10
cytokine	3.80E-10
immune response	4.60E-10
NOD-like receptor signaling pathway	1.70E-09
cytokine activity	2.70E-09
protein kinase cascade	3.00E-09
cell death	5.50E-09
death	8.70E-09
positive regulation of immune system process	1.20E-08
Type I diabetes mellitus	1.40E-08
apoptosis	1.50E-08
programmed cell death	1.60E-08
positive regulation of response to stimulus	3.10E-08
Graft-versus-host disease	6.10E-08
Cytosolic DNA-sensing pathway	1.10E-07
Apoptosis	1.40E-07
regulation of apoptosis	2.00E-07
regulation of immune effector process	2.10E-07
Allograft rejection	3.10E-07
MHC protein complex	3.20E-07

Table 4.5: Gene Ontology – Recovery (R) vs. Naïve (N)

Gene ontology terms were identified using DAVID based on differentially expressed suppressed genes identified using a 1.5 fold change and a *P* value of less than 0.05 ($p<0.05$).

Recovery vs. Naïve: Gene list down-regulated	
Term	***P*-value**
phosphoprotein	3.10E-23
zinc ion binding	9.40E-19
transition metal ion binding	1.00E-15
zinc	1.80E-15
nucleus	1.80E-15
Transcription	3.00E-15
transcription	3.70E-15
GTPase regulator activity	3.20E-13
metal-binding	6.90E-13
nucleoside-triphosphatase regulator activity	7.80E-13
regulation of transcription	1.50E-12
intracellular non-membrane-bounded organelle	1.10E-10
non-membrane-bounded organelle	1.10E-10
regulation of RNA metabolic process	3.40E-10
regulation of transcription, DNA-dependent	7.50E-10
alternative splicing	1.10E-09
regulation of small GTPase mediated signal transduction	1.20E-09
zinc-finger	1.40E-09
cell cycle	2.20E-09
GTPase activator activity	2.20E-09
DNA binding	4.10E-09
response to DNA damage stimulus	5.30E-09
metal ion binding	7.50E-09
small GTPase regulator activity	1.10E-08
DNA metabolic process	1.10E-08
cation binding	1.20E-08
cell cycle	1.40E-08
mitochondrion	1.60E-08
enzyme activator activity	2.00E-08
cellular response to stress	2.20E-08

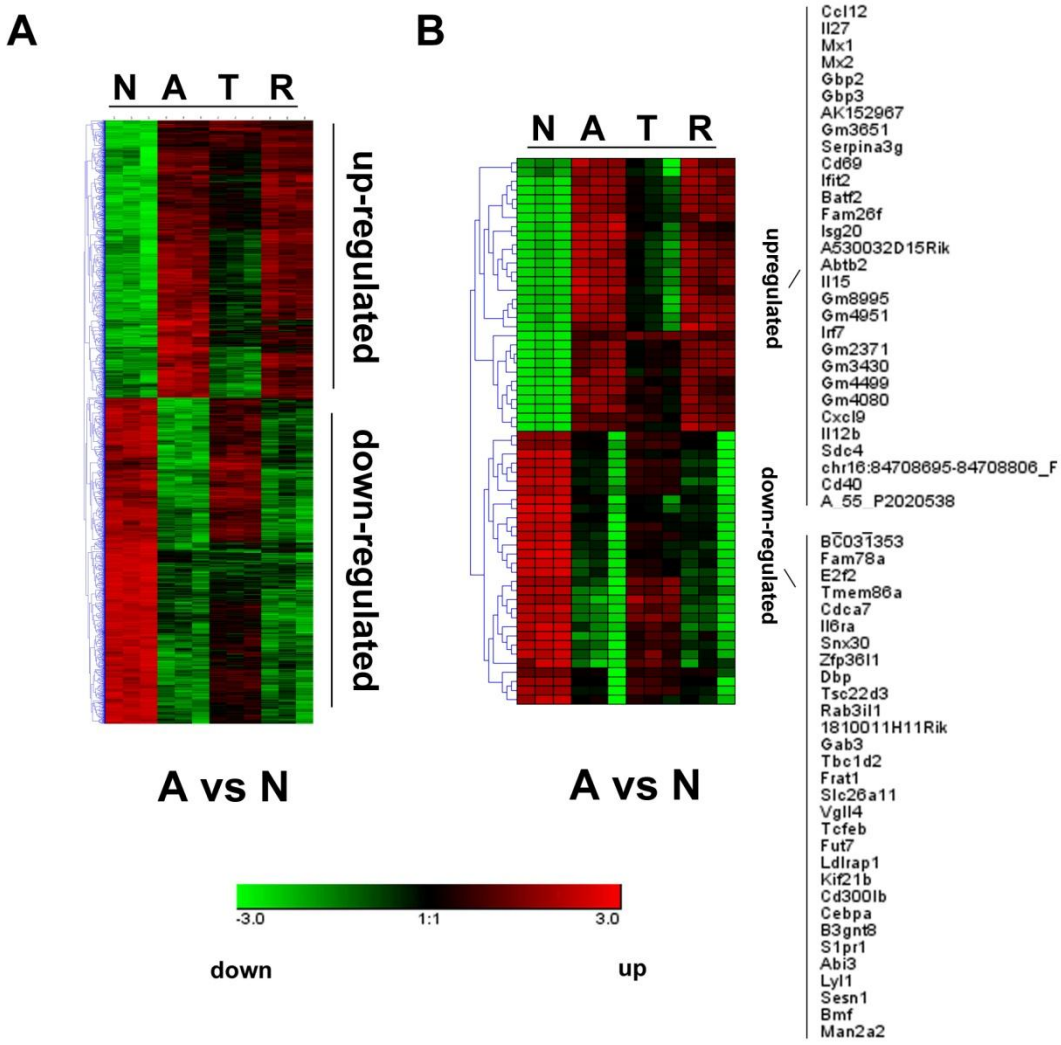

Figure 4.7: Differentially expressed genes: Acute response (A) vs. Naïve (N)

(A) Hierarchical clustering heatmap illustrating all up-regulated (red) and down regulated (green) genes identified by pairwise comparisons between the acute response group (A) relative to the Naïve (N) group. (B) Hierarchical clustering heatmap representing the top 30 (largest to smallest fold change) differentially expressed up-regulated and down-regulated genes in acute response group relative to the naïve group (data extrapolated from total differential expressed genes - Figure 4.7A). Differentially expressed genes were identified using fold change ± 1.5 fold (0.585 Log2) and a *P* value of less than 0.05 ($p<0.05$). N = Naïve, A = Activated, T = LPS Tolerance and R = Recovery.

Table 4.6: Top 30 up-regulated genes – Acute response (A) vs. Naive (N)

Differentially expressed genes were identified using a 1.5 fold change and a *P* value of less than 0.05 ($p<0.05$). Genes are ranked by largest to smallest fold change.

Rank	Gene Name	Fold change	*P* value
1	**Cd69**	129.61	2.63E-02
2	**Ifit2**	123.13	4.31E-02
3	**Gbp2**	108.91	4.69E-02
4	**Mx1**	101.97	4.52E-02
5	**Gm3651**	95.87	2.90E-02
6	**Cxcl9**	94.75	1.56E-03
7	**Mx2**	92.35	3.75E-02
8	**Cd40**	88.59	2.36E-02
9	**Gbp3**	85.98	3.83E-02
10	**Il12b**	73.52	1.80E-05
11	**Batf2**	69.74	3.55E-02
12	**Fam26f**	68.36	2.65E-02
13	**AK152967**	65.25	5.51E-03
14	**Ccl12**	64.85	3.92E-02
15	**Serpina3g**	63.08	6.39E-03
16	**Isg20**	62.99	4.07E-02
17	**Sdc4**	58.44	2.75E-02
18	**Gm3430**	56.85	4.20E-02
19	**Il27**	56.65	4.08E-02
20	**Gm2371**	54.83	4.79E-02
21	**A530032D15Rik**	54.76	2.02E-02
22	**Abtb2**	53.89	1.46E-02
23	**chr16:84708695-84708806_F**	51.63	7.47E-03
24	**Gm4499**	51.59	3.33E-02
25	**Irf7**	50.60	3.26E-02
26	**Il15**	50.46	1.77E-02
27	**Gm8995**	47.67	4.56E-02
28	**Gm4080**	47.54	2.97E-02
29	**Gm4951**	44.72	3.42E-02
30	**A_55_P2020538**	44.02	3.43E-02

Table 4.7: Gene ontology - Acute response to LPS (A) vs. Naive (N)

Gene ontology terms were identified using DAVID based on differentially expressed inducible genes identified using a 1.5 fold change and a *P* value of less than 0.05 ($p<0.05$).

Acute response to LPS vs. Naïve: Gene list up-regulated	
Term	***P* value**
phosphoprotein	1.40E-17
immune response	5.40E-07
nucleus	4.10E-07
Toll-like receptor signalling pathway	6.70E-07
nucleotide binding	1.30E-05
zinc-finger	3.70E-06
transcription regulation	5.40E-06
purine ribonucleotide binding	2.10E-05
ribonucleotide binding	2.10E-05
Cytosolic DNA-sensing pathway	5.80E-06
regulation of apoptosis	9.70E-05
regulation of programmed cell death	1.00E-04
regulation of cell death	8.90E-05
purine nucleotide binding	5.30E-05
RIG-I-like receptor signalling pathway	1.30E-05
regulation of cytokine production	1.30E-04
death	1.30E-04
apoptosis	1.20E-04
cell death	1.10E-04
programmed cell death	1.60E-04
activation of innate immune response	4.10E-04
Apoptosis	7.00E-05
cytoplasm	1.70E-04
NOD-like receptor signalling pathway	7.70E-05
Transcription	1.80E-04
response to peptidoglycan	1.10E-03
alternative splicing	2.90E-04
domain:PARP catalytic	1.50E-02
Apoptosis	3.30E-04
DNA binding	1.20E-03

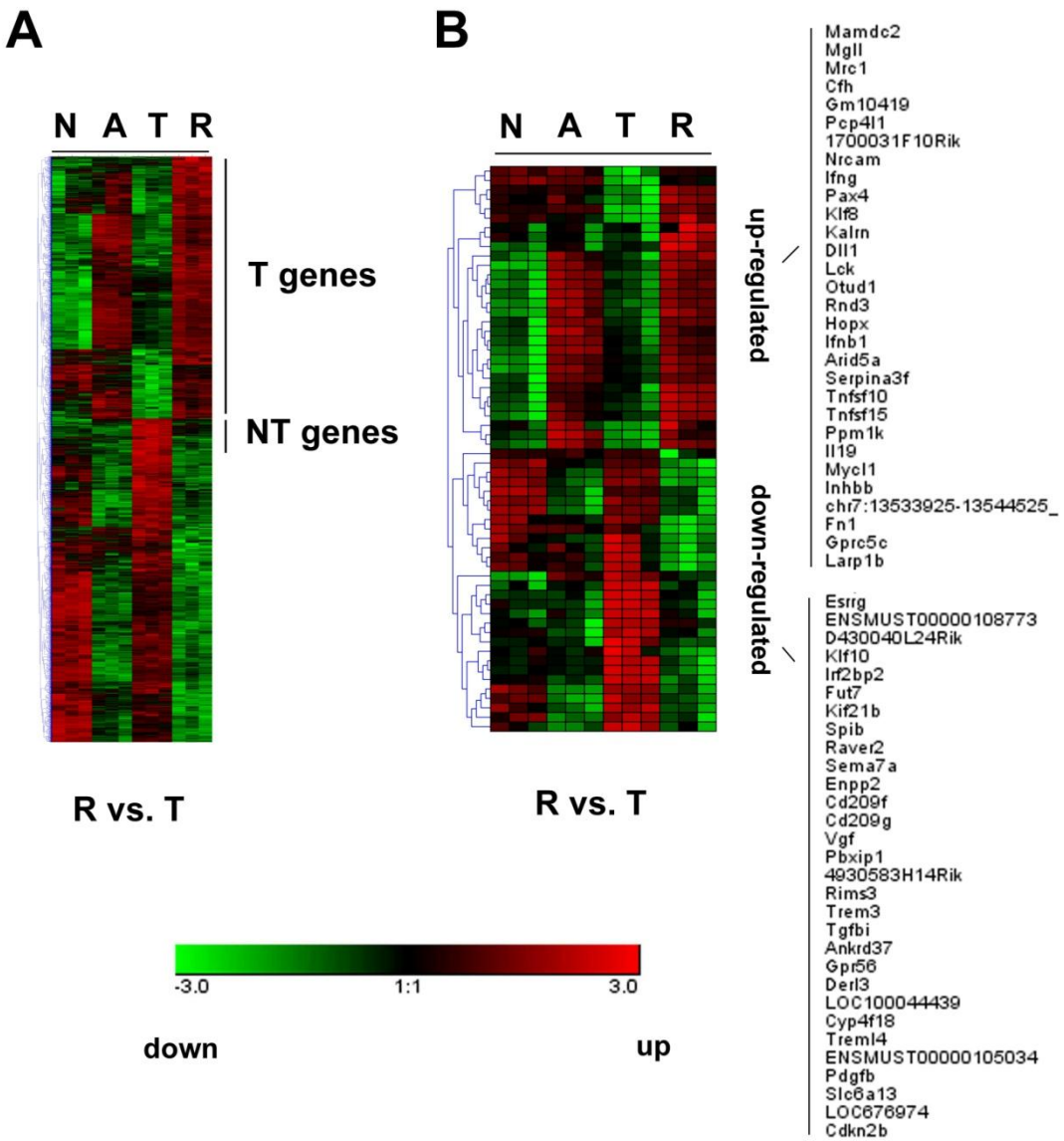

Figure 4.8 (A-B): Differentially expressed genes: Recovery (R) vs. LPS tolerant (T)

(A) Hierarchical clustering heatmap illustrating all up-regulated (red) and down regulated (green) genes identified by pairwise comparisons between the recovered group (R) relative to the LPS tolerant group (T). (B) Hierarchical clustering heatmap representing the top 30 (largest to smallest fold change) differentially expressed up-regulated and down-regulated genes in recovered group relative to the LPS tolerant group (data extrapolated from total differential expressed genes - Figure 4.8A). Differentially expressed genes were identified using fold change ± 1.5 fold (0.585 Log2) and a *P* value of less than 0.05 ($p<0.05$). N = Naïve, A = Activated, T = LPS Tolerance and R = Recovery.

Table 4.8: Top 30 up-regulated genes – Recovery (R) vs. LPS Tolerant (T)

Differentially expressed genes were identified using a 1.5 fold change and a *P* value of less than 0.05 ($p<0.05$). Genes are ranked by largest to smallest fold change.

Rank	Gene Name	Fold change	*P* value
1	**Mamdc2**	9.05	1.10E-03
2	**Hopx**	7.33	2.52E-03
3	**Mrc1**	7.05	1.52E-04
4	**Mycl1**	6.22	8.02E-04
5	**Inhbb**	6.20	2.49E-04
6	**Kalrn**	5.29	2.59E-04
7	**Mgll**	5.26	1.53E-04
8	**Cfh**	5.25	9.36E-04
9	**Klf8**	5.20	1.96E-04
10	**Arid5a**	5.16	1.75E-02
11	**Pax4**	5.01	6.30E-04
12	**Tnfsf10**	4.96	3.32E-03
13	**Ifnb1**	4.90	3.80E-02
14	**Tnfsf15**	4.73	1.41E-03
15	**Gm10419**	4.69	1.10E-05
16	**Dll1**	4.66	4.48E-04
17	**1700031F10Rik**	4.63	3.41E-02
18	**Lck**	4.58	7.84E-04
19	**Otud1**	4.53	4.19E-04
20	**Il19**	4.48	4.07E-03
21	**Serpina3f**	4.41	5.01E-03
22	**Nrcam**	4.39	7.58E-04
23	**Ppm1k**	4.29	3.76E-02
24	**Rnd3**	4.28	1.51E-04
25	**Fn1**	4.15	3.53E-02
26	**Gprc5c**	4.10	1.50E-03
27	**Ifng**	4.08	1.35E-03
28	**chr7:13533925-13544525_F**	4.07	1.48E-03
29	**Pcp4l1**	4.01	2.64E-04
30	**Larp1b**	4.00	6.10E-05

Table 4.9: Top 30 down-regulated genes – Recovery (R) vs. LPS Tolerant (T)

Differentially expressed genes were identified using a 1.5 fold change and a *P* value of less than 0.05 ($p<0.05$). Genes are ranked by largest to smallest fold change.

Rank	Gene Name	Fold change	*P* value
1	**LOC100044439**	-8.56	4.50E-04
2	**Cyp4f18**	-7.26	1.14E-04
3	**ENSMUST00000105034**	-6.40	1.14E-04
4	**Tgfbi**	-6.33	4.31E-02
5	**Spib**	-6.22	2.90E-04
6	**Pdgfb**	-6.02	9.44E-04
7	**Sema7a**	-5.97	6.36E-03
8	**Ankrd37**	-5.85	1.82E-03
9	**4930583H14Rik**	-5.84	2.95E-04
10	**Enpp2**	-5.79	1.19E-02
11	**ENSMUST00000108773**	-5.65	4.75E-04
12	**Cd209f**	-5.59	4.53E-03
13	**Derl3**	5.58	7.25E-03
14	**Rims3**	-5.54	4.23E-04
15	**Slc6a13**	-5.48	3.10E-04
16	**LOC676974**	-5.37	1.53E-03
17	**Treml4**	-5.36	1.79E-04
18	**Raver2**	-5.30	2.95E-03
19	**Irf2bp2**	-5.29	1.65E-02
20	**Pbxip1**	-5.21	3.18E-04
21	**Fut7**	-5.19	7.51E-04
22	**D430040L24Rik**	-5.18	1.38E-04
23	**Klf10**	-5.16	8.30E-05
24	**Trem3**	-5.05	2.69E-03
25	**Kif21b**	-4.97	4.38E-04
26	**Gpr56**	-4.96	1.40E-03
27	**Vgf**	-4.83	1.67E-03
28	**Esrrg**	-4.82	8.77E-03
29	**Cd209g**	-4.66	4.61E-03
30	**Cdkn2b**	-4.57	4.45E-04

Table 4.10: Gene Ontology – Recovery (R) vs. LPS Tolerant (T)

Gene ontology terms were identified using DAVID based on differentially expressed inducible genes identified using a 1.5 fold change and a *P* value of less than 0.05 ($p<0.05$).

Recovery vs. LPS Tolerance: Gene list up-regulated	
Term	***P*-value**
phosphoprotein	1.90E-16
cell cycle	5.10E-11
cell cycle process	7.30E-08
regulation of cytokine production	1.00E-07
cell cycle	5.50E-07
nuclear division	7.00E-07
mitosis	7.00E-07
M phase	8.90E-07
M phase of mitotic cell cycle	1.10E-06
mitotic cell cycle	1.10E-06
intracellular signaling cascade	1.30E-06
chromatin	1.50E-06
organelle fission	1.50E-06
mitosis	2.20E-06
cell cycle phase	2.70E-06
positive regulation of cytokine production	4.20E-06
chromosome	6.80E-06
transferase activity, transferring pentosyl groups	7.80E-06
positive regulation of biosynthetic process	1.00E-05
cell division	1.10E-05
response to wounding	1.10E-05
cell division	1.20E-05
regulation of cell proliferation	1.40E-05
NAD+ ADP-ribosyltransferase activity	1.40E-05
chromosomal part	1.40E-05
positive regulation of cellular biosynthetic process	1.50E-05
heart development	2.10E-05
regulation of immune effector process	2.50E-05
domain:PARP catalytic	3.10E-05
ubl conjugation	3.30E-05

Table 4.11: Gene Ontology – Recovery (R) vs. LPS Tolerant (T)

Gene ontology terms were identified using DAVID based on differentially expressed suppressed genes identified using a 1.5 fold change and a *P* value of less than 0.05 ($p<0.05$).

Recovery vs. LPS Tolerance: Gene list down-regulated	
Term	***P*-value**
mitochondrion	1.80E-16
zinc ion binding	6.50E-14
transcription	2.10E-13
Transcription	3.40E-13
zinc	5.30E-13
metal-binding	9.90E-13
transition metal ion binding	1.80E-12
regulation of transcription	1.30E-10
Glycolysis / Gluconeogenesis	1.10E-09
metal ion binding	1.40E-09
cation binding	5.00E-09
mitochondrial part	9.60E-09
ion binding	1.90E-08
phosphoprotein	5.50E-08
regulation of RNA metabolic process	6.30E-08
regulation of transcription, DNA-dependent	8.40E-08
nucleus	9.60E-08
membrane-enclosed lumen	1.70E-07
organelle lumen	2.10E-07
intracellular organelle lumen	3.20E-07
mitochondrion	3.40E-07
zinc finger region:C2H2-type 7	3.50E-07
monosaccharide catabolic process	5.50E-07
glycolysis	6.10E-07
mitochondrial membrane	1.40E-06
glucose catabolic process	1.50E-06
hexose catabolic process	1.50E-06
glycolysis	1.70E-06
alcohol catabolic process	2.60E-06
cellular carbohydrate catabolic process	3.10E-06

4.3.5 Recovery from LPS tolerance induces a unique transcriptional signature

Although COA analysis (PC1) revealed similar transcriptional profiles between the acute LPS response and re-stimulation of cells following recovery from LPS tolerance, clear differences in the expression of distinct groups of genes can be found (PC4). In support of this finding re-stimulation of macrophages with LPS following recovery from tolerance induced the expression of 310 genes not induced during the initial acute LPS response. Conversely 332 genes were found to be no longer induced by LPS following recovery from tolerance. The chemokine receptor CX3CR1, often used to distinguish between inflammatory and resident monocytes/macrophage lineages [128, 131, 132, 134, 210], was found to be one of the most significantly induced genes in the recovered group (R) not found in the acute LPS response group (A). Similarly the chemokine receptor CCR5, the folate receptor FOLR2, CCR3 and IFN-γ were specifically induced in the recovered group (R) (Figure 4.9, Figure 4.10, Table 4.12). The most significantly suppressed differentially expressed gene in the recovered group relative to the acute response group was the alarmin and pro-inflammatory gene IL-33. IL-33 is suppressed during LPS tolerance and remains "locked" in a tolerisable gene expression state following recovery from LPS tolerance (Figure 4.9, Figure 4.10 and Table 4.13).

Unsurprisingly, GO analysis of the 310 up-regulated differentially expressed genes in the recovered group relative to the acute response group were found to be enriched with numerous immune related processes and pathways. These included *immune response*, *response to wounding* and *inflammatory response* (Table 4.14). Of note, the most significant biological terms identified from the down-regulated differentially expressed genes were *antiviral response* and *response to virus* and

included the IFNA4, IFNA12, IFNA13, IFNA2, IFNA5 and IFNA7 genes (Figure 4.10) This was followed by *cytokine activity*, *immune system development* and *cytosolic DNA-sensing pathways* (Table 4.15) and included the anti-inflammatory cytokine IL-10 and the transcription factor NFIL3 (Figure 4.10). To validate these microarray findings gene expression of markers of RM cells was independently measured by qRT-PCR and by flow cytometry for the chemokine receptor CCR3 (Figure 4.11 and Figure 4.12).

Taken together, the transcriptional profile of the recovered group reflects many features of the LPS activated group however this data confirms recovery from LPS tolerance does not polarise macrophages strictly into an activated M1 pro-inflammatory macrophage. Importantly macrophages that recover from LPS tolerance have a unique transcriptional signature that identifies them as a novel macrophage activation state with altered expression of regulators of the anti-viral responses in addition to suppression of selective genes such as IL-33, an amplifier of LPS induced responses.

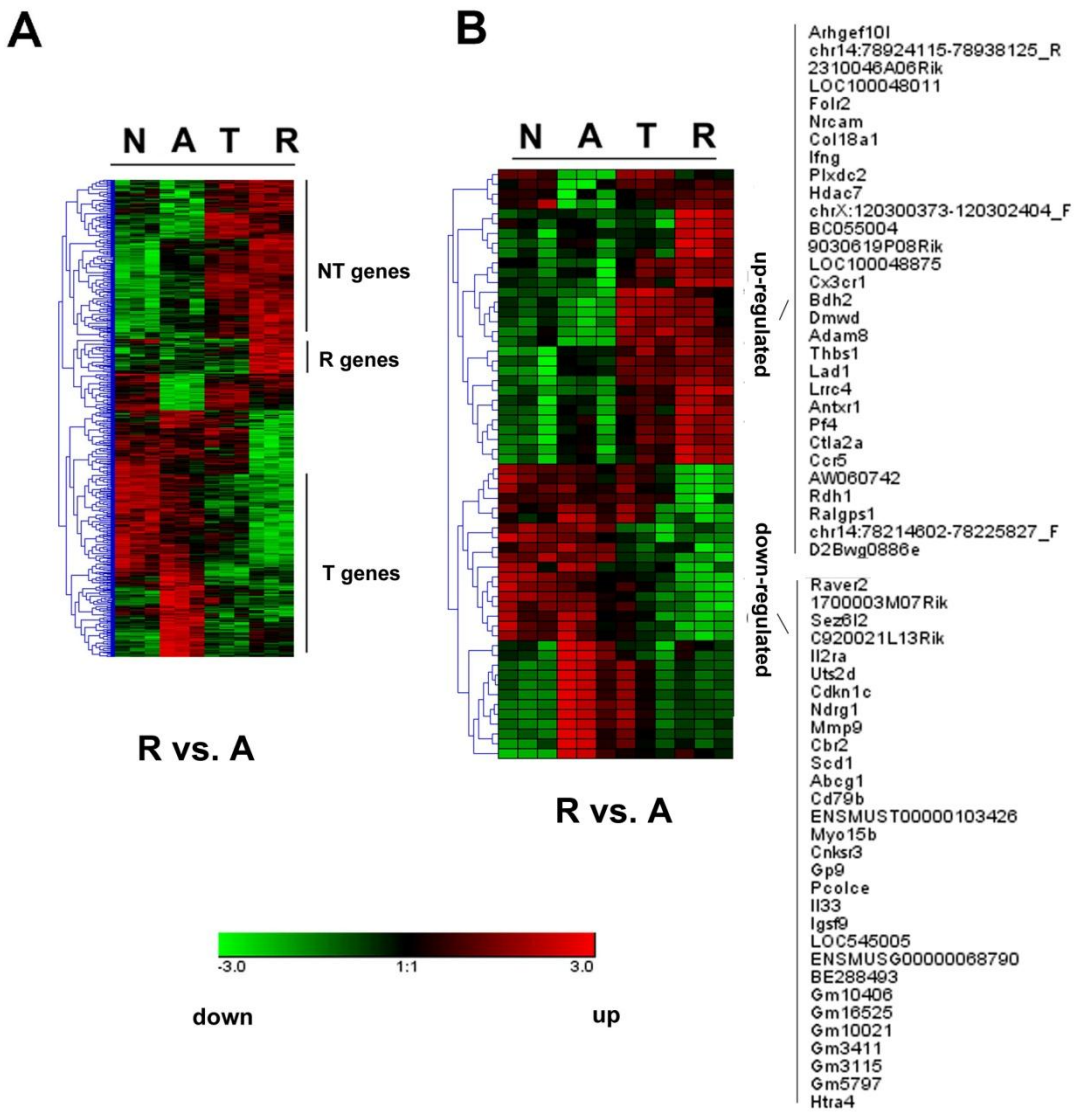

Figure 4.9 (A-B): Differentially expressed genes: Recovery (R) vs. activated (A)

(A) Hierarchical clustering heatmap illustrating all 310 up-regulated (red) and 332 down regulated (green) genes identified by pairwise comparisons between the recovered group (R) relative to the acute response group (A). (B) Hierarchical clustering heatmap representing the top 30 (largest to smallest fold change) differentially expressed up-regulated and down-regulated genes in recovered group (R) relative to the acute response group (A) (data extrapolated from total differential expressed genes - Figure 4.9A). Differentially expressed genes were identified using fold change ± 1.5 fold (0.585 Log2) and a *P* value of less than 0.05 ($p<0.05$). N = Naïve, A = Activated, T = LPS Tolerance and R = Recovery.

Table 4.12: Top 30 up-regulated genes – Recovery (R) vs. LPS activated (A)

Differentially expressed genes were identified using a 1.5 fold change and a *P* value of less than 0.05 ($p<0.05$). Genes are ranked by largest to smallest fold change.

Rank	Gene Name	Fold change	*P* value
1	**LOC100048875**	7.38	1.79E-02
2	**Ctla2a**	6.32	3.08E-02
3	**Cx3cr1**	6.06	2.54E-02
4	**Ccr5**	5.84	1.41E-02
5	**Hdac7**	4.54	2.80E-02
6	**chrX:120300373-120302404_F**	4.40	4.70E-02
7	**Lad1**	4.19	4.90E-02
8	**BC055004**	4.15	5.54E-03
9	**Antxr1**	4.09	2.59E-03
10	**Ifng**	3.84	1.82E-02
11	**AW060742**	3.82	4.48E-02
12	**Dmwd**	3.73	1.89E-02
13	**Folr2**	3.58	5.66E-03
14	**Bdh2**	3.56	1.37E-02
15	**Pf4**	3.39	4.12E-02
16	**Thbs1**	3.36	3.04E-02
17	**Nrcam**	3.30	2.41E-02
18	**Arhgef10l**	3.22	6.89E-03
19	**Lrrc4**	3.08	2.00E-02
20	**Col18a1**	3.06	1.10E-02
21	**2310046A06Rik**	3.06	2.64E-02
22	**chr14:78924115-78938125_R**	3.06	4.83E-02
23	**Rdh1**	3.05	4.24E-02
24	**chr14:78214602-78225827_F**	2.93	3.32E-02
25	**LOC100048011**	2.88	1.10E-02
26	**9030619P08Rik**	2.81	3.96E-02
27	**Adam8**	2.81	1.73E-03
28	**Plxdc2**	2.81	2.00E-02
29	**Ralgps1**	2.78	4.16E-02
30	**D2Bwg0886e**	2.77	3.00E-02

Table 4.13: Top 30 down-regulated genes – Recovery (R) vs. LPS activated (A)

Differentially expressed genes were identified using a 1.5 fold change and a *P* value of less than 0.05 ($p<0.05$). Genes are ranked by largest to smallest fold change.

Rank	Gene Name	Fold change	*P* value
1	**Il33**	-7.18	2.88E-02
2	**LOC545005**	-6.84	3.17E-02
3	**Raver2**	-6.55	1.44E-02
4	**ENSMUSG00000068790**	-5.83	2.61E-02
5	**Cdkn1c**	-5.76	2.57E-02
6	**BE288493**	-5.70	3.18E-02
7	**Mmp9**	-5.02	2.92E-02
8	**Gm10406**	-5.02	3.18E-02
9	**ENSMUST00000103426**	-4.86	1.29E-02
10	**Gm16525**	-4.85	1.89E-02
11	**Cbr2**	-4.60	1.49E-03
12	**Gm10021**	-4.42	3.04E-02
13	**Scd1**	-4.33	4.97E-02
14	**Gm3411**	-4.08	3.18E-02
15	**1700003M07Rik**	-4.00	3.18E-02
16	**Gm3115**	-3.86	2.80E-02
17	**Igsf9**	-3.81	2.00E-02
18	**Abcg1**	-3.80	1.49E-03
19	**Il2ra**	-3.62	3.85E-02
20	**Sez6l2**	-3.61	7.13E-03
21	**C920021L13Rik**	-3.59	1.01E-02
22	**Ndrg1**	-3.53	4.03E-02
23	**Gp9**	-3.51	2.33E-02
24	**Cnksr3**	-3.49	2.36E-02
25	**Cd79b**	-3.45	2.00E-02
26	**Uts2d**	-3.43	2.92E-02
27	**Gm5797**	-3.40	4.24E-02
28	**Myo15b**	-3.37	1.51E-02
29	**Pcolce**	-3.34	1.87E-02
30	**Htra4**	-3.26	3.73E-02

Table 4.14: Gene Ontology – Recovery (R) vs. LPS activated (A)

Gene ontology terms were identified using DAVID based on differentially expressed inducible genes identified using a 1.5 fold change and a *P* value of less than 0.05 ($p<0.05$).

Recovery vs. LPS activation: Gene list up-regulated	
Term	***P*-value**
disulfide bond	2.10E-07
disulfide bond	2.40E-06
glycoprotein	1.30E-05
signal	1.60E-05
immune response	2.30E-05
Systemic lupus erythematosus	3.40E-05
response to wounding	3.70E-05
signal peptide	3.80E-05
inflammatory response	4.80E-05
hydroxylation	8.90E-05
glycosylation site:N-linked (GlcNAc...)	1.20E-04
membrane	1.30E-04
defense response	1.60E-04
positive regulation of response to stimulus	2.60E-04
adaptive immune response	3.60E-04
adaptive immune response based on somatic recombination	3.60E-04
positive regulation of immune system process	5.40E-04
B cell mediated immunity	8.10E-04
positive regulation of immune response	8.70E-04
monoamine transport	1.00E-03
extracellular region part	1.20E-03
lymphocyte mediated immunity	1.60E-03
innate immunity	1.70E-03
blood vessel morphogenesis	1.80E-03
negative regulation of angiogenesis	1.80E-03
vasculature development	2.10E-03
topological domain:Cytoplasmic	2.10E-03
acute inflammatory response	2.20E-03
collagen	2.80E-03
activation of immune response	2.80E-03

Table 4.15: Gene Ontology – Recovery (R) vs. LPS activated (A)

Gene ontology terms were identified using DAVID based on differentially expressed suppressed genes identified using a 1.5 fold change and a *P* value of less than 0.05 ($p<0.05$).

Recovery vs. LPS activation: Gene list down-regulated	
Term	***P*-value**
Antiviral defense	3.70E-05
response to virus	3.40E-04
cytokine	1.60E-03
cytokine activity	2.40E-03
immune system development	3.50E-03
phosphoprotein	4.30E-03
atp-binding	4.70E-03
Natural killer cell mediated cytotoxicity	5.70E-03
Cytosolic DNA-sensing pathway	6.10E-03
kinase	6.70E-03
hemopoietic or lymphoid organ development	8.00E-03
allosteric enzyme	9.80E-03
extracellular space	9.90E-03
Regulation of autophagy	1.00E-02
transferase	1.20E-02
hemopoiesis	1.20E-02
regulation of I-kappaB kinase/NF-kappaB cascade	1.30E-02
Jak-STAT signaling pathway	1.60E-02
Focal adhesion	1.60E-02
Lectin	1.70E-02
ATP binding	1.90E-02
One carbon pool by folate	1.90E-02
adenyl ribonucleotide binding	2.20E-02
carbohydrate binding	2.20E-02
defense response	2.30E-02
negative regulation of cell morphogenesis involved in differentiation	2.40E-02
amino-acid biosynthesis	2.70E-02
negative regulation of cellular component organization	2.80E-02
nucleotide-binding	2.90E-02
basolateral plasma membrane	2.90E-02

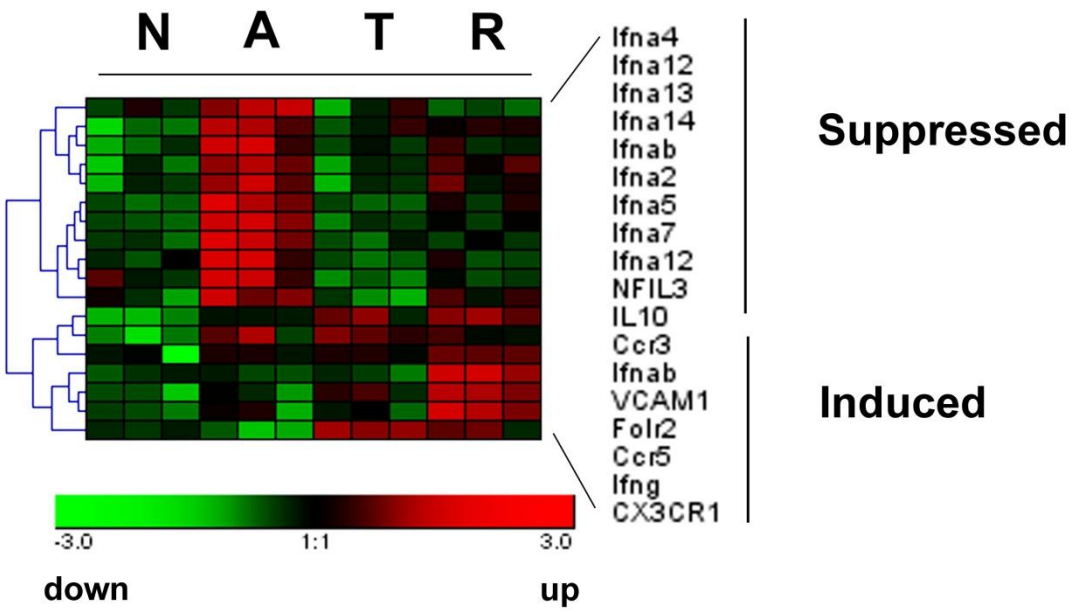

Figure 4.10: Recovery from LPS tolerance results in a unique transcriptional signature

Hierarchical clustering analysis of unique gene markers of the recovered group (R) (up-regulated (red) and down regulated (green) genes) identified by pairwise comparisons between the recovered group (R) relative to the acute response group (A). Differentially expressed genes were identified using fold change ± 1.5 fold (0.585 Log2) and a *P* value of less than 0.05 ($p<0.05$). N = Naïve, A = Activated, T = LPS Tolerance and R = Recovery.

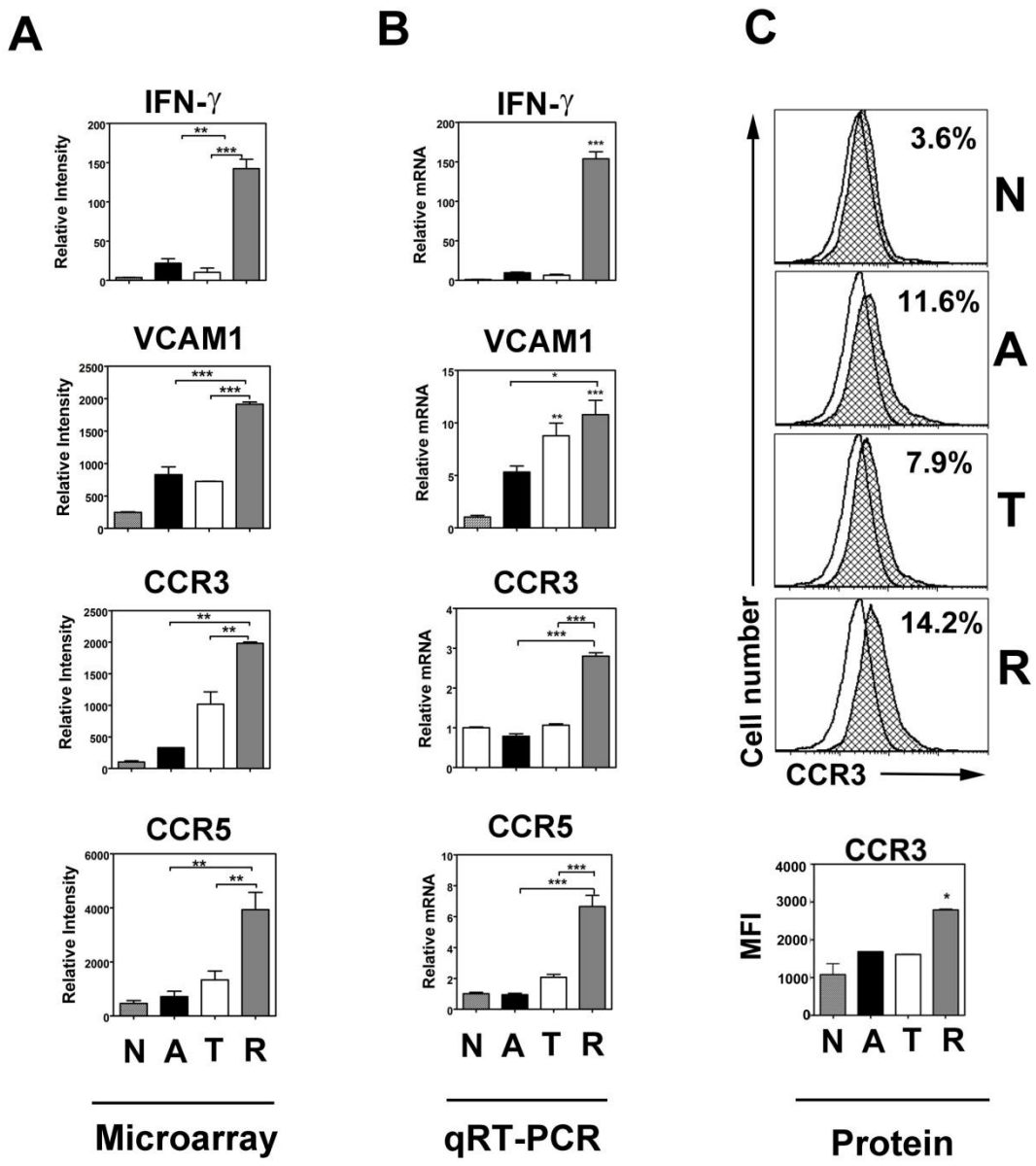

Figure 4.11: Recovered macrophages: Validated expression markers

Microarray intensities (A) and qRT-PCR (B) gene expression confirmation. Data is represented as relative mRNA or relative intensity (normalised microarray expression intensity). (C) CCR3 surface expression for all macrophage polarisation groups. Data is representative of three independent experiments with fluorescence minus one (FMO) and isotype controls. Data is represented as percentage gated cells and mean fluorescence intensity (MFI). N = Naïve, A = LPS activated, T = LPS Tolerance and R = Recovery. Differences between groups were determined using one-way ANOVA with Tukey's post hoc test with $p<0.001$ (***), $p<0.01$ (**) and $p<0.05$(*).

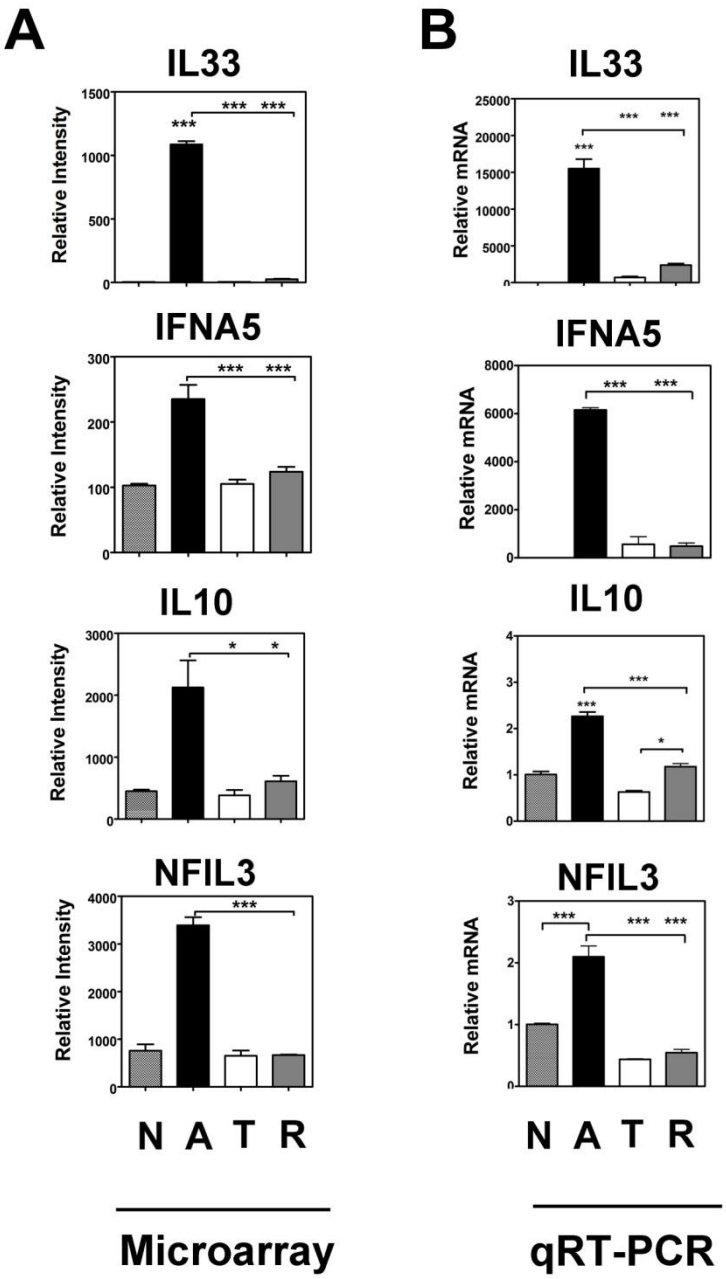

Figure 4.12: Recovered macrophages: Validated expression markers

Microarray intensities (A) and qRT-PCR (B) gene expression confirmation. Data is represented as relative mRNA or relative intensity (normalised microarray expression intensity) Differences between groups were determined using one-way ANOVA with Tukey's post hoc test with $p<0.001$ (***), $p<0.01$ (**) and $p<0.05$(*). N = Naïve, A = LPS activated, T = LPS Tolerance and R = Recovery.

4.3.6 Recovery from LPS tolerance induces a hybrid macrophage activation state, RM.

Antigen presentation is a classical feature of M1 macrophages while M2 anti-inflammatory macrophages display reduced capacity to present antigens to adaptive immune cells [127, 136]. LPS inducible CD86 mRNA levels were suppressed in both the LPS tolerant and recovered groups (Figure 4.13A-B) similar to IL-33, IL-10, NFIL3 and type 1 interferon gene expression (Figure 4.12). In addition we identified a large increase in the number of CD86 (46%) and CD80 (20.7%) F4/80 double positive cells following acute activation with LPS (Figure 4.13C). CD86 surface expression was suppressed during LPS tolerance (10.7%) and was not further inducible following recovery from LPS tolerance (9.8%). Similarly, LPS inducible CD80 surface expression was suppressed in the LPS tolerant group and was not inducible following recovery from LPS tolerance in a similar pattern to CD86 (Figure 4.13C). In contrast to suppression of co-stimulatory molecule expression, microbicidal activity and phagocytic capacity remained intact in the recovered group. NOS2 gene expression and nitrite production (greiss assay) was increased in the recovered group relative to the tolerant group confirming that recovery from LPS tolerance restores cytotoxic capacity in macrophages (Figure 4.14A-E).

In order to further define this inducible macrophage hybrid which we termed an RM macrophage state, we analysed M1 and M2 polarising markers from the microarray dataset. Using hierarchical clustering analysis we identified an overlap in M1 and M2 associated genes expressed following recovery from tolerance (Figure 4.15, Table 4.16, Table 4.17 and Table 4.18). The M1 polarisation markers IL-6, NOS2 and IL-12B [127, 136, 140] were significantly induced by LPS following recovery

from tolerance similar to the acute LPS response. In contrast, a number of M2 associated polarisation markers such as CCL17 and CCL24 [135] were found to be significantly induced following recovery from tolerance. Furthermore an increase in expression of the M2 polarisation markers mannose receptor (MRC1) and chitinase-3 like (chi3l3), [127, 135] were induced following recovery from tolerance (Figure 4.15, Table 4.16, Table 4.17 and Table 4.18). This data suggests that recovery from LPS tolerance may alter macrophage antigen presentation capacity and subsequent activation of the adaptive immune response. Our finding that following recovery from tolerance LPS may robustly induce iNOS gene expression suggests that these cells retain their cytotoxic microbicidal function. In addition, the expression of both M1 and M2 associated genes further emphasises that recovery from LPS tolerance induces a hybrid macrophage state with a unique transcriptional signature.

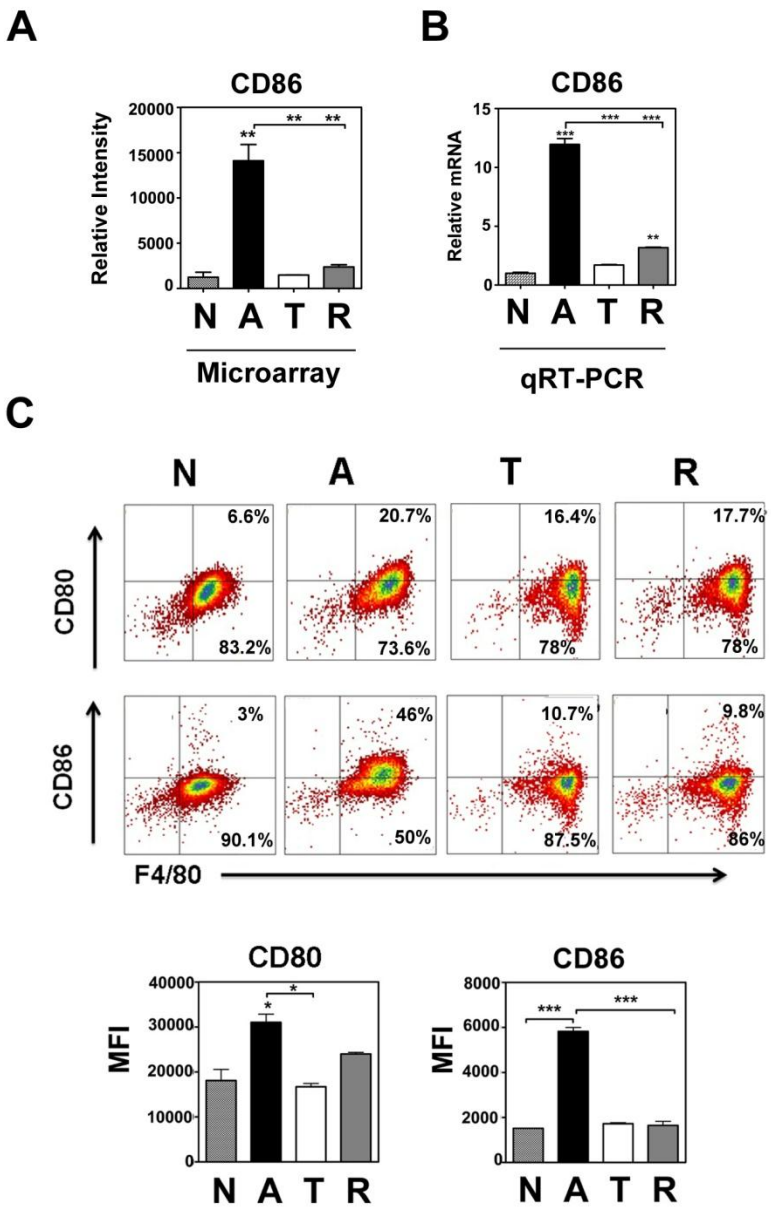

Figure 4.13: RM cells display alterations in regulators of antigen presentation

(A-B) Microarray and qRT-PCR validation of CD86 gene expression. Microarray gene expression is represented as relative intensity with qRT-PCR gene expression is represented as relative mRNA. (C) Surface staining for CD80 and CD86 co-stimulatory markers on each F4/80 positive group in the LPS tolerance recovery model (% Gated cells and mean fluorescence intensity – MFI). Data is representative of greater than three independent experiments. Flow cytometry data is normalised to fluorescence minus one (FMO) and isotype controls. Differences between groups determined by one way ANOVA with Tukey's post hoc test $p<0.001$ (***), $p<0.01$ (**) and $p<0.05$ (*). N = Naïve, A = LPS activated, T = LPS Tolerance, R = Recovery.

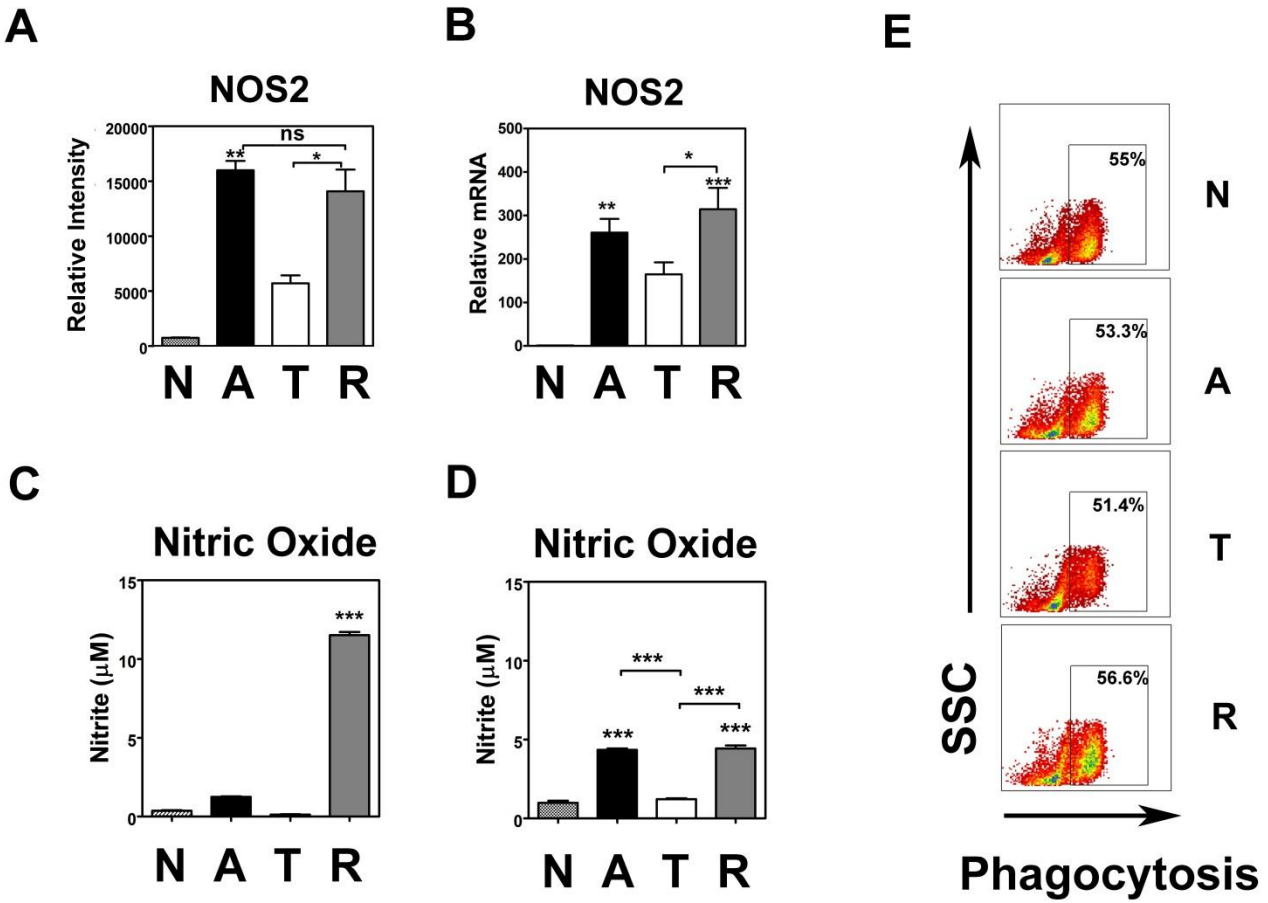

Figure 4.14: RM cells display intact phagocytic and cytotoxic capacity (Figure legend – Next page)

Figure 4.14: RM cells display intact phagocytic and cytotoxic capacity

(A-B) Microarray and qRT-PCR validation of NOS2 gene expression. Microarray gene expression is represented as relative intensity with qRT-PCR gene expression is represented as relative mRNA. Data is representative of greater than four independent experiments. (C-D) Measurement of nitric oxide production was measured using Greiss reagent. (C) NO production 24hr LPS re-stimulation. (D) NO production 24hr LPS re-stimulation (fresh media change prior to re-stimulation) (E) Phagocytosis capacity was determined by uptake of pHrodo particles. Ingested particles were measured by flow cytometry. Differences between groups determined by one way ANOVA with Tukey's post hoc test $p<0.001$ (***), $p<0.01$ (**) and $p<0.05$ (*). N = Naïve, A = LPS activated, T = LPS Tolerance and R = Recovery, NO = nitric oxide.

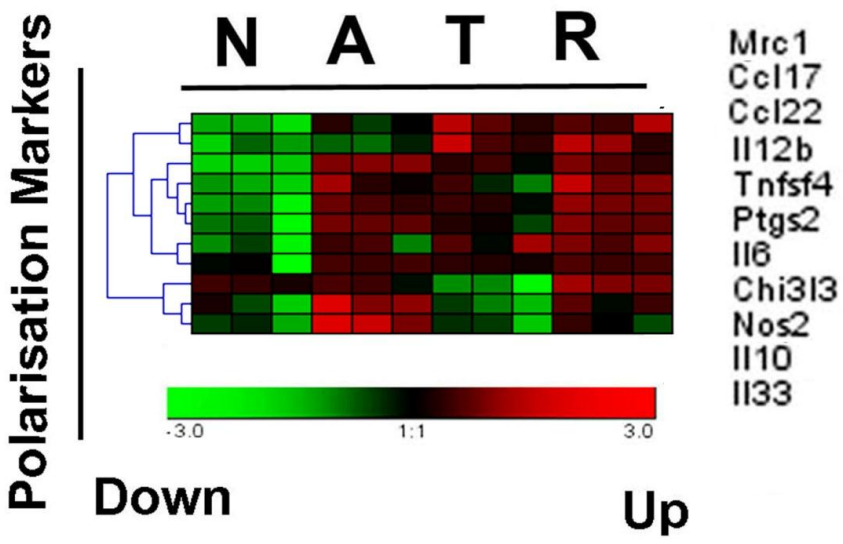

Figure 4.15: RM cells display a hybrid macrophage phenotype

Hierarchical clustering heatmap analysis of statistically significant M1 and M2 associated genes. Statistical significance was determined by log2 fold change ± 0.585 (1.5 fold) and $p<0.05$. N = Naïve, A = LPS activated, T = LPS Tolerance and R = Recovery.

Table 4.16: Differentially expressed macrophage polarisation genes – acute response (A) vs. Naïve (N)

Differentially expressed genes were identified using a 1.5 fold change and an adjusted *P* value of less than 0.05 ($p<0.05$). Differential expression corresponds to hierarchical clustering heatmap analysis of macrophage polarisation markers (Figure 4.15)

Gene Name	Fold change	*P* value
Mrc1	-1.02	9.73E-01
CCL17	1.71	2.64E-02
CCL22	1.20	4.69E-01
IL12B	47.21	1.80E-05
TNFSF4	4.57	7.41E-03
Ptgs2	21.32	2.29E-03
IL6	26.63	1.99E-03
Chi3L3	1.69	1.39E-01
NOS2	43.32	5.74E-02
IL10	2.95	7.58E-03
IL33	12.68	1.65E-03

Table 4.17 : Differentially expressed macrophage polarisation genes - LPS Tolerant (T) vs. Naïve (N)

Differentially expressed genes were identified using a 1.5 fold change and an adjusted *P* value of less than 0.05 ($p<0.05$). Differential expression corresponds to hierarchical clustering heatmap analysis of macrophage polarisation markers (Figure 4.15)

Gene Name	Fold change	*P* value
Mrc1	-3.95	4.99E-03
CCL17	2.38	3.27E-03
CCL22	1.85	1.51E-02
IL12B	11.66	2.71E-04
TNFSF4	2.36	1.32E-01
Ptgs2	12.53	1.19E-02
IL6	7.18	4.83E-02
Chi3L3	2.20	3.86E-02
NOS2	18.06	1.80E-01
IL10	0.73	5.02E-01
IL33	0.91	9.36E-01

Table 4.18: Differentially expressed macrophage polarisation genes - Recovered (R) vs. Naïve (N)

Differentially expressed genes were identified using a 1.5 fold change and an adjusted *P* value of less than 0.05 ($p<0.05$). Differential expression corresponds to hierarchical clustering heatmap analysis of macrophage polarisation markers (Figure 4.15)

Gene Name	Fold change	*P* value
Mrc1	1.78	4.58E-02
CCL17	2.39	2.31E-03
CCL22	1.93	2.04E-03
IL12B	25.65	1.00E-06
TNFSF4	7.93	1.65E-04
Ptgs2	27.59	6.00E-06
IL6	31.30	2.19E-02
Chi3L3	2.39	7.54E-03
NOS2	49.45	1.36E-02
IL10	1.73	1.10E-01
IL33	1.77	3.73E-01

4.3.7 Recovery from LPS tolerance is associated with a unique signalling and transcription factor profile in macrophages.

Macrophage polarisation is regulated by a number of transcription factors including the NF-κB, STAT and IRF families in addition to MAP kinase signalling. In order to assess the role of NF-κB in shaping macrophage responses following recovery from LPS tolerance we initially assessed the expression of NF-κB subunits by immunoblot. The levels of RelB, c-ReL and p65 subunits following recovery from tolerance were similar to those of the acute response group (Figure 4.16A-C). In contrast, LPS tolerised cells demonstrated elevated levels of RelB, c-ReL and p50 protein (Figure 4.16A) Interestingly, p50 levels remained elevated during recovery from LPS as demonstrated by both total and nuclear protein at 60 minutes of re-stimulation with LPS (Figure 4.16A-B). In addition, a re-stimulation step was important for movement of NF-κB into the nucleus with minimal detection of NF-κB subunits measured without LPS re-stimulation (Figure 4.16B). Furthermore, we observed no difference in total LPS-induced NF-κB binding activity following recovery from tolerance and the acute response group as shown by electrophoretic mobility shift assay (EMSA) (Figure 4.16C).

To assess LPS-induced signal transduction following recovery from LPS tolerance we measured ERK1/2 and p38 activation at 0, 15, 30 and 60 minutes following LPS stimulation using phospho-specific antibodies (Figure 4.17A). Following recovery from tolerance ERK1/2 was activated to levels comparable with the LPS activated group. Interestingly, p38 phosphorylation was increased following recovery from tolerance relative to the acute LPS response. p38 and ERK phosphorylation was suppressed in the tolerised group at 30 minutes in agreement with previous studies

[211] (Figure 4.17A). We next measured STAT1 and STAT3 in addition to IRF4 and IRF5 protein levels both of which have been previously been associated with macrophage polarisation [141, 149]. Interesting elevated phosphorylated STAT1 and STAT3 was measured in the LPS tolerant and recovered groups with IRF4 protein levels reduced in RM cells. No differences were observed in IRF5 protein (Figure 4.17B and C).

Interestingly hierarchical clustering analysis of transcription factor mRNA levels identified no significant difference in the expression of NF-κB and STAT proteins following recovery from tolerance (R) when compared to the acute LPS response group (A) (Figure 4.18, Table 4.19, Table 4.20 and Table 4.21). However, we did observe differences in the levels of the transcription factors NFIL3 and IRF8, a member of the IRF family of transcription factors. Both LPS inducible NFIL3 and IRF8 genes were suppressed following recovery from tolerance in a similar pattern to IL-33, IL-10 and type I interferon genes (Figure 4.10 and Figure 4.12). This data suggests that although no differences were observed in NF-κB protein levels, suppression of IRF4, IRF8 and NFIL3 may play a role in defining the transcriptional signature following recovery from LPS tolerance. Taken together, recovery from LPS tolerance induces a novel hybrid macrophage activation state with a unique transcriptional signature.

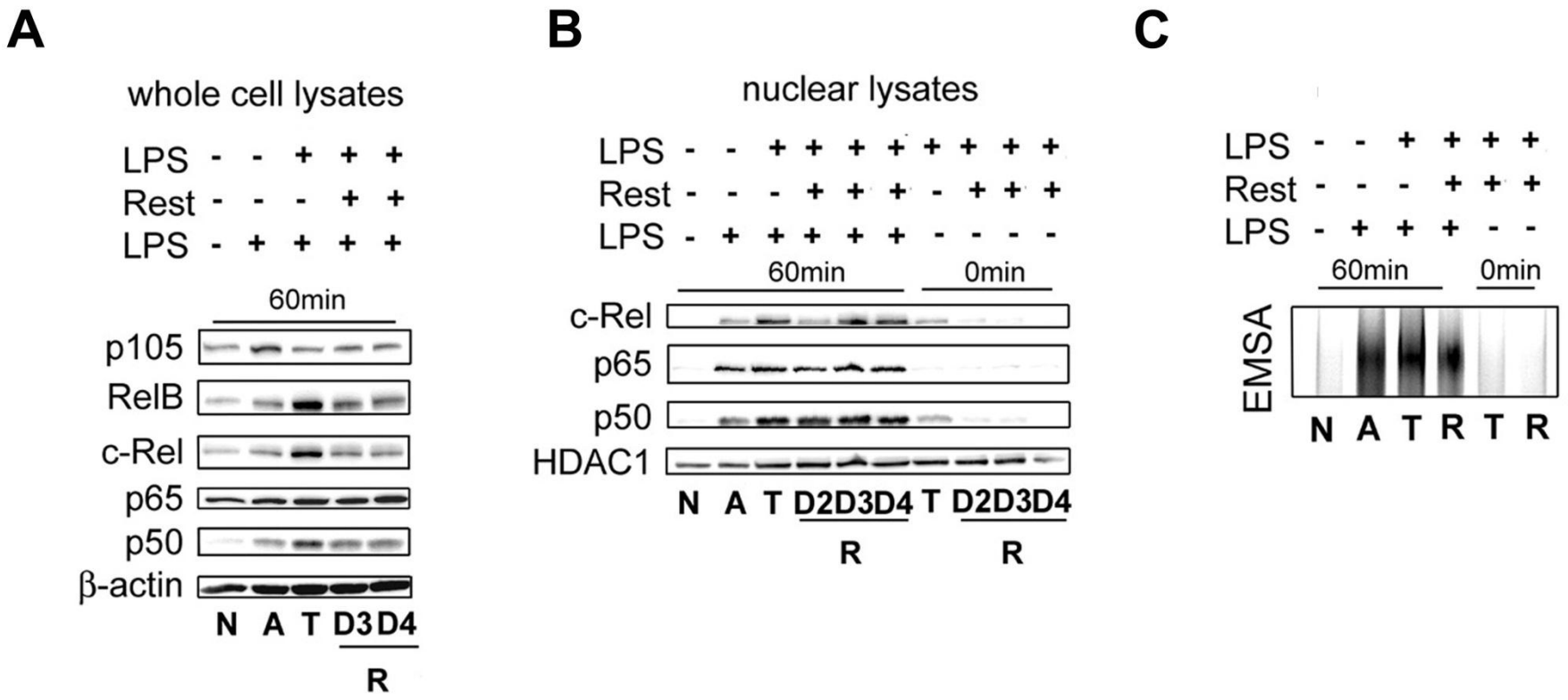

Figure 4.16: Recovery from LPS tolerance is reliant on NF-κB activation (Figure legend – Next page)

Figure 4.16: Recovery from LPS tolerance is reliant on NF-κB activation

(A-B) Immunoblot of total and nuclear NF-κB members during recovery from LPS tolerance. Nuclear and total protein was normalised to HDAC1 and β-actin loading controls respectively. (C) EMSA measurement of NF-κB binding in each macrophage group (N, A, T and R). N = Naïve, A = LPS activated, T = LPS Tolerance, R = Recovery (D2 = day 2, D3 = day 3, D4 = day 4). Data is representative of greater than three independent experiments.

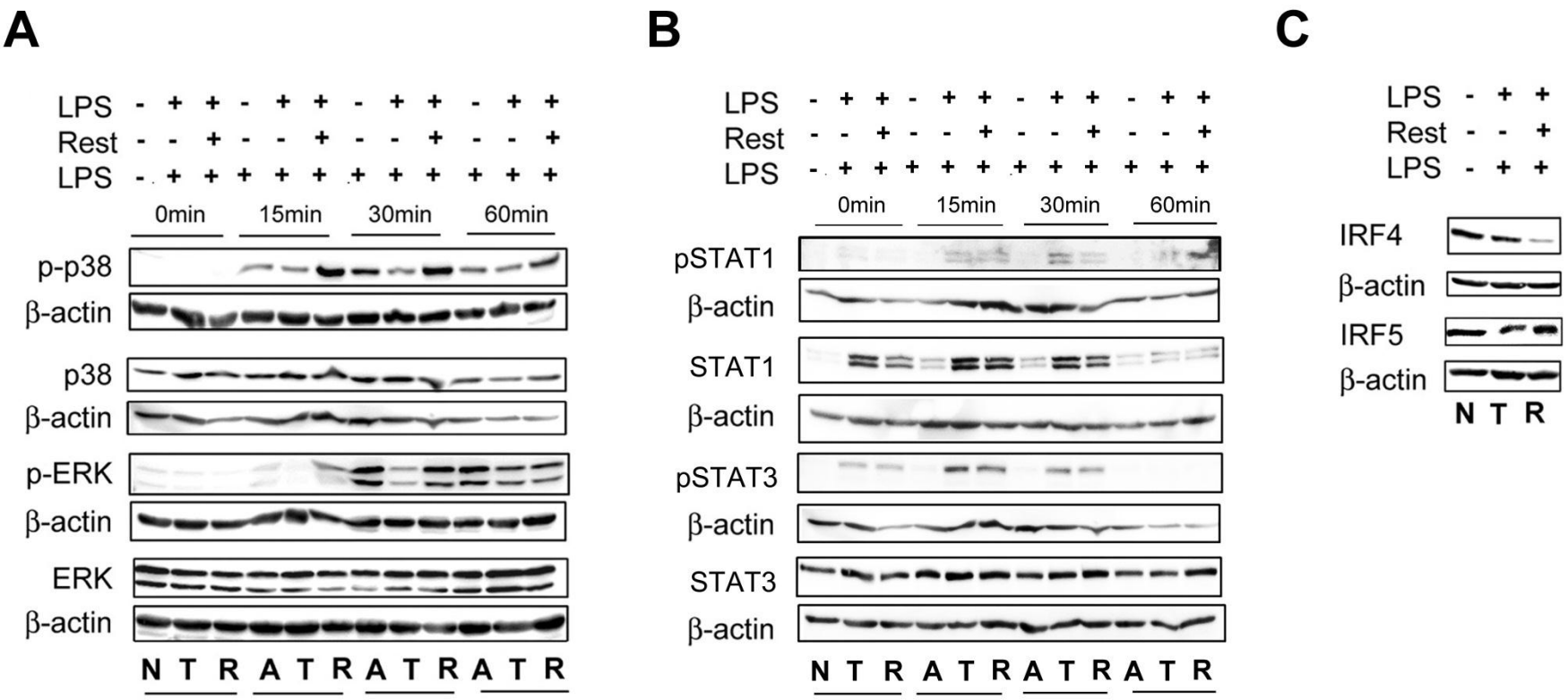

Figure 4.17: Recovery from LPS tolerance induces a unique signalling and transcription factor profile in macrophages (Figure legend – Next page)

Figure 4.17: Recovery from LPS tolerance induces a unique signalling and transcription factor profile in macrophages

(A-B) Immunoblot analysis of pp38, p38, ERK and pERK from whole cell lysates at 0, 15, 30 and 60 minutes of re-stimulation. Total protein was normalised to the β-actin loading control. (C) Immunoblot analysis for IRF4 and IRF5 protein from whole cell lysates. Total protein was normalised to the β-actin loading control. N = Naïve, A = LPS activated, T = LPS Tolerance, R = Recovery (D2 = day 2, D3 = day 3, D4 = day 4). Data is representative of greater than three independent experiments.

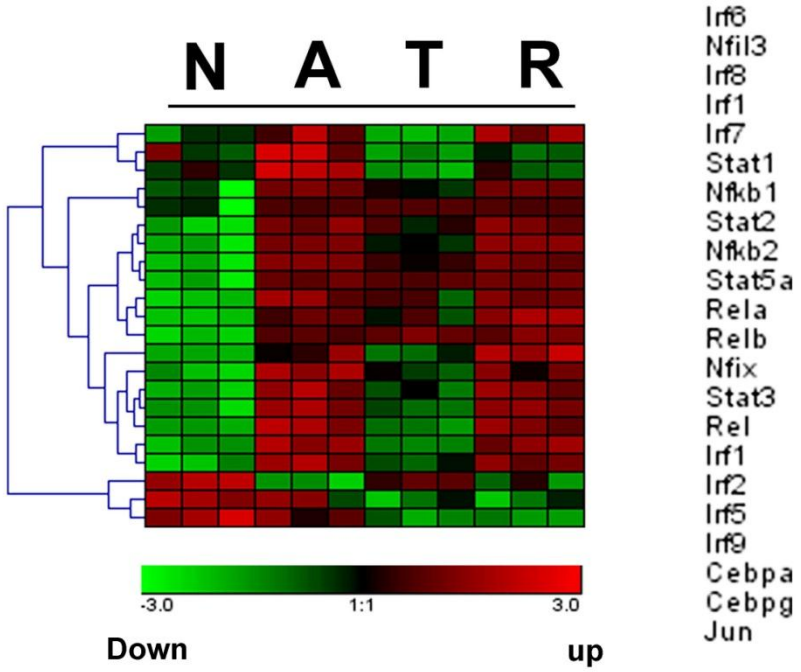

Figure 4.18: Recovery from LPS tolerance induces a unique signalling and transcription factor profile in macrophages

Hierarchical clustering analysis with complete linkage of transcription factor genes during LPS tolerance recovery. Statistical significance was determined by a Log2 fold change ±0.585 (1.5 fold) and a $p<0.05$. N = Naïve, A = LPS activated, T = LPS Tolerance, R = Recovery (D2 = day 2, D3 = day 3, D4 = day 4).

Table 4.19: Differential expressed transcription factor genes - Acute response (A) vs. Naïve (N)

Differentially expressed genes were identified using a 1.5 fold change and an adjusted *P* value of less than 0.05 ($p<0.05$). Differential expression corresponds to hierarchical clustering heatmap analysis of transcription factors (Figure 4.18)

Gene Name	Fold change	*P* value
Irf6	1.42	4.97E-02
Nfil3	2.03	2.99E-02
Irf8	2.29	8.28E-04
Irf1	3.85	8.50E-05
Irf7	50.60	3.26E-02
Stat1	3.03	1.02E-04
Nfkb1	4.61	2.20E-05
Stat2	4.63	2.60E-05
Nfkb2	5.98	5.30E-05
Stat5a	3.71	1.10E-04
Rela	1.70	6.21E-04
Relb	2.53	3.30E-05
Nfix	1.77	3.63E-03
Stat3	3.15	2.60E-05
Rel	5.15	1.12E-04
Irf2	3.34	4.90E-05
Irf5	2.13	1.14E-04
Irf9	1.64	1.26E-03
Cebpa	0.12	9.60E-05
Cebpg	0.84	4.93E-01
Jun	0.74	1.60E-01

Table 4.20: Differential expressed transcription factor genes - LPS tolerance (T) vs. Naïve (N)

Differentially expressed genes were identified using a 1.5 fold change and an adjusted *P* value of less than 0.05 ($p<0.05$). Differential expression corresponds to hierarchical clustering heatmap analysis of transcription factors (Figure 4.18)

Gene Name	Fold change	*P* value
Irf6	-1.24	2.82E-01
Nfil3	-1.61	1.73E-01
Irf8	-1.63	2.89E-02
Irf1	1.48	1.22E-01
Irf7	66.35	3.30E-02
Stat1	2.23	1.90E-03
Nfkb1	2.54	9.15E-04
Stat2	3.03	4.43E-04
Nfkb2	5.37	2.70E-04
Stat5a	2.30	4.22E-03
Rela	1.48	7.81E-03
Relb	2.61	1.23E-04
Nfix	1.14	5.14E-01
Stat3	1.49	4.83E-02
Rel	1.88	4.96E-02
Irf2	1.17	4.86E-01
Irf5	1.12	5.02E-01
Irf9	1.23	1.33E-01
Cebpa	0.43	3.99E-02
Cebpg	0.60	3.34E-02
Jun	0.45	2.50E-03

Table 4.21: Differential expressed transcription factor genes - Recovered (R) vs. Naïve (N)

Differentially expressed genes were identified using a 1.5 fold change and an adjusted P value of less than 0.05 ($p<0.05$). Differential expression corresponds to hierarchical clustering heatmap analysis of transcription factors (Figure 4.18)

Gene Name	Fold change	*P* value
Irf6	1.51	2.35E-02
Nfil3	-1.23	4.92E-01
Irf8	-1.10	8.05E-01
Irf1	3.50	6.00E-06
Irf7	55.41	5.84E-03
Stat1	3.03	1.40E-05
Nfkb1	5.29	2.35E-04
Stat2	4.11	1.00E-06
Nfkb2	6.44	1.00E-06
Stat5a	3.32	1.10E-05
Rela	2.01	1.10E-05
Relb	2.85	1.00E-06
Nfix	2.49	5.00E-05
Stat3	2.68	1.30E-05
Rel	4.57	1.30E-05
Irf2	2.72	7.00E-06
Irf5	1.98	4.04E-04
Irf9	1.53	5.43E-04
Cebpa	-4.98	3.67E-03
Cebpg	-1.44	5.51E-02
Jun	-2.32	1.58E-04

4.4 Discussion

The acute response towards LPS or endotoxin is one of the most extensively studied immune processes owing to its powerful effect on host immunity and disease. In this study we utilised a transcriptomics approach to characterise the transcriptional signature of macrophages post LPS tolerance induction. We identified that recovery from LPS tolerance induced a novel macrophage activation state (RM) resulting from a global transcriptional shift from an anti-inflammatory profile to a M1-M2 hybrid macrophage state. While a large proportion of tolerisable pro-inflammatory gene expression (IL-6, TNF-α and CXCL10) was restored, a number of pro-inflammatory (IL-33, type 1 interferons), anti-inflammatory (IL-10) and immune regulatory genes (NFIL3, CD86) remained locked in a tolerisable state thus failing to recover from LPS tolerance. In addition, RM cells expressed a number of unique markers not expressed in the other macrophage groups. Taken together this data confirms that recovery from LPS tolerance does not polarise macrophages back into a pro-inflammatory M1 activation state, but rather a hybrid macrophage state with a unique transcriptional signature.

Macrophages are key components of the innate immune response and central mediators of inflammation and defence. These cells also play important physiological roles involving tissue repair and remodelling, phagocytosis of cellular debris and apoptotic cells in addition to having important metabolic functions [127]. This range of biological roles is reflected in an increasingly recognised spectrum of macrophage activation states largely focused around the M1 pro-inflammatory /M2 anti-inflammatory classification system. M1 macrophages are mainly recruited under inflammatory conditions such as bacterial or viral infections. These cells are highly

cytotoxic, produce significant quantities of pro-inflammatory cytokines and are powerful activators of Th1 adaptive immune responses. On the contrary, M2 macrophages are important in wound healing, tissue remodelling and parasitic infections and polarised by IL-4 and IL-13 [127, 135, 136, 140, 212]. Many additional stimuli can be found *in vivo* including glucocorticoids, IL-10, TGF-β, parasitic infections, immune complexes and TLR engagement. Therefore macrophages are heterogeneous cells with many hybrid polarisation states existing in the emerging spectrum of macrophage polarisation [127, 135]. In addition, many resident macrophage populations adopt a hybrid anti-inflammatory-like state dependent on the local microenvironment. These include liver Kupffer cells, intestinal macrophages, placental macrophages, LPS tolerant macrophages and tumour associated macrophages [131, 135, 153-155, 157, 163].

In this study, we identified a novel macrophage activation state that shares many properties of both M1 and M2 macrophage populations. Recovered macrophages (RM) express highly inducible levels of pro-inflammatory cytokines and have cytotoxic capacity as illustrated by inducible iNOS expression and nitrite production suggesting that these cells are more pro-inflammatory M1-like. However, the expression of markers of M2 activation (CCL17, CCL22) in addition to the reduced expression of co-stimulatory molecules (CD80, CD86) following recovery from LPS tolerance would suggest that RM display features of both M1 and M2 polarisation states. Importantly, RM cells expressed reduced levels of two associated M2 polarising markers (IL-33, IRF4) which may be critical to promoting this novel hybrid state. IL-33 is a pro-inflammatory cytokine, alarmin and amplifier of LPS activation [213-217]. The lack of IL-33 expression in RM may be important in limiting the amplification of LPS responses and M2 polarisation through paracrine

signalling. Reduced expression of the M2 polarising transcription factor IRF4 [73, 149] may play a role in facilitating recovery from LPS tolerance by limiting the potential for maintenance of an M2-like macrophage polarisation state. In addition, we found increased expression of CX3CR1 in both RM and LPS tolerant cells. CX3CR1 is expressed on some resident macrophage populations and has been implicated in cellular survival. Thus, increased expression of CX3CR1 in RM cells may regulate survival post inflammatory challenge [218, 219]. While reduced expression of a number of type 1 interferons in RM cells may render macrophages more susceptible to viral infections, suppression of these genes may be important to limit their unnecessary production post bacterial inflammatory challenge. Taken together our data suggests that RM cells are distinct from LPS tolerised macrophages and represent a unique macrophage population primed to respond to new inflammatory challenges under strict environmental conditions.

The plasticity of macrophages can have both positive and negative outcomes depending on the local environmental requirements and activation stimuli that macrophages encounter. While an endotoxin tolerant state may limit potentially devastating consequences of excessive inflammation, prolonged tolerance can have harmful effects. Monocytes isolated from patients with sepsis or cystic fibrosis display reduced responsiveness towards *ex vivo* challenges with LPS as determined by pro-inflammatory cytokine production [159]. These cells remained locked in a tolerant state which coincided with patient mortality due to inability to produce a robust inflammatory response to secondary infections. Interestingly, patients who recovered from sepsis are responsive towards LPS upon LPS challenge *ex vivo* [159, 160]. This suggests that recovery from endotoxin tolerance may be a critical physiological response to maintain host protection to invading microbial challenges.

On the contrary, under normal homeostatic conditions, intestinal macrophages adopt a regulatory tolerant-like state towards the local environmental microbial community. This environment is rich in the cytokines IL-10 and TGF-β which contribute to generating an anti-inflammatory tolerant environment in the gut [131]. In addition, the resident macrophage population (Kupffer cells) in the liver adopt an anti-inflammatory tolerised-like phenotype specific to the liver microenvironment where they are exposed to a vast array of gut derived and environmental toxins under the normal physiologic conditions [163-165]. These two macrophage populations represent environments where prolonged tolerance is a physiological protection mechanism. The loss of this normal tolerance state is associated with alcoholic liver disease, HCV viral infections and IBD [158, 167]. Of note, deficiencies in IL-10 and the transcription factor NFIL3 have been associated with chronic inflammation in the gut [220], two genes that are locked in a tolerised state in RM cells. In addition, CD14+ lamina propria mononuclear cells from Crohn's disease and ulcerative colitis patients showed reduced NFIL3 gene expression in comparison to non-inflamed cells [220]. NFIL3 is a regulator of IL-12B expression with IL-10 acting as a co-factor in NFIL3 induction in macrophages. Although we measured no difference in IL12B gene expression in RM cells, suppression of both IL-10 and NFIL3 in RM cells may facilitate the recovery from LPS tolerance. Thus this data suggests that a recovery from LPS tolerance is central to restoring normal physiological responses following microbial infections. Importantly recovery from this tolerant state may be environment specific due to the positive and negative effects a loss of tolerance can have on host immunity.

In summary, we have identified a novel transcriptional signature following recovery from LPS tolerance which has both pro-inflammatory and anti-inflammatory

characteristics. Recovery from LPS tolerance may represent a physiological response of macrophages following microbial infection which is important to controlling and limiting excessive inflammation. Macrophages that are in an LPS tolerance state could be more susceptible towards new microbial challenges due to reduced iNOS activity and antigen presentation capability. Macrophages remaining locked in this tolerised state would likely have deleterious consequences to the host upon new microbial challenges. Recovery from LPS tolerance may therefore allow macrophages to be primed towards mounting an effective immune response towards new microbial challenges while still maintaining a level of tolerance that protects against unnecessary over-activation of the inflammatory response.

5. Regulation of cytokine secretion following recovery from LPS Tolerance

5.1 Abstract

Cytokines and chemokines play a fundamental role in orchestrating the inflammatory response through recruitment and expansion of immune cell populations in addition to modulating the immunological functions of these cells. Excessive or uncontrolled cytokine and chemokine production can have both pathological and immune suppressive consequences; therefore their production is tightly controlled transcriptionally through induction of TLR tolerance under normal homeostatic conditions. In this chapter functional analysis of cytokine and chemokine production was performed by fluorescent microscopy and ELISA to investigate the regulation of cytokine secretion following recovery from LPS tolerance. We demonstrate a novel mechanism of TLR tolerance in macrophages at the level of protein secretion through degradation of pro-inflammatory cytokine protein. We identify that pro-inflammatory cytokine (IL-6, TNF-α and IL-12) and anti-inflammatory cytokine (IL-10) secretion is selectively suppressed in RM cells despite inducible mRNA and total intracellular protein levels measured in these cells. Furthermore, we identified that TNF-α cytokine secretion is regulated in a lysosomal dependent process, independent of autophagy and acidic protease, calpain and cathepsin dependent degradative processes. In addition, we identify that a second independent inflammatory signal including IL-1β can restore TNF-α secretion thereby restoring immune competency in RM cells. Our data describes a unique mechanism of

regulation of TLR tolerance post transcriptionally through degradation of translated cytokine protein.

5.2 Introduction

Cytokines and chemokines belong to a diverse family of proteins that play a fundamental role in shaping the inflammatory response following recognition of pathogen and tissue injury signals. These glycoproteins display a range of pleiotropic effects which can function in an autocrine, feedback or synergistic network to tailor appropriate inflammatory responses towards specific microbial and host derived stimuli. Cytokine and chemokine families largely mediate recruitment of immune effector cells such as inflammatory monocytes and neutrophils from circulation to sites of infections. In addition, secretion of these proteins by immune cells such as macrophages, leads to priming and activation of other innate and adaptive immune cell functions including cytotoxicity and antigen presentation in addition to promoting the expansion of Th1, Th2, Th17 and B cell populations and their cellular responses [3, 221].

Microbial recognition by PRRs such as TLR4 leads to rapid production and secretion of pro-inflammatory cytokines and chemokines including TNF-α, IL-6, IL-12 and RANTES in addition to type 1 interferons and anti-microbial peptides [1]. Induction of these pro-inflammatory proteins is associated with a powerful cytotoxic macrophage state promoting TH1 immune responses. Cytokine and chemokine secretion is regulated transcriptionally during LPS tolerance. Expression of multiple negative regulators of TLR signalling and TLR induced transcription such as IRAK-M, A20, ST2 and Bcl-3 are central to promoting an anti-inflammatory regulatory state in macrophages in addition to transcriptional suppression of pro-inflammatory cytokine and chemokine production [35, 39, 47, 49, 111]. While induction of a pro-inflammatory state is essential in order to mount effective immunity against microbial infection, excessive and dysregulated production of immune modulators

underlies the pathology of a number of chronic inflammatory conditions ranging from IBD, chronic obstructive pulmonary disease (COPD), asthma, obesity and cancer [222-224]. In contrast, prolonged suppression of these immuno-modulatory proteins can lead to a state of immunosuppression rendering the host more susceptible to developing opportunistic secondary infections [36, 160, 225].

Recently suppression of TNF-α secretion has been observed in macrophages isolated from Crohn's disease (CD) patients [226]. TNF-α protein was found within CD macrophages despite suppressed TNF-α secretion. It was proposed that lysosomal degradation was implicated in suppressing cytokine secretion in CD macrophages [226]. This study provides physiological evidence of a disconnect between mRNA and protein secretion in macrophages suggesting that post transcriptional regulation of cytokine secretion may play a role in the pathogenesis of CD. Importantly whether suppressed cytokine secretion is a pathophysiological consequence of CD remains to be determined. On the contrary, colonic macrophages under normal environmental conditions have been associated with a hyporesponsive state with reduced production of pro-inflammatory cytokines including TNF-α despite inducible mRNA and intracellular protein measured in these cells [162, 227]. In addition a recent study has demonstrated that secretion of the pro-inflammatory cytokine IL-1β by intestinal macrophages is controlled by NLRC4 inflammasome activation [228]. In this study, colonic macrophages demonstrate a hyporesponsive state through suppressed TNF-α and IL-6 production. Furthermore, these cells were shown to contain high levels of pro-IL-1β however the mature cytokine was not secreted. Secretion of mature IL-1β was dependent on activation of the NLRC4 inflammasome upon pathogenic infection as a result of NLRC4 activation of caspase 1 and subsequent cleavage of pro-IL-1β. Interestingly, this study demonstrates discrimination between pathogenic

and commensal bacteria is dependent on the NLRC4 inflammasome with mature IL-β not produced in response to commensal bacteria exposure [228]. These studies further emphasise a disconnect between mRNA and protein secretion in a macrophage population that reside in the unique tolerant environment of the gut. These studies highlight that cytokine secretion is regulated post transcriptionally. Thus performing transcriptional profiling alone of macrophages that recover from LPS tolerance as described in chapter 4 is not sufficient to determine the global activation status of RM cells. Therefore in this chapter we performed functional analysis of cytokine secretion in RM cells to complement our transcriptional profiling data to determine the global impact of recovery from LPS tolerance on the activation status of macrophage.

As described in Chapter 4, recovery from LPS tolerance induces a global switch in the gene expression profile of macrophages resulting in a novel macrophage activation state with a unique transcriptional signature (RM). Transcriptional suppression of many pro-inflammatory genes was alleviated following recovery from LPS tolerance, as assessed by microarray profiling however post transcriptional analysis of pro-inflammatory cytokine and chemokine expression remained to be elucidated in RM cells. In this chapter we used a functional approach to analyse the regulation of cytokine production following recovery from LPS tolerance. Similarly to transcriptional profiling experiments, we utilised the model of LPS activation of murine macrophages to generate naïve (N), LPS activated/ acute response (A = M1), LPS tolerised (T) and recovered (R = RM) polarisation states. Our data demonstrates that while recovery from LPS tolerance restores transcription of many pro-inflammatory genes, secretion of pro-inflammatory cytokines and chemokines remains suppressed in RM cells despite pro-inflammatory cytokine mRNA actively

being translated into protein. This chapter illustrates a novel mechanism of regulation of TLR tolerance through regulation of cytokine secretion in RM cells.

5.3 Results

5.3.1 Recovery from LPS tolerance restores cytokine and chemokine gene transcription in RM cells

Using the designed *ex vivo* model of recovery from LPS tolerance as previously outlined in Chapter 4, the cytokine and chemokine expression profile was analysed in RM cells. As previously discussed, LPS tolerance (T) was induced by stimulation of BMDMs with LPS (100ng/ml) for 8 hours followed by washout and resting of cells for an additional 16 hours prior to re-stimulation with LPS (100ng/ml). Recovery from LPS tolerance (R) was induced in macrophages by extending the rest period to 3 days following LPS washout. The acute response to LPS (A) was measured in cells which received no pre-stimulation with LPS prior to stimulation with 100ng/ml LPS (A). The duration of LPS re-stimulation was dependent on the experimental endpoint. Messenger RNA levels were measured following 4 hours LPS re-stimulation. TNF-α protein was measured following 1.5 hours LPS re-stimulation for fluorescent microscopy experiments. Intracellular cytokine protein was measured at 8 hours post LPS re-stimulation for both immunoblotting and intracellular staining by flow cytometry. Cytokine and chemokine secreted protein was measured in supernatants removed from cells following 8 and 24 hours LPS re-stimulation. Naive macrophages (N) remained untreated (Figure 5.1).

Gene expression of LPS inducible cytokines and chemokines was measured by microarray profiling and visualised by hierarchical clustering analysis in all groups (N, A, T and R). Gene expression profiling revealed a robust increase in cytokine and chemokine mRNA levels following a single stimulation with LPS (A) as determined using a 1.5 fold change difference and p value cut off of 0.05. These

included pro-inflammatory cytokines and chemokines such as IL-6, CXCL10, IL-12 and RANTES. A large number of these genes were suppressed following LPS tolerance induction (T) and re-inducible upon recovery from LPS tolerance (R) to levels comparable with the acute response group (A). In addition a number of *non-tolerisable* cytokines and chemokines including RANTES remained inducible following recovery from LPS tolerance (Figure 5.2). In support of these findings, qRT-PCR validation of cytokine and chemokine gene expression (IL-6, CXCL10, CXCL1, TNF-α, RANTES and CXCL2) revealed a robust increase in mRNA levels following recovery from LPS tolerance (R) confirming the microarray gene expression findings (Figure 5.3).

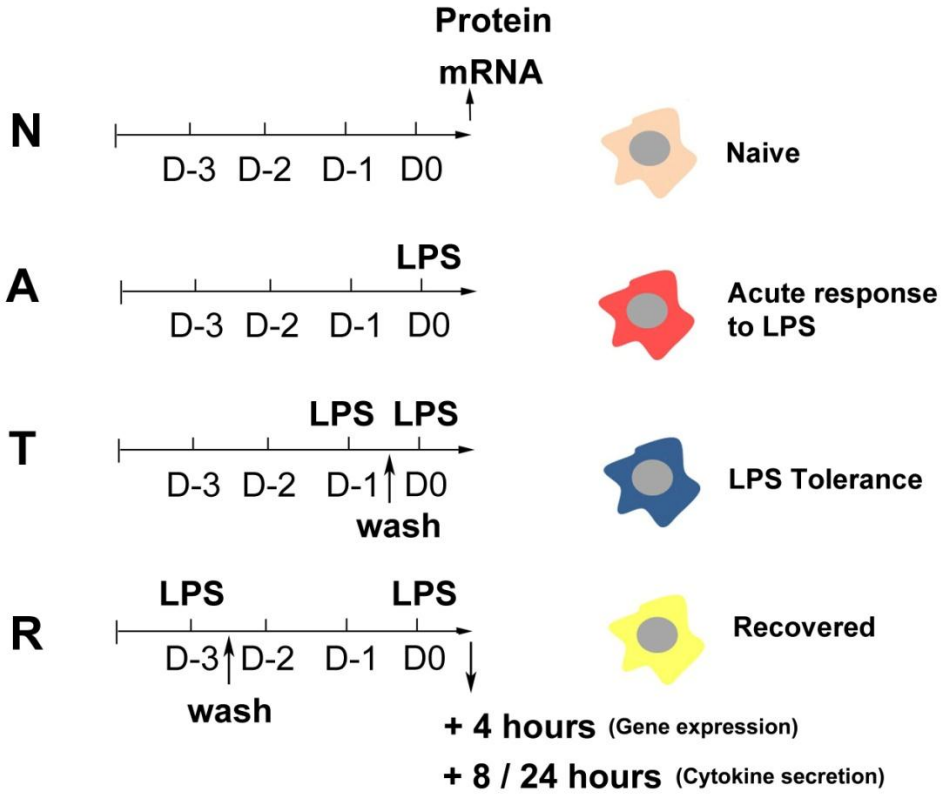

Figure 5.1: LPS Tolerance Recovery Model

Ex-vivo model of recovery from LPS tolerance using murine BMDM. Briefly, four unique macrophage polarisation groups were induced. N = Naïve, A = acute response to LPS, T = LPS Tolerance and R = Recovery (RM).

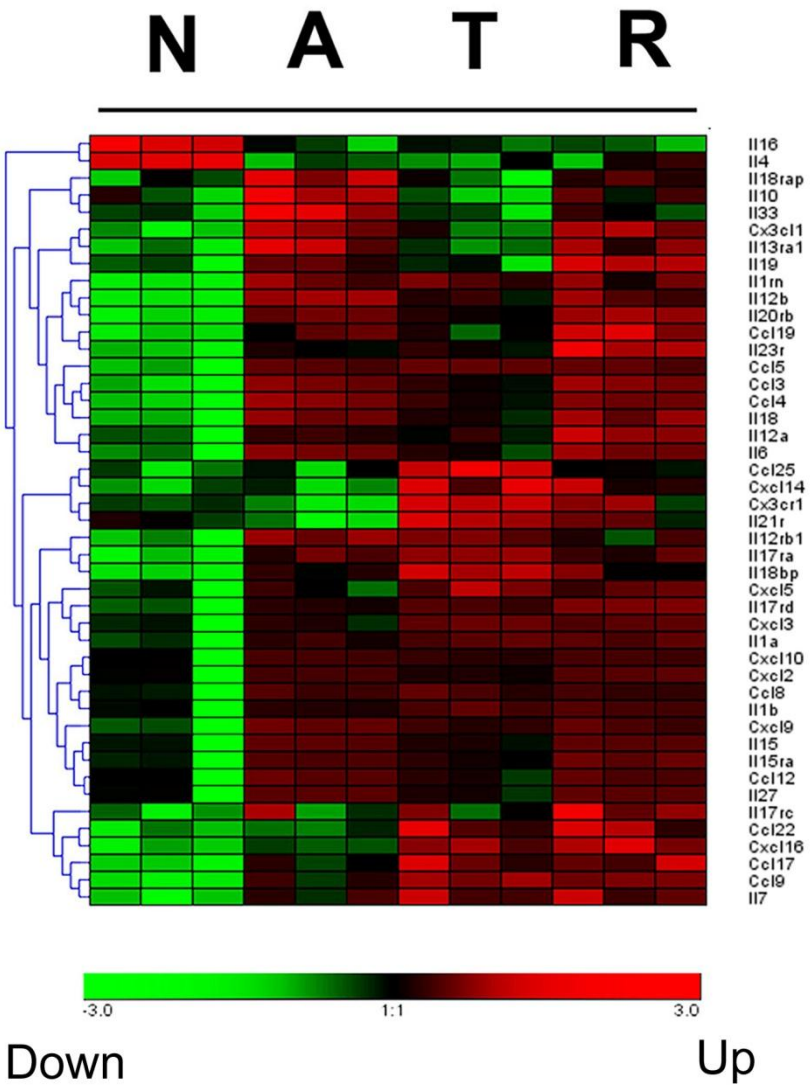

Figure 5.2: Cytokine and chemokine transcriptional profile

Hierarchical clustering analysis of cytokine and chemokine microarray gene expression. Statistical significance was determined using Benjamini Hochberg multiple correction testing and with a fold change of ± 1.5 fold (0.585 Log2) and a *P* value cut off of less than 0.05 ($p<0.05$). Normalised expression data is represented in Log2. Up-regulated (up) and down-regulated (down) genes are represented in red and green respectively. N = Naïve, A = acute response to LPS, T = LPS Tolerance and R = Recovery.

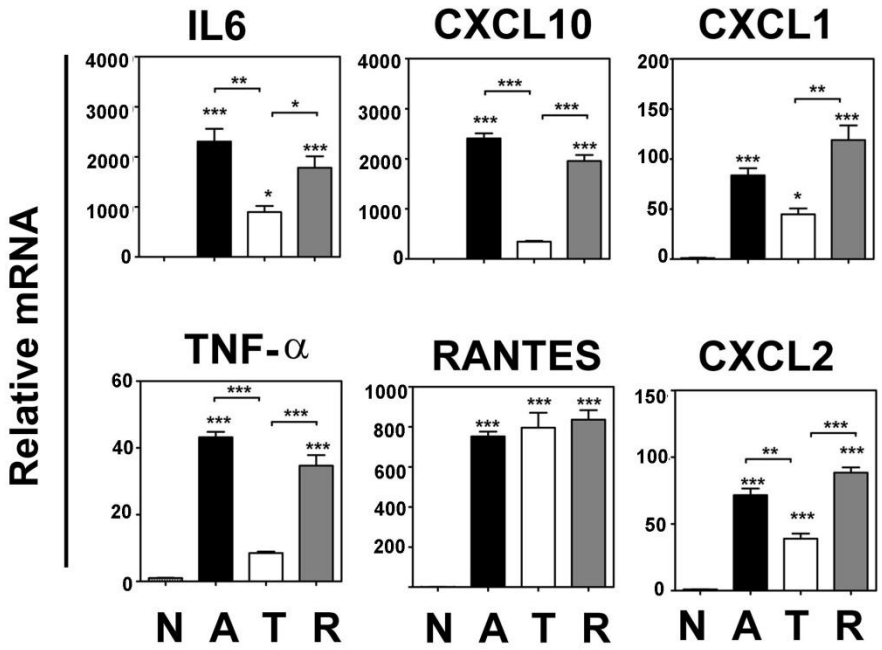

Figure 5.3: qRT-PCR validation of cytokine and chemokine gene expression

Gene expression of CXCL10**,** IL-6, CXCL1, RANTES, CXCL2 and TNF-α was analysed by qRT-PCR. Differences between groups were measured by one-way ANOVA with Tukey's post hoc test with $p<0.05$ (*), $p<0.01$ (**) and $p<0.001$ (***). Data is representative of greater than four independent experiments and measured as relative mRNA as determined by the $2^{-\Delta\Delta CT}$ method. N = Naïve, A = acute response to LPS, T = LPS Tolerance and R = Recovery.

5.3.2 Recovery from LPS Tolerance restores intracellular TNF-α protein

To confirm restoration of cytokine and chemokine protein expression following recovery from LPS tolerance, intracellular TNF-α protein expression was measured by flow cytometry and immunoblot analysis following 8 hours LPS re-stimulation in the presence or absence of the protein secretion inhibitor Brefeldin A (1μg/10^6 cells) (Figure 5.4A and B). TNF-α was highly inducible following an initial stimulation with LPS (A) with 62% of cells staining double positive for TNF-α and F4/80. In contrast only 10.6% of F4/80 positive cells contained TNF-α protein in the LPS tolerant group (T). In agreement with the gene expression results, TNF-α protein expression was induced in the recovered group (R) (57.8%) to levels comparable with the acute response group (A) as determined by intracellular staining and immunoblotting analysis (Figure 5.4A and B). This data confirms that suppression of pro-inflammatory cytokines and chemokines during LPS tolerance is a transient and temporary transcriptional event with both gene expression and intracellular cytokine protein restored in RM cells as determined by TNF-α expression.

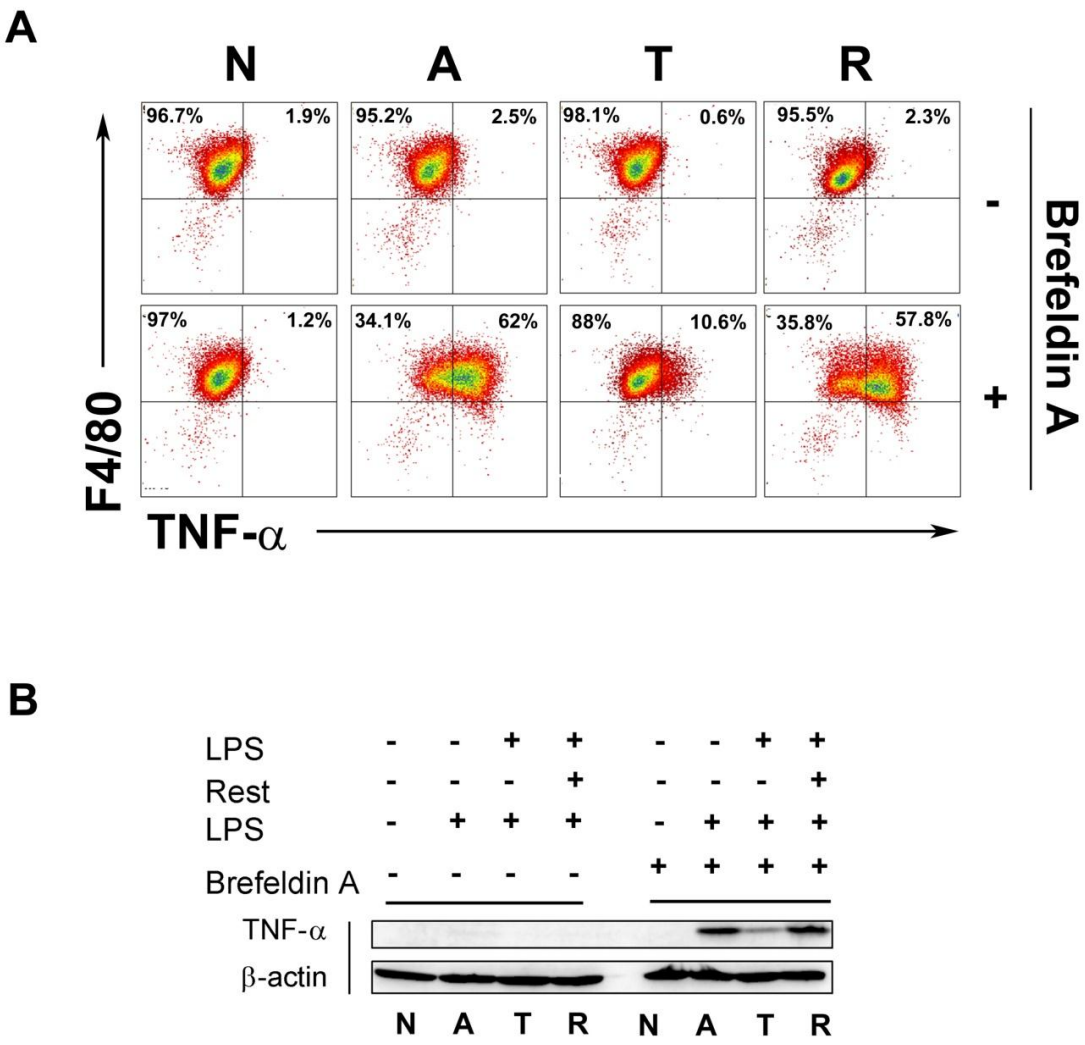

Figure 5.4: Recovery from LPS Tolerance restores intracellular TNF-α protein expression

(A) Intracellular TNF-α protein was measured in F4/80 positive cells from each group ± brefeldin A (1μg/10^6 cells – BD Golgi Plug). Data was controlled for with isotype specific and FMO controls. (B) Immunoblot measurement of total TNF-α protein ± brefeldin A. TNF-α protein was normalised to β-actin control protein. Data is representative of greater than four independent experiments with protein expression measured 8 hours post LPS re-stimulation. N = Naïve, A = acute response to LPS, T = LPS Tolerance and R = Recovery.

5.3.3 Suppression of pro-inflammatory cytokine secretion following recovery from LPS tolerance

We next analysed cytokine secretion in each macrophage group (N, A, T and R) by ELISA. Unexpectedly we were unable to detect significant levels of TNF-α, IL-6, IL-10 and IL-12p70 when compared with the acute response group (A) (Figure 5.5A). These cytokines remained suppressed in a LPS tolerisable state despite inducible intracellular TNF-α protein expression measured by intracellular staining and immunoblot analysis in the presence or absence of brefeldin A (1μg/10^6 cells) for 8 hours during LPS re-stimulation (Figure 5.4A and B).

To further analyse the secretion of cytokines and chemokines in the recovered group (R) we used an independent method involving an antibody membrane array. We screened a panel of thirty two cytokines including IL-6, IL-12p70, IL-12p40/p70, RANTES, CXCL1, CXCL2 and CCL3 (Appendix 1 and Appendix 2). Cells from each macrophage group (N, A, T and R) were treated as described in the LPS tolerance recovery model with cells re-stimulated with LPS for 24 hours. Supernatants removed from these cells were incubated with individual cytokine antibody membrane arrays for each group (N, A, T and R). This was followed by incubation of the membrane with a cocktail of biotinylated antibodies and subsequent labelling with streptavidin HRP. The membrane was visualised using a chemiluminescence imaging system. Using densitometric analysis we confirmed that IL-6, IL-12p70, CCL3 and IL-12p40/p70 secretion remained suppressed in the recovered group (R) with levels similar to that of the tolerant group (T) when compared with the acute response group (A). No significant difference in the secretion of the chemokines CXCL1, RANTES and CXCL2 was found between the

groups (A, T and R) (Figure 5.5B and Appendix 1). This data demonstrates that cytokine secretion is a regulated process and that cytokine synthesis does not lead to cytokine secretion in RM cells. In addition, this data suggests that cytokine secretion is regulated post transcriptionally through selective inhibition of pro-inflammatory cytokine secretion following recovery from LPS tolerance.

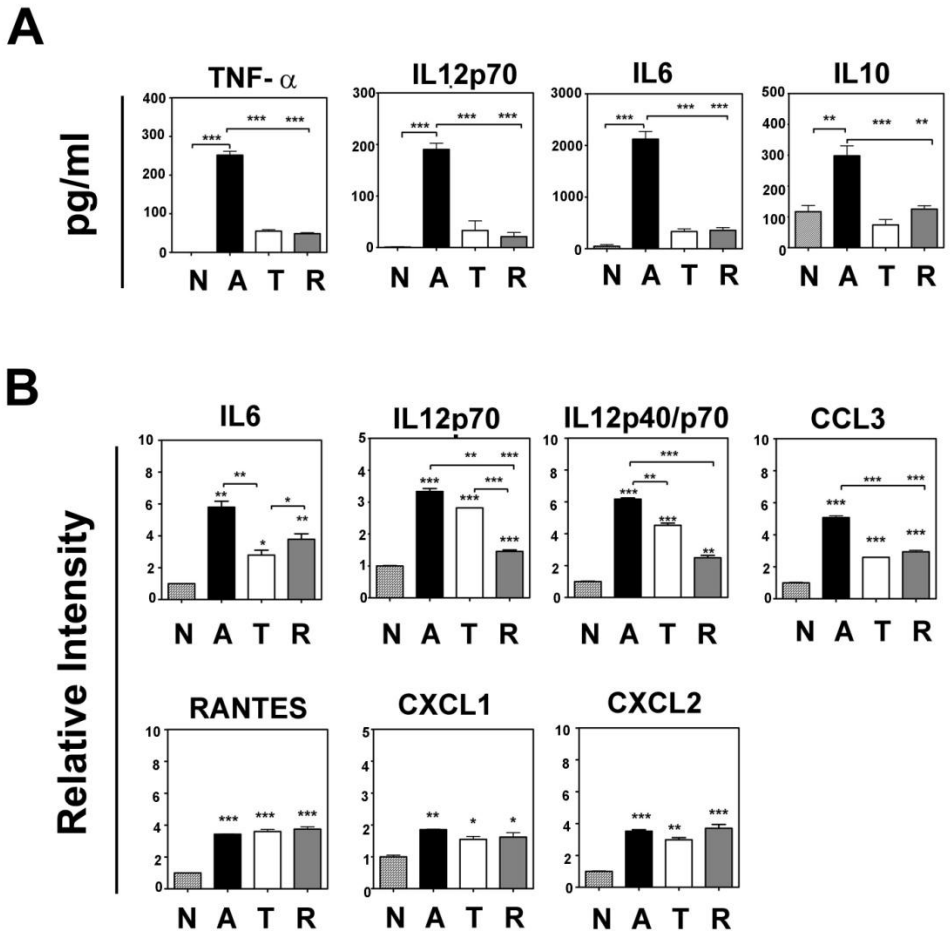

Figure 5.5: Suppression of pro-inflammatory cytokine secretion following recovery from LPS tolerance

(A) Pro-inflammatory cytokine secretion is measured by ELISA (pg/ml); TNF-α (8 hours), IL-6, IL-12p70, IL-10 (24 hours). (B) Pro-inflammatory cytokine and chemokine secretion (24 hours LPS re-stimulation); cytokine membrane array. Data is represented as relative intensity with all groups compared to the Naïve group (N) as determined by densitometric analysis. Densitometric analysis was performed using Image J software. Data is representative of greater than four independent experiments. N = Naïve, A = acute response to LPS, T = LPS Tolerance and R = Recovery.

5.3.4 TNF-α cytokine secretion is regulated through a bafilomycin A sensitive compartment

TNF-α translated protein is trafficked through a classical secretory route via the golgi intracellular compartment to recycling endosomes before delivery to the cell surface via the phagocytic cup for enzymatic cleavage and release of mature protein [229]. To investigate the disconnect between cytokine transcription and translation with that of cytokine secretion in RM cells, we measured TNF-α intracellular protein levels during the early stages in TNF-α cytokine trafficking through the Golgi. Intracellular TNF-α trafficking within each macrophage group (N, A, T and R) was analysed by fluorescence microscopy using antibodies against TNF-α and a marker of the Golgi intracellular apparatus, GM130. Trafficking of TNF-α through the Golgi was measured by analysis of GM130 and TNF-α co-localisation within cells and quantified by measuring the percentage co-localisation of GM130/TNF-α per field of view at 100X magnification. We identified that 1.5 hours of LPS re-stimulation was the optimal time point for analysis of GM130/TNF-α co-localisation in each macrophage group. This time point identified a disconnect in TNF-α intracellular protein trafficking through the Golgi between cells of the acute response (A) and RM cells (Figure 5.6 - Figure 5.12). This disconnect in TNF-α trafficking through the Golgi compartment was not evident at later time points as determined by GM130/TNF-α co-localisation.

Upon acute exposure to LPS (A) (1.5 hours), 60% of cells of the acute LPS response (A) were found to contain TNF-α co-localising with the Golgi compartment as determined by co-localisation with the Golgi marker GM130. In contrast, reduced TNF-α protein was measured within the Golgi in the LPS tolerant group (T) with

less than 10% of cells containing TNF-α protein co-localising with the Golgi marker GM130. This data is in agreement with reduced intracellular TNF-α expression levels as measured by flow cytometry and immunoblotting in addition to TNF-α transcriptional suppression demonstrated by qRT-PCR in the tolerant group (T) (Figure 5.3 and Figure 5.4). Despite inducible mRNA levels of TNF-α in RM cells to a level equal to the acute response group (A) (Figure 5.3), an average of 20% of RM cells were found to contain TNF-α protein co-localising with the Golgi compartment as determined by GM130/TNF-α co-localisation. Importantly a two fold significant difference was identified in the level of TNF-α co-localising within the Golgi compartment between cells of the acute LPS response (A) and RM cells ($p<0.001$) (Figure 5.6B, Figure 5.7B, Figure 5.8B and Figure 5.9B). This data correlated with the previous finding of suppressed cytokine secretion in RM cells at 8 hours post LPS re-stimulation (Figure 5.5).

Reduced TNF-α co-localisation within the Golgi compartment in RM cells despite inducible mRNA and total intracellular TNF-α protein (Figure 5.3 and Figure 5.4) suggests that TNF-α cytokine secretion is a regulated process. The lack of secretion of TNF-α is accompanied by increased total intracellular levels of TNF-α in RM cells suggesting that the synthesised protein is being degraded intracellularly. To test this hypothesis a panel of inhibitors used to target intracellular proteases (pepstatin A), calcium dependent proteases (MDL28170 - calpain III inhibitor) and cathepsin B (ca074me) to investigate if these enzymes were involved in degrading TNF-α protein in RM cells. Macrophages from each group were re-stimulated for 1.5 hours with LPS in the presence of absence of individual inhibitors (pepstatin A - 10μM, ca074me – 10μM and MDL28170 - 10μM). TNF-α protein trafficking through the golgi was measured by fluorescence microscopy in each macrophage group (N, A, T

and R) and represented as percentage GM130/TNF-α co-localisation per field of view at 100X magnification.

Treatment of macrophages from each group with the cathepsin B inhibitor ca074me or pepstatin A did not affect TNF-α co-localisation within the Golgi or restore cytokine secretion in RM cells despite cathepsin B previously being shown to be involved in post-transcriptional processing of TNF-α (Figure 5.6 and Figure 5.7) [230]. Although treatment with the calpain inhibitor MDL28170 led to an increase in GM130/TNF-α co-localisation in RM cells, a significant difference ($p<0.001$) remained in GM130/TNF-α co-localisation between the acute LPS response group (A) and RM cells (Figure 5.8A and B). In addition, while MDL28170 treatment lead to increased TNF-α secretion in both the acute LPS response (A) and RM cells, MDL28170 treatment did not restore TNF-α secretion in RM cells to levels comparable with the acute LPS response groups (A) as determined by ELISA (Figure 5.8C).

We next treated all macrophage groups with bafilomycin A, a vacuolar type H^+ ATPase, an inhibitor of intracellular organelle acidification and an inhibitor of the late stages of autophagy through inhibition of autophagosome and lysosome fusion, to determine if TNF-α protein was being degraded intracellularly in RM cells. Re-stimulation of groups A, T and R with LPS in the presence or absence of bafilomycin A (1μM) for 1.5 hours (including the naïve group) resulted in increased levels of intracellular TNF-α protein co-localising within the Golgi compartment in both the acute response (A) and recovered groups (R) (Figure 5.9A and B). An increase in GM130/TNF-α co-localisation was measured in the acute response group (A) treated with bafilomycin A with roughly 80% of cells of the acute response (A) co-localising within the Golgi compartment when compared with non bafilomycin A

treated acute response cells (A). However a significantly larger fold increase (2 fold) in GM130/TNF-α co-localisation was measured following recovery from LPS tolerance with 60% of RM cells containing TNF-α co-localising within the Golgi in the presence of bafilomycin A when compared with non bafilomycin A treated RM cells. In contrast GM130/TNF-α co-localisation was found to be relatively unchanged in the LPS tolerant group (T) upon treatment with bafilomycin A (Figure 5.9A and B). Bafilomycin A treatment during LPS re-stimulation of cells for 8 hours led to a 4.5 fold increase ($p<0.001$) in TNF-α secretion in the acute response group (A) when compared with non bafilomycin A treated cells (Figure 5.9C). Importantly, treatment of RM cells with bafilomycin A led to a 10 fold increase in TNF-α secretion following 8 hours of LPS re-stimulation when compared with RM cells without bafilomycin treatment ($p<0.001$) (Figure 5.9C). Furthermore, bafilomycin A treatment led to restoration of TNF-α secretion in RM cells to levels comparable with the acute response group (A) (Figure 5.9C). A statistically significant increase in TNF-α mRNA levels was measured in RM cells however this increase in gene expression is not biologically significant when compared with the 10 fold increase in secreted TNF-α protein in RM cells treated with bafilomycin A (Figure 5.9D). This data demonstrates that a bafilomycin sensitive compartment is involved in the regulation of TNF-α cytokine secretion following recovery from LPS tolerance.

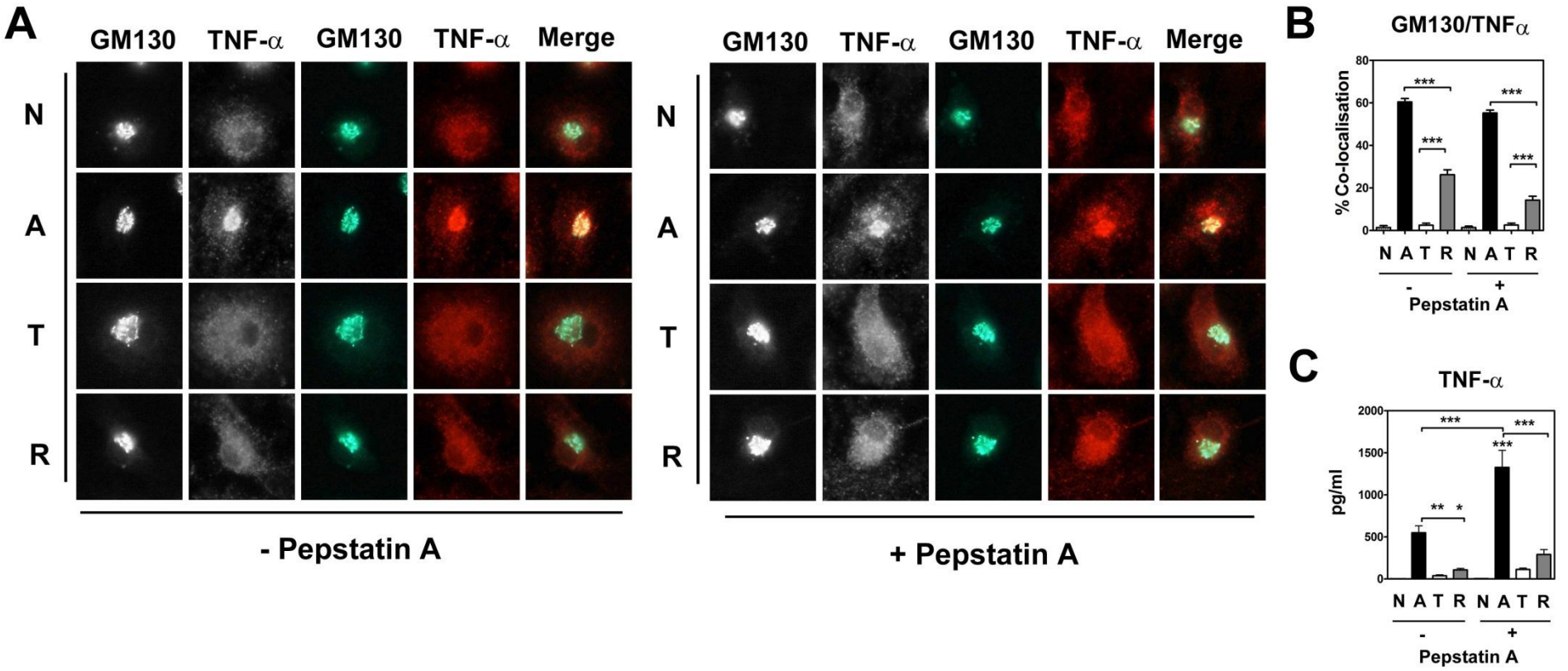

Figure 5.6: Pepstatin A inhibition does not restore TNF-α protein levels in RM cells (Figure legend – Next page)

Figure 5.6: Pepstatin A inhibition does not restore TNF-α protein levels in RM cells

(A) GM130/TNF-α co-localisation following 1.5 hour LPS re-stimulation ± protease inhibitor pepstatin A (10μM). Immunofluorescence images are representative of individual fields of view (10 fields of view analysed at 100X). (B) Quantification of GM130/TNF-α co-localisation (% co-localisation). Quantification was performed on greater than 10 fields of view at 100X magnification from greater than two independent experiments. (C) TNF-α secretion ± pepstatin A (8 hours LPS re-stimulation) Differences between groups were measured by one-way ANOVA with Tukey's post hoc test; $p<0.001$ (***), $p<0.01$ (**) $p<0.05$ (*). N = Naïve, A = acute response to LPS, T = LPS Tolerance and R = Recovery.

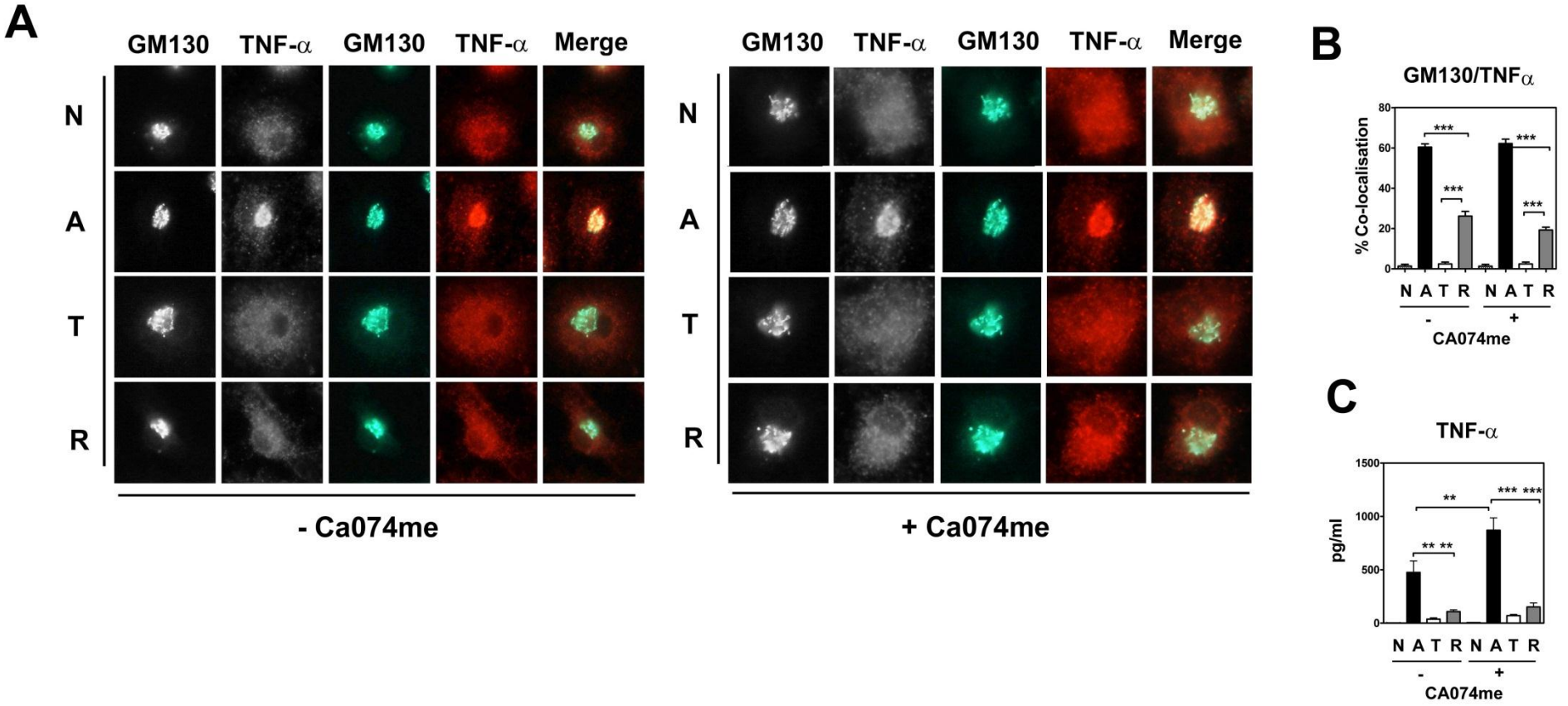

Figure 5.7: Cathepsin B inhibition does not restore TNF-α protein levels in RM cells (Figure legend – Next page)

Figure 5.7: Cathepsin B inhibition does not restore TNF-α protein levels in RM cells

(A) GM130/TNF-α co-localisation following 1.5 hour LPS re-stimulation ± cathepsin inhibitor ca074me (10μM). Immunofluorescence images are representative of individual fields of view (10 fields of view analysed at 100X). (B) Quantification of GM130/TNF-α co-localisation (% co-localisation). Quantification was performed on greater than 10 fields of view at 100X magnification from greater than two independent experiments. (C) TNF-α secretion ± ca074me (8 hours LPS re-stimulation) Differences between groups were measured by one-way ANOVA with Tukey's post hoc test; $p<0.001$ (***), $p<0.01$ (**) $p<0.05$ (*). N = Naïve, A = acute response to LPS, T = LPS Tolerance and R = Recovery.

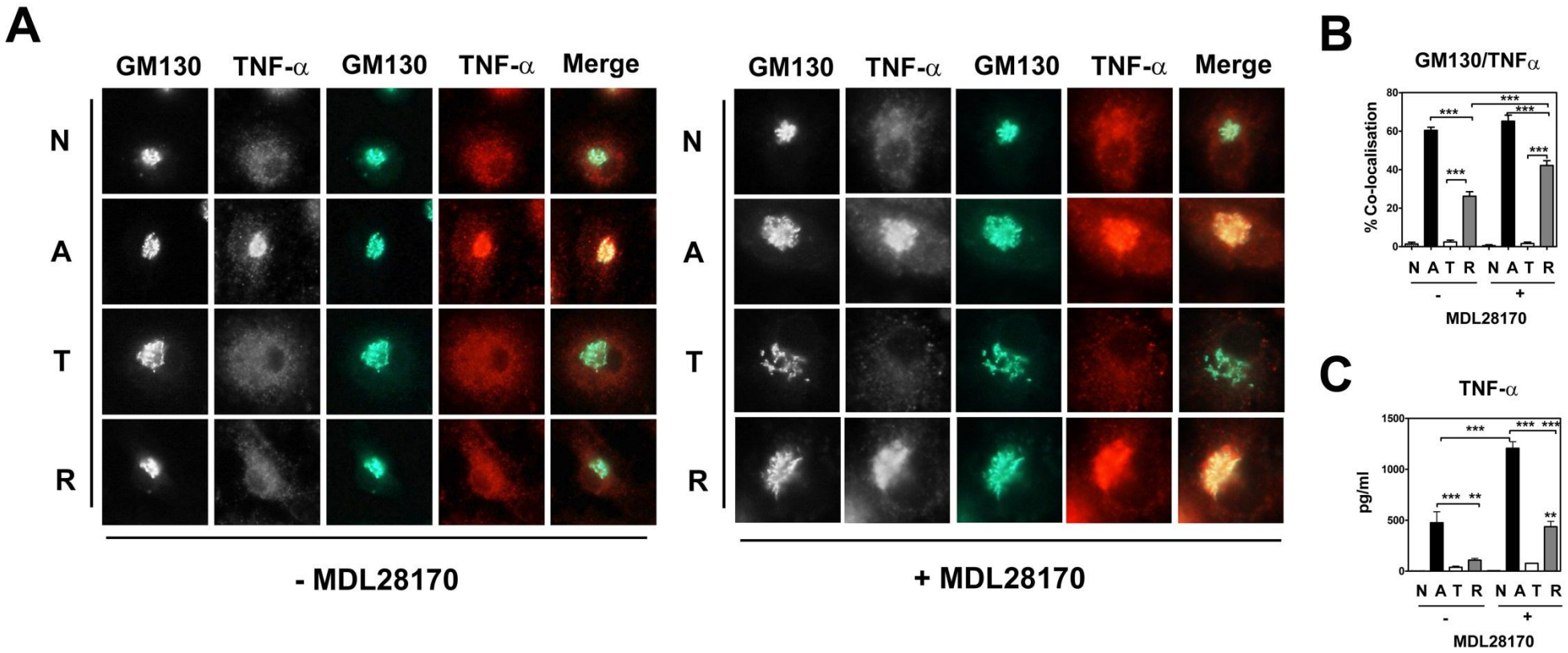

Figure 5.8: Calpain inhibition does not restore TNF-α protein levels in RM cells (Figure legend – Next page)

Figure 5.8: Calpain inhibition does not restore TNF-α protein levels in RM cells

(A) GM130/TNF-α co-localisation following 1.5 hour LPS re-stimulation ± calpain III inhibitor MDL28170 (10μM). Immunofluorescence images are representative of individual fields of view (10 fields of view analysed at 100X). (B) Quantification of GM130/TNF-α co-localisation (% co-localisation). Quantification was performed on greater than 10 fields of view at 100X magnification from greater than two independent experiments. (C) TNF-α secretion ± MDL28170 (8 hours LPS re-stimulation) Differences between groups were measured by one-way ANOVA with Tukey's post hoc test; $p<0.001$ (***), $p<0.01$ (**) $p<0.05$ (*). N = Naïve, A = acute response to LPS, T = LPS Tolerance and R = Recovery.

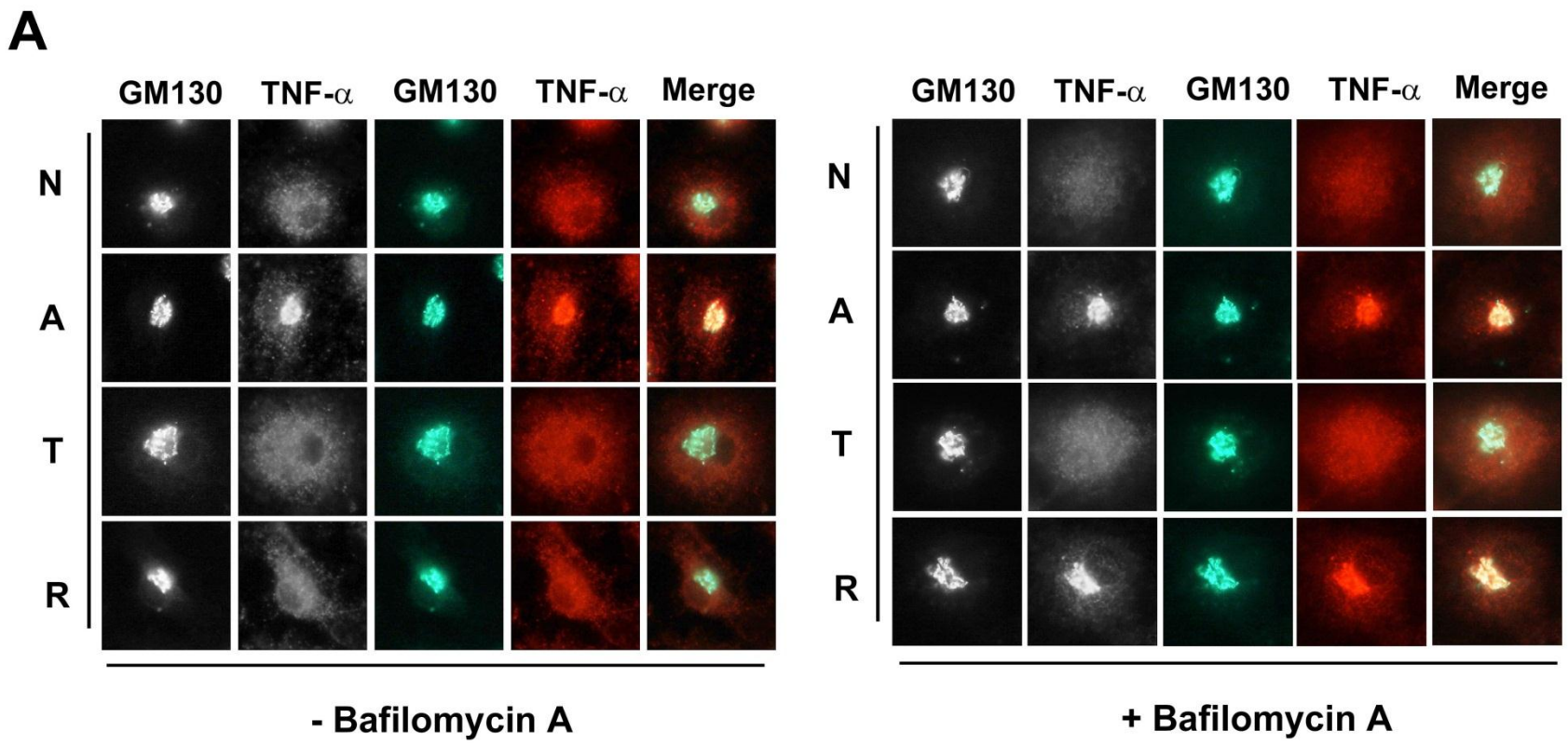

Figure 5.9: TNF-α secretion is regulated through a Bafilomycin A sensitive compartment in RM cells

(A) GM130/TNF-α co-localisation following 1.5 hour LPS re-stimulation ± bafilomycin A (1μM). Immunofluorescence images are representative of total field of view at 100X magnification.

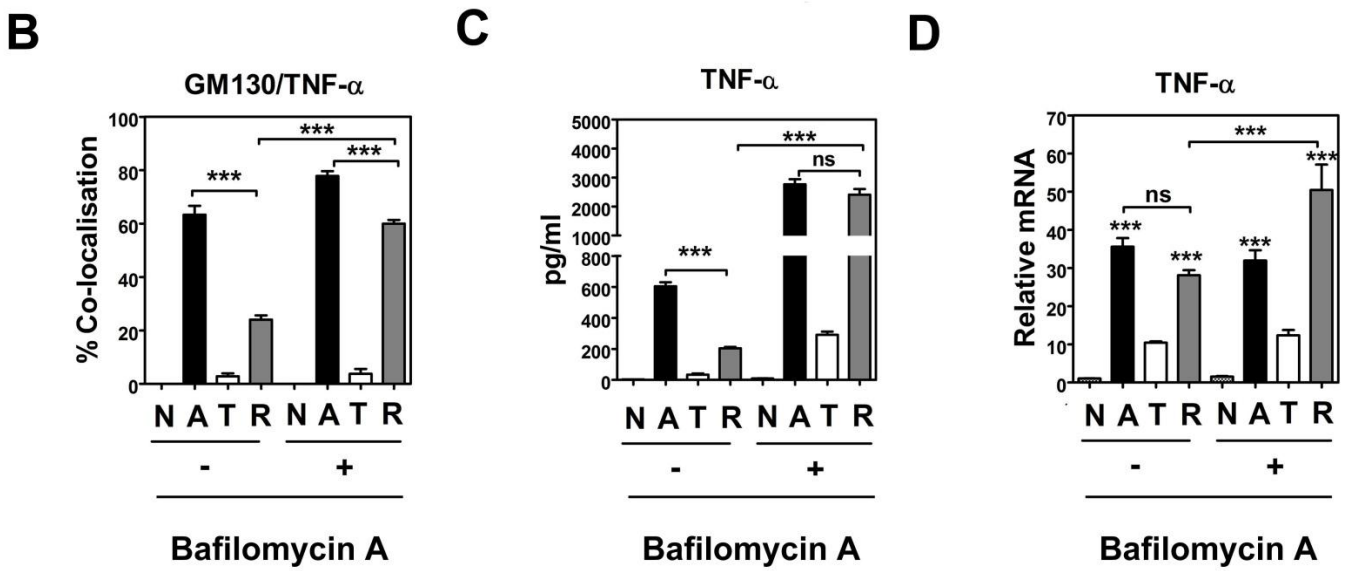

Figure 5.9: TNF-α secretion is regulated through a Bafilomycin A sensitive compartment in RM cells

(B) Quantification of GM130/TNF-α co-localisation (% co-localisation) following 1.5 hour LPS re-stimulation ± bafilomycin A (1μM) at 100X magnification. (C) TNF-α secretion (pg/ml) ± bafilomycin A (8 hours). (D) TNF-α gene expression ± bafilomycin A represented as relative mRNA. Differences between groups were measured by one-way ANOVA with Tukey's post hoc test; $p<0.001$ (***), $p<0.01$ (**) $p<0.05$ (*). Quantification of GM130/TNF-α co-localisation was measured from greater than 10 fields of view at 100X magnification. Data is representative of greater than three independent experiments. N = Naïve, A = acute response to LPS, T = LPS Tolerance and R = Recovery.

5.3.5 Loss of Atg16L1 does not restore TNF-α secretion in RM cells

Autophagy is an evolutionarily conserved process important in maintaining cell and tissue homeostasis through removal of cellular proteins and organelles by targeting them for degradation within lysosomes while recycling cellular energy and nutrients [231, 232]. Autophagy is a physiological host response and has also been shown to be important in controlling cytokine secretion by regulating inflammasome activation targeting pro-IL-1β for cleavage by caspase 1[231, 233]. In addition, autophagy has been shown to be important in regulating IL-23 secretion through the regulation of IL-1 family of cytokines [232, 234]. Atg16L1 is an important component of the autophagy apparatus with Atg16L1 deficiency leading to defective recruitment of the Atg12-Atg5 complex resulting in inhibition of autophagosome formation [235]. Furthermore Atg16L1 has been identified as a Crohn's disease susceptibility gene [236] in addition to being important in regulating LPS induced IL-1β secretion in BMDMs [72]. Therefore to investigate if suppressed cytokine secretion in RM cells was controlled by an autophagy dependent degradative process, we tested if TNF-α secretion could be restored in RM cells to levels comparable to cells of the acute response (A) in the absence of Atg16L1 using Atg16L1 deficient BMDMs.

WT and Atg16L1 deficient BMDMs were treated as described in the LPS tolerance recovery model (Figure 5.1). No difference in TNF-α gene expression was measured between WT and Atg16L1$^{-/-}$ cells following 4 hours re-stimulation of macrophage groups (A, T and R) with LPS (Figure 5.10A). Similarly no difference in total intracellular TNF-α protein was found between WT and Atg16L1$^{-/-}$ cells as determined by immunoblot and intracellular staining by flow cytometry following 8

hours LPS re-stimulation in the presence or absence of brefeldin A (1μg/10^6 cells) (Figure 5.10B and C).

We next measured TNF-α trafficking through the Golgi compartment by measuring the percentage of cells containing TNF-α co-localising with the Golgi marker GM130 following 1.5 hours LPS re-stimulation. A 2 fold significant increase was measured in the number of Atg16L1$^{-/-}$ RM cells containing TNF-α co-localising within the Golgi (GM130/TNF-α co-localisation) in comparison to that of wild type RM cells (Figure 5.11A and B). However this did not fully restore GM130/TNF-α co-localisation in Atg16L1 deficient RM cells to levels comparable with Atg16L1 deficient cells of the acute response (A) as determined quantitatively by measuring the percentage of GM130/TNF-α positive cells (Figure 5.11A and B). These data correlate with treatment of RM cells with bafilomycin A, which led to an increase in TNF-α co-localising within the Golgi compartment when compared with non bafilomycin treated RM cells (Figure 5.9B). Importantly, despite Atg16L1 deficiency in RM cells leading to a 2 fold increase GM130/TNF-α co-localisation similar to bafilomycin treatment of RM cells, Atg16L1 deficiency did not restore TNF-α secretion in RM cells when compared with Atg16L1 deficient acute LPS response cells (A) (Figure 5.11C). This data is in contrast to the ability of bafilomycin A treatment of RM cells to induce a 10 fold increase in TNF-α secretion in comparison to non bafilomycin A treated RM cells Figure 5.9C). Taken together this data suggests that a bafilomycin A dependent cellular process through inhibition of organelle acidification other than autophagy may be involved in regulation of TNF-α secretion in RM cells.

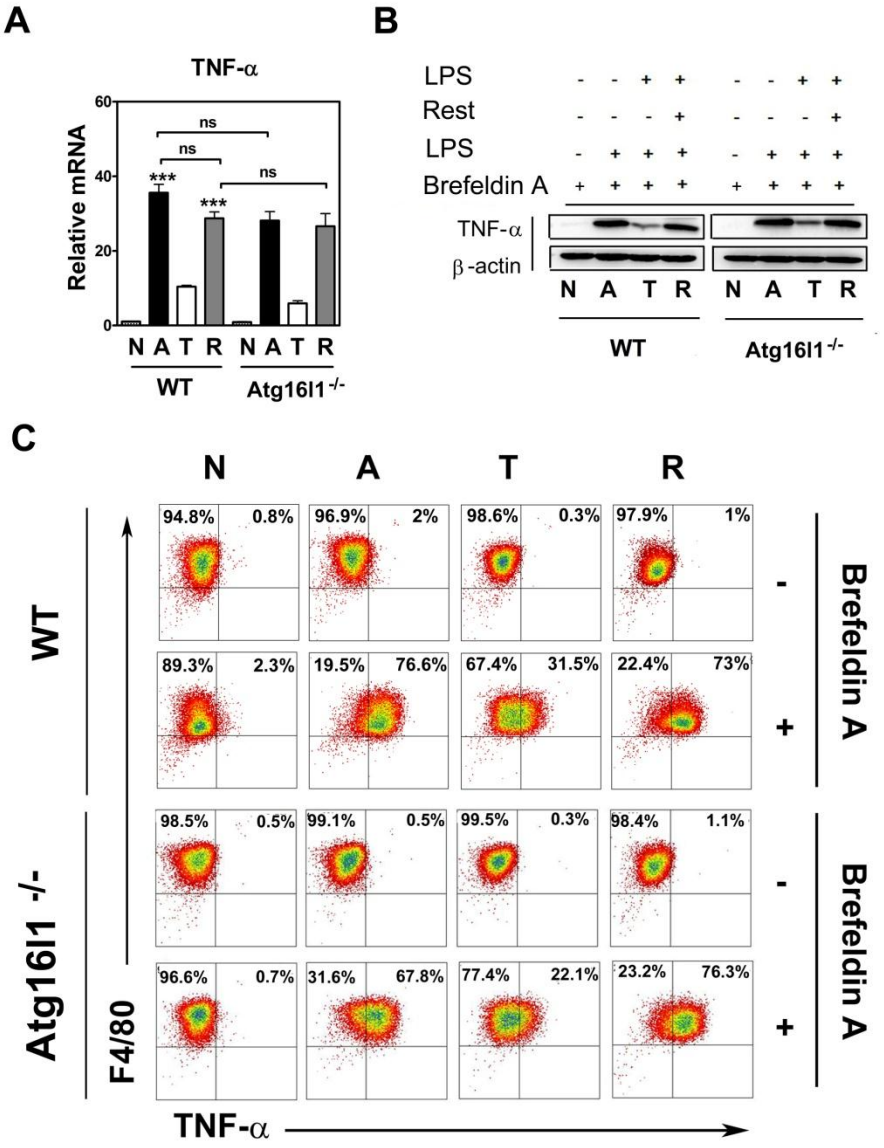

Figure 5.10: Atg16L1 deficiency does not affect TNF-α transcription and translation following recovery from LPS tolerance

Wild type (WT) and Atg16L1$^{-/-}$ BMDMs (A) TNF-α gene transcription (relative mRNA) following 4 hours LPS re-stimulation. (B) Immunoblot of total TNF-α protein ± brefeldin A (8 hours LPS re-stimulation) normalised to β-actin control protein. (C) Intracellular TNF-α protein was measured in F4/80 positive cells from each group (N, A, T and R) ± brefeldin A (8 hours LPS re-stimulation). Data was controlled for with isotype specific and FMO controls. Differences between groups were measured by one-way ANOVA with Tukey's post hoc test; $p<0.001$ (***), $p<0.01$ (**) $p<0.05$ (*). Data is representative of greater than three independent experiments. N = Naïve, A = acute response to LPS, T = LPS Tolerance and R = Recovery.

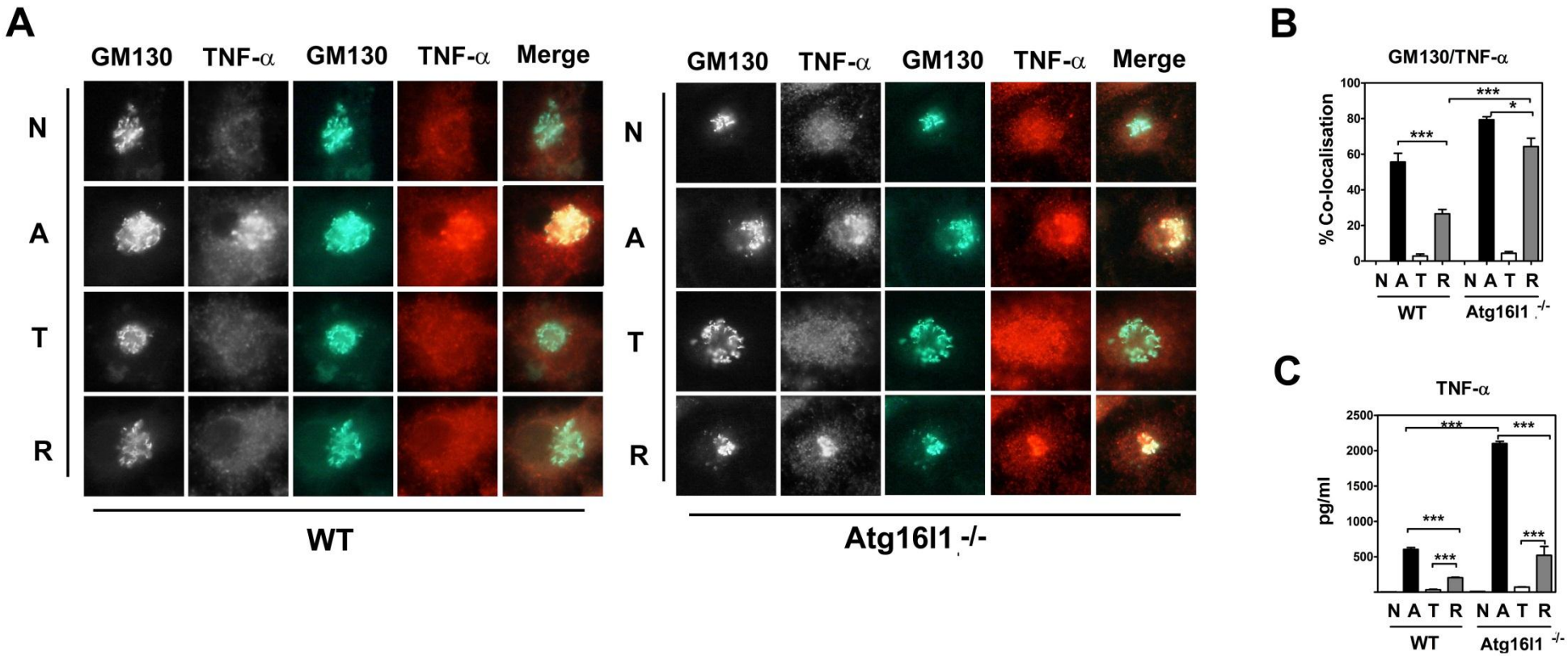

Figure 5.11: TNF-α secretion in RM cells is not regulated by autophagy (Figure legend – Next page)

Figure 5.11: TNF-α secretion in RM cells is not regulated by autophagy

WT and Atg16L1$^{-/-}$ BMDMs (A) TNF-α/GM130 co-localisation following 1.5 hour LPS re-stimulation. Immunofluorescence images are representative of total field of view at 100X magnification. (B) Quantification of TNF-α/GM130 co-localisation (% co-localisation) was measured from greater than 10 fields of view at 100X magnification. (C) TNF-α secretion (pg/ml) was measured at 8 hours post re-stimulation. Differences between groups were measured by one-way ANOVA with Tukey's post hoc test; $p<0.001$ (***), $p<0.01$ (**) $p<0.05$ (*). Data is representative of greater than three independent experiments. N = Naïve, A = acute response to LPS, T = LPS Tolerance and R = Recovery.

5.3.6 TNF-α co-localisation within the Golgi is restored in RM cells upon treatment with monensin

To further investigate the consequences of blocking acidification of intracellular organelle compartments, GM130 co-localisation with TNF-α was measured in the presence or absence of the monovalent ionophore monensin. Monensin treatment raises the pH of acidic intracellular compartments such as lysosomes by facilitating the exchange of sodium ions for protons. In a similar pattern to bafilomycin A treatment of cells (Figure 5.9), monensin (2μM) treatment for 1.5 hours during LPS re-stimulation led to a significant increase in GM130/TNF-α co-localisation in RM cells comparable with cells of the acute LPS response (A) (Figure 5.12A and B). Despite alterations in Golgi structure associated with treatment with monensin or brefeldin A [237], co-localisation of TNF-α within this fragmented compartment was easily measured. Monensin treatment of cells of the acute LPS response (A) led to a small increase in intracellular TNF-α co-localising within the Golgi however monensin treatment completely restored GM130/TNF-α co-localisation (90%) in RM cells to levels comparable with cells of the acute response group. Collectively, this data suggests that TNF-α is directed towards acidic intracellular compartments such as lysosomes for degradation in RM cells rather than being trafficked to the cell surface for cleavage and subsequent secretion of mature TNF-α protein.

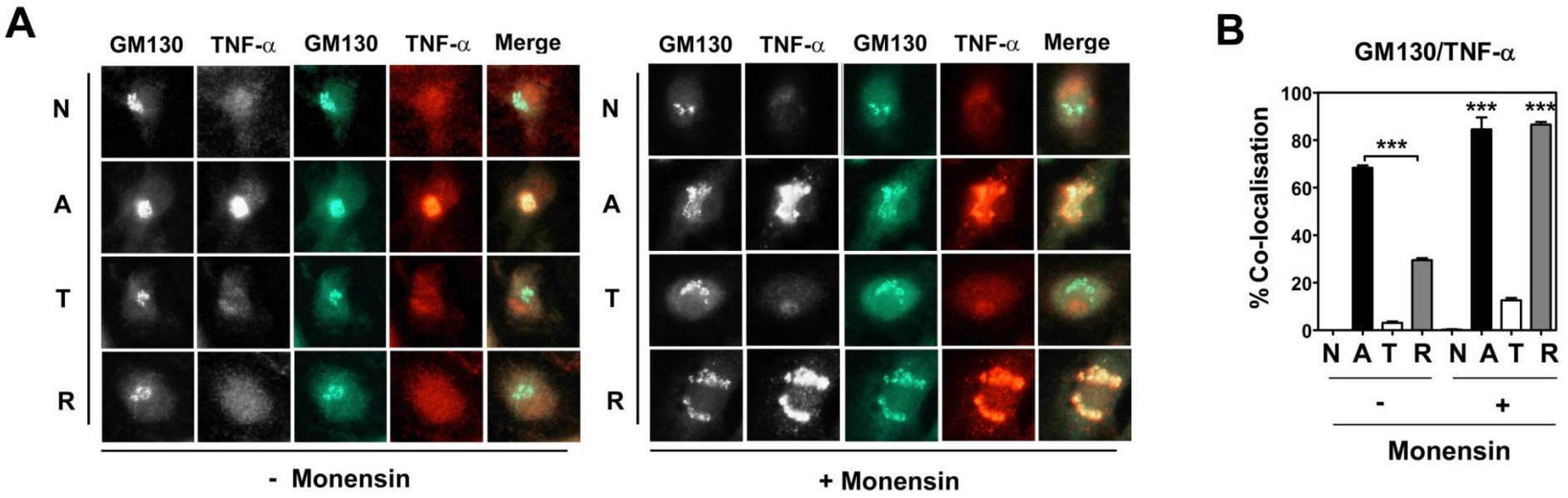

Figure 5.12: TNF-α secretion may be regulated in a lysosomal dependent process

(A) TNF-α/GM130 co-localisation following 1.5 hour LPS re-stimulation ± monensin. Immunofluorescence images are representative of total field of view at 100X magnification. (B) Quantification of TNF-α/GM130 co-localisation (% co-localisation) was measured from greater than 10 fields of view at 100X magnification. Differences between groups were measured by one-way ANOVA with Tukey's post hoc test; $p<0.001$ (***), $p<0.01$ (**) $p<0.05$ (*). Data is representative of greater than three independent experiments. N = Naïve, A = acute response to LPS, T = LPS Tolerance and R = Recovery.

5.3.7 Restoration of cytokine secretion in RM cells upon stimulation with a second independent signal

Suppression of cytokine secretion despite intact total intracellular cytokine protein expression (Figure 5.4) levels in RM cells would appear to be a wasteful use of cellular energy resources. In addition, inhibition of cytokine secretion in RM cells may render the host more susceptible to secondary opportunistic infections due to the inability to recruit other innate immune cells including neutrophils and monocytes mediated by cytokines and chemokines. In addition induction of cytotoxicity, antigen presentation activities and expansion of Th1, Th2, Th17 and B cell populations and their cellular responses are all key functions of cytokines and chemokines which would be reduced if cytokine secretion is inhibited. Therefore to investigate the ability of RM cells to mount an effective immune response towards secondary infections, cytokine secretion was measured in RM cells upon challenge with a second independent inflammatory signal.

Macrophages from each group were treated as described in the LPS tolerance recovery model prior to re-stimulation (Figure 5.1). Macrophages were then re-stimulated with a combination of LPS and an additional inflammatory signal such as IL-1β (10ng/ml) or a TLR2 agonist Pam3CSK4 (100ng/ml) or the TLR9 agonist CpG (1μM) or IFN-γ (50ng/ml) or CD40L (10μg/ml) for 8 hours (TNF-α secretion) and 24 hours (IL-6 secretion). Supernatants were removed from each group (N, A, T and R) that were re-stimulated with different combinations of ligands described. Cytokine secretion was analysed by ELISA. TNF-α cytokine secretion was restored in RM cells to levels comparable to the acute response group (A) upon combined re-stimulation with LPS and IL-1β. The LPS and IL-1β combined stimulation resulted

in a 2 fold increase in TNF-α secretion in RM cells. Treatment of group A, T and R with LPS and Pam3CSK4 or LPS and CpG resulted in a robust increase in cytokine secretion in all groups. Treatment of RM cells with LPS and Pam3CSK4 resulted in a 20 fold increase in TNF-α secretion while LPS and CpG co-treatment of RM cells resulted in an 18 fold increase in TNF-α secretion (Figure 5.13). Interestingly this coincided with increased mRNA levels of TNF-α in the macrophage groups (A, T and R) upon Pam3CSK4 and CpG challenge but not that of IL-1β challenge. Importantly increased mRNA levels in RM cells did not account for restoration of secretion of TNF-α as no difference in mRNA levels were found between the acute LPS response group (A) and RM cells following co-treatment with LPS and IL-1β or LPS and Pam3CSK4 or LPS and CpG (Figure 5.13). Importantly, re-stimulation of tolerant cells (T) with LPS and IL-1β, or LPS and Pam3CSK4, or LPS and CpG did not alter TNF-α secretion with TNF-α secretion and gene expression remaining suppressed when compared with the acute response group (A) (Figure 5.13).

The restoration of TNF-α cytokine secretion was found to be stimulus dependent with combined LPS stimulation with IFN-γ or LPS and CD40L, two powerful activators of inflammation, failing to restore TNF-α secretion in RM cells when compared with the acute LPS response group (A). TNF-α secretion levels were found be comparable to the LPS tolerant group (T) (Figure 5.14). Furthermore restoration of cytokine secretion was specific to TNF-α with secretion of IL-6 remaining suppressed upon re-stimulation with LPS and IL-1β or LPS and Pam3CSK4 or LPS and CpG when compared with the acute response group (A) (Figure 5.15). Taken together this data suggests that RM cells are primed to respond and secrete TNF-α upon independent inflammatory signals such IL-1β. Furthermore

this highlights that restoration of pro-inflammatory cytokine secretion is tightly regulated in a stimulus dependent manner.

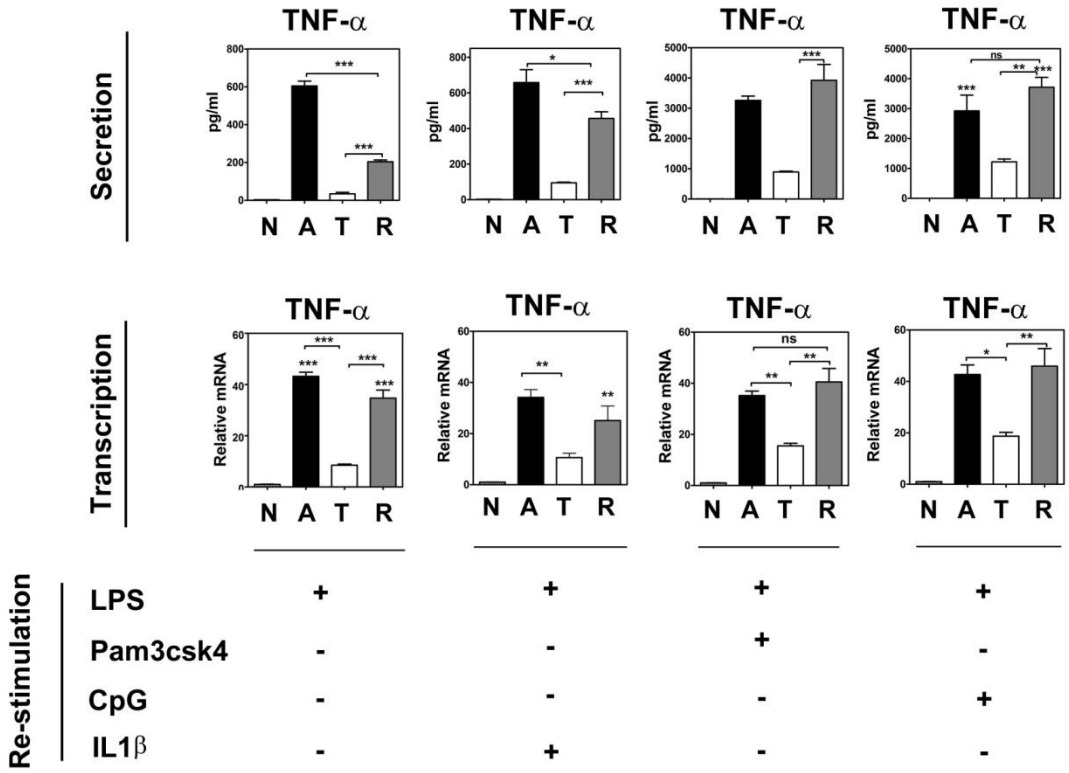

Figure 5.13: An independent inflammatory stimulus restores TNF-α secretion in RM cells

TNF-α secretion (pg/ml) and TNF-α gene expression was measured post re-stimulation with LPS ± Pam3CSK4 (100ng/ml), CpG (1μM) or IL-1β (10ng/ml). Secretion and gene expression were measured 8 and 4 hours post re-stimulation respectively. Gene expression is measured as relative mRNA. Differences between groups were measured by one-way ANOVA with Tukey's post hoc test; $p<0.001$ (***), $p<0.01$ (**) $p<0.05$ (*). Data is representative of greater than three independent experiments. N = Naïve, A = acute response to LPS, T = LPS Tolerance and R = Recovery.

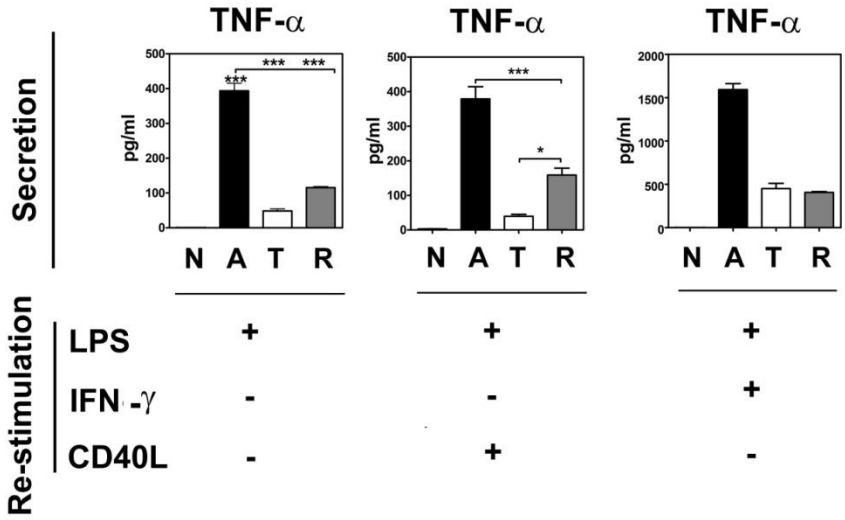

Figure 5.14: Restoration of TNF-α secretion in RM cells is stimulus specific

TNF-α secretion (pg/ml) was measured post re-stimulation with LPS ± IFN-γ (50ng/ml) or CD40L (10μg/ml). Secretion was measured 8 post re-stimulation. Differences between groups were measured by one-way ANOVA with Tukey's post hoc test; $p<0.001$ (***), $p<0.01$ (**) $p<0.05$ (*). Data is representative of greater than three independent experiments. N = Naïve, A = acute response to LPS, T = LPS Tolerance and R = Recovery.

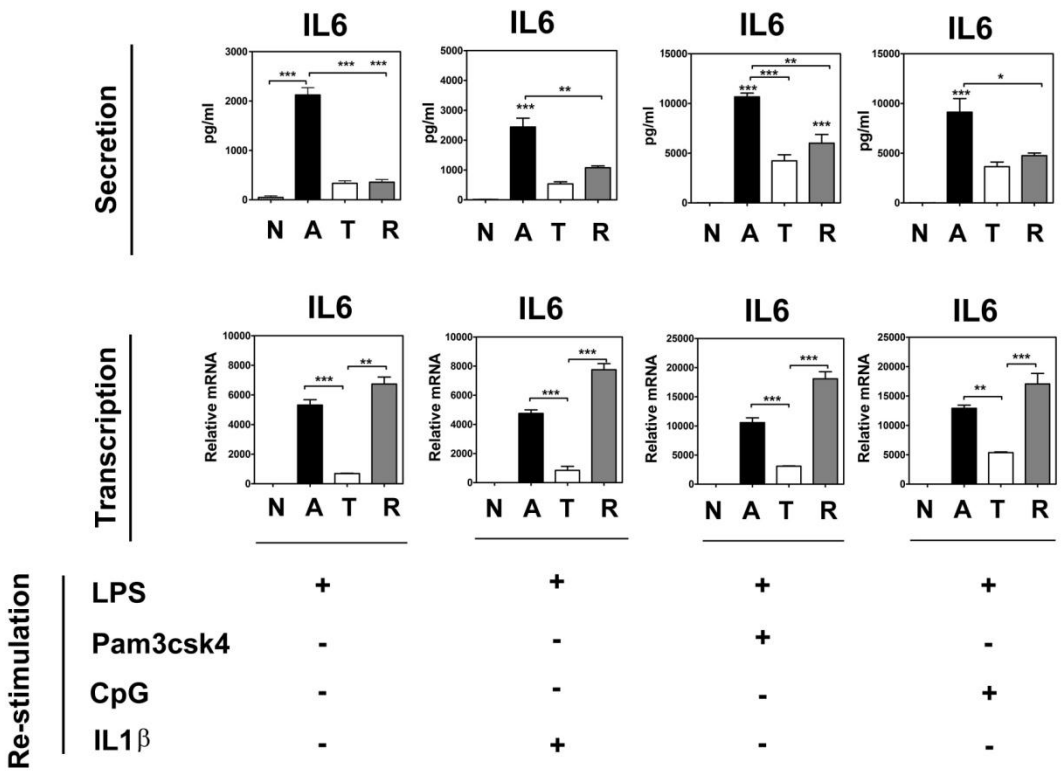

Figure 5.15: Pam3CSK4, CpG and IL-1β does not restore IL-6 secretion in RM cells

IL-6 secretion (pg/ml) and IL-6 gene expression were measured post re-stimulation with LPS ± Pam3CSK4 (100ng/ml), CpG (1μM) or IL-1β (10ng/ml). Secretion and gene expression were measured 24 hours and 4 hours post re-stimulation respectively. Gene expression is measured as relative mRNA. Differences between groups were measured by one-way ANOVA with Tukey's post hoc test; $p<0.001$ (***), $p<0.01$ (**) $p<0.05$ (*). Data is representative of greater than three independent experiments. N = Naïve, A = acute response to LPS, T = LPS Tolerance and R = Recovery.

5.4 Discussion

TLR induced inflammation is a highly orchestrated and tightly regulated immunological response to infection and injury. While extensive research has been undertaken to elucidate the regulation of TLR immune responses, much of this focus has been largely centred on the TLR signalling pathway and transcriptional regulation of TLR responses [2, 3, 30, 75]. Here we illustrate a novel mechanism of regulation of TLR inflammatory responses post translationally at the level of cytokine secretion. Using the model of acute response to LPS, regulation of cytokine protein was analysed in Naïve (N), acute LPS response (A), LPS tolerant (T) and RM recovered cells (R = RM). Transcriptomic analysis revealed that gene expression of interleukin, CXCL and CCL pro-inflammatory cytokine and chemokine families were inducible upon recovery from LPS tolerance. Tolerisable cytokines including TNF-α, CXCL10, CXCL1 and IL-6 were induced in RM cells to levels comparable with that of the acute response to LPS (A). Furthermore non-tolerisable cytokine and chemokine genes including RANTES, CCL17, CCL9 and CCL22 remained inducible in RM cells. In agreement with these findings, intracellular levels of TNF-α were measured following recovery from LPS tolerance (R) confirming that TNF-α mRNA was translated and not inhibited through post transcriptional regulatory events [238]. In contrast, secretion of TNF-α in addition to IL-6, IL-10, CXCL10, CCL3, and IL-12p70 was dramatically reduced in RM cells. Furthermore we identified that a second independent specific stimulus may selectively restore cytokine secretion upon recovery from LPS tolerance.

Cytokine and chemokine secretion during infection or injury is fundamental to mounting an effective and tailored immunological response to specific inflammatory

stimuli. These key immune-modulatory proteins initiate immune cell recruitment in addition to modulating immune cellular functions and expansion of adaptive immune cell populations to fight and clear infection, thus restoring immune and tissue homeostasis [3]. Despite playing a fundamental protective immunological role, excessive production of cytokines and chemokines underlie the pathology of many chronic inflammatory and autoimmune diseases. Cytokines produced from multiple cellular sources including macrophages play a central role in the pathogenesis of rheumatoid arthritis (RA) [222]. Although numerous cytokines and chemokines have been implicated in RA, TNF-α is widely found in synovial membranes of these patients. Over-expression studies in mice with TNF-α demonstrated the ability to develop spontaneous arthritis [222]. Similarly, excessive cytokine production has been a central component of the pathogenesis of inflammatory bowel disease [239]. Of note, neutralising TNF-α protein with TNF-α targeting antibodies (infliximab and adalimuab) are widely used in the clinic as part of the treatment and management of both RA and IBD [222, 239]. The development of therapeutics targeting cytokines specifically highlights the central role cytokines play in the pathology of these diseases.

Tissue resident macrophages that are found in healthy non-obese adipose tissue have an anti-inflammatory like phenotype dependent on the local adipokine microenvironment to perform tissue specific regulatory functions. During obesity this metabolic environment is disrupted as a result of increased levels of pre-adipocytes. Increased levels of these cells can lead to increased production of pro-inflammatory cytokines and induction of unnecessary inflammation. Increased production of TNF-α and IL-6 has been implicated in the development of insulin resistance and type 2 diabetes [127]. Furthermore, excessive and uncontrolled

cytokine and chemokine production has been implicated in asthma and lung diseases including COPD [223]. Similarly, extensive vascular inflammation has been associated with the pro-inflammatory environment created within atherosclerotic plaques [240]. On the contrary, dysregulation of cytokine production has been implicated in immunosuppressive states including sepsis [117, 159, 225]. Prolonged and unregulated suppression of pro-inflammatory cytokine production by monocytes mirrors a state of endotoxin tolerance in sepsis patients [36]. Furthermore, monocytes isolated from cystic fibrosis patients demonstrate a similar tolerant-like profile [42, 113, 241]. Additionally, inability to regulate cytokine production correlates with increased susceptibility to secondary opportunistic infections and subsequent patient mortality [160].

The variety of chronic inflammatory and immunosuppressive conditions associated with dysregulated cytokine and chemokine production demonstrates the importance for tight regulation of cytokine secretion following acute inflammatory responses. This study suggests that inflammation is regulated post translationally through modulation of cytokine secretion following recovery from LPS tolerance. To decipher the regulatory mechanism involved in inhibiting TNF-α secretion, RM cells were treated with bafilomycin A, a known inhibitor of autophagy and vacuolar type H^+ATPase which inhibits acidification of cellular compartments including lysosomes and endosomes. Restoration of TNF-α secretion and increased levels of TNF-α co-localising within the Golgi in RM cells upon bafilomycin A treatment suggested that translated TNF-α may be alternatively trafficked within RM cells towards lysosomal compartments to prevent secretion. Treatment with additional inhibitors of intracellular proteases including pepstatin A, in addition to a calpain inhibitor and cathepsin B inhibitor did not have the same effect as bafilomycin A in restoring

TNF-α secretion in RM cells suggesting that an alternative intracellular compartment that is bafilomycin A sensitive is involved in TNF-protein degradation. Additionally, RM cells deficient in Atg16L1, an autophagy protein involved in recruitment of the Atg12-Atg5 complex which is involved in autophagosome formation in the autophagy pathway [235] did not demonstrate restored TNF-α secretion despite defects in the autophagy pathway implicated in the alterations in IL-1β production [72, 231, 232, 234]. This suggests that an alternative bafilomycin sensitive compartment may be involved in the regulation of cytokine secretion in RM cells. In support of bafilomycin A restoration of TNF-α secretion in RM cells, treatment of cells with an additional inhibitor of lysosomal acidification, monensin, led to increased levels of TNF-α protein co-localising within the Golgi compartment thereby preventing trafficking of TNF-α towards these intracellular acidic compartments. Collectively this data suggests that recovery from LPS tolerance regulates inflammation through altering TNF-α trafficking towards a degradative pathway that is independent of autophagy and intracellular acidic proteases, calpain and cathepsin B enzyme degradation.

Interestingly, suppression of TNF-α secretion has been observed in macrophages isolated from Crohn's disease (CD) patients [226]. Smith et al found intracellular TNF-α protein within CD macrophages despite reduced protein secretion. Smith et al proposed that lysosomal degradation was implicated in suppressing cytokine secretion in CD macrophages [226]. This study provides solid evidence for post translational regulation of cytokine secretion as a mechanism for regulating macrophage responses to TLRs. Whether suppressed cytokine secretion is a consequence of CD pathology remains to be determined.

In light of this work we propose that TLR tolerance is not only regulated at the mRNA level, but also at the level of secretion. In chapter 4 transcriptional profiling identified LPS tolerance as a transient state with transcriptional repression of pro-inflammatory mRNA alleviated following recovery from this state. In this chapter measurement of total intracellular TNF-α protein further highlighted restoration of inflammatory potential post LPS tolerance. Furthermore, this confirmed that post transcriptional regulatory events involving mRNA stability were not implicated in suppressing cytokine secretion [238]. Reduced TNF-α secretion following recovery from LPS tolerance suggests that RM cells do not restore full pro-inflammatory potential similar to macrophages of the acute response to LPS. Requirement of a secondary independent signal highlighted that macrophages post LPS tolerance adopt an immune primed phenotype that is regulated through cytokine secretion. This level of regulation of inflammation suggests that following recovery from LPS tolerance, macrophages may retain a memory of a prior inflammatory response. Thus these cells are able to respond rapidly upon additional specific infections, in environments where maintaince of a tolerant state is critical to maintain tissue homeostasis such as in the gut or that of adipose tissue.

Recent studies have demonstrated a role for the multiprotein inflammasome complex in the regulation of inflammatory responses in intestinal phagocytes through NLRC4 driven IL-β production [228]. *Franchi et al* demonstrated that CD11b positive intestinal phagocytes (iMPs) were anergic to TLR stimulation however produced high levels of pro-IL-1β [228]. Upon pathogenic infection with *Salmonella* or *Pseudomonas* species NLRC4 drives mature IL-1β production which in turn orchestrates the inflammatory response to these infections in the intestine [228]. Interestingly, we identified that IL-1β co-stimulation with LPS restored TNF-α

secretion in RM cells suggesting that activation of the inflammasome complex may play a role in the regulation of cytokine secretion following recovery from LPS tolerance.

Ueda et al demonstrated that colonic macrophages are hyporesponsive towards TLR stimulation with IL-10 production central to controlling secretion of inflammatory cytokines including IL-6 and TNF-α [162]. In addition, this study demonstrated that STAT3 or IL-10 deficient mice were hyperresponsive to LPS with increased TNF-α and IL-6 secretion measured in colonic macrophages [162]. In chapter 4 we measured increased phosphorylated STAT1 and STAT3 in both LPS tolerant (T) and RM cells (Figure 4.17) suggesting that these transcription factors may play a role regulation of cytokine secretion in RM cells. A recent study has characterised colonic macrophage populations under steady state and inflammatory conditions [227]. This study demonstrated that resident colonic macrophages were responsive toward TLR challenge with mRNA and intracellular TNF-α protein increased in these cells [227]. While TNF-α secretion was not measured in these cells, previous studies by *Franchi et al* [228] and *Ueda et al* [162] did not detect secretion of TNF-α or IL-6 upon TLR stimulation. These two studies isolated colonic macrophages using CD11b MACS separation or CD11b flow cytometry cell sorting, however *Bain et al* describe a novel isolation protocol for resident colonic macrophages using a panel of colonic macrophage specific markers [227]. As a result, it would be important to measure cytokine production from these cells upon TLR challenge to confirm the suppressed cytokine secretion identified in the previous studies. Taken together these studies correlate with the suppressed cytokine secretion findings in RMs of this study suggesting that TLR tolerance may also be regulated at the level of cytokine secretion under physiological conditions in the intestine.

These three studies also highlight the importance of measuring both cytokine secretion and mRNA levels to determine the activation status of cells. LPS tolerance results from transcriptional repression of pro-inflammatory gene expression and subsequent suppression of cytokine synthesis and secretion [75]. Measurement of restored mRNA levels of tolerisable cytokines including TNF-α alone would suggest that recovery from LPS tolerance restored inflammatory potential of macrophage to levels comparable with LPS M1 macrophages. Measurement of cytokine secretion by ELISA alone would suggest that RM cells remain in a LPS tolerisable state which does not fit the profile of RM cells that we describe here. Therefore analysis of gene expression cytokine synthesis and cytokine secretion is critical to identifying the full activation status of RM cells. Taken together this approach has identified a novel mechanism of regulating TLR tolerance at the level of secretion with RM cells retaining the ability to restore immune competency through regulation of cytokine secretion upon appropriate inflammatory challenge.

6. General Discussion

The mammalian immune system comprises a complex network of innate and adaptive components including mucosal barriers, soluble factors and specialised immune cells that recognise noxious stimuli and mount powerful immune responses. While these responses are fundamental to host defence and protection, dysregulation of the inflammatory response is the central hallmark of immune deficient, autoimmune and chronic inflammatory conditions. Due to the costly pathological consequences of uncontrolled inflammation, TLR tolerance is pivotal in regulating TLR induced inflammation by preventing excessive and uncontrolled inflammation while also promoting the resolution of inflammation [2, 75, 242].

Extensive research has been carried out in deciphering the regulation of TLR responses [29, 30, 32, 75] however the plasticity of this state has not been explored. Therefore the aims of this thesis were to investigate the regulation of TLR tolerance using two models of inflammation. Firstly, utilising a murine model of intestinal inflammation, the role of the negative regulator of TLR responses Bcl-3 was investigated to decipher its role in the regulation of microbial tolerance in the gut in addition to its contribution to the pathogenesis of intestinal inflammatory diseases. Secondly, a transcriptomics approach was employed to analyse the transcriptional plasticity of LPS tolerance in macrophages upon additional TLR exposure. Simultaneously, functional analysis of TLR tolerance plasticity led to the discovery of a novel mechanism regulating TLR responses involving inhibition of cytokine secretion through intracellular degradation.

Chapter 3 describes an *in vivo* study of intestinal inflammation utilising the DSS induced colitis model in mice deficient in Bcl-3. Bcl-3 is a nuclear member of the IκB family which binds only homodimers of the p50 or p52 NF-κB subunits. Since these subunits lack a transactivation domain they are associated with repression of NF-κB transcription [90]. Bcl-3 was originally identified in a subset of chronic lymphocytic leukaemia (B-CLL) patients containing a recurring t(14:19) chromosomal translocation [91, 92]. As a result Bcl-3 has since been implicated in cell survival and tumorigenesis [93-96]. Bcl-3 deficient T cells showed reduced survival while over-expression of Bcl-3 increased T cell survival [100-102]. Bcl-3 is a regulator of cyclin D1 and is important in cell cycle regulation. Over-expression of Bcl-3 has been shown to shorten the G1 phase of cell cycle in breast cancer epithelial cells which coincided with elevated cyclin D1 expression levels [96]. Furthermore, Bcl-3 also regulates HDM2, an inhibitor of p53 induced apoptosis by promoting its expression [103]. Bcl-3 plays a critical role in immunological development via negative regulation of autoreactive thymocytes in addition to altering T cell responses [104-106]. Recently Bcl-3 has been identified as a negative regulator of essential TLR induced responses [111] with Bcl-$3^{-/-}$ cells and mice demonstrating hyper-responsiveness to TLR stimulation. Additionally Bcl-$3^{-/-}$ mice have demonstrated increased susceptibility to microbial infections with *Klebsiella pneumoniae*, *Streptococcus pneumoniae* and *Listeria monocytogenes* [68, 108, 111, 112]. Importantly Bcl-$3^{-/-}$ macrophages and mice show a lack of lipopolysaccharide (LPS) tolerance induction and increased susceptibility to LPS toxicity [111].

Maintenance of a tolerant co-existence between the intestinal microbial community and the underlying mucosal immune cellular network is essential to promote tissue homeostasis. Preventing excessive and uncontrolled inflammation is critical in this

unique environment as unnecessary inflammation can lead to the development of severe chronic inflammatory conditions including Crohn's disease and ulcerative colitis [131, 243]. Recently, a single nucleotide polymorphism (SNP) associated with reduced Bcl-3 gene expression has been identified as a potential risk factor for Crohn's disease [170]. However, the role of Bcl-3 in regulation of intestinal inflammation and inflammatory bowel disease has not been investigated to date. Therefore we hypothesised that Bcl-3 may play a role in contributing to the regulation of the host immune and intestinal microbial interactions through maintaining a level of microbial tolerance between both groups.

The study presented in chapter 3 identifies Bcl-3 as a negative regulator of intestinal epithelial cell proliferation during intestinal colitis which suggests additional physiological functions for Bcl-3 beyond its role as a negative regulator of pro-inflammatory gene expression. Interestingly Bcl-3 deficient mice developed milder colitis than their WT litter mate control mice as determined by daily disease activity scoring. However upon further examination, we measured no differences in inflammatory scores between both WT and Bcl-$3^{-/-}$ mice. Histological observations of significant oedema and leukocyte infiltration correlated with quantification of infiltrating leukocytes and pro-inflammatory mucosal gene expression which revealed equivalent inflammatory scores between both Bcl-$3^{-/-}$ and WT groups. Of note, gene expression and histological analysis was performed at the experimental endpoint on day 8, a time point where WT mice demonstrated a more severe colitis phenotype than Bcl-$3^{-/-}$ mice as determined by DAI scores. At this time point mice had stopped DSS treatment and the barrier of WT mice was severely disrupted as demonstrated by DAI scoring and histological analysis of distal colon tissue. However during DSS treatment up to day 6, DAI scores demonstrated that both WT

and Bcl-3$^{-/-}$ mice displayed similar levels of inflammation, therefore there may have been increased inflammation during DSS treatment at an earlier time point that led to significant infiltration of leukocytes and cytokine production in Bcl-3$^{-/-}$ mice. Thus analysis of gene expression and cellular infiltration at an earlier time point during DSS treatment would give additional information of the role of Bcl-3 in the induction of intestinal inflammation.

These findings of reduced severity of DSS induced colitis in Bcl-3$^{-/-}$ mice are in contrast to previous studies examining the role of additional TLR signalling negative regulators in DSS induced colitis. Both IRAK-M$^{-/-}$ and SOC1$^{+/-}$ mice revealed severe colitis induction in comparison to their WT counterparts [244, 245]. In addition microbial models of infection revealed a hyperresponsive state in Bcl-3 deficient mice [108, 112]. *Klebsiella pneumoniae* lung infection in Bcl-3$^{-/-}$ mice resulted in increased lung damage, reduced bacterial clearance and subsequent dissemination of bacteria into the bloodstream. This study highlights the importance of Bcl-3 in regulation of lung inflammation through clearance of Gram negative bacteria [112]. Similarly, Schwarz et al demonstrated the importance of Bcl-3 in the clearance of *Listeria monocytogenes* infection with Bcl-3$^{-/-}$ mice demonstrating a 2 fold enhanced bacterial load in their spleens when compared with their WT counterparts. Furthermore, this study showed that Bcl-3$^{-/-}$ were highly susceptible to *Streptococcus pneumoniae* infection as a result of the lack of a competent humoral immune response required to fight and clear this Gram positive pathogen. As a result of a deficiency in Bcl-3, survival of mice was severely affected in comparison to WT infected mice [108].

In support of our findings, the resistance of Bcl-3$^{-/-}$ mice to experimentally induced colitis correlates with our analysis of Bcl-3 expression in the colon of IBD patients which was significantly increased when compared to healthy individuals. Histological analysis revealed intact epithelial structures within the colonic tissue architecture of Bcl-3$^{-/-}$ mice. This corresponded with a significant enhancement in epithelial cell proliferation as determined by Ki67 immunofluorescence staining and suggests that the resistance of Bcl-3$^{-/-}$ mice to DSS-induced colitis results from increased regeneration of the epithelium. Therefore it is possible that the identified SNPs [170] implicating reduced Bcl-3 levels as a potential IBD risk factor may lead to increased Bcl-3 expression rather than decreased expression as predicted. Thus, our findings suggest that increased expression of Bcl-3 rather than reduced expression may be a potential risk factor for IBD. Given that the proliferation of intestinal epithelial cells is normal in Bcl-3$^{-/-}$ mice, it is likely that inflammation induced expression of Bcl-3 in the epithelium during colitis contributes to the development of disease. Furthermore, our data suggests that increased expression of Bcl-3 leads to reduced epithelial regenerative capacity and therefore may contribute to the development of IBD. Thus, by targeting Bcl-3 it may be possible to enhance epithelial cell proliferation and regeneration without exacerbating inflammation in the intestine. The potential therapeutic benefits to IBD are highlighted by the reduced clinical score and lack of weight loss in DSS-treated Bcl-3$^{-/-}$ mice.

This report suggests that targeting Bcl-3 in colitis may be therapeutically beneficial in IBD through increasing tissue regeneration and repair in the colon without exacerbating the inflammatory response. Therefore it would be interesting to further investigate the role of Bcl-3 in the pathogenesis of murine colitis using additional models of colitis. The model of DSS induced colitis was utilised in our study as this

model mimics intestinal inflammation in ulcerative colitis. Furthermore administration of DSS is of short duration and is technically straightforward with induction of colitis being highly reproducible. However human IBD is a heterogeneous disease and modelling IBD is complex in the mouse as no one model replicates that of human IBD. However the variety of genetic, chemical, T cell mediated and spontaneously induced colitis models provide significant insight into the different factors involved in the pathogenesis of IBD [65, 171, 172, 174].

DSS induced colitis is a chemical model mediating destruction of the mucosal/epithelial barrier driving intestinal inflammation [173, 174]. However this model may not encompass important features of murine colitis and human IBD including bacterial induced colitis and T cell mediated intestinal inflammation. These important feature are studied in additional murine models of IBD including, TNBS and oxazolone induced colitis in addition to *Citrobacter rodentium* induced colitis [246, 247]. Therefore analysis of Bcl-3 deficiency in a bacterial induced colitis model such as *Citrobacter rodentium* or *Salmonella typhimurium* would provide significant insight into the role of Bcl-3 in response to pathogenic infections in the gut mediating intestinal inflammation. Furthermore a T cell model of murine colitis would provide additional insight into the role of Bcl-3 in the pathogenesis of IBD particularly when Bcl-3 has previously been shown to be involved in T cell responses [106]. We analysed Bcl-3 deficiency in an acute model of DSS induced colitis hence examination of epithelium regeneration and immunological responses during the chronic regenerative phase of DSS induced colitis would be important. This phase of the DSS induced colitis model represents a longer duration of intestinal inflammation and repair. This phase also consists of a different cellular population infiltrating the colon with a change from that of a macrophage heavy

load during the acute phase to an T cell load from day 12 to 25 of the chronic phase of DSS induced colitis [172]. Therefore, owing to the role Bcl-3 plays in T cell responses [101, 106], examination of Bcl-3$^{-/-}$ mice immune responses during the chronic DSS induced colitis phase would be of interest particularly due to the new role for Bcl-3 we identified in the regulation of epithelial cell proliferation in the colon. In addition, due to the importance of an intact epithelial barrier in the regulation of inflammation in the gut, a study of barrier function by measuring serum FITC levels of Bcl-3$^{-/-}$ mice fed with FITC dextran [178] and Ki67 staining of the intestinal epithelium throughout the study duration would be important. Furthermore analysis of barrier function using these strategies in additional chemical models of colitis including TNBS and Oxazolone induced colitis which result in intestinal epithelial destruction, in addition to bacterial models of colonic hyperplasia induced in the *Citrobacter rodentium* induced colitis model would be important to provide further insight into the role of Bcl-3 in the regulation of epithelial regeneration during intestinal inflammation [246, 248]. Importantly, investigation of the molecular mechanisms involved in regulation of intestinal epithelial cells by Bcl-3 is merited. Bcl-3 is a multifaceted member of the atypical IκB family of regulators of NF-κB activation therefore, Bcl-3 may transcriptionally repress NF-κB target genes involved in resolution of inflammation to prevent regeneration of the intestinal epithelium during colitis or in human IBD.

In this study we identified Bcl-3 as a negative regulator of intestinal epithelial cell proliferation. Given that Bcl-3 is a putative oncogene and a regulator of cyclin D1 [92, 96, 196], we were surprised that Bcl-3 deficiency resulted in increased epithelial cell proliferation. In support of our findings Bcl-3 expression has been associated with colorectal cancer [249]. Furthermore enhanced epithelial cell proliferation in

the colon has been shown to be protective against colitis associated cancer [250]. However given the role of Bcl-3 in tumorigenesis [91, 95, 97], further studies to investigate the implications of Bcl-3 deficiency in the development of colitis associated cancer are merited. Collectively, we have shown that increased Bcl-3 is a potential risk factor in IBD which may be involved in regulating regeneration of the epithelium. Thus future studies will provide a significant opportunity to target Bcl-3 therapeutically.

The work carried out in chapter 4 and 5 of this thesis represents an *ex vivo* study of TLR tolerance using LPS to investigate the plasticity of TLR tolerance in macrophages. Macrophages are professional phagocytes with important physiological and metabolic roles however these cells are also essential mediators of inflammation and central to host defence. [127]. This range of biological roles is reflected in an emerging spectrum of macrophage activation states largely focused around the M1 pro-inflammatory /M2 anti-inflammatory classification system. M1 macrophages are mainly recruited under inflammatory conditions such as bacterial or viral infections. These cells are highly cytotoxic, produce high levels of pro-inflammatory cytokines and are powerful activators of Th1 adaptive immune responses. In contrast, M2 macrophages are anti-inflammatory cells important in wound healing, tissue remodelling and parasitic infections [127, 135, 136, 140, 212]. Regulatory macrophages are immune regulatory cells that display both anti-inflammatory and pro-inflammatory features through suppression of some pro-inflammatory genes and increased production of IL-10, while maintaining antigen presenting capacity. Immune complexes in conjunction with TLR activation in addition to other stimuli including glucocorticoids, prostaglandins and apoptotic cells have been implicated in regulatory macrophage polarisation. While regulatory

macrophages are distinct from both M1 and M2 macrophages, these cells share some overlapping anti-inflammatory properties with M2 cells [127]. These three macrophage populations represent the main groups in the emerging spectrum of macrophage polarisation however many hybrid macrophage activation states exist owing to the large number of activation stimuli that macrophages encounter *in vivo*. Tumour associated macrophages, intestinal macrophages, liver Kupffer cells, placental macrophages and LPS tolerised macrophages are described as representing hybrid macrophage populations which share overlapping M1/M2 and regulatory properties while expressing distinct features unique to their polarisation state and the microenvironment where they reside. [127, 135, 152-155, 163].

Using a model of acute LPS responses in murine BMDMs, we demonstrated that LPS tolerance is a transient transcriptional immunological state with recovery from LPS tolerance promoting a global switch in the gene expression profile of macrophages. Bioinformatics analysis revealed a large shift in macrophage gene expression with correspondence analysis (COA) initially revealing transcriptional overlap between macrophages of the acute LPS response (A) and RM cells. The expression of many pro-inflammatory genes in RM cells was inducible at levels comparable to the acute response group (A). However further examination of correspondence analysis data (PC4) revealed that the acute response group (A) did not fully overlap with RM cells which confirmed a unique transcriptional profile in RM cells. In addition RM cells displayed some transcriptional features of LPS tolerant cells. These included suppression of co-stimulatory molecules and genes involved in regulation of antiviral responses despite restoration of cytotoxic capacity in RM cells as determined by NOS2, CD86 and type 1 interferon expression. Importantly this data emphasised that LPS tolerance is a plastic transcriptional state

in macrophages resulting in induction of a previously un-described hybrid macrophage activation state with a unique transcriptional signature distinct from M1 and M2 polarisation states.

M1 and M2 classification of macrophage polarisation is largely based upon *in vitro* studies and therefore does not aptly describe the physiological polarisation states of macrophages. Tissue resident macrophage polarisation is largely influenced by the specific microenvironment they reside in and therefore these physiological phagocytes adopt a hybrid phenotype. In addition inflammatory macrophages recruited to sites of infection are also polarised into different activation states dependent on the specific environmental stimulus, largely focused around M1 and M2 states however many overlapping hybrid states exist [127]. Therefore re-addressing macrophage polarisation states under physiological conditions is merited. Our data demonstrates that LPS tolerance is a transcriptionally regulated plastic state in macrophages with recovery from this state polarising macrophage into a unique immune primed hybrid state which may mimic a macrophage phenotype post microbial infection *in vivo*.

Secretion of cytokines and chemokines during infection or injury is fundamental to mounting an effective and tailored immunological response [2, 221]. These key immuno modulatory proteins initiate immune cell recruitment in addition to modulating immune cellular functions and expansion of adaptive immune cell populations to fight and clear infection thereby restoring immune and tissue homeostasis [2, 3]. Despite these proteins playing a fundamental protective immunological role, excessive production of cytokines and chemokines underlies the pathology of many chronic inflammatory and autoimmune diseases ranging from rheumatoid arthritis to IBD [221-224, 251]. During LPS tolerance the potentially

deleterious effects of pro-inflammatory cytokine secretion are suppressed transcriptionally through induction of negative regulators of TLR signalling and TLR induced gene transcription in addition to epigenetic chromatin modelling [30, 32, 75]. As described in chapter 4 recovery from LPS tolerance restored gene expression of a large proportion of tolerisable genes including pro-inflammatory cytokine and chemokines.

The data presented in chapter 5 re-enforces the highly plastic nature of macrophage transcriptional responses with RM cells displaying inducible mRNA levels of these cytokines including TNF-α, IL-6 and CXCL10. Further examination revealed however that TNF-α secretion was un-coupled from protein synthesis. We measured increased intracellular TNF-α in RM cells which confirmed that the protein was actively translated and TNF-α was not subject to post transcriptional regulation of its mRNA through ARE (adenine/uridine rich elements) dependent regulation of mRNA stability [238]. In contrast cytokine secretion remained suppressed in RM cells suggesting that TNF-α was being alternatively trafficked within the cell towards a storage or degradative compartment. To decipher the regulatory mechanism involved in inhibiting TNF-α secretion, RM cells were treated with a panel of intracellular enzyme inhibitors to investigate if TNF-α was being degraded by a particular enzyme family. Treatment with inhibitors of intracellular proteases including pepstatin A, in addition to a calpain inhibitor and cathepsin B inhibitor did not restore TNF-α secretion in RM cells. However, treatment of RM cells with bafilomycin A, a known inhibitor of autophagy and vacuolar type H^+ATPase which inhibits acidification of cellular compartments including lysosomes and endosomes led to increased TNF-α protein trafficking through the Golgi compartment and restoration of TNF-α secretion in RM cells. Bafilomycin A restoration of TNF-α

secretion confirmed that TNF-α protein was being trafficking to a bafilomycin A sensitive compartment where it was potentially being degraded in an autophagy dependent manner.

Autophagy is an evolutionarily conserved process important in maintaining cell and tissue homeostasis through removal of cellular proteins and organelles by targeting them for degradation within lysosomes while recycling cellular energy and nutrients [231, 232]. Autophagy is a physiological host response and has also been shown to be important in controlling cytokine secretion by regulating inflammasome activation targeting pro-IL-1β for caspase 1 cleavage and subsequent production of mature IL-1β protein [231, 233]. In addition, autophagy has been shown to be important in regulating IL-23 secretion through the regulation of the IL-1 family of cytokines [232, 234]. Atg16L1 is an important component of the autophagy apparatus with Atg16L1 deficiency demonstrating defective recruitment of the Atg12-Atg5 complex resulting in inhibition of autophagosome formation [235]. Atg16L1 has also been shown to being important in regulating LPS induced IL-1β secretion in BMDMs [72].

Regulation of IL-1β cytokine secretion has previously been shown to be regulated in an autophagy dependent manner with cleavage of pro-IL-1β occurring within the autophagosome intracellular compartment [233]. While regulation of TNF-α secretion under normal classical TLR induced inflammation is distinct from that of inflammasome regulated secretion of IL-1β [231, 233, 252], we postulated that the suppressed cytokine secretion profile in RM cells may be regulated in an autophagy dependent manner, independent of the classical secretory route for TNF-α via the trans Golgi network to the cell surface via the phagocytic cup [253-256]. Based upon this hypothesis and our findings that bafilomycin A restored TNF-α secretion in RM

cells, we measured TNF-α secretion in Atg16L1$^{-/-}$ BMDMs [175]. Despite a robust increase in TNF-α mRNA and protein levels within macrophages in all LPS stimulated groups (A, T and R), this did not restore TNF-α secretion in RM cells. This data suggested that the block in TNF-α cytokine secretion in RM cells is independent of autophagy but dependent on a bafilomycin sensitive degradative process. This was further supported by treatment of RM cells with monensin, an inhibitor of endosomal and lysosomal acidification [257] which demonstrated increased levels of TNF-α detected within the Golgi in RM cells, similar to bafilomycin A treatment of RM cells. This data demonstrates that cytokine secretion is a regulated process and that cytokine synthesis does not lead to cytokine secretion in RM cells. Collectively this data suggests that recovery from LPS tolerance regulates inflammation through altering TNF-α trafficking towards a lysosomal degradative pathway that is independent of autophagy and intracellular acidic proteases, calpain and cathepsin B enzyme degradation.

A recent study has demonstrated the plasticity of dendritic cells to respond to an independent inflammatory signal despite developing reduced responsiveness towards LPS as measured by suppressed pro-inflammatory cytokine secretion [258]. *Abdi et al* revealed that these "exhausted" (LPS tolerised) dendritic cells retained responsiveness toward specific inflammatory signals such as activated T cells including CD40L. This study demonstrated that LPS tolerised dendritic cells were primed to respond to an adaptive immune signal suggesting that that TLR tolerance is a plastic state in dendritic cells [258]. Based upon this theory, we hypothesised that regulation of cytokine secretion in RM cells may be controlled by an independent secondary signal including a secondary opportunistic microbial infection or activation of the inflammasome complex. Treatment of RM cells with an

additional independent inflammatory signal including IL-1β and additional TLR ligands (Pam3CSK4 and CpG) restored cytokine secretion in RM cells. In contrast to the study performed by Abdi and colleagues [258], CD40L co-stimulation with LPS of RM cells did not restore TNF-α secretion suggesting that restoration of cytokine secretion is stimulus specific in RM cells. This data implies that RM cells are primed to respond to secondary signals but require an additional activation signal to restore full activation capacity.

Recent studies have demonstrated a role for the multiprotein inflammasome complex in the regulation of inflammatory responses in intestinal phagocytes through NLRC4 driven IL-1β production [228]. *Franchi et al* demonstrated that CD11b positive intestinal phagocytes (iMPs) were anergic to TLR stimulation as determined by IL-6 and TNF-α secretion however these cells produced high levels of pro-IL-1β [228]. Upon pathogenic infection with *Salmonella* or *Pseudomonas* species NLRC4 drives mature IL-1β production which in turn orchestrates the inflammatory response to these infections in the intestine [228]. Interestingly, we identified that IL-1β co-stimulation with LPS restored TNF-α secretion in RM cells suggesting that activation of the inflammasome complex may switch TNF-α trafficking within RM cells from that from a lysosomal compartment to directly trafficking to the cell surface for enzymatic cleavage and subsequent secretion. Discrimination between pathogenic and commensal bacteria is regulated by the NLRC4 inflammasome [228], thus inflammasome activation in RM cells upon exposure to specific pathogenic stimuli *in vivo* may represent a potential mechanism for restoring cytokine secretion through increased production of IL-1β by RM cells.

IL-1β signalling is a potent activator of pro-inflammatory cytokine and chemokine transcription and subsequent secretion in response to inflammatory stimuli. TNF-α

protein is trafficked in macrophages through a classical secretory route through the Golgi and trans-Golgi network where it is then delivered to recycling endosomes and subsequently to the phagocytic cup at the cell surface where it is cleaved into its mature form by the enzyme TACE [229, 253-256]. IL-1β autocrine signalling resulting from inflammasome activation in RM cells may drive TNF-α protein trafficking in RM cells back to the classical secretory route as described above. Investigation of the potential mechanism of IL-1β modulating TNF-α trafficking from an alternative degradative route to the classical secretory route is essential and requires functional trafficking analysis of TNF-α protein which is beyond the scope of this thesis. However, inflammasome activation of IL-1β production may play an important role in the regulation of cytokine secretion following recovery from LPS tolerance particularly when a similar observation was described in intestinal phagocytes capacity to discriminate between pathogenic and commensal bacteria.

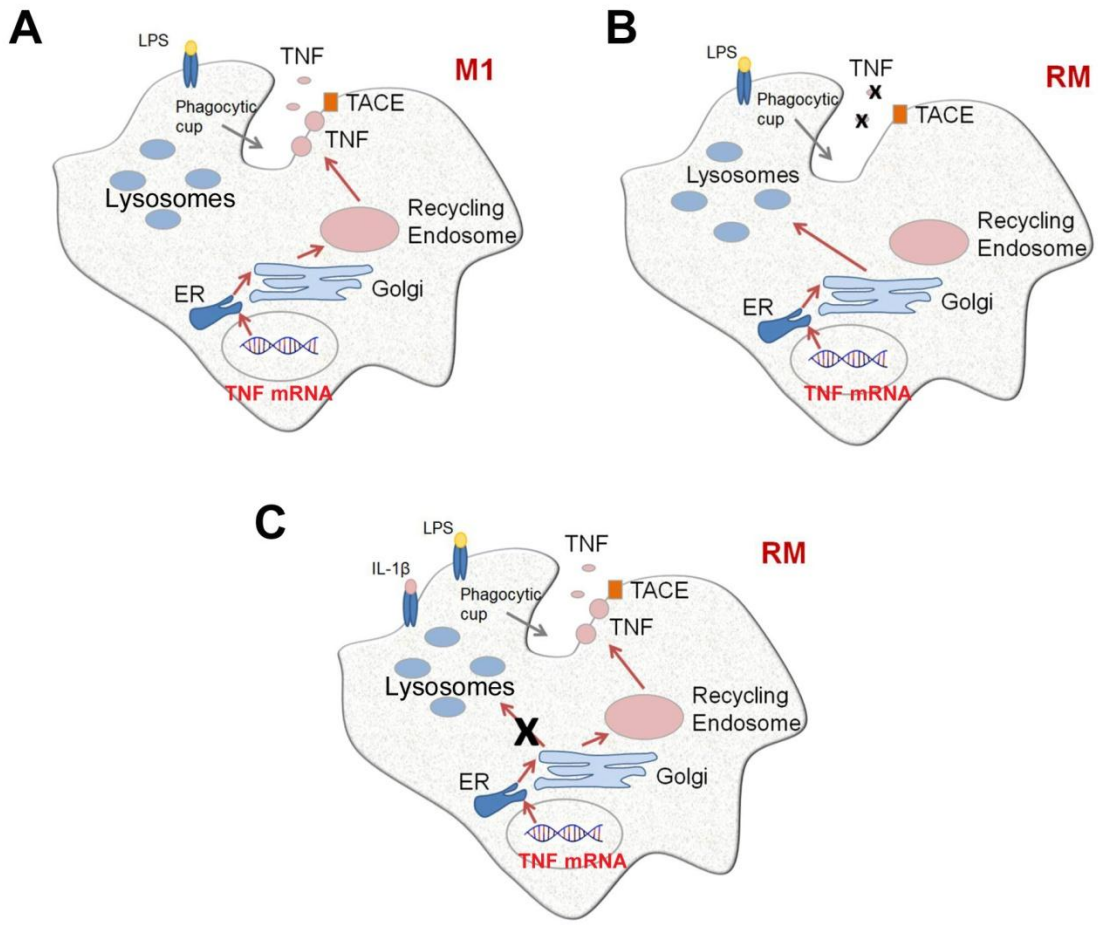

Figure 6. 1: Proposed mechanism of regulation of TNF-α secretion in RM cells

(A) Classical intracellular trafficking of TNF-α from gene transcription to protein synthesis and delivery to the cell surface for enzymatic cleavage within the phagocytic cup. (B) Proposed alternative trafficking of TNF-α protein from the golgi to lysosomes for degradation of protein in RM cells. (C) Proposed mechanism of restored TNF-α secretion in RM cell upon IL-1β and LPS co-stimulation following inflammasome activation and cleavage of pro-IL-1β. Co-stimulation of RM cells with LPS and IL-1β restores TNF-α secretion through directing TNF-α trafficking back towards the classical TNF-α trafficking route to the cell surface. RM = recovered macrophage, M1 = acute response to LPS. Arrow represents the direction of TNF-α trafficking within cells.

The variety of chronic inflammatory and immunosuppressive conditions associated with dysregulated cytokine and chemokine production demonstrates the importance of tight regulation of cytokine secretion following acute inflammatory responses. Recently suppression of TNF-α secretion has been observed in macrophages isolated from Crohn's disease (CD) patients [226]. Interestingly, *Smith et al* demonstrated similar findings to the TNF-α secretion data in RM cells with translated TNF-α protein found within CD macrophages despite reduced protein secretion. Lysosomal degradation of cytokines was implicated in suppressing cytokine secretion in CD macrophages [226]. This study provides patho-physiological evidence for post translational regulation of cytokine secretion however whether suppressed cytokine secretion is a pathophysiological consequence of CD remains to be determined. Suppression of secreted TNF-α through neutralising of secreted protein with TNF-α targeting antibodies (infliximab and adalimuab) is a widely utilised therapeutic strategy used in the treatment and management of inflammation in RA and IBD patients [221, 222, 259, 260]. Therapeutic strategies mediating suppression of cytokine responses further indicates that suppression of cytokine secretion in RM cells under non chronic inflammatory pathologies may represent a physiological immune response post microbial tolerance induction with secretion restored upon specific inflammatory signals such as pathogenic infections. This is further supported by reduced secretion of pro-inflammatory cytokines in lamina propria macrophages under normal physiological conditions where they are constantly exposed to the intestinal microbial community. Furthermore, germ free mice have been shown to secrete increased levels of pro-inflammatory cytokines upon inflammatory challenge suggesting that suppressed secretion of cytokines regulates a

level of tolerance between the intestinal commensal microbial community and the underlying immune cellular network [162, 228].

Septic shock results from dysregulation of inflammatory responses mediated through an initial inflammatory phase followed by an immunosuppressive state in patients. This immunosuppressive phenotype observed in sepsis renders these patients more susceptible to developing secondary opportunistic infections which can have a significant effect on patient morbidity and mortality. In contrast to non-survival cases of septic shock, monocytes isolated from patients that recovered from this immunosuppressive septic state demonstrated restoration of cytokine secretion upon LPS challenge [117, 159] suggesting that survival may be attributed to restoration of immune competency. Our observations of restored immune competency in RM cells through restoration of cytokine secretion upon IL-1β or TLR treatment supports our hypothesis that regulation of cytokine secretion post tolerance is a important physiological response in the regulation of inflammation. This further suggests that cytokine suppression following inflammatory insult and post microbial tolerance may represent a unique level of regulation of inflammation.

Chapter 4 and chapter 5 demonstrate the highly plastic nature of LPS tolerance with recovery from such state important in restoring immune competency which is regulated post translationally through modulation of cytokine secretion. This may represent an important physiological response in macrophages not only in response to LPS but to microbial infection. Therefore it would be beneficial to apply this model of recovery from LPS tolerance to additional inducers of TLR-induced inflammation including ligands representing Gram positive bacteria including peptidoglycan and Pam3CSK4. It would be particularly interesting to investigate the polarisation profile of RM macrophages following stimulation with viral associated

ligands in addition to viral infection of RM cells as these cells display alterations in regulators of anti-viral responses.

Macrophages perform a diverse range of fundamental physiological and immunological roles to maintain tissue homeostasis therefore analysis of some of these functions in RM cells merits further investigation. Firstly, alterations in the patterns of expression of regulators involved in interaction with T cells e.g CD86 suggested that interaction with adaptive immune cells is suppressed in RM cells similar to that observed during LPS tolerance. Therefore functional analysis of antigen presenting capacity would be interesting to measure *in vivo* by performing a mixed lymphocytic reaction. Recently, macrophage polarisation was shown to influence natural killer cell responses with endotoxin tolerant macrophage unable to induce NK cell activation [261]. Thus, it would be particularly be interesting to study the functional outcomes of NK cell polarisation by RM cells.

Finally analysis of TLR tolerance plasticity needs to be investigated further *in vivo* to gain a greater understanding of the physiological relevance of this state under both homeostatic and pathophysiological conditions. *Ueda el at* demonstrated that colonic macrophages are hyporesponsive towards TLR stimulation with IL-10 production central to controlling reduced secretion of inflammatory cytokines including IL-6 and TNF-α [162]. In addition, this study demonstrated that STAT3 and IL-10 deficient mice were hyperresponsive to LPS with increased TNF-α and IL-6 secretion measured in colonic macrophages [162]. In Chapter 4 we measured increased phosphorylated STAT1 and STAT3 in both LPS tolerant (T) and RM cells suggesting that these transcription factors may play a role in regulation of cytokine secretion in RM cells. A recent study has characterised colonic macrophage populations under steady state and inflammatory conditions [227]. This study

demonstrated that resident colonic macrophages were responsive toward TLR challenge with mRNA and intracellular TNF-α protein increased in these cells [227]. While TNF-α secretion was not measured in these cells, previous studies by *Franchi et al* [228] and *Ueda et al* [162] measured no secretion of TNF-α or IL-6 upon TLR stimulation. These two studies isolated colonic macrophages using CD11b MACS separation or CD11b flow cytometry cell sorting. However, *Bain et al* describe a novel isolation protocol for resident colonic macrophages using a panel of colonic macrophage specific markers [227]. As a result, it would be important to measure cytokine production from these cells upon TLR challenge to confirm suppressed cytokine secretion identified in these previous studies. Taken together these studies correlate with the suppressed cytokine secretion findings in RMs of this study suggesting that TLR tolerance may also be regulated at the level of cytokine secretion under physiological conditions such as that of the intestine. Based on functional analysis of cytokine secretion in RM cells, lysosomal degradation of intracellular TNF-α protein may represent a potential mechanism suppressing cytokine secretion in colonic macrophage populations under physiological conditions in response to the intestinal microbiota.

These studies highlight the importance of measuring both cytokine secretion and mRNA levels to determine the activation status of cells. LPS tolerance results from transcriptional repression of pro-inflammatory gene expression and subsequent suppression of cytokine synthesis and secretion [75]. Measurement of restored mRNA levels of tolerisable cytokines including TNF-α alone would suggest that recovery from LPS tolerance restored inflammatory potential of macrophage to levels comparable with LPS M1 macrophages. Measurement of cytokine secretion by ELISA alone would suggest that RM cells remain in a LPS tolerisable state which

does not fit the profile of RM cells that we describe here. Thus, analysis of gene expression, cytokine synthesis and cytokine secretion is central to identifying the activation status of RM cells. Furthermore, using this strategy we identified a novel mechanism of regulation of TLR tolerance independent of mRNA regulation, through lysosomal degradation of synthesised TNF-α protein resulting in inhibition of TNF-α secretion.

The findings of this thesis demonstrate that LPS tolerance is a highly plastic physiological response towards microbial challenge. We have identified a novel physiological role for Bcl-3 as a negative regulator of intestinal epithelial cell proliferation during intestinal colitis distinct from its essential role in the negative regulation of TLR induced inflammatory responses. Furthermore, the plasticity of the LPS tolerant state resulted in polarisation of macrophages to a distinct activation state with a unique transcriptional signature. In addition identification of this unique macrophage population led to a novel insight into the regulation of inflammation at the level of cytokine secretion. Collectively this thesis provides significant insight into the plasticity and regulation of TLR tolerance which provides solid groundwork for downstream physiological analysis and subsequent understanding of the pathophysiology of chronic inflammatory diseases.

7. References

1. Takeuchi, O. and S. Akira, Pattern Recognition Receptors and Inflammation. Cell, 2010. 140(6): p. 805-820.
2. Medzhitov, R., Origin and physiological roles of inflammation. Nature, 2008. 454(7203): p. 428-435.
3. Nathan, C., Points of control in inflammation. Nature, 2002. 420(6917): p. 846-852.
4. Janeway, C.A., Jr., Approaching the asymptote? Evolution and revolution in immunology. Cold Spring Harb Symp Quant Biol, 1989. 54 Pt 1: p. 1-13.
5. Akira, S., S. Uematsu, and O. Takeuchi, Pathogen Recognition and Innate Immunity. Cell, 2006. 124(4): p. 783-801.
6. Medzhitov, R., Recognition of microorganisms and activation of the immune response. Nature, 2007. 449(7164): p. 819-826.
7. Kerrigan, A.M. and G.D. Brown, C-type lectins and phagocytosis. Immunobiology, 2009. 214(7): p. 562-575.
8. Plüddemann, A., S. Mukhopadhyay, and S. Gordon, Innate immunity to intracellular pathogens: macrophage receptors and responses to microbial entry. Immunological Reviews, 2011. 240(1): p. 11-24.
9. O'Neill, L.A.J., D. Golenbock, and A.G. Bowie, The history of Toll-like receptors [mdash] redefining innate immunity. Nat Rev Immunol, 2013. 13(6): p. 453-460.
10. Rutschmann, S., et al., The Rel Protein DIF Mediates the Antifungal but Not the Antibacterial Host Defense in Drosophila. Immunity, 2000. 12(5): p. 569-580.
11. Medzhitov, R., P. Preston-Hurlburt, and C.A. Janeway, Jr., A human homologue of the Drosophila Toll protein signals activation of adaptive immunity. Nature, 1997. 388(6640): p. 394-7.
12. Kawai, T. and S. Akira, Toll-like Receptors and Their Crosstalk with Other Innate Receptors in Infection and Immunity. Immunity, 2011. 34(5): p. 637-650.
13. Kawai, T. and S. Akira, The role of pattern-recognition receptors in innate immunity: update on Toll-like receptors. Nat Immunol, 2010. 11(5): p. 373-384.

14. Frey, E.A., et al., Soluble CD14 participates in the response of cells to lipopolysaccharide. The Journal of Experimental Medicine, 1992. 176(6): p. 1665-1671.
15. Schumann, R.R., et al., Structure and function of lipopolysaccharide binding protein. Science, 1990. 249(4975): p. 1429-31.
16. Wright, S.D., et al., CD14, a receptor for complexes of lipopolysaccharide (LPS) and LPS binding protein. Science, 1990. 249(4975): p. 1431-3.
17. Kirkland, T.N., et al., Identification of lipopolysaccharide-binding proteins in 70Z/3 cells by photoaffinity cross-linking. J Biol Chem, 1990. 265(16): p. 9520-5.
18. Park, B.S., et al., The structural basis of lipopolysaccharide recognition by the TLR4-MD-2 complex. Nature, 2009. 458(7242): p. 1191-1195.
19. Hoshino, K., et al., Cutting Edge: Toll-Like Receptor 4 (TLR4)-Deficient Mice Are Hyporesponsive to Lipopolysaccharide: Evidence for TLR4 as the Lps Gene Product. The Journal of Immunology, 1999. 162(7): p. 3749-3752.
20. Carty, M., et al., The human adaptor SARM negatively regulates adaptor protein TRIF-dependent Toll-like receptor signaling. Nat Immunol, 2006. 7(10): p. 1074-1081.
21. Carmody, R.J. and Y.H. Chen, Nuclear factor-kappaB: activation and regulation during toll-like receptor signaling. Cell Mol Immunol, 2007. 4(1): p. 31-41.
22. Horng, T., et al., The adaptor molecule TIRAP provides signalling specificity for Toll-like receptors. Nature, 2002. 420(6913): p. 329-333.
23. Kawai, T., et al., Unresponsiveness of MyD88-Deficient Mice to Endotoxin. Immunity, 1999. 11(1): p. 115-122.
24. Araki, A., et al., MyD88-deficient mice develop severe intestinal inflammation in dextran sodium sulfate colitis. Journal of Gastroenterology, 2005. 40(1): p. 16-23.
25. Suzuki, N., et al., Severe impairment of interleukin-1 and Toll-like receptor signalling in mice lacking IRAK-4. Nature, 2002. 416(6882): p. 750-756.
26. Picard, C., et al., Pyogenic Bacterial Infections in Humans with IRAK-4 Deficiency. Science, 2003. 299(5615): p. 2076-2079.
27. Kawai, T., et al., Lipopolysaccharide Stimulates the MyD88-Independent Pathway and Results in Activation of IFN-Regulatory Factor 3 and the

Expression of a Subset of Lipopolysaccharide-Inducible Genes. The Journal of Immunology, 2001. 167(10): p. 5887-5894.

28. Yamamoto, M., et al., Role of adaptor TRIF in the MyD88-independent toll-like receptor signaling pathway. Science, 2003. 301(5633): p. 640-3.
29. Liew, F.Y., et al., Negative regulation of Toll-like receptor-mediated immune responses. Nat Rev Immunol, 2005. 5(6): p. 446-458.
30. Kondo, T., T. Kawai, and S. Akira, Dissecting negative regulation of Toll-like receptor signaling. Trends Immunol, 2012. 33(9): p. 449-58.
31. Lang, T. and A. Mansell, The negative regulation of Toll-like receptor and associated pathways. Immunol Cell Biol, 2007. 85(6): p. 425-434.
32. Hedl, M. and C. Abraham, Negative regulation of human mononuclear phagocyte function. Mucosal Immunol, 2013. 6(2): p. 205-23.
33. Iwami, K.-i., et al., Cutting Edge: Naturally Occurring Soluble Form of Mouse Toll-Like Receptor 4 Inhibits Lipopolysaccharide Signaling. The Journal of Immunology, 2000. 165(12): p. 6682-6686.
34. Hyakushima, N., et al., Interaction of Soluble Form of Recombinant Extracellular TLR4 Domain with MD-2 Enables Lipopolysaccharide Binding and Attenuates TLR4-Mediated Signaling. The Journal of Immunology, 2004. 173(11): p. 6949-6954.
35. Brint, E., et al., ST2 is an inhibitor of interleukin 1 receptor and Toll-like receptor 4 signaling and maintains endotoxin tolerance. Nat Immunol, 2004. 5: p. 373 - 9.
36. Biswas, S.K. and E. Lopez-Collazo, Endotoxin tolerance: new mechanisms, molecules and clinical significance. Trends in immunology, 2009. 30(10): p. 475-487.
37. Wald, D., et al., SIGIRR, a negative regulator of Toll-like receptor-interleukin 1 receptor signaling. Nat Immunol, 2003. 4(9): p. 920-927.
38. Qin, J., et al., SIGIRR Inhibits Interleukin-1 Receptor- and Toll-like Receptor 4-mediated Signaling through Different Mechanisms. Journal of Biological Chemistry, 2005. 280(26): p. 25233-25241.
39. Kobayashi, K., et al., IRAK-M Is a Negative Regulator of Toll-like Receptor Signaling. Cell, 2002. 110(2): p. 191-202.

40. Biswas, A., et al., Negative regulation of Toll-like receptor signaling plays an essential role in homeostasis of the intestine. European Journal of Immunology, 2011. 41(1): p. 182-194.
41. Balaci, L., et al., IRAK-M Is Involved in the Pathogenesis of Early-Onset Persistent Asthma. American journal of human genetics, 2007. 80(6): p. 1103-1114.
42. del Fresno, C., et al., Potent Phagocytic Activity with Impaired Antigen Presentation Identifying Lipopolysaccharide-Tolerant Human Monocytes: Demonstration in Isolated Monocytes from Cystic Fibrosis Patients. The Journal of Immunology, 2009. 182(10): p. 6494-6507.
43. Zhang, G. and S. Ghosh, Negative Regulation of Toll-like Receptor-mediated Signaling by Tollip. Journal of Biological Chemistry, 2002. 277(9): p. 7059-7065.
44. Burns, K., et al., Tollip, a new component of the IL-1RI pathway, links IRAK to the IL-1 receptor. Nat Cell Biol, 2000. 2(6): p. 346-51.
45. Burns, K., et al., Inhibition of Interleukin 1 Receptor/Toll-like Receptor Signaling through the Alternatively Spliced, Short Form of MyD88 Is Due to Its Failure to Recruit IRAK-4. The Journal of Experimental Medicine, 2003. 197(2): p. 263-268.
46. Janssens, S., et al., Regulation of interleukin-1- and lipopolysaccharide-induced NF-kappaB activation by alternative splicing of MyD88. Curr Biol, 2002. 12(6): p. 467-71.
47. Boone, D.L., et al., The ubiquitin-modifying enzyme A20 is required for termination of Toll-like receptor responses. Nat Immunol, 2004. 5(10): p. 1052-1060.
48. Saitoh, T., et al., A20 Is a Negative Regulator of IFN Regulatory Factor 3 Signaling. The Journal of Immunology, 2005. 174(3): p. 1507-1512.
49. Wertz, I.E., et al., De-ubiquitination and ubiquitin ligase domains of A20 downregulate NF-[kappa]B signalling. Nature, 2004. 430(7000): p. 694-699.
50. Hitotsumatsu, O., et al., The Ubiquitin-Editing Enzyme A20 Restricts Nucleotide-Binding Oligomerization Domain Containing 2-Triggered Signals. Immunity, 2008. 28(3): p. 381-390.

51. Vereecke, L., et al., Enterocyte-specific A20 deficiency sensitizes to tumor necrosis factor–induced toxicity and experimental colitis. The Journal of Experimental Medicine, 2010. 207(7): p. 1513-1523.
52. Hammer, G.E., et al., Expression of A20 by dendritic cells preserves immune homeostasis and prevents colitis and spondyloarthritis. Nat Immunol, 2011. 12(12): p. 1184-1193.
53. Thomson, W., et al., Rheumatoid arthritis association at 6q23. Nat Genet, 2007. 39(12): p. 1431-1433.
54. Musone, S.L., et al., Multiple polymorphisms in the TNFAIP3 region are independently associated with systemic lupus erythematosus. Nat Genet, 2008. 40(9): p. 1062-1064.
55. Zhou, F., et al., Ubiquitin-specific Protease 4 Mitigates Toll-like/Interleukin-1 Receptor Signaling and Regulates Innate Immune Activation. Journal of Biological Chemistry, 2012. 287(14): p. 11002-11010.
56. Massoumi, R., et al., Cyld Inhibits Tumor Cell Proliferation by Blocking Bcl-3-Dependent NF-κB Signaling. Cell, 2006. 125(4): p. 665-677.
57. Yoshida, H., et al., The Tumor Suppressor Cylindromatosis (CYLD) Acts as a Negative Regulator for Toll-like Receptor 2 Signaling via Negative Cross-talk with TRAF6 and TRAF7. Journal of Biological Chemistry, 2005. 280(49): p. 41111-41121.
58. An, H., et al., SHP-2 Phosphatase Negatively Regulates the TRIF Adaptor Protein-Dependent Type I Interferon and Proinflammatory Cytokine Production. Immunity, 2006. 25(6): p. 919-928.
59. Kinjyo, I., et al., SOCS1/JAB Is a Negative Regulator of LPS-Induced Macrophage Activation. Immunity, 2002. 17(5): p. 583-591.
60. Nakagawa, R., et al., SOCS-1 Participates in Negative Regulation of LPS Responses. Immunity, 2002. 17(5): p. 677-687.
61. Mansell, A., et al., Suppressor of cytokine signaling 1 negatively regulates Toll-like receptor signaling by mediating Mal degradation. Nat Immunol, 2006. 7(2): p. 148-155.
62. Lu, Q. and G. Lemke, Homeostatic Regulation of the Immune System by Receptor Tyrosine Kinases of the Tyro 3 Family. Science, 2001. 293(5528): p. 306-311.

63. Shi, M., et al., TRIM30[alpha] negatively regulates TLR-mediated NF-[kappa]B activation by targeting TAB2 and TAB3 for degradation. Nat Immunol, 2008. 9(4): p. 369-377.
64. Zhao, W., et al., E3 Ubiquitin Ligase Tripartite Motif 38 Negatively Regulates TLR-Mediated Immune Responses by Proteasomal Degradation of TNF Receptor-Associated Factor 6 in Macrophages. The Journal of Immunology, 2012. 188(6): p. 2567-2574.
65. Elson, C.O., et al., Experimental models of inflammatory bowel disease reveal innate, adaptive, and regulatory mechanisms of host dialogue with the microbiota. Immunological Reviews, 2005. 206(1): p. 260-276.
66. Chang, J., S.L. Kunkel, and C.-H. Chang, Negative regulation of MyD88-dependent signaling by IL-10 in dendritic cells. Proceedings of the National Academy of Sciences, 2009. 106(43): p. 18327-18332.
67. Kuwata, H., et al., IL-10-inducible Bcl-3 negatively regulates LPS-induced TNF-α production in macrophages. Blood, 2003. 102(12): p. 4123-4129.
68. Riemann, M., et al., The IκB Protein Bcl-3 Negatively Regulates Transcription of the IL-10 Gene in Macrophages. The Journal of Immunology, 2005. 175(6): p. 3560-3568.
69. Sly, L.M., et al., LPS-Induced Upregulation of SHIP Is Essential for Endotoxin Tolerance. Immunity, 2004. 21(2): p. 227-239.
70. Naiki, Y., et al., Transforming Growth Factor-β Differentially Inhibits MyD88-dependent, but Not TRAM- and TRIF-dependent, Lipopolysaccharide-induced TLR4 Signaling. Journal of Biological Chemistry, 2005. 280(7): p. 5491-5495.
71. Hirsch, E., et al., Functions of interleukin 1 receptor antagonist in gene knockout and overproducing mice. Proceedings of the National Academy of Sciences, 1996. 93(20): p. 11008-11013.
72. Saitoh, T., et al., Loss of the autophagy protein Atg16L1 enhances endotoxin-induced IL-1[bgr] production. Nature, 2008. 456(7219): p. 264-268.
73. Negishi, H., et al., Negative regulation of Toll-like-receptor signaling by IRF-4. Proceedings of the National Academy of Sciences of the United States of America, 2005. 102(44): p. 15989-15994.

74. Sun, H., et al., TIPE2, a Negative Regulator of Innate and Adaptive Immunity that Maintains Immune Homeostasis. Cell, 2008. 133(3): p. 415-426.
75. Foster, S.L., D.C. Hargreaves, and R. Medzhitov, Gene-specific control of inflammation by TLR-induced chromatin modifications. Nature, 2007. 447(7147): p. 972-978.
76. Saijo, K., et al., A Nurr1/CoREST Pathway in Microglia and Astrocytes Protects Dopaminergic Neurons from Inflammation-Induced Death. Cell, 2009. 137(1): p. 47-59.
77. Kimura, A., et al., Aryl hydrocarbon receptor in combination with Stat1 regulates LPS-induced inflammatory responses. J Exp Med, 2009. 206(9): p. 2027-35.
78. Baltimore, D., et al., MicroRNAs: new regulators of immune cell development and function. Nat Immunol, 2008. 9(8): p. 839-845.
79. Taganov, K.D., et al., NF-kappaB-dependent induction of microRNA miR-146, an inhibitor targeted to signaling proteins of innate immune responses. Proc Natl Acad Sci U S A, 2006. 103(33): p. 12481-6.
80. Nahid, M.A., et al., Regulation of TLR2-Mediated Tolerance and Cross-Tolerance through IRAK4 Modulation by miR-132 and miR-212. The Journal of Immunology, 2013. 190(3): p. 1250-1263.
81. Sheedy, F.J., et al., Negative regulation of TLR4 via targeting of the proinflammatory tumor suppressor PDCD4 by the microRNA miR-21. Nat Immunol, 2010. 11(2): p. 141-147.
82. O'Connell, R.M., et al., Inositol phosphatase SHIP1 is a primary target of miR-155. Proceedings of the National Academy of Sciences, 2009. 106(17): p. 7113-7118.
83. Tili, E., et al., Modulation of miR-155 and miR-125b Levels following Lipopolysaccharide/TNF-α Stimulation and Their Possible Roles in Regulating the Response to Endotoxin Shock. The Journal of Immunology, 2007. 179(8): p. 5082-5089.
84. Tang, B., et al., Identification of MyD88 as a novel target of miR-155, involved in negative regulation of Helicobacter pylori-induced inflammation. FEBS Lett, 2010. 584(8): p. 1481-6.

85. Medzhitov, R. and T. Horng, Transcriptional control of the inflammatory response. Nat Rev Immunol, 2009. 9(10): p. 692-703.
86. Whitmore, M.M., et al., Negative Regulation of TLR-Signaling Pathways by Activating Transcription Factor-3. The Journal of Immunology, 2007. 179(6): p. 3622-3630.
87. Gilchrist, M., et al., Systems biology approaches identify ATF3 as a negative regulator of Toll-like receptor 4. Nature, 2006. 441(7090): p. 173-178.
88. Tanaka, T., M.J. Grusby, and T. Kaisho, PDLIM2-mediated termination of transcription factor NF-[kappa]B activation by intranuclear sequestration and degradation of the p65 subunit. Nat Immunol, 2007. 8(6): p. 584-591.
89. Kuwata, H., et al., IκBNS Inhibits Induction of a Subset of Toll-like Receptor-Dependent Genes and Limits Inflammation. Immunity, 2006. 24(1): p. 41-51.
90. Palmer, S. and Y. Chen, Bcl-3, a multifaceted modulator of NF-κB-mediated gene transcription. Immunologic Research, 2008. 42(1): p. 210-218.
91. Crossen, P.E., Cytogenetic and molecular changes in chronic B-cell leukemia. Cancer Genet Cytogenet, 1989. 43(2): p. 143-50.
92. Ohno, H., G. Takimoto, and T.W. McKeithan, The candidate proto-oncogene bcl-3 is related to genes implicated in cell lineage determination and cell cycle control. Cell, 1990. 60(6): p. 991-997.
93. McKeithan, T.W., et al., BCL3 rearrangements and t(14;19) in chronic lymphocytic leukemia and other B-cell malignancies: A molecular and cytogenetic study. Genes, Chromosomes and Cancer, 1997. 20(1): p. 64-72.
94. Martin-Subero, J.I., et al., A comprehensive genetic and histopathologic analysis identifies two subgroups of B-cell malignancies carrying a t(14;19)(q32;q13) or variant BCL3-translocation. Leukemia, 2007. 21(7): p. 1532-1544.
95. Maldonado, V. and J. Melendez-Zajgla, Role of Bcl-3 in solid tumors. Mol Cancer, 2011. 10: p. 152.
96. Westerheide, S.D., et al., The Putative Oncoprotein Bcl-3 Induces Cyclin D1 To Stimulate G1 Transition. Molecular and Cellular Biology, 2001. 21(24): p. 8428-8436.

97. Cogswell, P.C., et al., Selective activation of NF-kappa B subunits in human breast cancer: potential roles for NF-kappa B2/p52 and for Bcl-3. Oncogene, 2000. 19(9): p. 1123-31.
98. Thornburg, N.J., R. Pathmanathan, and N. Raab-Traub, Activation of Nuclear Factor-κB p50 Homodimer/Bcl-3 Complexes in Nasopharyngeal Carcinoma. Cancer Research, 2003. 63(23): p. 8293-8301.
99. Massoumi, R., et al., Cyld Inhibits Tumor Cell Proliferation by Blocking Bcl-3-Dependent NF-ºB Signaling. Cell, 2006. 125(4): p. 665-677.
100. Bauer, A., et al., The NF-κB regulator Bcl-3 and the BH3-only proteins Bim and Puma control the death of activated T cells. Proceedings of the National Academy of Sciences, 2006. 103(29): p. 10979-10984.
101. Mitchell, T.C., et al., Immunological adjuvants promote activated T cell survival via induction of Bcl-3. Nat Immunol, 2001. 2(5): p. 397-402.
102. Rangelova, S., et al., FADD and the NF-κB family member Bcl-3 regulate complementary pathways to control T-cell survival and proliferation. Immunology, 2008. 125(4): p. 549-557.
103. Kashatus, D., P. Cogswell, and A.S. Baldwin, Expression of the Bcl-3 proto-oncogene suppresses p53 activation. Genes & Development, 2006. 20(2): p. 225-235.
104. Franzoso, G., et al., Mice Deficient in Nuclear Factor (NF)-κB/p52 Present with Defects in Humoral Responses, Germinal Center Reactions, and Splenic Microarchitecture. The Journal of Experimental Medicine, 1998. 187(2): p. 147-159.
105. Zhang, X., et al., A Role for the IκB Family Member Bcl-3 in the Control of Central Immunologic Tolerance. Immunity, 2007. 27(3): p. 438-452.
106. Corn, R.A., et al., Opposing Roles for RelB and Bcl-3 in Regulation of T-Box Expressed in T Cells, GATA-3, and Th Effector Differentiation. The Journal of Immunology, 2005. 175(4): p. 2102-2110.
107. Paxian, S., et al., Abnormal organogenesis of Peyer's patches in mice deficient for NF-κB1, NF-κB2, and Bcl-3. Gastroenterology, 2002. 122(7): p. 1853-1868.
108. Schwarz, E.M., et al., Immunological defects in mice with a targeted disruption in Bcl-3. Genes & Development, 1997. 11(2): p. 187-197.

109. Kreisel, D., et al., Bcl3 prevents acute inflammatory lung injury in mice by restraining emergency granulopoiesis. The Journal of Clinical Investigation, 2011. 121(1): p. 265-276.
110. Ruan, Q., et al., Roles of Bcl-3 in the Pathogenesis of Murine Type 1 Diabetes. Diabetes, 2010. 59(10): p. 2549-2557.
111. Carmody, R.J., et al., Negative Regulation of Toll-Like Receptor Signaling by NF-κB p50 Ubiquitination Blockade. Science, 2007. 317(5838): p. 675-678.
112. Pène, F., et al., The IκB Family Member Bcl-3 Coordinates the Pulmonary Defense against Klebsiella pneumoniae Infection. The Journal of Immunology, 2011. 186(4): p. 2412-2421.
113. Beeson, P.B., Development of tolerance to typhoid bacterial pyrogen and its abolition by reticulo-endothelial blockade. Proc Soc Exp Biol Med, 1946. 61: p. 248-50.
114. Beeson, P.B., TOLERANCE TO BACTERIAL PYROGENS : I. FACTORS INFLUENCING ITS DEVELOPMENT. J Exp Med, 1947. 86(1): p. 29-38.
115. Beeson, P.B., TOLERANCE TO BACTERIAL PYROGENS : II. ROLE OF THE RETICULO-ENDOTHELIAL SYSTEM. J Exp Med, 1947. 86(1): p. 39-44.
116. Freedman, H.H., Passive transfer of tolerance to pyrogenicity of bacterial endotoxin. J Exp Med, 1960. 111: p. 453-63.
117. Cavaillon, J.M. and M. Adib-Conquy, Bench-to-bedside review: endotoxin tolerance as a model of leukocyte reprogramming in sepsis. Crit Care, 2006. 10(5): p. 233.
118. Berczi, I., Neurohormonal Host Defense in Endotoxin Shock. Annals of the New York Academy of Sciences, 1998. 840(1): p. 787-802.
119. Freudenberg, M.A. and C. Galanos, Induction of tolerance to lipopolysaccharide (LPS)-D-galactosamine lethality by pretreatment with LPS is mediated by macrophages. Infection and Immunity, 1988. 56(5): p. 1352-1357.
120. Poltorak, A., et al., Defective LPS Signaling in C3H/HeJ and C57BL/10ScCr Mice: Mutations in Tlr4 Gene. Science, 1998. 282(5396): p. 2085-2088.
121. Fujihara, M., et al., Lipopolysaccharide-triggered desensitization of TNF-α mRNA expression involves lack of phosphorylation of IκBα in a murine

macrophage-like cell line, P388D1. Journal of Leukocyte Biology, 2000. 68(2): p. 267-276.

122. Medvedev, A.E., K.M. Kopydlowski, and S.N. Vogel, Inhibition of Lipopolysaccharide-Induced Signal Transduction in Endotoxin-Tolerized Mouse Macrophages: Dysregulation of Cytokine, Chemokine, and Toll-Like Receptor 2 and 4 Gene Expression. The Journal of Immunology, 2000. 164(11): p. 5564-5574.
123. Fujihara, M., et al., Molecular mechanisms of macrophage activation and deactivation by lipopolysaccharide: roles of the receptor complex. Pharmacology & Therapeutics, 2003. 100(2): p. 171-194.
124. Medvedev, A.E., et al., Dysregulation of LPS-Induced Toll-Like Receptor 4-MyD88 Complex Formation and IL-1 Receptor-Associated Kinase 1 Activation in Endotoxin-Tolerant Cells. The Journal of Immunology, 2002. 169(9): p. 5209-5216.
125. Medvedev, A.E., et al., Invited review: Tolerance to microbial TLR ligands: molecular mechanisms and relevance to disease. Journal of Endotoxin Research, 2006. 12(3): p. 133-150.
126. Yan, Q., et al., Nuclear factor-κB binding motifs specify Toll-like receptor-induced gene repression through an inducible repressosome. Proceedings of the National Academy of Sciences, 2012. 109(35): p. 14140-14145.
127. Mosser, D.M. and J.P. Edwards, Exploring the full spectrum of macrophage activation. Nat Rev Immunol, 2008. 8(12): p. 958-969.
128. Geissmann, F., S. Jung, and D.R. Littman, Blood Monocytes Consist of Two Principal Subsets with Distinct Migratory Properties. Immunity, 2003. 19(1): p. 71-82.
129. van Furth, R., et al., The mononuclear phagocyte system: a new classification of macrophages, monocytes, and their precursor cells. Bull World Health Organ, 1972. 46(6): p. 845-52.
130. Murray, P.J. and T.A. Wynn, Protective and pathogenic functions of macrophage subsets. Nat Rev Immunol, 2011. 11(11): p. 723-737.
131. Mowat, A.M. and C.C. Bain, Mucosal Macrophages in Intestinal Homeostasis and Inflammation. Journal of Innate Immunity, 2011. 3(6): p. 550-564.

132. Ginhoux, F., et al., Fate Mapping Analysis Reveals That Adult Microglia Derive from Primitive Macrophages. Science, 2010. 330(6005): p. 841-845.
133. Schulz, C., et al., A Lineage of Myeloid Cells Independent of Myb and Hematopoietic Stem Cells. Science, 2012. 336(6077): p. 86-90.
134. Geissmann, F., et al., Unravelling mononuclear phagocyte heterogeneity. Nat Rev Immunol, 2010. 10(6): p. 453-460.
135. Biswas, S.K. and A. Mantovani, Macrophage plasticity and interaction with lymphocyte subsets: cancer as a paradigm. Nat Immunol, 2010. 11(10): p. 889-896.
136. Edwards, J.P., et al., Biochemical and functional characterization of three activated macrophage populations. Journal of Leukocyte Biology, 2006. 80(6): p. 1298-1307.
137. Galli, S.J., N. Borregaard, and T.A. Wynn, Phenotypic and functional plasticity of cells of innate immunity: macrophages, mast cells and neutrophils. Nat Immunol, 2011. 12(11): p. 1035-1044.
138. Murray, P.J. and T.A. Wynn, Obstacles and opportunities for understanding macrophage polarization. Journal of Leukocyte Biology, 2011. 89(4): p. 557-563.
139. Grimm, M.J., et al., Monocyte- and Macrophage-Targeted NADPH Oxidase Mediates Antifungal Host Defense and Regulation of Acute Inflammation in Mice. The Journal of Immunology, 2013. 190(8): p. 4175-4184.
140. Lawrence, T. and G. Natoli, Transcriptional regulation of macrophage polarization: enabling diversity with identity. Nat Rev Immunol, 2011. 11(11): p. 750-761.
141. Krausgruber, T., et al., IRF5 promotes inflammatory macrophage polarization and TH1-TH17 responses. Nat Immunol, 2011. 12(3): p. 231-238.
142. Darnell, J.E., Jr., I.M. Kerr, and G.R. Stark, Jak-STAT pathways and transcriptional activation in response to IFNs and other extracellular signaling proteins. Science, 1994. 264(5164): p. 1415-21.
143. Meraz, M.A., et al., Targeted Disruption of the Stat1 Gene in Mice Reveals Unexpected Physiologic Specificity in the JAK STAT Signaling Pathway. Cell, 1996. 84(3): p. 431-442.

144. Varin, A. and S. Gordon, Alternative activation of macrophages: Immune function and cellular biology. Immunobiology, 2009. 214(7): p. 630-641.
145. Gordon, S. and F.O. Martinez, Alternative Activation of Macrophages: Mechanism and Functions. Immunity, 2010. 32(5): p. 593-604.
146. Harris, J., et al., T Helper 2 Cytokines Inhibit Autophagic Control of Intracellular Mycobacterium tuberculosis. Immunity, 2007. 27(3): p. 505-517.
147. Herbert, D.B.R., et al., Alternative Macrophage Activation Is Essential for Survival during Schistosomiasis and Downmodulates T Helper 1 Responses and Immunopathology. Immunity, 2004. 20(5): p. 623-635.
148. Brombacher, F., et al., Analyzing Classical and Alternative Macrophage Activation in Macrophage/Neutrophil-Specific IL-4 Receptor-Alpha-Deficient Mice, in Macrophages and Dendritic Cells, N.E. Reiner, Editor 2009, Humana Press. p. 225-252.
149. Satoh, T., et al., The Jmjd3-Irf4 axis regulates M2 macrophage polarization and host responses against helminth infection. Nat Immunol, 2010. 11(10): p. 936-944.
150. Ruffell, D., et al., A CREB-C/EBPβ cascade induces M2 macrophage-specific gene expression and promotes muscle injury repair. Proceedings of the National Academy of Sciences, 2009. 106(41): p. 17475-17480.
151. Jenkins, S.J., et al., Local Macrophage Proliferation, Rather than Recruitment from the Blood, Is a Signature of TH2 Inflammation. Science, 2011. 332(6035): p. 1284-1288.
152. Rajaiah, R., et al., Dissociation of Endotoxin Tolerance and Differentiation of Alternatively Activated Macrophages. The Journal of Immunology, 2013. 190(9): p. 4763-4772.
153. Pena, O.M., et al., Endotoxin Tolerance Represents a Distinctive State of Alternative Polarization (M2) in Human Mononuclear Cells. The Journal of Immunology, 2011. 186(12): p. 7243-7254.
154. Porta, C., et al., Tolerance and M2 (alternative) macrophage polarization are related processes orchestrated by p50 nuclear factor κB. Proceedings of the National Academy of Sciences, 2009. 106(35): p. 14978-14983.
155. Mantovani, A., et al., Macrophage plasticity and polarization in tissue repair and remodelling. The Journal of Pathology, 2013. 229(2): p. 176-185.

156. Gustafsson, C., et al., Gene Expression Profiling of Human Decidual Macrophages: Evidence for Immunosuppressive Phenotype. PLoS One, 2008. 3(4): p. e2078.
157. Bain, C.C. and A.M. Mowat, Intestinal macrophages – specialised adaptation to a unique environment. European Journal of Immunology, 2011. 41(9): p. 2494-2498.
158. Dolganiuc, A., et al., Viral and host factors induce macrophage activation and loss of toll-like receptor tolerance in chronic HCV infection. Gastroenterology, 2007. 133(5): p. 1627-36.
159. Munoz, C., et al., Dysregulation of in vitro cytokine production by monocytes during sepsis. The Journal of Clinical Investigation, 1991. 88(5): p. 1747-1754.
160. Cavaillon, J.-M. and M. Adib-Conquy, Bench-to-bedside review: Endotoxin tolerance as a model of leukocyte reprogramming in sepsis. Critical Care, 2006. 10(5): p. 233.
161. del Fresno, C., et al., Inflammatory responses associated with acute coronary syndrome up-regulate IRAK-M and induce endotoxin tolerance in circulating monocytes. Journal of Endotoxin Research, 2007. 13(1): p. 39-52.
162. Ueda, Y., et al., Commensal microbiota induce LPS hyporesponsiveness in colonic macrophages via the production of IL-10. International Immunology, 2010. 22(12): p. 953-962.
163. Callery, M.P., M.J. Mangino, and M.W. Flye, A biologic basis for limited Kupffer cell reactivity to portal-derived endotoxin. Surgery, 1991. 110(2): p. 221-230.
164. Hafenrichter, D.G., et al., The Kupffer Cell in Endotoxin Tolerance: Mechanisms of Protection Against Lethal Endotoxemia. Shock, 1994. 2(4): p. 251-256.
165. Uhrig, A., et al., Development and functional consequences of LPS tolerance in sinusoidal endothelial cells of the liver. Journal of Leukocyte Biology, 2005. 77(5): p. 626-633.
166. Enomoto, N., et al., Alcohol causes both tolerance and sensitization of rat Kupffer cells via mechanisms dependent on endotoxin. Gastroenterology, 1998. 115(2): p. 443-51.

167. Fava, F. and S. Danese, Intestinal microbiota in inflammatory bowel disease: friend of foe? World J Gastroenterol, 2011. 17(5): p. 557-66.
168. Seksik, P., et al., Sera from patients with Crohn's disease break bacterial lipopolysaccharide tolerance of human intestinal epithelial cells via MD-2 activity. Innate Immunity, 2010. 16(6): p. 381-390.
169. Louvet, A., et al., Cannabinoid CB2 receptors protect against alcoholic liver disease by regulating Kupffer cell polarization in mice. Hepatology, 2011. 54(4): p. 1217-1226.
170. Fransen, K., et al., Analysis of SNPs with an effect on gene expression identifies UBE2L3 and BCL3 as potential new risk genes for Crohn's disease. Human Molecular Genetics, 2010. 19(17): p. 3482-3488.
171. Gottfries, J., S. Melgar, and E. Michaëlsson, Modelling of Mouse Experimental Colitis by Global Property Screens: A Holistic Approach to Assess Drug Effects in Inflammatory Bowel Disease. PLoS One, 2012. 7(1): p. e30005.
172. Hall, L., et al., Induction and Activation of Adaptive Immune Populations During Acute and Chronic Phases of a Murine Model of Experimental Colitis. Digestive Diseases and Sciences, 2011. 56(1): p. 79-89.
173. Vowinkel, T., et al., Impact of dextran sulfate sodium load on the severity of inflammation in experimental colitis. Dig Dis Sci, 2004. 49(4): p. 556-64.
174. Wirtz, S., et al., Chemically induced mouse models of intestinal inflammation. Nat. Protocols, 2007. 2(3): p. 541-546.
175. Cadwell, K., et al., A key role for autophagy and the autophagy gene Atg16l1 in mouse and human intestinal Paneth cells. Nature, 2008. 456(7219): p. 259-263.
176. Murphy, C.T., et al., Technical Advance: Function and efficacy of an α4-integrin antagonist using bioluminescence imaging to detect leukocyte trafficking in murine experimental colitis. Journal of Leukocyte Biology, 2010. 88(6): p. 1271-1278.
177. Cummins, E.P., et al., The Hydroxylase Inhibitor Dimethyloxalylglycine Is Protective in a Murine Model of Colitis. Gastroenterology, 2008. 134(1): p. 156-165.e1.

178. Tambuwala, M.M., et al., Loss of Prolyl Hydroxylase-1 Protects Against Colitis Through Reduced Epithelial Cell Apoptosis and Increased Barrier Function. Gastroenterology, 2010. 139(6): p. 2093-2101.
179. Livak, K.J. and T.D. Schmittgen, Analysis of Relative Gene Expression Data Using Real-Time Quantitative PCR and the 2−ΔΔCT Method. Methods, 2001. 25(4): p. 402-408.
180. Gentleman, R.C., et al., Bioconductor: open software development for computational biology and bioinformatics. Genome Biol, 2004. 5(10): p. R80.
181. Smyth, G.K., Linear models and empirical bayes methods for assessing differential expression in microarray experiments. Stat Appl Genet Mol Biol, 2004. 3: p. Article3.
182. Johnson, W.E., C. Li, and A. Rabinovic, Adjusting batch effects in microarray expression data using empirical Bayes methods. Biostatistics, 2007. 8(1): p. 118-27.
183. Huang, D.W., B.T. Sherman, and R.A. Lempicki, Systematic and integrative analysis of large gene lists using DAVID bioinformatics resources. Nat. Protocols, 2008. 4(1): p. 44-57.
184. Sturn, A., J. Quackenbush, and Z. Trajanoski, Genesis: cluster analysis of microarray data. Bioinformatics, 2002. 18(1): p. 207-208.
185. Costello, C.M., et al., Dissection of the Inflammatory Bowel Disease Transcriptome Using Genome-Wide cDNA Microarrays. PLoS Med, 2005. 2(8): p. e199.
186. Ghosh, S. and M.S. Hayden, New regulators of NF-[kappa]B in inflammation. Nat Rev Immunol, 2008. 8(11): p. 837-848.
187. Hayden, M.S. and S. Ghosh, Shared Principles in NF-κB Signaling. Cell, 2008. 132(3): p. 344-362.
188. Schreiber, S., S. Nikolaus, and J. Hampe, Activation of nuclear factor κB in inflammatory bowel disease. Gut, 1998. 42(4): p. 477-484.
189. Wullaert, A., M.C. Bonnet, and M. Pasparakis, NF-[kappa]B in the regulation of epithelial homeostasis and inflammation. Cell Res, 2011. 21(1): p. 146-158.

190. Karrasch, T., et al., Gnotobiotic IL-10−/−;NF-κBEGFP Mice Reveal the Critical Role of TLR/NF-κB Signaling in Commensal Bacteria-Induced Colitis. The Journal of Immunology, 2007. 178(10): p. 6522-6532.
191. Zhang, J., et al., Impaired regulation of NF-κB and increased susceptibility to colitis-associated tumorigenesis in CYLD-deficient mice. The Journal of Clinical Investigation, 2006. 116(11): p. 3042-3049.
192. Neurath, M.F., et al., Local administration of antisense phosphorothiate olignucleotides to the p65 subunit of NF-[kappa]B abrogates established experimental colitis in mice. Nat Med, 1996. 2(9): p. 998-1004.
193. Nenci, A., et al., Epithelial NEMO links innate immunity to chronic intestinal inflammation. Nature, 2007. 446(7135): p. 557-561.
194. Steinbrecher, K.A., et al., Loss of Epithelial RelA Results in Deregulated Intestinal Proliferative/Apoptotic Homeostasis and Susceptibility to Inflammation. The Journal of Immunology, 2008. 180(4): p. 2588-2599.
195. Rakoff-Nahoum, S., et al., Recognition of Commensal Microflora by Toll-Like Receptors Is Required for Intestinal Homeostasis. Cell, 2004. 118(2): p. 229-241.
196. Kerr, L.D., et al., The proto-oncogene bcl-3 encodes an I kappa B protein. Genes & Development, 1992. 6(12a): p. 2352-2363.
197. Nolan, G.P., et al., The bcl-3 proto-oncogene encodes a nuclear I kappa B-like molecule that preferentially interacts with NF-kappa B p50 and p52 in a phosphorylation-dependent manner. Molecular and Cellular Biology, 1993. 13(6): p. 3557-3566.
198. Dann, S.M., et al., IL-6-dependent mucosal protection prevents establishment of a microbial niche for attaching/effacing lesion-forming enteric bacterial pathogens. J Immunol, 2008. 180(10): p. 6816-26.
199. Tao, Y., et al., Soluble factors from Lactobacillus GG activate MAPKs and induce cytoprotective heat shock proteins in intestinal epithelial cells. Am J Physiol Cell Physiol, 2006. 290(4): p. C1018-30.
200. Ota, N., et al., IL-22 bridges the lymphotoxin pathway with the maintenance of colonic lymphoid structures during infection with Citrobacter rodentium. Nat Immunol, 2011. 12(10): p. 941-948.
201. O'Connor Jr, W., et al., A protective function for interleukin 17A in T cell-mediated intestinal inflammation. Nat Immunol, 2009. 10(6): p. 603-609.

202. Zenewicz, L.A., et al., Innate and Adaptive Interleukin-22 Protects Mice from Inflammatory Bowel Disease. Immunity, 2008. 29(6): p. 947-957.
203. Mähler, M., et al., Differential susceptibility of inbred mouse strains to dextran sulfate sodium-induced colitis. American Journal of Physiology - Gastrointestinal and Liver Physiology, 1998. 274(3): p. G544-G551.
204. Mahler, M., et al., Genetic analysis of susceptibility to dextran sulfate sodium-induced colitis in mice. Genomics, 1999. 55(2): p. 147-56.
205. Dobrovolskaia, M.A. and S.N. Vogel, Toll receptors, CD14, and macrophage activation and deactivation by LPS. Microbes and Infection, 2002. 4(9): p. 903-914.
206. Cook, D.N., D.S. Pisetsky, and D.A. Schwartz, Toll-like receptors in the pathogenesis of human disease. Nat Immunol, 2004. 5(10): p. 975-979.
207. Piao, W., et al., Endotoxin tolerance dysregulates MyD88- and Toll/IL-1R domain-containing adapter inducing IFN-β-dependent pathways and increases expression of negative regulators of TLR signaling. Journal of Leukocyte Biology, 2009. 86(4): p. 863-875.
208. Xiong, Y. and A.E. Medvedev, Induction of endotoxin tolerance in vivo inhibits activation of IRAK4 and increases negative regulators IRAK-M, SHIP-1, and A20. Journal of Leukocyte Biology, 2011. 90(6): p. 1141-1148.
209. Fleetwood, A.J., et al., GM-CSF- and M-CSF-dependent macrophage phenotypes display differential dependence on Type I interferon signaling. Journal of Leukocyte Biology, 2009. 86(2): p. 411-421.
210. Chorro, L., et al., Langerhans cell (LC) proliferation mediates neonatal development, homeostasis, and inflammation-associated expansion of the epidermal LC network. The Journal of Experimental Medicine, 2009. 206(13): p. 3089-3100.
211. Chen, J. and L.B. Ivashkiv, IFN-γ abrogates endotoxin tolerance by facilitating Toll-like receptor-induced chromatin remodeling. Proceedings of the National Academy of Sciences, 2010. 107(45): p. 19438-19443.
212. Benoit, M., B. Desnues, and J.-L. Mege, Macrophage Polarization in Bacterial Infections. The Journal of Immunology, 2008. 181(6): p. 3733-3739.

213. Schmitz, J., et al., IL-33, an interleukin-1-like cytokine that signals via the IL-1 receptor-related protein ST2 and induces T helper type 2-associated cytokines. Immunity, 2005. 23: p. 479 - 90.
214. Espinassous, Q., et al., IL-33 enhances lipopolysaccharide-induced inflammatory cytokine production from mouse macrophages by regulating lipopolysaccharide receptor complex. J Immunol, 2009. 183: p. 1446 - 55.
215. Joshi, A., et al., Interleukin-33 contributes to both M1 and M2 chemokine marker expression in human macrophages. BMC Immunology, 2010. 11(1): p. 52.
216. Ali, S., et al., The Dual Function Cytokine IL-33 Interacts with the Transcription Factor NF-κB To Dampen NF-κB–Stimulated Gene Transcription. The Journal of Immunology, 2011. 187(4): p. 1609-1616.
217. Ohno, T., et al., Paracrine IL-33 Stimulation Enhances Lipopolysaccharide-Mediated Macrophage Activation. PLoS One, 2011. 6(4): p. e18404.
218. Landsman, L., et al., CX3CR1 is required for monocyte homeostasis and atherogenesis by promoting cell survival. Blood, 2009. 113(4): p. 963-972.
219. Boehme, S.A., et al., The Chemokine Fractalkine Inhibits Fas-Mediated Cell Death of Brain Microglia. The Journal of Immunology, 2000. 165(1): p. 397-403.
220. Kobayashi, T., et al., NFIL3 Is a Regulator of IL-12 p40 in Macrophages and Mucosal Immunity. The Journal of Immunology, 2011. 186(8): p. 4649-4655.
221. Kopf, M., M.F. Bachmann, and B.J. Marsland, Averting inflammation by targeting the cytokine environment. Nat Rev Drug Discov, 2010. 9(9): p. 703-718.
222. McInnes, I.B. and G. Schett, Cytokines in the pathogenesis of rheumatoid arthritis. Nat Rev Immunol, 2007. 7(6): p. 429-442.
223. Barnes, P.J., The cytokine network in asthma and chronic obstructive pulmonary disease. The Journal of Clinical Investigation, 2008. 118(11): p. 3546-3556.
224. Lin, W.-W. and M. Karin, A cytokine-mediated link between innate immunity, inflammation, and cancer. The Journal of Clinical Investigation, 2007. 117(5): p. 1175-1183.

225. Hotchkiss, R.S., et al., The sepsis seesaw: tilting toward immunosuppression. Nat Med, 2009. 15(5): p. 496-497.
226. Smith, A.M., et al., Disordered macrophage cytokine secretion underlies impaired acute inflammation and bacterial clearance in Crohn's disease. The Journal of Experimental Medicine, 2009. 206(9): p. 1883-1897.
227. Bain, C.C., et al., Resident and pro-inflammatory macrophages in the colon represent alternative context-dependent fates of the same Ly6Chi monocyte precursors. Mucosal Immunol, 2013. 6(3): p. 498-510.
228. Franchi, L., et al., NLRC4-driven production of IL-1[beta] discriminates between pathogenic and commensal bacteria and promotes host intestinal defense. Nat Immunol, 2012. 13(5): p. 449-456.
229. Lacy, P. and J.L. Stow, Cytokine release from innate immune cells: association with diverse membrane trafficking pathways. Blood, 2011. 118(1): p. 9-18.
230. Ha, S.-D., et al., Cathepsin B Is Involved in the Trafficking of TNF-α-Containing Vesicles to the Plasma Membrane in Macrophages. The Journal of Immunology, 2008. 181(1): p. 690-697.
231. Dupont, N., et al., Autophagy-based unconventional secretory pathway for extracellular delivery of IL-1[beta]. EMBO J, 2011. 30(23): p. 4701-4711.
232. Harris, J., Autophagy and cytokines. Cytokine, 2011. 56(2): p. 140-144.
233. Harris, J., et al., Autophagy Controls IL-1β Secretion by Targeting Pro-IL-1β for Degradation. Journal of Biological Chemistry, 2011. 286(11): p. 9587-9597.
234. Peral de Castro, C., et al., Autophagy Regulates IL-23 Secretion and Innate T Cell Responses through Effects on IL-1 Secretion. The Journal of Immunology, 2012. 189(8): p. 4144-4153.
235. Fujita, N., et al., The Atg16L Complex Specifies the Site of LC3 Lipidation for Membrane Biogenesis in Autophagy. Molecular Biology of the Cell, 2008. 19(5): p. 2092-2100.
236. Hampe, J., et al., A genome-wide association scan of nonsynonymous SNPs identifies a susceptibility variant for Crohn disease in ATG16L1. Nat Genet, 2007. 39(2): p. 207-211.
237. Dinter, A. and E.G. Berger, Golgi-disturbing agents. Histochemistry and Cell Biology, 1998. 109(5-6): p. 571-590.

238. Anderson, P., et al., Post-transcriptional regulation of proinflammatory proteins. Journal of Leukocyte Biology, 2004. 76(1): p. 42-47.
239. Papadakis, K.A. and S.R. Targan, Role of Cytokines in the Pathogenesis of Inflammatory Bowel Disease. Annual Review of Medicine, 2000. 51(1): p. 289-298.
240. Miller, A.M. and I.B. McInnes, Cytokines as therapeutic targets to reduce cardiovascular risk in chronic inflammation. Curr Pharm Des, 2011. 17(1): p. 1-8.
241. del Fresno, C., et al., Monocytes from Cystic Fibrosis Patients Are Locked in an LPS Tolerance State: Down-Regulation of TREM-1 as Putative Underlying Mechanism. PLoS One, 2008. 3(7): p. e2667.
242. Medzhitov, R., D.S. Schneider, and M.P. Soares, Disease Tolerance as a Defense Strategy. Science, 2012. 335(6071): p. 936-941.
243. Wu, H.-J. and E. Wu, The role of gut microbiota in immune homeostasis and autoimmunity. Gut Microbes, 2012. 3(1): p. 4-14.
244. Horino, J., et al., Suppressor of cytokine signaling-1 ameliorates dextran sulfate sodium-induced colitis in mice. International Immunology, 2008. 20(6): p. 753-762.
245. Berglund, M., et al., IL-1 receptor-associated kinase M downregulates DSS-induced colitis. Inflamm Bowel Dis, 2010. 16(10): p. 1778-86.
246. Murphy, C.T., et al., The Sphingosine-1-Phosphate Analogue FTY720 Impairs Mucosal Immunity and Clearance of the Enteric Pathogen Citrobacter rodentium. Infection and Immunity, 2012. 80(8): p. 2712-2723.
247. Powrie, F., et al., Phenotypically distinct subsets of CD4+ T cells induce or protect from chronic intestinal inflammation in C. B-17 scid mice. Int Immunol, 1993. 5(11): p. 1461-71.
248. Wirtz, S. and M.F. Neurath, Mouse models of inflammatory bowel disease. Advanced Drug Delivery Reviews, 2007. 59(11): p. 1073-1083.
249. Puvvada, S.D., et al., NF-kB and Bcl-3 activation are prognostic in metastatic colorectal cancer. Oncology, 2010. 78(3-4): p. 181-8.
250. Ustyugova, I.V., et al., IEX-1 Deficiency Protects against Colonic Cancer. Molecular Cancer Research, 2012. 10(6): p. 760-767.
251. Bamias, G., et al., New insights into the dichotomous role of innate cytokines in gut homeostasis and inflammation. Cytokine, 2012. 59(3): p. 451-459.

252. Latz, E., T.S. Xiao, and A. Stutz, Activation and regulation of the inflammasomes. Nat Rev Immunol, 2013. 13(6): p. 397-411.
253. Lieu, Z.Z., et al., A trans-Golgi network golgin is required for the regulated secretion of TNF in activated macrophages in vivo. Proceedings of the National Academy of Sciences, 2008. 105(9): p. 3351-3356.
254. Murray, R.Z., et al., A Role for the Phagosome in Cytokine Secretion. Science, 2005. 310(5753): p. 1492-1495.
255. Stow, J.L., et al., Cytokine secretion in macrophages and other cells: Pathways and mediators. Immunobiology, 2009. 214(7): p. 601-612.
256. Stow, J.L. and R.Z. Murray, Intracellular trafficking and secretion of inflammatory cytokines. Cytokine & growth factor reviews, 2013.
257. Stenseth, K. and J. Thyberg, Monensin and chloroquine inhibit transfer to lysosomes of endocytosed macromolecules in cultured mouse peritoneal macrophages. Eur J Cell Biol, 1989. 49(2): p. 326-33.
258. Abdi, K., N.J. Singh, and P. Matzinger, Lipopolysaccharide-Activated Dendritic Cells: "Exhausted" or Alert and Waiting? The Journal of Immunology, 2012. 188(12): p. 5981-5989.
259. Feldmann, M., Many cytokines are very useful therapeutic targets in disease. The Journal of Clinical Investigation, 2008. 118(11): p. 3533-3536.
260. Targan, S.R., et al., A Short-Term Study of Chimeric Monoclonal Antibody cA2 to Tumor Necrosis Factor α for Crohn's Disease. New England Journal of Medicine, 1997. 337(15): p. 1029-1036.
261. Bellora, F., et al., The interaction of human natural killer cells with either unpolarized or polarized macrophages results in different functional outcomes. Proceedings of the National Academy of Sciences, 2010. 107(50): p. 21659-21664.

Appendix 1

Cytokine antibody Array

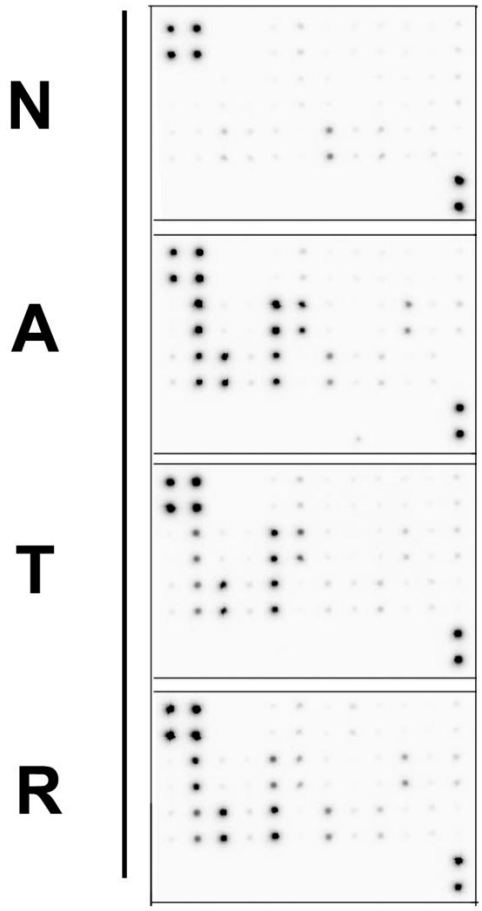

Appendix 2

Cytokine antibody array layout

	A	B	C	D	E	F	G	H	I	J	K	L
1	pos	pos	neg	neg	6Ckine	CTACK	Eotaxin	G-CSF	GM-CSF	IL-2	IL-3	IL-4
2	pos	pos	neg	neg	6Ckine	CTACK	Eotaxin	G-CSF	GM-CSF	IL-2	IL-3	IL-4
3	IL-5	IL-6	IL-9	IL-10	IL-12p40/p70	IL-12p70	IL-13	IL-17	IFN-γ	KC	Leptin	MCP1
4	IL-5	IL-6	IL-9	IL-10	IL-12p40/p70	IL-12p70	IL-13	IL-17	IFN-γ	KC	Leptin	MCP1
5	MCP5	MIPα	MIP2	MIP3β	RANTES	SCF	sTNFR1	TARC	TIMP1	TNFα	TP	VEGF
6	MCP5	MIPα	MIP2	MIP3β	RANTES	SCF	sTNFR1	TARC	TIMP1	TNFα	TP	VEGF
7	Blank	Blank	Blank	Blank	Blank	Blank	Blank	Blank	Blank	Blank	Blank	pos
8	Blank	Blank	Blank	Blank	Blank	Blank	Blank	Blank	Blank	Blank	Blank	pos